95

MATHEMATICAL SIMULATION OF DYNAMIC BEHAVIOUR OF SECONDARY SETTLING TANKS

by

Alison Emslie Ozinsky

BSc (Chem Eng), MSc (Cape Town), Pr Eng

Thesis submitted in fulfillment of the requirements for the degree of Doctor of Philosophy at the University of Cape Town

Department of Civil Engineering

University of Cape Town

August 1993

The University of Cape Town has been given the right to [illegible] in whole or in part. Copyright is held by the author.

The copyright of this thesis vests in the author. No quotation from it or information derived from it is to be published without full acknowledgement of the source. The thesis is to be used for private study or non-commercial research purposes only.

Published by the University of Cape Town (UCT) in terms of the non-exclusive license granted to UCT by the author.

University of Cape Town

DECLARATION BY CANDIDATE

I hereby declare that this thesis
is my own work and that it has not been submitted
for a degree at another University.

Signed by candidate

Alison Emslie Ozinsky
August 1993

ABSTRACT

MATHEMATICAL SIMULATION OF DYNAMIC BEHAVIOUR OF SECONDARY SETTLING TANKS

The main objective of this thesis was to bring the theoretical and practical aspects of secondary settling tank developments closer together. This was achieved firstly, by evaluating and developing empirical relationships from which the flux theory constants may be derived from simpler sludge settleability measures; and secondly, by developing a computer model for the simulation of dynamic behaviour of full scale secondary settling tanks. The model was initially developed for and tested on laboratory scale data. It was then calibrated with full scale data and used to verify the flux theory by comparing the simulated predictions and the measured results.

The simulations demonstrated that a calibrated and verified dynamic settling tank model based on the flux theory and incorporating various refinements such as turbulent diffusivity implicitly encompasses such features of secondary settling tank behaviour such as maximum underflow concentration and sludge storage concentration and capacity. It was concluded that the simulation program is an improvement on previous simulation programs based purely on the steady state flux theory and should be used as a starting point for developing design theories based on the flux theory.

Alison Emslie Ozinsky
Department of Civil Engineering
University of Cape Town
Private Bag Rondebosch
Cape Town
7700

13 August 1993

SYNOPSIS

Although much effort has been expended on work on secondary settling tanks over the past few decades, theoretical and practical developments have remained separate. Theoretical developments have centred mainly on understanding the processes happening inside the settling tank by means of the flux theory, which has already formed the basis for a number of computer simulation models of varying degrees of sophistication and refinement. Practical advances have been mainly in the development of settling tank design procedures which recognise sludge settleability, the two most advanced being the German Abwasser Technische Vereiniging (1973, 1976) (ATV) and Stichiting Toegepast Onderzoek Reiniging Afvalwater (1981) (STORA) design procedures. These two procedures are based on the diluted sludge volume index (DSVI), which is an improvement on the conventional SVI in that it is not dependent on sludge concentration. These two procedures are extremely comprehensive, in that they provide guidance for all the major criteria for secondary settling tank design, such as surface area, depth, sludge storage concentration and capacity and maximum underflow concentration and recycle ratio.

One of the main reasons for the lack of integration between theory and practice is that the two constants required for specifying the sludge settleability in the flux theory, V_o and n, necessitate multiple batch zone settling velocity - concentration (ZSV-X) measurements. In contrast to the simpler sludge settleability tests such as the $SSVI_{3.5}$ and DSVI tests, the ZSV-X test is tedious and time consuming, and consequently is not popular with workers in the field. The preference for the simpler tests have resulted in these being incorporated into improved design procedures that recognise sludge settleability such as the ATV and STORA procedures.

In English speaking countries, improved design procedures recognising sludge settleability were developed based on the flux theory. This was achieved by formulating relationships between the simpler sludge settleability parameters (SSP) and the V_o and n constants describing the ZSV-X relationship. With these relationships, the

flux theory could be used with a knowledge of any one of the sludge settleability parameters. However, these developments are limited in that the flux theory gives guidance only on the surface area and none on the other important settling tank parameters mentioned earlier.

Despite the easier access to the flux theory with the V_o and n - SSP relationship, it has still not become widely accepted as a design tool, the principle reason being that the theory has not yet been definitively verified. This has resulted in a lack of confidence in its predictive abilities, even as regards the surface area determination. Therefore, a comprehensive verification of the flux theory, including a demonstration that it implicitly embraces such aspects as maximum underflow concentration, sludge storage concentration and capacity, will go a long way towards instilling confidence in the flux theory as a design tool or a model from which design guidelines can be obtained.

In this light, the main objective of this investigation was to bring the theoretical and practical aspects of secondary settling tank developments closer together. This was achieved in the following ways:

1. by evaluating and developing relationships from which the flux theory constants, V_o and n, may be derived from the simpler sludge settleability measures: sludge volume index (SVI), stirred specific volume index ($SSVI_{3.5}$) and diluted sludge volume index (DSVI) measurements,

2. by developing a computer model for the simulation of dynamic behaviour of full scale secondary settling tanks. This model was initially developed for and tested on laboratory scale data. It was then calibrated with full scale data collected in an extensive investigation sponsored by STORA (1981) and used to verify the flux theory by comparing the simulated predictions and the measured results. Although the STORA (1981) data is impressive in its detail and comprehensiveness, the ZSV-X tests, were not correctly performed.

Consequently, in order to obtain the flux theory V_o and n values, it was necessary to derive these from the $SSVI_{3.5}$ or DSVI measurements.

3. by demonstrating that a calibrated and verified dynamic settling tank model based on the flux theory and incorporating diffusivity implicitly encompasses such features such as maximum underflow concentration and sludge storage concentration and capacity.

DEVELOPING RELATIONSHIPS BETWEEN SLUDGE SETTLEABILITY PARAMETERS

From the published literature, 12 different data sets for the SVI were obtained. These consisted of 1548 individual ZSV-X values in 190 groups with distinct SVI measurements. For the $SSVI_{3.5}$, nine different data sets were found, totalling 1123 individual ZSV-X values in 212 groups with distinct $SSVI_{3.5}$ measurements. For the DSVI, only five different data sets were found, totalling 354 individual ZSV-X values in 137 groups with distinct DSVI measurements.

Recognising that the data sets were measured on different plants operating under different conditions, specific F tests were conducted to check which of the data sets could be pooled and treated as one set. For the SVI, only five of the 12 sets could be pooled into a family comprising 713 ZSV-X values in 190 SVI groups. None of the remaining sets could be pooled together and had to be treated individually. The pooled family comprises data sets representative of two different activated sludge plant types: biological N and biological N and P removal plants. For the $SSVI_{3.5}$, five of the nine sets could be pooled into a family comprising 603 ZSV-X values in 68 $SSVI_{3.5}$ groups. None of the remaining sets could be pooled into a subgroup. For the DSVI, only three of the five sets could be pooled into a family comprising 239 ZSV-X values in 34 DSVI groups. The remaining two sets could not be paired.

The statistical analysis for pooling the groups was based on the ZSV-X and V_o-SSP relationship being exponential and the n-SSP relationship being linear with the result that:

$$\ln V_o = \ln\alpha - \beta * SSP - \gamma * X - \delta * SSP * X \qquad (A)$$

Statistical and graphical evaluation of the data indicated that these functional forms satisfactorily represent the trends in the data.

Having established the largest family of data for each of the three SSP's, linear least squares regression analyses were conducted to determine the constants α, β, γ and δ in Equation (A). Two different methods were used, the best results being obtained for the "single-step" method, where the constants α, β, γ and δ were determined simultaneously by regression analysis.

For the single step method, the α, β, γ and δ values for the three SSP's are as follows:

$$\begin{aligned} \ln V_o &= 2.14370 - 0.00165 * SVI - 0.20036 * X - 0.00091 * SVI * X \\ (r^2 &= 0.842) \end{aligned} \qquad (B)$$

$$\begin{aligned} \ln V_o &= 2.45095 - 0.00636 * SSVI_{3.5} - 0.16756 * X - 0.00218 * SSVI_{3.5} * X \\ (r^2 &= 0.849) \end{aligned} \qquad (C)$$

$$\begin{aligned} \ln V_o &= 2.30854 - 0.00297 * DSVI - 0.29721 * X - 0.00095 * DSVI * X \\ (r^2 &= 0.776) \end{aligned} \qquad (D)$$

In evaluating the reliability of these functions, it was concluded that the $SSVI_{3.5}$ relationship was the best because (i) the $SSVI_{3.5}$ is itself a better sludge settleability measure than the SVI and (ii) it is based on a much larger data family than the DSVI. Furthermore, the $SSVI_{3.5}$ gave more consistent results for the pooling procedure in that the five data sets that could be pooled were all from essentially long sludge age, N removal plants. The data from N and P removal plants and from fully aerobic plants could not be pooled.

It was concluded that the primary objective of the statistical evaluation had been achieved and that the V_o and n could be reliably obtained from the STORA data with the correlation for $SSVI_{3.5}$ in Equation (C) because the data sets contributing to this relationship were measured at plants similar to those at which the STORA data was collected.

With regard to the generality of these functions, caution should be exercised when using them to obtain V_o and n values. The fact that not all the data could be pooled and that, for the $SSVI_{3.5}$, the pooling seemed to be specific to plant type, indicate that plant type needs to be take into account. For the SVI, this appears not to be the case, but this may be caused by the fact that the SVI is itself a poor sludge settleability measure.

THE SECONDARY SETTLING TANK SIMULATION PROGRAM

Of the numerous secondary settling tank dynamic models that have been developed, Anderson's (1981) model was found to be the most refined and true application of the flux theory to the modelling problem. For this reason, it was decided to use Anderson's model as a starting point for developing a dynamic computer simulation program for secondary settling tanks. Anderson developed the settling tank model as part of a full wastewater treatment plant model for the Detroit Wastewater and Sewage Department (DWSD). He concluded that, in order to obtain a good simulation of the entire plant effluent quality, the secondary settling tank model had to be an improvement on past models.

The algorithm upon which the model is based is an implicit second order, non-iterative finite difference algorithm which solves the set of equations describing the dynamic behaviour of settling sludge in secondary settling tanks. The equations describing the continuous sedimentation process are partial differential hyperbolic equations which are, unfortunately, susceptible to generating multiple physically meaningless solutions when solved by finite difference methods. Anderson's strategy to ensure that a single

correct solution is generated was to introduce a small amount of diffusivity into the hyperbolic partial differential equation (PDE), thus rendering it parabolic. Parabolic partial differential equations do not generate multiple solutions and are uniquely determined by their initial conditions. The addition of diffusivity into the equation, besides being mathematically advantageous, also has physical relevance in that diffusivity in the form of turbulence does exist in the secondary settling tank. Anderson proposed that the diffusivity is highest at the feed point and dies away, approaching zero, in the regions furthest from the feed point. Anderson's algorithm allowed the diffusivity to follow this pattern, thus rendering the partial differential equations parabolic in the region near the feed point and hyperbolic in the region away from the feed point.

Anderson further improved his algorithm by the inclusion of switching functions to resolve discontinuities in the final solution. These discontinuities (or shocks) are a feature of hyperbolic partial differential equations and manifest themselves in the settling tank as abrupt changes in concentration with depth.

The relevant section of Anderson's program was reconstructed into a self contained FORTRAN program called SETTLER (revision 1), dedicated to simulate only the secondary settling tank section of an activated sludge plant. The program SETTLER was progressively tested, modified and refined in four successive steps by comparing the simulation results against

1. Anderson's own data collected at the Detroit WWTP,
2. idealised flux theory calculations
3. laboratory scale measurements,
4. full scale data collected by STORA.

TESTING OF SETTLER (revision 1) AGAINST THE DWWTP DATA

The objective of testing the program SETTLER against the DWWTP data was to confirm that SETTLER is an accurate reconstruction of the secondary settling tank component of Anderson's own program. A number of deficiencies in the program were identified and resolved during the course of this investigation:

1. Although Anderson stated that his algorithm was valid throughout the depth of the tank i.e. for both the parabolic and hyperbolic partial differential equations, he proposed no strategy to deal with problem of physically meaningless multiple solutions generated by hyperbolic partial differential equations.

2. Although Anderson stated that the diffusivity in the settling tank is proportional to the feed flow rate and inversely proportional to the distance from the feed point, his computer program does not take this into account, as the diffusivity is set at a constant value for most of the depth of the tank. It appears that the magnitude of the diffusivity in the settling tank was calibrated specifically for the geometry of the Detroit Wastewater Treatment Plant settling tanks and thus may not be applicable for the general case.

3. Various other problems in the computer program were also identified.

The results obtained for the simulation with SETTLER were the same as those obtained by Anderson and thus it was concluded that SETTLER (revision 1) could be considered to be essentially the same as Anderson's program.

It was noted that neither the measured data nor the results generated by SETTLER (revision 1) preserved the mass balance over the settling tank. This was considered to be a problem of some concern but was dealt with in a subsequent revision of SETTLER.

TESTING OF SETTLER (revision 2) AGAINST IDEALISED FLUX THEORY PREDICTIONS

Application of SETTLER to other test cases was confounded by the lack of clarity regarding an appropriate form and magnitude for the diffusivity function. It was thus decided to select a series of idealised test cases where it would be possible to eliminate the effects of diffusivity entirely. The absence of diffusivity makes the PDE's hyperbolic, thus enabling any other non diffusivity related deficiencies in the program to be identified before complicating the simulation with the additional problem of the diffusivity function.

Four theoretical idealised test cases were simulated with SETTLER (revision 2), each one falling into a different region of the design and operating chart and therefore representative of different modes of over- and underloaded operating conditions. The idealised concentration profile for each test case was calculated with the flux theory, and the predictions of the program compared with these expected results.

Only after the following major modifications were made to SETTLER did it generate accurate solutions for each of the test cases with a variety of initial conditions:

1. Since the set of equations to be solved were hyperbolic partial differential equations, a strategy for avoiding the physically meaningless solutions characteristic of these equations needed to be incorporated into the program. This was achieved by using the flux theory to identify the appropriate solution and initiating the solution procedure with this value.

2. It was necessary to introduce diffusivity into the equations at the feed point only to ensure that, for the overloaded case, the sludge blanket propagated upwards past the feed point. Trial and error simulations were carried out to establish the value of the diffusivity constant necessary to ensure that the predicted concentration profile matched the idealised flux theory concentration profile.

3. Inconsistencies in the switching functions generated incorrect concentration profiles for some of the underloaded test cases with overloaded initial conditions.

4. It was necessary to correct the definition of the bulk velocity at the feed point for overloaded conditions to ensure that the correct concentration profile was generated when the critical concentration was initiated at the feed point and not in the bottom of the tank.

With these modifications incorporated into SETTLER, it was also found to preserve the mass balance on sludge solids over extended simulation periods for each of the test cases.

With confidence in the ability of SETTLER to predict accurate results for idealised (hyperbolic) theoretical test cases with no diffusivity, and to conform to the concentration profiles expected from the flux theory calculations, SETTLER (revision 3) was tested against laboratory scale measurements.

TESTING OF SETTLER (revision 3) AGAINST LABORATORY SCALE DATA

A tall, thin laboratory scale column was selected as a physical situation in which vertical flow dominates and horizontal effects are negligible. Diffusivity effects in the column were assumed to be very small, and all diffusivity constants in the program were set to zero. SETTLER (revision 3) was tested against two cases representative of the range of laboratory scale data and was found to accurately simulate the behaviour in the laboratory column. The next step in the development of the computer simulation program was to check it against full scale data.

TESTING OF SETTLER (revision 4) AGAINST FULL SCALE DATA

Of the 44 settling tank test cases measured by STORA on 22 different settling tanks, 11 critical cases were selected for the purposes of simulation. Except for those cases

where the data was missing or suspect, all overloaded cases that ended in failure were simulated. These were five tests on the settling tank at Rijen, one at Wijk bij Duurstede and one at Uden-Veghel. The four "safe" cases that were simulated were chosen because these fell close to the theoretical (flux calculations) dividing line between safe and failed cases. This was to test the ability of SETTLER to distinguish between failed and safe cases. The inconclusive test cases and the underloaded cases that fell far in the safe region were not simulated as these tests were not regarded as being informative for the purposes of developing the simulation program.

Initially, SETTLER (revision 4) was tested against two of the overloaded Rijen tests, the Rijen 1 test and the Rijen 4 test. The predicted results deviated considerably from the measured results and two major reasons were identified for the discrepancies:

1. the absence of diffusivity in all but the feed point layer of the tank is an inadequate reflection of the extensive turbulent effects found in full scale tanks and

2. the lack of any strategy to model the thickening zone of the settling tank causes erroneous predictions for the underflow concentration.

SETTLER was modified to overcome these problems with the incorporation of a diffusivity function to model the diffusivity at all layers of the tank and a completely mixed stirred tank reactor (CSTR) at the bottom of the settling tank to simulate the time delay of the sludge in the thickening zone.

Calibration of SETTLER on the Rijen tests

The diffusivity function incorporated into SETTLER had the following features: it was greatest at the feed point (diftop), dying away exponentially above the feed point (α_1) and below the feed point (α_2). For the lower layers of the tank, it was found that the diffusivity needed to be set at a small constant value (difbot), not only to avoid

generating hyperbolic partial differential equations in these layers but also to predict realistic sludge concentration depth profiles. During the process of calibrating the diffusivity function, it was determined that:

1. α_1 should be set at a constant value for all full scale settling tanks,

2. α_2 and diftop are dependent on tank geometry only,

3. difbot is dependent on the operating parameters as well as on tank geometry.

After these modifications had been incorporated, SETTLER (revision 5) was then tested against the five overloaded Rijen tests and reasonable results obtained for all the simulations.

Once a degree of confidence had been obtained in the ability of SETTLER (revision 5) to accurately simulate the measured results for the Rijen test cases, the next step was to extend the program to take into account both differing tank geometries and operating conditions. The overloaded settling tank test at the smaller Wijk bij Duurstede settling tank was used for calibration.

On the basis of the Wijk test, it was concluded that α_2 should be scaled on the basis of settling tank surface area and that diftop should be scaled on the basis of settling tank volume. The depth of the CSTR was scaled down to account for the smaller size of the Wijk settling tank. For these values of the diffusivity constants and the CSTR depth, reasonable simulation results were obtained for the test at Wijk.

The next step was to develop a function allowing the diffusivity constants to be calculated for different circular settling tanks. Equations for calculating α_2 on the basis of surface area and diftop on the basis of volume were developed. On the basis of the previous six simulations, an equation for calculating difbot as a function of feed flow rate, surface area, diftop and α_2 was developed. The test at Uden-Veghel was then

simulated to check the validity of the calculated diffusivity constants. Reasonable simulation results were obtained, and it was concluded that a satisfactory model for predicting the behaviour of secondary settling tanks under overloaded conditions had been developed.

Four underloaded test cases (2 at Oss, 1 at Rijen and 1 at Gieten) were then simulated to check that SETTLER (revision 5) correctly distinguished between safe and failed cases. In the process of conducting these simulations, it was found that a minimum value of difbot needed to be determined to ensure realistic simulations.

SETTLER (revision 5) was then used to investigate one of the known deficiencies of the flux theory. The flux theory has been found to overpredict the maximum permissable solids loading, thus overestimating the storage capacity of full scale settling tanks. SETTLER (revision 5) was used to simulate five theoretical full scale cases, each at a different percentage of the flux theory maximum solids loading. SETTLER predicted failure for the cases where the applied solids loading was greater than 80% of the predicted maximum solids loading, thus verifying earlier findings and confirming that the flux theory overpredicts the maximum solids loading.

Further simulations were carried out with SETTLER to examine the effect of changing the depth of the feed point. The program was found to be valid for all reasonable feed point depths.

A last simulation was performed to confirm that SETTLER is able to predict a third form of settling tank failure. This form of failure occurs when the required underflow concentration to preserve the mass balance exceeds realistically attainable values. Under these conditions, although the flux theory predicts underloaded conditions, the settling tank will fail due to compaction limitations. SETTLER was found to correctly predict this form of failure.

It was concluded that SETTLER was adequately able to predict both underloaded and overloaded conditions in full scale settling tanks. With the incorporation of diffusivity at all layers in the tank and a CSTR to model the thickening region, the program was an improvement on previous simulation programs based purely on the steady state flux theory. The inclusion of diffusivity in the program enables it to correctly predict the limitations on the maximum attainable underflow concentration and to overcome the tendency in the flux theory to overpredict the maximum solids loading. These aspects are not considered by the flux theory, although they have been recognised by and incorporated into the ATV and STORA design procedures.

It was further noted that, although SETTLER was considered to have successfully achieved the major objective of bringing practical and theoretical developments in settling tanks closer together, it is not appropriate in its present form for design and operation. Its value as a model lies primarily in its usefulness in assessing the applicability of the idealised flux theory to full scale tanks.

The recommendations of this investigation are that:

1. the relationships formulated in this thesis that link V_o and n to the sludge settleability measures SVI, $SSVI_{3.5}$ and DSVI be used with caution, as they are known to be applicable only under certain conditions. The relationship for $SSVI_{3.5}$ particularly, appears to be plant type specific, and should only be applied to plants of the extended aeration type from which the pooled data was collected.

2. if further work is carried out in collecting sludge settleability data, then other relevant parameters besides the concentration and SSP measurements must also be collected. These parameters include plant type, temperature and organism type, as well as other parameters that could possibly influence the sludge settleability measure,

REFERENCES

Abwasser Technik Verband, "Arbeitsbericht des ATV-fachausschiusses 2.5 absetzverfarhen. Die bemussung der nachlarbecken von belebungsanlangen", Korrespondenz Abwasser, 8, 20, 193 (1973)

Abwasser Technik Verband, "Erlaterungen und erganzungenzum arbeitsbericht des ATV-fachausschiusses 2.5 absetzverfarhen. Die demessung der nachlarbecken von belebungsanlangen", Korrespondenz Abwasser, 8, 23, 231, (1976)

Anderson H.M., "A dynamic simulation model for wastewater renovation systems", PhD thesis, Wayne State University, Detroit, Michigan, (1981)

STORA (Stichting Toegepast Onderzoek Reiniging Afvalwater), "Hydraulische en technologische aspecten van het nabezink-process", Rapport 1-Literatuur, Rapport 2-Ronde nabezinktanks (Praktijkonderzoek), Rapport 3-Rondenabezinktanks (Ontwerpgegevens en bedrijfservaring), (1981)

White M.J.D., "Settling of activated sludge", Technical Report TR11, Water Research Centre, England, (1975)

ACKNOWLEDGEMENTS

It would like to express my sincere thanks and appreciation to :

* my supervisor, Prof George Ekama, for his guidance and support throughout the project,

* my second supervisor, Prof Daya Reddy, and Prof GvR Marais for their availability, wisdom and advice,

* the Water Research Commission and the Foundation for Research and Development for providing financial support,

* Tim Casey, Craig Peters and all my colleagues in the Civil Engineering Department for their support and encouragement during the long hours,

* Cheryl Baker, who helped me to discover that I could be a person during the process.

I would like to express a special thanks to Max Ozinsky for his life-saving technical help and for his support and love.

DEDICATION

During the years that I have spent at UCT, I received an education that has hopefully equipped me to play a useful role in South Africa. I would like to take this opportunity to dedicate my skills to working for change and development in this country and to express the hope that I can contribute to building a society based on the principles of peace and justice.

LIST OF SYMBOLS

α, β, γ, δ	constants fitted to the settling velocity equation by least squares regression
α_1	die off rate of diffusivity above the feed point (layer^{-1})
α_2	die off rate of diffusivity below the feed point (layer^{-1})
β_i	true slope of the regression function in the population
β_m	true regression coefficient for the means
β_w	true pooled within groups regression coefficient
σ_E	standard deviation
υ_1, υ_2	degrees of freedom associated with S_1, S_2, S_3 and S_4
A	surface or cross sectional area (m^2)
b_i	estimated slope for the ith group
b_m	regression coefficient for the regression of the means
b_w	regression coefficient computed from the "pooled within" values
cas0	concentration at time t=0 (kgm^{-3})
cast	concentration at time t=t (kgm^{-3})
cdif	concentration difference between layers (i) and (i-1) (kgm^{-3})
conc (i)	concentration in layer (i) (kgm^{-3})
CSTR	completely mixed stirred tank reactor
d_{CSTR}	depth of the CSTR (m)
difbot	turbulent diffusivity in the lower layers of the tank (m^2h^{-1})
diftop	diffusivity at the feed point layer (m^2h^{-1})
DSVI	diluted sludge volume index (mlg^{-1})
dt	length of time interval (h)
dx	depth of each modelling layer (m)
E_i	turbulent diffusivity in layer i (m^2h^{-1})
F	F statistic for the theoretical F distribution

fdif	flux difference between layers (i) and (i-1) ($kgm^{-2}h^{-1}$)
flux (i)	flux in layer (i) ($kgm^{-2}h^{-1}$)
G_{ap}	applied flux ($kgm^{-2}h^{-1}$)
G_b	bulk flux ($kgm^{-2}h^{-1}$)
G_g	gravity flux ($kgm^{-2}h^{-1}$)
G_L	limiting flux ($kgm^{-2}h^{-1}$)
G_{per}	maximum permissable solids loading rate ($kgm^{-2}h^{-1}$)
G_s	solids flux ($kgm^{-2}h^{-1}$)
G_s	source or sink terms present as boundary conditions ($kgm^{-2}h^{-1}$)
G_t	total flux ($kgm^{-2}h^{-1}$)
G_{up}	flux moving upwards ($kgm^{-2}h^{-1}$)
i	layer number
jsw	shock direction
k	number of data groups
nfq	feed point layer (layer no.)
n_i	number of observations in the ith group
nsw	difference operator
q0	feed flow at time t=0 (m^3h^{-1})
qdown	volumetric underflow rate (m^3h^{-1})
Q_f	volumetric feed flow rate (m^3h^{-1})
Q_i	volumetric influent flow rate (m^3h^{-1})
Q_r	volumetric underflow rate (m^3h^{-1})
qt	feed flow at time t=t (m^3h^{-1})
r^2	multiple correlation coefficient
s	underflow recycle ratio (Q_r/Q_i)
S	shock velocity (mh^{-1})
S_1	pooled sum of squares of deviations from the regression
S_2	sum of squares of deviations among the k group regression coefficients

S_3	sum of squares of the deviations of the Y-means from the regression of Y-means on X-means
$SSVI_{3.5}$	stirred specific volume index at a standard concentration of $3.5gl^{-1}$ (mlg^{-1})
S_T	total sum of squares of the deviations
SV_{30}	30 minute settled volume (ml)
SVI	sludge volume index (mlg^{-1})
t	t statistic for the theoretical t distribution
u_o	overflow rate ($=Q_i/A$) (mh^{-1})
u_u	underflow rate ($=Q_r/A$) (mh^{-1})
V	volume of settling tank (m^3)
V_1	velocity below the feed point layer (mh^{-1})
V_2	velocity above the feed point layer (mh^{-1})
V_3	velocity at the feed point layer (mh^{-1})
V_b	particle velocity due to the bulk fluid motion (mh^{-1})
V_g	settling velocity of the particles due to gravitational acceleration (mh^{-1})
V_o, n	flux theory constants describing the settling characteristics of the sludge (mh^{-1} and m^3kg^{-1})
V_R	volume of the biological reactor (m^3)
V_s	settling velocity (mh^{-1})
X	sludge concentration ($kgMLSSm^{-3}$)
X_{40}	underflow concentration introduced into the CSTR at time t=0 (kgm^{-3})
X_{af}	limiting concentration above the feed point (kgm^{-3})
X_{dz}	dilute zone concentration (kgm^{-3})
X_{ef}	solids concentration lost with the effluent (kgm^{-3})
X_i	sludge concentration in layer (i) (kgm^{-3})
X_L	limiting concentration below the feed point (kgm^{-3})
X_o	solids concentration in the biological reactor (kgm^{-3})
X_r	underflow concentration (kgm^{-3})

X_{rl}	final concentration in the CSTR (kgm^{-3})
X_{rL}	limiting underflow concentration (kgm^{-3})
X_{ro}	initial concentration in the CSTR (kgm^{-3})
z	distance in the vertical direction (m)
ZSV	zone settling velocity (mh^{-1})

CHAPTER 1
INTRODUCTION

1.1 FUNCTIONS OF THE SECONDARY SETTLING TANK

The function of the secondary settling tank in the activated sludge system is twofold: firstly to separate the sludge produced in the activated sludge reactor from the treated wastewater (clarification), thus producing clear effluent as the overflow; and secondly to produce a concentrated sludge stream from the bottom (thickening) for recycling back to the activated sludge reactor. The performance of an activated sludge plant is directly dependent on both of these functions of the secondary settling tank. If the settling tank does not thicken the sludge sufficiently, then the concentration of the sludge recycled to the biological reactor may not be sufficient to maintain the required biological reactor sludge concentration. If the clarification function is not achieved, effluent quality standards may be compromised due to the solids that are lost with the effluent and discharged to receiving waters.

1.2 CONSEQUENCES OF SETTLING TANK FAILURE

In the activated sludge system, the secondary settling tank is a crucial component because failure results in a dramatic increase in effluent suspended solids. This gross loss of solids with the effluent can be so dramatic that the effluent solids concentration can exceed that of the influent wastewater, defeating the objectives of treating the wastewater in the first place.

The settling tank is also the "bottleneck" which limits the treatment capacity of the activated sludge plant. Any increase in load, either in the form of higher influent COD concentration or higher influent flows, results in higher solids concentrations and flow through the biological reactor and consequently also through the secondary settling tank. These higher solids concentrations and flows can usually be accommodated by

the biological reactor but not necessarily by the secondary settling tank. When the applied solids loading on the settling tank exceeds the limit defined by its surface area and by the sludge settleability, the settling tank fails and gross solids loss with the effluent occurs. Because sludge settleability varies, the treatment capacity of the secondary settling tank in terms of flow and load also varies, decreasing as sludge settleability deteriorates. Thus, the time that a plant reaches its treatment capacity will always be apparent first in the settling tank by gross solids loss at peak wet or dry weather flows. The situation is all the more serious because failure of a settling tank is a sudden occurrence. A settling tank may have produced a very low effluent suspended solids concentration for many years and one day, possibly due to a deterioration in sludge settleability or a progressive increase in flow and load on the treatment plant, the settling tank suddenly manifests gross solids loss in the effluent at the high flow period of the day. This is because, once the solids and hydraulic loading limits of a settling tank are exceeded, the settling tank will inevitably fail. The principal factors that affect the permissable solids and hydraulic loading of a settling tank are the feed concentration from the biological reactor and the sludge settleability.

1.3 EMPIRICAL DESIGN CRITERIA

Even though it has long been recognised by design engineers that the feed concentration and sludge settleability limit the permissable solids and hydraulic loading on settling tanks, these two parameters have not been incorporated into conventional empirical design criteria. These design criteria, which have been established from practice and experience, take the form of simple hydraulic and/or solids loading limits such as maximum permissable overflow rate or maximum permissable solids loading. However, should the reactor concentration and/or sludge settleability fall outside the range implicitly incorporated in these criteria, then the settling tank will fail. This empirical approach needed to be adopted because, at least in the English speaking world, there was no better method available.

scale secondary settling tank performance. It presents in a simple codified form the pertinent behavioral characteristics that need to be recognised for design of settling tanks such as feed solids concentration, sludge settleability, sludge storage capacity, settling tank depth, maximum underflow concentration and sludge storage concentration. At the time, the best the flux theory could achieve was an idealised model of settling tank behaviour from which a tank surface area could be determined. It did not address the issues of sludge storage capacity and concentration, settling tank depth and maximum underflow concentration. These deficiencies, exacerbated by the uncertainty in the accuracy of even the most well defined estimate of the surface area from the flux theory, resulted in the continued use of the conventional design criteria. In countries where the German ATV procedures were unknown, in particular the English speaking countries, the conventional hydraulic and/or solids loading criteria continued to be used for design. This was despite the fact that in these countries the most notable contributions to the flux theory had been made.

In the English speaking countries, attempts to overcome the obvious deficiencies of the hydraulic and/or solids loading design criteria resulted in numerous researchers developing sludge settleability relationships to obtain V_o and n, the flux theory constants, from SVI measurements. This was an attempt to bypass the tedious ZSV-X test necessary to obtain the V_o and n values. However, these attempts failed to address the major perceived deficiency of the flux theory, namely its inability to correctly predict the maximum permissable solids loading on a secondary settling tank.

In Europe, where the German ATV design procedure had a considerable influence, other countries like Holland began adopting the procedure. However, before doing so, researchers in Holland conducted an extensive full scale investigation into full scale settling tank behaviour, conducting 44 solids loading tests at 22 different plants.From the results of these tests, STORA (1981) verified the major elements of the ATV procedure and confirmed such factors as maximum underflow concentration and sludge storage concentration, both of which are dependent on the DSVI. The only aspect that was modified by STORA was the permissable overflow rate for poorly settling sludges

at high reactor feed concentrations. From their measurements and observations, STORA developed a design procedure for Holland based on the DSVI. The STORA procedure is essentially the same as the ATV procedure in all the important elements. Unfortunately, with their work being reported in Dutch it, like the German work on which the ATV procedure is based, is virtually unknown in the English speaking world.

In this light, the major objective of this work was to verify the flux theory and overcome some of its critical deficiencies, thereby promoting its use as both a design and simulation tool. This objective was approached by using the data measured by STORA at the Dutch plants to calibrate and verify a computer simulation model for dynamic behaviour of full scale secondary settling tanks. In order to achieve this, it would also be necessary to develop reliable relationships to link the STORA sludge settleability measure ($SSVI_{3.5}$) to the flux theory constants V_o and n. The objective of this was twofold: firstly to simulate the STORA results; and secondly to provide a link between existing design procedures and the flux theory so that these can be compared and integrated if possible.

The flux theory has already been incorporated into a number of computer models for simulating dynamic behaviour of secondary settling tanks. Over the decade 1971 to 1981, major advances took place in the development of flux theory based models with the emergence of a series of models that each significantly improved on its predecessors. This advancement in the sophistication of flux theory based models culminated with the model of Anderson (1981). Since 1991, a spate of models have been presented, but none of these significantly develop the modelling of secondary settling tanks beyond Anderson's model. This is mainly because these models have mostly been developed with the aim of incorporating them into combined activated sludge/secondary settling tank models. Because of this aim, the models have focused on parameters critical to the whole activated sludge process such as effluent quality and underflow concentration, and none have focused extensively on the processes occurring inside the settling tank itself.

In order to fulfil the major objective of this work, it was intended to use Anderson's model as a starting point. The model would then be modified and refined in the process of calibrating and verifying it with the data collected by STORA (1981).

Besides the aim of advancing progress in secondary settling tank modelling, the overall aim of this thesis was to set about verifying the flux theory for full scale settling tanks, thereby fashioning a link between the two distinct paths of work on secondary settling tanks and furthering the process of integration between them.

REFERENCES

Anderson H.M., "A dynamic simulation model for wastewater renovation systems", PhD thesis, Wayne State University, Detroit, Michigan, (1981)

STORA (Stichting Toegepast Onderzoek Reiniging Afvalwater), "Hydraulische en technologische aspecten van het nabezink-process", Rapport 1-Literatuur, Rapport 2-Ronde nabezinktanks (Praktijkonderzoek), Rapport 3-Rondenabezinktanks (Ontwerpgegevens en bedrijfservaring), (1981)

Abwasser Technik Verband, "Arbeitsbericht des ATV-fachausschiusses 2.5 absetzverfarhen. Die bemussung der nachlarbecken von belebungsanlangen", Korrespondenz Abwasser, 8, 20, 193 (1973)

Abwasser Technik Verband, "Erlaterungen und erganzungenzum arbeitsbericht des ATV-fachausschiusses 2.5 absetzverfarhen. Die demessung der nachlarbecken von belebungsanlangen", Korrespondenz Abwasser, 8, 23, 231, (1976)

CHAPTER 2
LITERATURE REVIEW
SECONDARY SETTLING TANK DESIGN, THEORY AND MODELS

2.1 INTRODUCTION

Over the past few decades, work on secondary settling tanks has progressed along two parallel but distinct paths. The one path has focused mainly on strategies for settling tank design and operation which have been based primarily on empirical criteria. The other path has focused on developing the flux theory and incorporating it into models for secondary settling tank simulation. Not much integration has taken place between the two paths, with the result that the theoretical developments have not been well integrated into the practical field of secondary settling tank design and operation. One of the main reasons for this lack of integration has been the tediousness of performing the necessary multiple batch zone settling velocity - concentration (ZSV-X) measurements required for determination of the sludge settleability measure in the flux theory. Simpler sludge settleability measures are preferred by engineers and operators in the field which has resulted in the development of a wealth of conventional design and operation experience and criteria based on these simpler measures. Consequently, work on the flux theory has fallen mainly into the realm of research.

In this chapter the basic developments in the two parallel paths are reviewed so that the principle objective of this thesis i.e. bringing the parallel paths closer together by creating areas of integration will come into sharper focus. Two area of integration are developed: firstly refinement of the relationships between the various sludge settleability measures; and secondly verification of the flux theory as a reliable model for the secondary settling tank simulation program. In this review, the conventional design criteria and procedures as well as the flux theory as design tools are briefly

reviewed followed by the developments in the application of the flux theory as a basis for secondary settling tank simulation models.

2.2 CONVENTIONAL DESIGN CRITERIA

The simplest sludge settleability measure is the sludge volume index (SVI) test. Although it has received much adverse criticism over the last three decades on a number of aspects, even today it is still the conventional measure in practice for determining sludge settleability. The principal weaknesses of the SVI are that:

1. It is not independent of sludge concentration,
2. it is not independent of cylinder diameter and depth,
3. it is affected by gentle stirring,
4. it has no observable relation to rheological properties of sludge and
5. it appears to have little relation to the zone settling velocity.

Because the SVI has been found inadequate as a settleability measure, it has not featured explicitly in design criteria for settling tanks but has rather entered in an indirect fashion. The design criteria, which generally take the form of hydraulic or sludge loading limits which should not be exceeded, usually provide adequate functioning of the settling tank over a range of sludge settling behaviour that can arise. These criteria, being empirically based, implicitly accept that the sludge settling characteristics will not deteriorate below a certain minimum quality, a quality unknown but in conformity with past experience of similar sludges. The settleability of the sludge is thus "hidden" in the empirical design criteria.

Examples of such criteria are those recommended by

1. the Institute for Water Pollution Control - for example (from the IWPC designers' handbook, 1973):

a. the overflow rate must not exceed $1m^3m^{-2}h^{-1}$ at Peak Wet Weather Flow (PWWF) - gives surface area,

b. the retention time must not be less than 1.5h at Peak Dry Weather Flow (PDWF) - gives depth,

c. Maximum discharge per unit length of effluent weir is $8.3m^3h^{-1}m^{-1}$ - gives maximum diameter.

2. the United States Environmental Protection Agency (1975) (see Table 2.1) and

Table 2.1 Secondary settling tank design criteria for activated sludge plants recommended by the US Environmental Protection Agency

TYPE OF PROCESS	HYDRAULIC LOADING		SOLIDS LOADING		SIDE WALL DEPTH
	AVERAGE	PEAK	AVERAGE	PEAK	
UNITS	mh^{-1}		$kgTSSm^{-2}h^{-1}$		m
Air activated sludge	0.68-1.36	1.70-2.04	4.08-6.08	10.17	3.66-4.57
Oxygen activated sludge	0.68-1.36	1.70-2.04	5.08-7.13	10.17	3.66-4.57
Extended aeration	0.34-0.68	1.36	4.08-6.08	10.17	3.66-4.57

3. the Great Lakes - Upper Mississippi River Board of State Sanitary Engineers (1978) (see Table 2.2)

Because of the inadequacies of the SVI and the fact that empirical design criteria do not recognise sludge settleability, considerable research effort has been expended since 1950 in developing improved sludge settleability measures and incorporating these into rational design procedures for settling tanks that do recognise sludge settleability. Over

Table 2.2 Secondary settling tank design criteria for activated sludge plants recommended by the Great Lakes Upper Mississippi River Board of State Sanitary Engineers

TYPE OF PROCESS	HYDRAULIC LOADING		SOLIDS LOADING		WEIR LOADING RATE	
	AVERAGE	PEAK	AVERAGE	PEAK	AVERAGE	PEAK
UNITS	mh^{-1}		$kgTSSm^{-2}h^{-1}$		m	
All activated sludge plants		2.04		10.17		7.75

the years three such measures have been developed and integrated into a settling tank theory or design procedure i.e.

1. the multiple batch zone settling velocity - concentration (ZSV-X) test and the flux theory,

2. the diluted SVI (DSVI) and the ATV (1973, 1976) and STORA (1981) design procedures and

3. the stirred specific volume index ($SSVI_{3.5}$) and its associated WRC (White (1975)) design procedure.

Each of these developments are discussed in some detail below.

2.3 THE FLUX THEORY

The flux theory is the most rational model available for describing the behaviour of secondary settling tanks. A comprehensive description of the flux theory can be found in Appendix A. Since its development by Coe and Clevenger in 1916, its value and usefulness as a conceptual model for secondary settling tanks has been well established by the contributions of, *inter alia*, Kynch (1952), Yoshioka *et al* (1957), Vesilind

(1968), Dick and co-workers, (1967, 1972) Alkema (1971), Keinath and co-workers, (1977, 1973, 1983), Pitman (1980, 1984) and Ekama *et al* (1984). Yoshioka *et al* (1957) developed a graphical approach which gave significant insight into the design and operation of secondary settling tanks with due consideration being taken of the settling characteristics of the sludge. However, the graphical procedure is tedious and can be restrictive. To facilitate analytical solutions, many mathematical expressions linking the settling velocity and sludge concentration have been proposed. The two that are most widely accepted and which give the closest correlation with measured data are those proposed by Vesilind (1968) in Equation (2.1)

$$V_s = V_o e^{-nX} \qquad (2.1)$$

and Dick and Young (1972) in Equation (2.2)

$$V_s = V_o X^{-n} \qquad (2.2)$$

where V_o and n are constants that describe the settleability of the sludge and are called the flux theory constants.

The first expression can be represented by a straight line on a log V_s vs natural X plot (i.e. a semi-log plot), the second by a straight line on a log V_s vs log X plot (i.e. a log-log plot). In reviewing these expressions, Smollen and Ekama (1984) concluded that Equation (2.1) is superior to Equation (2.2) because it gives over the entire concentration range

1. a theoretically consistent description of the observed gravity flux curve with defined turning and inflexion points,

2. a closer correlation with data measured on laboratory, pilot and full scale plants over a number of years ($r^2 > 0.95$) and

3. an internally consistent secondary settling tank model in which the various modes of settling tank failure are continuous and logically integrated.

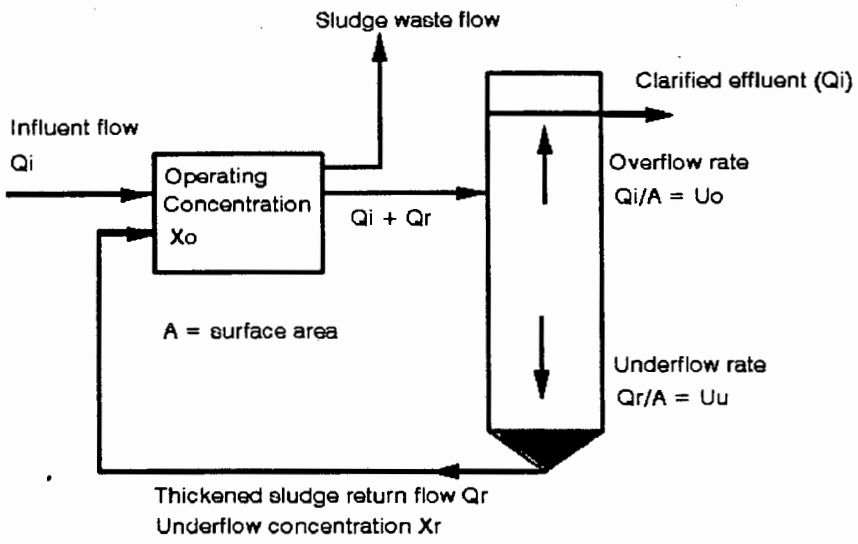

Figure 2.1 Schematic representation of the secondary settling tank in the activated sludge process

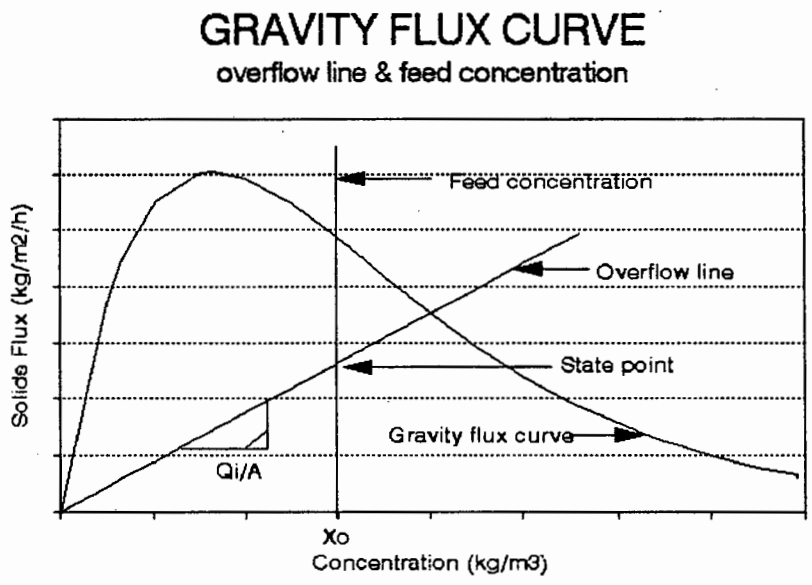

Figure 2.2 Gravity flux curve showing the overflow line and the state point

(flatter slope) than this one will cause settling tank failure. This is illustrated in Figure 2.3.

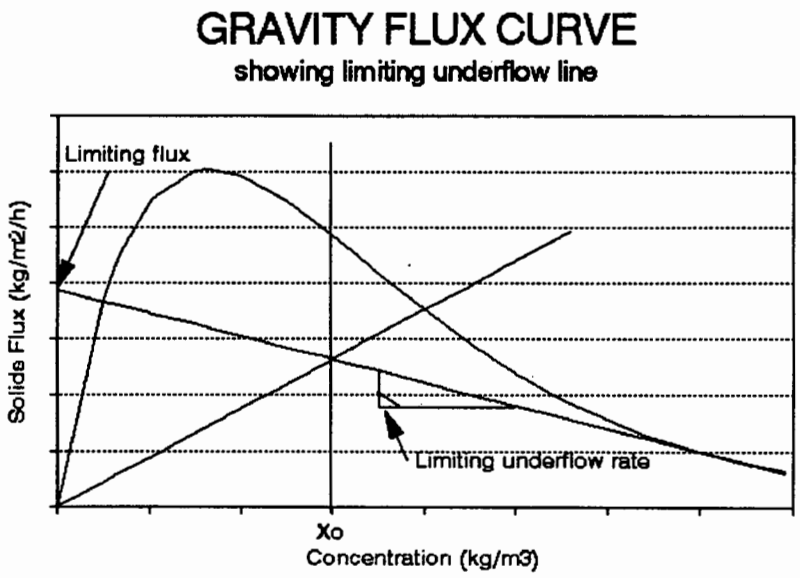

Figure 2.3 Gravity flux curve showing the limiting underflow rate for a chosen overflow rate and feed concentration

The limiting flux given on the vertical axis (Figure 2.3) is called the solids flux limit A criterion and it only applies whilst the underflow line is sufficiently flat to enable a tangent to be drawn to the gravity flux curve. If the underflow line is too steep to enable a tangent to be drawn to the gravity flux curve, then another criterion - solids flux limit B applies. For this criterion to be met, the intersection of the lines for the overflow rate and the feed concentration (the state point) must lie within the envelope of the gravity flux curve (see Figure 2.4) and its limit is defined when the state point lies on the gravity flux curve with the underflow line steeper than the slope of the gravity flux curve at the inflexion point. The underflow line can only make tangents to the gravity flux curve when it has a slope flatter than that of the inflexion point, which is solids flux limit A.

For design purposes this graphical construction is a tedious procedure, as repeated selections of underflow and overflow rates must be made in order to be able to determine the necessary surface area for safe operation.

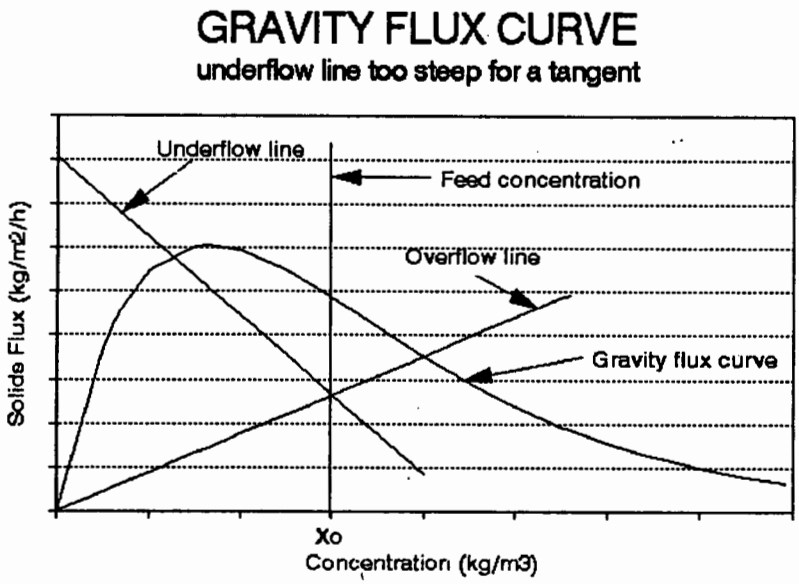

Figure 2.4 Gravity flux curve showing the underflow rate too steep to form a tangent - solids flux limit B

To eliminate the repetitive graphical procedure described above, the same principles i.e. solids flux limits A and B can be applied analytically to construct a design and operating chart for flux theory constants V_o and n and specified feed concentration X_o. By plotting overflow rate (Q_i/A) against recycle ratio (Q_r/Q_i) for a particular feed concentration (or a few feed concentrations), the design and operating chart illustrated in Figure 2.5 is obtained. For details, see Ekama *et al* (1984). On the figure, solids flux limit A, solids flux limit B and the underflow line tangent limit are indicated where the last mentioned represents the transition point from solids flux limit A to B. It is in this respect that the semilog model for the ZSV-X function is superior to the log-log model. With the latter the transition from solids limits A to B is not continuous across the underflow line tangent limit hyperbola in Figure 2.5.

With the aid of the design and operating chart, design of a secondary settling tank is greatly streamlined. For a specified reactor concentration, it is necessary only to choose an operating overflow rate/ recycle ratio pair such that it falls below the solid flux limit A or B criteria in order for safe settling tank operation to be ensured.

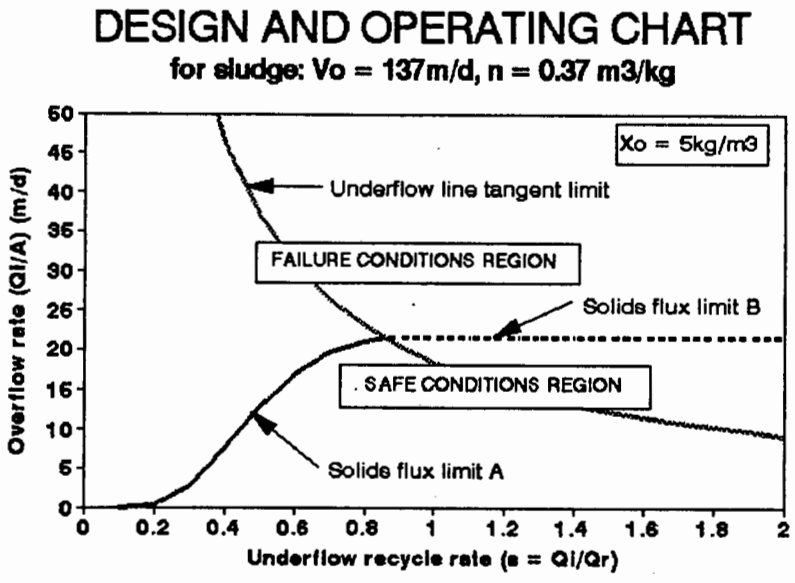

Figure 2.5 Design and operating chart showing failed and safe regions for a chosen reactor concentration

Despite the apparent usefulness of the flux theory, it has not been widely adopted for design and operation principally for three reasons:

1. It requires time consuming and tedious multiple batch stirred settling column tests (6 to 10) over a range of concentrations (X) from about 2 to 12gl^{-1} to obtain the zone settling velocity (ZSV) vs concentration (X) relationship. The stirred ZSV test is conducted in a gently stirred (1rpm) column of about 100mm diameter and 600mm deep. About 2 to 3 minutes after the column has been filled with sludge of a known concentration and stirring commenced, the solid liquid interface begins to subside and zone settling commences. During stirred zone settling, the subsidence rate of the interface is called the Zone Settling Velocity (ZSV) and is measured from the slope of the straight line portion of the interface height-time plot. Because the sludge concentration of the zone settling region remains constant during zone settling and is equal to the concentration with which the column was originally filled, the ZSV is associated with the original sludge concentration. By repeating the test at different concentrations a set of ZSV-X data can be assembled. Clearly, this is a tedious undertaking.

2. Owing to its tediousness, measurement of ZSV-X data is not common practice so that little data is available relating this measure to full scale settling tank operation.

3. Although conceptually a sound theory, the flux theory has not been definitively verified against full scale settling tank operation with the result that practising engineers and operators have not had much confidence in its predictive power for full scale tanks.

These difficulties with the flux theory, in particular the tedious ZSV-X measurement, prompted the development of the two other simpler settleability measures i.e. DSVI and $SSVI_{3.5}$ and their associated design procedures.

Because of the simplicity and popularity of the SVI, the two modifications of the SVI test that have been proposed are attempts to improve it as a sludge settleability parameter, in particular to eliminate its dependence on sludge concentration. The two modifications are: (i) dilution, which leads to the DSVI (Diluted Sludge Volume Index) and (ii) stirring, which leads to the $SSVI_{3.5}$ (Stirred Specific Volume Index). Neither test measures the ZSV-X relationship of the sludge required for the flux theory but both parameters feature in design procedures based directly on them.

There are three main design procedures that have been developed based on the DSVI and $SSVI_{3.5}$:

1. ATV (Abwasser Technische Vereiniging) (1973, 1976) design procedure using the DSVI,

2. STORA (Stichiting Toegepast Onderzoek Reiniging Afvalwater) (1981) design procedure using the DSVI,

3. the WRC (Water Research Centre) White (1975) approach using the $SSVI_{3.5}$.

2.3.1 THE DSVI AND THE STORA AND ATV DESIGN PROCEDURES

In investigating the SVI's dependence on sludge concentration, Stobbe (1964) showed that the test results are largely independent of concentration if in the 1l graduated cylinder the 30 min settled volume (SV_{30}) is less than 250ml. This is demonstrated in Figure 2.6 from Dick and Vesilind (1969), showing that when the SV_{30} is less than about $200ml l^{-1}$, the SVI remains approximately constant with concentration.

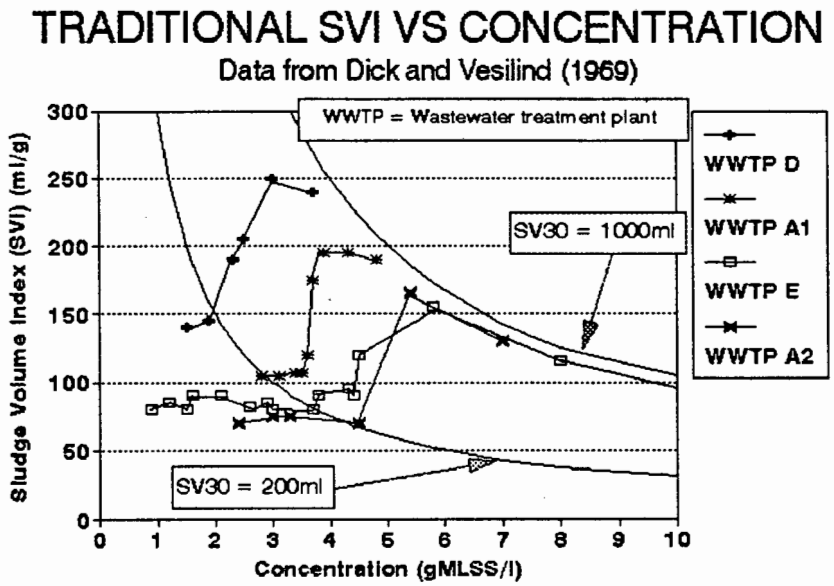

Figure 2.6 SVI vs concentration data taken from Dick and Vesilind (1969)

Stobbe's DSVI therefore is found in exactly the same way as the conventional SVI except that instead of a single test being done, 3 to 4 tests are done on several dilutions of sludge (1:1, 0.5:1, 0.25:1, etc) and the SVI of the first dilution that has an $SV_{30} < 200ml$ is the DSVI. Apart from largely eliminating the effect of concentration, Lee *et al* (1983) demonstrated a number of additional advantages of the DSVI test, the most significant being its consistent relationship to filamentous bulking and total extended filament length (see also Ekama and Marais (1984)).

Because the DSVI is relatively insensitive to sludge concentration, it is permissable to multiply sludge concentration by the DSVI and obtain a specific sludge volume - the

SV_{30} in ml^{-1} or lm^{-3}. This approach is adopted in both the ATV and STORA design procedures where the sludge concentration and DSVI are selected to be the reactor sludge concentration and its settleability respectively. This specific sludge volume, denoted VS_V in the two design procedures, is then empirically related to the permissable overflow rate (denoted in their symbols, q_A) found from experience to give safe designs.

Using their symbols:

$$VS_V = G_a * I_{SV} \tag{2.3}$$

where VS_V = specific sludge volume (ml^{-1})

G_a = biological reactor sludge concentration (gl^{-1})

I_{SV} = DSVI (mlg^{-1})

For ATV:

$$q_A = 2400(VS_V)^{-1.34}$$

$$\text{subject to} \tag{2.4}$$

$$q_A < 1.6mh^{-1}$$

For STORA:

$$q_A = \frac{1}{3} + \frac{200}{VS_V}$$

$$\text{subject to} \tag{2.5}$$

$$300 < q_A.VS_V < 400l/(m^2h^{-1})$$

$$\text{and } q_A < 2.0mh^{-1}$$

Important features of the ATV and STORA design procedures are:

1. The q_A-VS_V relationships hold equally for dry and wet weather flows with the peak wet weather flow usually being the governing condition.

2. They allow storage of sludge in the settling tank so that during wet weather flow the reactor concentration decreases causing a reduction in the specific sludge volume (VS_V) and therefore allowing an increased overflow rate (q_A). However, the reduction in concentration is limited to 30% and it may never fall below $2gl^{-1}$.

3. For the ATV procedure, the depth of the tank is calculated empirically depending on the DSVI of the sludge and the mass (or volume) of sludge to be stored during peak wet weather flow. For the STORA procedure the depth of the side wall and depth of the tank are fixed at 2 to 3m but the calculation of the area takes into account the mass of sludge that needs to be stored at peak wet weather flow.

4. The underflow recycle ratio is calculated on the basis of the maximum attainable underflow concentrations at dry and wet weather flow conditions. These depend on the DSVI of the sludge.

The ATV procedure is based on a large body of research and full scale plant experience obtained in the 1970's at the Technical University of Munich by such workers as Pflantz (1969), Merkel (1971, 1974) and Billmeier (1978) and has been adopted as the standard guideline for design of settling tanks in Germany. The STORA procedure is essentially a modification of the ATV procedure based on information obtained in a comprehensive full scale settling tank evaluation undertaken in Holland in the early 1980's. The STORA information is described in Chapter 3 and is extensively used in Chapter 8 for the verification of the dynamic simulation model based on the flux theory.

Reviewing the German and Dutch information on which the ATV and STORA procedures are based, one finds that the flux theory and all the developments associated with it are not considered; instead from astute observation and careful practice a reliable secondary settling tank design approach has been built up. Similarly,

the ATV and STORA design procedures and the information on which they are based (being written in German and Dutch) are virtually unknown in the English speaking world, where the attention seems to have been focused on the flux theory and empirical design and operation procedures flowing from this i.e. White (1975), Wilson (1983), Riddel *et al* ((1983), Koopman and Cadee (1983) and Daigger and Roper (1985). Therefore it seems that two traditions of secondary settling tank design and practice have evolved over the past 20 years with little interaction between them. An objective of this research in using the STORA information to verify a dynamic simulation model for secondary settling tank based on the flux theory is to promote interaction between the German/Dutch ATV/STORA practice and the English flux theory based practice.

Of the design procedures flowing from the flux theory, only the procedure developed by White, known as the Water Research Centre Procedure, is briefly discussed because with it the improved sludge settleability measure $SSVI_{3.5}$ was developed to obviate the tedious ZSV-X tests. The other procedures either used the ZSV directly (See Wilson (1983) and Riddel *et al* (1983)) or developed relationships linking the flux theory constants V_o and n to the SVI (Daigger and Roper(1985)) or DSVI (Koopman and Cadee (1983)). These relationships are reviewed in greater detail in Chapter 4.

Extensive research at full scale plants has demonstrated that the ATV and STORA procedures predict permissable overflow rates with reasonable accuracy from DSVI measurements.

2.3.2 THE WATER RESEARCH CENTRE DESIGN PROCEDURE USING THE STIRRED SPECIFIC VOLUME INDEX AND BASED ON THE FLUX THEORY

White (1975) modified the SVI by introducing gentle stirring during settling. He found that this improved flocculation and reduced short circuiting and bridge formation effects, thereby creating conditions more in keeping with those in the settling tank.

More importantly, gentle stirring induces a linear relationship between the 30 min settled volume (SV_{30}) and sludge concentration thereby to a large extent eliminating the effect of concentration. He called this test the stirred specific volume index ($SSVI_{3.5}$) which is calculated in an identical fashion as the SVI (i.e. SV_{30}/X) where the SV_{30} is the 30 minute settled volume with gentle (1-2rpm) stirring in a 100mm diameter, 600mm tall (4.6l) column known as a settleometer. For most sludges that White investigated, the $SSVI_{3.5}$ was independent of the initial sludge concentration. However, for some sludges (the very poorly settling ones) this was not the case. To accommodate this difficulty he proposed a standard concentration of $3.5gl^{-1}$ for reporting the SSVI data, denoting it the $SSVI_{3.5}$.

White developed the Water Research Centre theory by measuring the $SSVI_{3.5}$ and the flux theory constants V_o and n at a number of full scale plants in England. With the aid of the flux theory, he then calculated the maximum permissable solids loading (or limiting flux) for different underflow rates. From the calculated results, he developed an empirical function relating the calculated maximum permissable solid loading rate (G_L) to the underflow rate (Q_r/A) and sludge settleability in terms of $SSVI_{3.5}$ i.e.

$$G_L = 8.85 \left[\frac{100}{SSVI_{3.5}}\right]^{0.77} \left[\frac{Q_r}{A}\right]^{0.68} \quad (kgm^{-2}h^{-1}) \qquad (2.6)$$

In verifying Equation (2.6), White found that the calculated maximum solids loading correlated to within $\pm 20\%$ with that observed in a number of full scale settling tanks. A detailed comment on and verification of the WRC procedure is given by Ekama and Marais (1986). Important features of the flux theory and related design procedures are:

1. Only a surface area for the settling tank can be calculated.

2. No guidance for the depth of the tank is given - depths are usually arrived at from practical experience (see Parker (1983) and Stukenberg *et al* (1983)).

3. Reduction in reactor concentration and sludge storage during peak dry and wet weather conditions are not implicitly taken into account. These features can be incorporated into the design approach but are purely dependent on the ingenuity and experience of the design engineer. No guidance implicit in the procedures is given.

4. No limits for the maximum attainable underflow concentration are specified so there is no guidance given regarding the design of the underflow recycle ratio for different conditions.

5. To date relatively little information is available demonstrating the reliability and dependability of the flux theory for full scale settling tank design with the result that there is not much confidence in the theory as a design tool.

From the above it is clear that, compared to the ATV and STORA procedures, the flux theory and its associated design procedures have not addressed real design needs by giving no guidance for the selection of the tank depth, sludge storage capacity and recycle ratio. Clearly, while the flux theory is the most rational model for understanding secondary settling tank behaviour, it is inadequate for design compared to the DSVI based ATV and STORA procedures. Anyone aware of the additional features of these two design procedures would no doubt prefer to use them, but then would need to use the DSVI for the sludge settleability measure.

2.3.3 THE FLUX THEORY AND ITS RELATED PROCEDURES AS A DESIGN TOOL

From the above it can be seen that design, operation and practical application is quite remote from the flux theory, despite this theory being the most rational model for secondary settling tank behaviour. As mentioned earlier, various attempts have been made to bring the flux theory into common usage either by presenting relationships from which the V_o and n values could be estimated from the SVI, $SSVI_{3.5}$ or DSVI or

by presenting simplified procedures for using the flux theory itself such as the WRC procedure developed by White (1975). In the former group are Daigger and Roper (1985), Pitman (1984), Koopman and Cadee (1983) and Ekama and Marais (1986) who developed empirical relationships from which the V_o and n values could be calculated from the three different settleability tests SVI, $SSVI_{3.5}$ and DSVI. Ekama and Marais (1986) showed that for the DSVI and $SSVI_{3.5}$ reasonable estimates of the V_o and n values could be obtained from their own and some published data sets, and that there was a reasonably good correspondence between the estimates from the same DSVI or $SSVI_{3.5}$ from different data sets. However, this was not the case for the SVI. Although the Daigger and Roper (1985) and Pitman (1984) SVI data yield very similar relationships for V_o/n, the actual V_o and n values were significantly different for the same SVI. This, and the whole aspect of developing relationships between SVI, $SSVI_{3.5}$ and DSVI and the V_o and n values is considered in detail in Chapter 4. With the relationships between V_o and n known, these researchers present procedures and diagrams from which to calculate the maximum solids loading capacity of the settling tank for a known SVI, $SSVI_{3.5}$ or DSVI in a similar manner to that of the WRC procedure.

Although all these procedures certainly simplify the use of the flux theory for design, they do not address the issue of the lack of confidence in the reliability of the flux theory for accurately estimating the maximum solids loading capacity of the settling tank. Although it can be construed that to a limited extent White indirectly verified the flux theory when verifying the WRC procedure, his finding that it is accurate only to within $\pm 20\%$ constitutes a very large margin of error.

Ekama and Marais (1986) undertook a verification of the flux theory for design of full scale settling tanks with the aid of the extensive settling tank evaluation undertaken by STORA (Stofkoper and Trentelman (1982)). As mentioned earlier, this information is described in detail in Chapter 3. Because the ZSV-X data measured by STORA could not be used (see Chapter 3), Ekama and Marais calculated the V_o and n values from the measured DSVI and $SSVI_{3.5}$ data. With the V_o and n values, the maximum solids

loading was calculated from the flux theory and compared with the measured solids loading in 44 full scale settling tank tests taking note whether or not the test ended in solids overload (failure) or not (safe). This is illustrated in Figure 2.7 in which the data points for the inconclusive cases have been excluded.

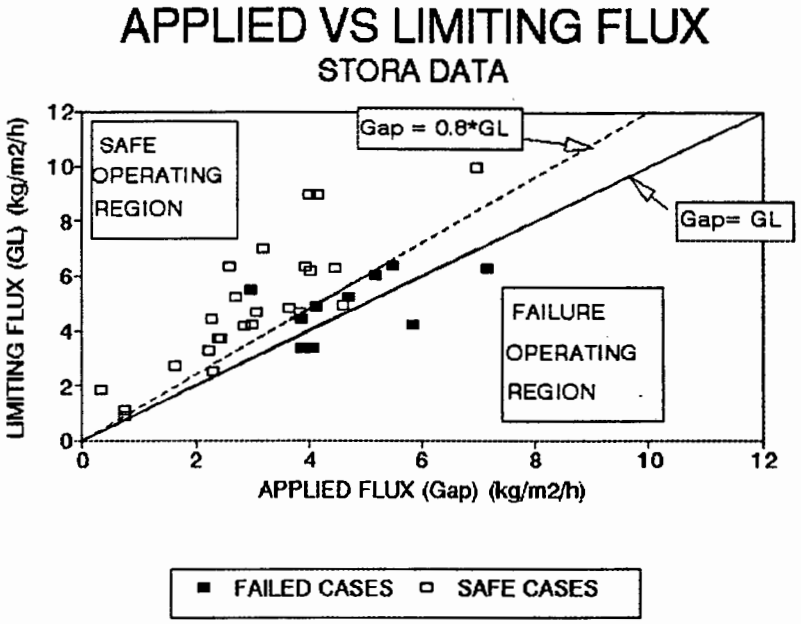

Figure 2.7 Applied vs limiting flux for the STORA data as presented by Ekama and Marais (1986)

For perfect prediction by the flux theory, all the overloaded cases should fall below the diagonal, and all the underloaded cases above. This was found not to be the case. Six overloaded cases fell incorrectly above the diagonal, but no underloaded cases fell incorrectly below the diagonal. This indicated that the flux theory tended to overpredict the limiting flux. If the limiting flux was reduced to 80% (as indicated by the line (G_{ap} = 0.8*G_L) in Figure 2.7), all except one of the overloaded cases were correctly positioned indicating that the flux theory tends to overestimate the maximum solids loading on the settling tank and that the permissable solids loading is about 80% of that predicted.

This considerably narrowed the margin of error of ±20% and gives a clear indication of the reliability of the flux theory for use in design.

Other interesting information presented by Ekama and Marais (1986) is that

1. Pitman's (1984) and White's (1975) V_o and n relationships in terms of $SSVI_{3.5}$ were virtually identical, rendering their procedures essentially the same,

2. the IWPC hydraulic criterion of $1mh^{-1}$ maximum overflow rate would provide safe settling tank designs for settleabilities better than a DSVI of $150mlg^{-1}$ or $SSVI_{3.5}$ of $100mlg^{-1}$.

The latter point in a sense indicates the wisdom of the previous generation of sanitary engineers because DSVI's greater than $150mlg^{-1}$ are often regarded as bulking sludges (Jenkins *et al* (1984)). The sludge settleability implicit in the EPA and GLUMRB design criteria (Tables 2.1 and 2.2) also can be estimated from the diagrams presented by Ekama and Marais (1986).

2.3.4 INTERIM CONCLUSION

From the above review, it is apparent that as a design tool the flux theory and its related design procedures are inadequate compared to the DSVI based ATV and STORA procedures. However, significant steps towards bringing the flux theory into popular use have been made. Nevertheless, the following three issues still need to be addressed:

1. the difficulty of obtaining the flux theory constants V_o and n either by direct measurement or by calculation; in the former case the measurements are tedious and time consuming and in the latter, the relationships linking V_o and n to SVI, $SSVI_{3.5}$ or DSVI are not precise or consistent between data sets,

2. no guidance is given regarding settling tank depth, sludge storage capacity or recycle rates,

3. inadequate verification of the flux theory as a design tool for calculation of the maximum solids loading has lead to a lack of confidence in the theory.

Despite these problems, and because the flux theory remains the most rational and fundamental model for describing secondary settling tank behaviour, the flux theory has been incorporated into a number of computer models for simulating dynamic behaviour of settling tanks. Before drawing final conclusions, the application of the flux theory and other theories to dynamic modelling of secondary settling tank behaviour is first reviewed.

2.4 REVIEW OF EXISTING SIMULATION MODELS FOR SECONDARY SETTLING TANKS

Over the last twenty years a number of models have emerged which propose to simulate the processes occurring in a secondary settling tank. Although each of the individual models have different objectives, they can be divided broadly into two categories i.e. (a) layer based sedimentation models and (b) hydraulic models.

a. Layer based sedimentation models

These models for secondary settling tanks are all based on the flux theory and have mostly been developed with the aim of being incorporated into integrated activated sludge/secondary settling tank models. With the settling tank model incorporated, realistic return sludge mass flows and sludge hold up times were sought to be obtained for more realistic activated sludge simulation models. Also, because the settling tank inevitably limits the activated sludge treatment capacity, incorporation of a settling tank model would also give a more realistic activated sludge system model with which the system treatment capacity could be estimated. Because of these intended applications, the focus of the settling tank models has been on the sedimentation process of the sludge in the settling tank under various operating conditions. An important consideration has been the

ability of the models to accurately predict the principal settling tank performance parameters i.e. effluent solids concentrations (clarification function) and underflow concentrations (thickening function). Existing models propose numerous ways of dealing with these functions with varying degrees of effectiveness.

b. Hydraulic models

Hydraulic models have mainly been developed with the aim of being able to assess the effect of the settling tank geometry on the hydraulic performance of the tank. The focus has been on determining the hydraulic velocity distribution profiles in the tank in order to minimise the effects of density currents and to optimise the inflow construction, underflow geometry and overflow weir placement, for example. These models are mostly not intended to be used in conjunction with an activated sludge process model.

2.4.1 LAYER BASED SEDIMENTATION MODELS

The layer based sedimentation models are all based on the flux theory, which is described in detail in Appendix A. The major concept of the flux theory is that of the layer of limiting flux and its associated limiting concentration, which determines the maximum solids transport capacity of a secondary settling tank. The limiting solids flux can be visualised as the "bottleneck" in the settling tank, constraining the maximum solids flux that can be processed by the tank. If the load on the settling tank is less than the limiting flux, then the settling tank can safely process all the influent solids, and failure will not occur. If the load on the settling tank is greater than the limiting flux, then solids in the settling tank will build up at the limiting concentration and eventually the excess solids will be lost out of the top of the tank with the effluent flow i.e. failure will occur. The limiting flux governs the behaviour of the tank in that other effects such as effluent solids and underflow concentrations are consequences of

it. All the sedimentation models make use of this concept in order to simulate the processes occurring in the settling tank.

The flux theory on its own specifies only idealized concentration profiles in the settling tank at steady state (See Appendix A). It is only when the flux theory equations are incorporated into a mass balance, or continuity equation, that the unsteady state concentration profiles can be determined. The number of continuity equations that need to be solved is determined by the number of layers into which the settling tank is divided. The usefulness and accuracy of a model depends on the number of layers considered as well as the nature of the mathematical algorithm which solves the continuity equation(s). Generally, the more layers and the more comprehensive the algorithm, the more refined the model and the more realistic the simulation results. The models developed by Alkema (1971), Tracy and Keinath (1973), Attir *et al* (1977) and finally Anderson (1981) are all based on the flux theory, and represent progressive refinements in the development of a flux based dynamic model for secondary settling tanks. The contribution of each model is described in more detail below.

Alkema (1971)

Alkema developed a two layer model based on the flux theory which calculates the response of the settling tank to a step change in input parameters such as influent flow rate, underflow rate and feed concentration. The model uses the flux theory equations to determine whether the step change causes the tank to be underloaded or overloaded and then calculates the final idealised steady state concentration profile. The "transient" between the two steady states (initial conditions and final conditions) is simulated by identifying a series of critical "events" and estimating the time after the step change at which each of these events occur. For the overloaded case, the critical events include the time at which:

a. the zone of limiting concentration (X_L) reaches the feed point,

b. solids first appear in the effluent,

c. the underflow concentration (X_r) attains the limiting underflow concentration (X_{rL}).

The algorithm traces these events in a stepped manner rather then simultaneously. Taking a step increase in feed concentration leading to overloaded conditions as an example, first the increased solids need to reach the bottom of the tank while the underflow concentration remains constant. Then the zone of limiting concentration is formed and moves upwards in the tank until it reaches the feed point whilst the underflow concentration increases in response to the increased flux. Then the underflow concentration increases to its limiting value while the sludge layer builds up above the feed point. When the sludge layer reaches the top, loss of solids with the effluent commences. Calculation of the time at which various events take place is done with a mass balance incorporating the flux theory equations. Because the flux theory gives the solids transport rate at different concentrations, the idealised velocity of movement of the different concentration regions in the settling tank can be calculated. From these velocities, the time of each of the critical events in the tank is determined.

The model developed by Alkema is a very simple layer based model which divides the settling tank into only two layers (one above and one below the feed point). Consequently, it is not able to make any predictions about the variation of concentration with depth in the settling tank. Furthermore, it is not a dynamic model, as it considers only the stepwise change between two steady state conditions and makes no predictions about the transient states between them, except for identifying the "critical events" mentioned above. The model is further limited because of the "sequential events" approach of the algorithm. In practice, the processes in a settling tank occur simultaneously with the result that the sequential events approach, besides being unrealistic, also leads to incorrect solutions.

Tracy and Keinath (1973)

Tracy and Keinath developed a model based on the same principles as those of Alkema, but improved the algorithm to allow moment by moment by dynamic simulation. It is a more sophisticated layer based model than Alkema's, as the settling tank is sliced into three fixed depth horizontal layers representative of the different regions in the settling tank. These are a thickening region and two zone settling regions; one below and one above the feed point. The settling region below the feed point is further divided into 1 to 4 layers depending on the depth of the limiting concentration layer at any point in time. The algorithm identifies whether the tank is underloaded, overloaded or critically loaded and selects an appropriate subroutine. The continuity equations between the layers are set up with the aid of sludge mass balance and flux equations around each layer and, similarly to Alkema's model, the velocity of the movement of the different concentration regions is calculated from these equations. The concentration in each layer is determined sequentially, starting from the top and working down to the bottom of the tank.

Tracy and Keinath's model is a significant improvement on the model developed by Alkema in that it is a dynamic simulation model able to deal with, amongst others, the transient conditions between two steady states (and not just the time of critical events). However, the model is not able to predict a complete sludge concentration depth profile in the settling tank because it specifies only three different regions of constant concentration. Furthermore, the sequential logic of the algorithm is deficient in that if the input conditions are changed such that the step change moves simultaneously from the top down and the bottom up (e.g. when feed and underflow rates are changed simultaneously), the sequential layer approach fails to correctly monitor the concentration changes during the progress of the transient.

Attir, Denn and Petty (1977)

Attir *et al* criticized the two previous models stating that under certain conditions these models violate certain entropy restrictions known as Lax's (1957) generalised entropy condition. In very general terms, this condition requires that an increase in flux is associated with an increase in concentration i.e. the flux curve must be strictly convex for all concentrations encountered. Attir *et al* maintained the same clarifier layer subdivision as Tracy and Keinath but they improved the numerical algorithms taking due consideration of entropy restrictions. This was achieved by checking at every time step and layer boundary whether or not the entropy condition has been violated between any two layers. If it has been violated, then a series of discrete layers is inserted between the two offending layers. The unallowed concentration discontinuity (or shock) is then "spread out" over the inserted layers such that the convexity of the flux curve is reinstated and the entropy restriction no longer violated. Attir *et al* then carried out simulations to show that whereas under some conditions the earlier algorithms which neglected the entropy condition predicted a safe (no sludge overflow) condition, the improved algorithm with entropy restrictions predicted a failed (sludge overflow) condition in conformity with experimental observation.

Anderson (1981)

Anderson (see also Anderson and Edwards (1980), (1981)) developed a secondary settling tank model which was part of a comprehensive simulation model of the entire wastewater renovation system for metropolitan Detroit. Because of the settling tank's important role in limiting effluent suspended solids, Anderson concluded that in order to simulate the wastewater treatment plant effluent quality accurately a good secondary settling tank simulation model was required. He criticized previous models by Tracy and Keinath (1973) and Attir *et al* (1977) on the basis that they only accounted for convective transport in the

secondary settling tank and ignored hydraulic effects, turbulence and density currents which are known to influence settling tank performance to a greater or lesser extent. He therefore incorporated a turbulent diffusion term into the flux equation to account for dispersive and turbulent effects. The inclusion of a turbulent diffusion term also has the advantage of ensuring that no entropy rule violations take place. Anderson also refined the calculation algorithm by incorporating switching functions and dividing the settling tank into 40 layers. The switching functions reduce the spurious oscillations that develop when solving hyperbolic (no turbulent diffusion)/ parabolic (with turbulent diffusion) partial differential equations by finite difference techniques. Also, the significantly larger number of layers in Anderson's model compared to previous models enabled well defined sludge concentration depth profiles to be determined. Anderson solved the continuity equations for each layer simultaneously which eliminated the problems with the sequential logic of earlier models and allowed concentration shocks to move upwards and downwards simultaneously. Anderson's model is a significant improvement over previous ones and so far represents the most refined application of the flux theory to dynamic modelling of secondary settling tanks. Anderson's model is reviewed more extensively in Chapter 5.

Comment on recently developed settling tank models

The developments towards the Anderson model took place over the decade 1971 to 1981 and since that time no major development has taken place in the layer based flux theory sedimentation models approach. A number of models have been presented since 1991, such as those of Hartel and Popel (1992), Dupont and Henze (1992), Grau (1992), Takacs *et al* (1991) and Otterpohl and Freund (1992). It is interesting to note that all of these models have appeared in the last two years, after research in this thesis had commenced. It is likely that the appearance of the activated sludge simulation models, such as those of the IAWQ (Henze *et al* (1987)), University of Cape Town (Dold *et al* (1991)) and Gujer

(1990) prompted this spate of secondary settling tank models. With the kinetics and modelling of the activated sludge biological reactor very well advanced it became obvious that the most serious deficiency in modelling the activated sludge system was modelling of the secondary settling tank. In this respect each of the secondary settling tank models that appeared over the past two years do not develop the modelling of secondary settling tanks significantly beyond that of Anderson. Indeed, some are not as advanced as Anderson's and appear to have been developed to obtain an improved activated sludge-settling tank system model rather than an activated sludge biological reactor model only. Consequently, these settling tank models do not focus much on the settling behaviour in the settling tank but rather on the materials that come out of the settling tank. As a consequence, many models incorporate features which allow estimation of the effluent suspended solids based on, for example, flocculation behaviour of the activated sludge. In contrast, the secondary settling tank models developed during the 1970's focused on the settling behaviour inside the settling tank, the materials flowing out of the tank being a consequence of the settling behaviour. Despite the different emphasis, the recently presented models are briefly reviewed for interest.

Hartel and Popel (1992)

Hartel and Popel developed a layer based sedimentation model which was eventually integrated into a dynamic activated sludge biochemical reaction model. The secondary settling tank part of the model describes the settling of activated sludge in the dilute zone according to the flux theory. They incorporated an Ω-correction function to adjust the settling properties of the sludge in the hindered settling and thickening regions. Hartel and Popel assumed that above the feed point no flocculation took place, and that the settling velocity of the flocs could be described by the maximum initial velocity of hindered settling. Their model was only partly calibrated due to insufficient data from full scale settling tanks.

In addition, it is only valid for low surface loading rates ($< 1 mh^{-1}$) and does not consider turbulent and dispersive effects.

Dupont and Henze (1992)

Dupont and Henze developed a dynamic model of the activated sludge plant including the secondary settling tank which was intended to be a first attempt at modelling the two processes as a combined unit. They developed a layer based sedimentation model based on the flux theory but included an additional empirical function to take into account non-settleable solids in the effluent. Turbulent and dispersive effects were not considered. Because of a lack of comprehensive data, the model could not be fully verified. In addition, the model is specific to the plant for which it was developed and must be recalibrated if it is to be applied to another plant.

Grau (1992)

Grau developed a layer based sedimentation model which included settling, horizontal and vertical mixing and enmeshment of fine particles in the sludge blanket. Grau criticized models based on the flux theory as being deficient in predicting effluent solids concentrations and sludge blanket height as well as idealizing sludge withdrawal and ignoring the potential and kinetic energy introduced into the settling tank with the feed flow. Grau's model, however, does use the flux theory to formulate a set of differential equations for a layer based model. The differential equations were modified to incorporate mixing and enmeshment processes and then solved simultaneously. Dispersive and turbulent effects were not considered. The model applies only to a steady state condition and requires extensive calibration in order to ascertain the constants for settling, mixing and entrainment. In addition, the assumption regarding the nature of the feed flow to the settling tank (equal distribution into all layers below the influent

well edge) is a situation which is specific to certain designs of secondary settling tank. It is more common to have the feed flow enter the tank at a specific depth.

Takacs, Patry and Nolasco (1991)

Takacs *et al* proposed a model which was intended to provide a unified framework for the simulation of both the clarification and thickening functions of a secondary settling tank. Their layer based model employed the flux theory and was eventually coupled to an activated sludge process model to give a complete representation of the plant. They proposed a modification to the Vesilind (1968) zone settling velocity - concentration equation to model the settling process in dilute regions in an attempt to more accurately predict the suspended solids concentration in the effluent. Turbulent and dispersive effects were not considered. Calibration of the parameters for the secondary clarifier is required in order to accurately simulate the behaviour of a full scale tank, apparently a time consuming and tedious task. Due to lack of data, no full scale tank verification was carried out on the model for overloaded conditions. However, the model appears to perform satisfactorily for underloaded conditions.

Otterpohl and Freund (1992)

Otterpohl and Freund maintained that only layer models are able to represent secondary settling tanks simply enough such that they can be incorporated into complete activated sludge process simulations. Even if hydraulic considerations were to be included, these would overcomplicate the model and render it less useful for the purpose of simulating entire activated sludge processes. Layer based models, they maintained, generally give good results, rendering it unnecessary to simulate the hydraulic conditions in detail (see below). They developed a layer based sedimentation model although they criticized previous layer models on the basis that they are not able to accurately predict effluent solids concentrations during wet and dry weather flow. Their solution to this

problem was to model micro and macro flocs separately. They also used the Ω-correction function for thickening developed by Hartel and Popel (1992) but did not consider turbulent and dispersive effects. The model was verified for wet and dry weather flows by comparison with full scale plant data. Although there was good correspondence between measured and predicted results for the dry weather flow simulations, the effluent solids concentrations were consistently underpredicted for the wet weather flow simulations.

2.4.2 HYDRAULIC MODELS

Most hydraulic models focus on qualitative assessment of the effect of tank geometry on the hydraulic velocity profile in secondary settling tanks, this being the major factor influencing behaviour of materials in the tank. They generally consider the sedimentation process to be of secondary importance. At present, it appears that no models exist that consider both hydraulic and sedimentation effects to be of equivalent importance. Indeed, as stated by Otterpohl and Freund (1992), the objectives of these two types of models are usually quite different, and it may not even be desirable to develop integrated (and complex) models which simulate both hydraulic and sedimentation phenomena. In the light of this, an extensive review of existing hydraulic models is not within the scope of this thesis. However, in the interests of completeness, a brief review of three existing hydraulic models is presented below.

A deficiency in all presently existing hydraulic models is the lack of information as to the nature of the eddy viscosity field (see below for more explanation of this term). Because the eddy viscosity field is a crucial parameter in so far as turbulence and velocity flow fields are concerned, this lack of information represents a significant deficiency in these models.

Krebbs (1991)

Krebbs analysed the flow field in a rectangular secondary settling tank and presented an hydraulic model which simulates the density currents in the tank. The settling tank was modelled two dimensionally, the velocity and volume fraction fields being calculated by the program PHOENICS (Rosten and Spalding (1987)). A constant turbulent viscosity term approximates the turbulent flow. The intention of the simulations was to show qualitatively the effects of different geometric or hydraulic conditions on the flow field in the tank. Eventually the model was used as a tool in optimising the inlet construction. It was also used to investigate the effect on flow conditions of introducing other physical measures such as angle bars and a dividing wall. The drawbacks of this model are twofold. Firstly, it has been developed for a rectangular secondary settling tank and, because the results are geometry specific, it is not applicable to circular tanks. Secondly, the use of a constant turbulent viscosity term to approximate turbulent flow is not empirically justified (see below).

Imam, Mccorquodale and Bewtra (1983)

Imam, McCorquodale and Bewtra presented an hydraulic model to simulate the settling process in rectangular settling tanks. Their model establishes the velocity field in the tank by finite difference solution of the Reynolds equations. These equations are a time averaged form of the Navier-Stokes equations (equations of motion with constant density and viscosity). The problem with the solution of the Reynolds equations is that they require a value for the term representing the (dissipating) influence of turbulent fluctuations on the flow field. This term (known as "turbulence stresses") can be found if the eddy viscosity is known. Imam, McCorquodale and Bewtra used a constant value for eddy viscosity in their hydraulic model.

Mccorquodale, Yuen, Vitasovic and Dittmar (1991)

McCorquodale *et al* (1991) applied a two dimensional transport model to sedimentation tank flow for circular tanks using an empirically derived eddy viscosity field. The numerical model was used to evaluate the influence of underflow geometry on sedimentation tank performance. This approach has been criticised by its authors on the basis of empirical limitations. If turbulent transport is a critical feature determining the flow field, then an empirically derived eddy viscosity field is not adequate. It also cannot be really predictive for tanks of differing geometry. Samstag *et al* (1992) in their review paper criticized the method of assuming a constant value for eddy viscosity on the basis that it is empirically unjustified. A constant value is only applicable for applications where the overall effect of turbulence is small (such as flows in coastal embayments and estuaries).

2.5 CONCLUSIONS

From the above, it is clear that, if the intention is to develop a layer based sedimentation model which focuses on the processes within the settling tank itself, then Anderson's model, being the most advanced and refined application of the flux theory to a model, would be the best place to start.

REFERENCES

Abwasser Technik Verband, "Arbeitsbericht des ATV-fachausschiusses 2.5 absetzverfarhen. Die bemussung der nachlarbecken von belebungsanlangen", Korrespondenz Abwasser, 8, 20, 193 (1973)

Abwasser Technik Verband, "Erlaterungen und erganzungenzum arbeitsbericht des ATV-fachausschiusses 2.5 absetzverfarhen. Die demessung der nachlarbecken von belebungsanlangen", Korrespondenz Abwasser, 8, 23, 231, (1976)

Alkema. K.L., "The effect of settler dynamics on the activated sludge process", MSc thesis, Dept of Chemical Engineering, Univ. of Colorado, (1971)

Anderson H.M. and R.V. Edwards, "Combined sewer overflow modelling: STPSIM2, A dynamic model of the wastewater treatment plant", Paper presented at the 91st National Meeting of the AIChE, Detroit, Michigan, (1981)

Anderson H.M. and R.V Edwards, "A finite differencing scheme for the dynamic simulation of continuous sedimentation", AIChE Symposium Series, Water, (1980)

Anderson H.M., "A dynamic simulation model for wastewater renovation systems", PhD thesis, Wayne State University, Detroit, Michigan, (1981)

Attir U., Denn M.M. and C.A. Petty, "Dynamic simulation of continuous sedimentation", AIChE Symposium Series, 73, No. 167, 49, (1977)

Billmeier E., "Verbesserte bemessungsvorschlage fur horizontal durchstromte nachklarbecken von belebungsanlagen", Berichte aus Wasserguterwirtschaft und Gesundheitdsingenieurwesen, T.U. Munchen, Band 21, (1978)

Coe H.S. and G.H. Clevenger, "Methods for determining the capacities of slime settling tanks", Trans Am Inst of Mining Engineers, 55, 356, (1916)

Daigger G.T. and R.E. Roper, "The relationship between SVI and activated sludge settling characteristics", JWPCF, Vol 57, No 8, pp 859-866, (1985)

Dick R. I. and K.W. Young, "Analysis of thickening performance of final settling tanks", Procs 27th Purdue International Waste Conf, Lafayette, Indiana, (1972)

Dick R. I. and B.B. Ewing, "Evaluation of activated sludge thickening theories", J San Eng Div, ASCE, 93, SA, (4), (1967)

Dick R. and P.A. Vesilind, "The Sludge Volume Index - What is it?", JWPCF, 41, 7, pp 1285-1291, (1969)

Dold P. L., Wentzel M.C., Billing A.E., Ekama G.A. and G.v.R. Marais, "Activated sludge simulation programs", Version 1.0, WRC, (1991)

Dupont R. and M. Henze, "Modelling of the secondary clarifier combined with the activated sludge model no. 1", Wat Sci Tech, Vol 25, No. 6, pp 285-300, (1992)

Ekama G.A. and G.v.R Marais, "Two improved sludge settleability parameters", IMIESA, 9, (6), 20, (1984)

Ekama G.A., Pitman A.R., Smollen M. and G.v.R. Marais, "Secondary settling tanks", Chapter 8 in "Theory Design and Operation of Nutrient Removal Processes", Published by Water Research Commission of South Africa, (1984)

Ekama G.A. and G.v.R. Marais, "Sludge settleability and secondary settling tank design procedures", Wat Pollut Control, Vol 5, No. 1, (1986)

Grau P., "New concepts in final clarifiers. Modelling, design and operation", Personal Communication, (1992)

Great Lakes - Upper Mississippi River Board of State Sanitary Engineers, "Recommended standards for sewage works", (1978)

Gujer W., "Activated sludge simulation program", ASIM, MS-DOS, public domain, (1990)

Hartel L. and H.J. Popel, "A dynamic secondary clarifier model including processes of sludge thickening", Wat Sci Tech, Vol 25, No. 6. pp 267-284 (1992)

Henze M., Grady C.P.L., Guyer W., Marais G.v.R. and T. Matsuo, "A general model for single-sludge wastewater treatment systems", Wat Res, 21, 5, pp 505 - 515, (1987)

Imam E., McCorquodale J.A. and J.K. Bewtra, "Numerical modelling of sedimentation tanks", Journal of Hyd Eng, ASCE, Vol 109, 12, (1983)

Institute of Water Pollution Control, "A guide to the design of sewage purification works", IWPC, P.O. Box 81249, Parkhurst 2120, (1973)

Jenkins D., Richard M. and G.T. Daigger, "Manual on the causes and control of activated sludge bulking and foaming", Published by the Water Research Commission of South Africa, P.O. Box 824, Pretoria, 0001, (1984)

Keinath T.M., Ryckman M.D., Dana C.H. and D.A. Hofer, "Activated sludge - Unified system design and operation", J Enviro Eng Div, ASCE, 103, EE5, 829, (1977)

Koopman B. and K. Cadee, "Prediction of thickening capacity using diluted sludge volume index", Water Research, 17, (10), 1427, (1983)

Krebbs P., "The hydraulics of final settling tanks", Wat Sci Tech, Vol 23, Kyoto, pp 1037-1046, (1991)

Kynch J.J., "A theory of sedimentation", Trans Faraday Society, 148, 166, (1952)

Laquidara V.D. and T.M. Keinath, "Mechanism of clarification failure", JWPCF, 55, (1), 54, (1983)

Lax, P.D., "Hyperbolic systems of conservation laws II", Comm Pure Appl Math, Vol 10, No 2 , pp 537-566, (1957)

Lee S.E., Koopman B., Bode H. and D. Jenkins, "Evaluation of alternative sludge settleability indices", Water Research, 17, 10, pp 1421-1426, (1983)

McCorquodale J.A., Yuen E.M., Vitasovic Z. and D. Dittmar, "Numerical simulation of unsteady conditions in clarifiers", Accepted for publication, Wat Pollut, Research Journal of Canada, (1991)

Merkel W., "Die bemessung horizontal durchstrometer nachklarbecken von belebungsanlagen", gwf-Wasser/Abwasser, 115, H(6), 272, (1974)

Merkel W., "Untersuchungen u das verhalten des belebten schlammes im system belebungsbeken - nachklarbecken", Gewasserschutz, Wasser-Abwasser, Aachen, (1971)

Otterpohl R. and M. Freund, "Dynamic models for clarifiers of activated sludge plants with dry and wet weather flows", Wat Sci Tech, Vol 26, No 5-6, pp 1391-1400, (1992)

Parker D.S., "Assessment of secondary clarifier design concepts", JWPCF, 55, (4), 349, (1983)

Pflantz P., "Performance of activated sludge secondary sedimentation basins", Procs 4th IAWPR, Prague, ed. S.H. Jenkins, Pergamon Press, Oxford, (1969)

Pitman A.R., "Settling properties of extended aeration sludge", JWPCF, 52, (3), 524 (1980)

Pitman A.R., "Settling of nutrient removal activated sludges", Procs of 12th IAWPRC Conference, Amsterdam, Wat Sci Tech, 17, 493, (1984)

Riddel M.D.R., Lee J.S. and T.E. Wilson, "Method for estimating the capacity of an activated sludge plant", JWPCF, Vol 55, No. 4, (1983)

Rosten H.I. and D.B. Spalding, "The PHOENICS reference manual", Cham Ltd, London, Report TR200, (1987)

Samstag R.W., McCorquodale J.A. and S.P Zhou, "Prospects for transport modelling of process tanks", Wat Sci Tech, Vol 26, no 5-6, pp 1401-1410, (1992)

Smollen M. and G.A. Ekama, "Comparison of empirical settling velocity equations in flux theory for secondary settling tanks", Water SA, 10, (4), 175, (1984)

Stobbe C.T., "Ueber das verhalten von belebten schlammes in aufsteingender waserbewegung", Verffentlichungen des Institutes for Siedlungswasserwirtschaft der Technischen Hochschule Hannover, 18, Hannover, (1964)

Stofkoper J.A. and C.C.M. Trentelman, "Richtlijnen voor het dimensioneren von ronde nabezinktanks voor actiefslibinstallaties", $HO6_2O$, 15, (14), 344, (1982)

STORA (Stichting Toegepast Onderzoek Reiniging Afvalwater), "Hydraulische en technologische aspecten van het nabezink-process", Rapport 1-Literatuur, Rapport 2-Ronde nabezinktanks (Praktijkonderzoek), Rapport 3-Rondenabezinktanks (Ontwerpgegevens en bedrijfservaring), (1981)

Stukenberg J.R., Rodman L.C. and J.E. Touslee, "Activated sludge clarifier design improvements", JWPCF, 55, (4), 341, (1983)

Takacs I., Patry G.C. and D. Nolasco, "A dynamic model of the clarification-thickening process", Wat Res, Vol 25, No 10, pp 1263-1271, (1991)

Tracy K.D. and T.M. Keinath, "Dynamic model for thickening of activated sludge", AIChE Symposium series, 70, (136), 291, (1973)

United States Environmental Protection Agency, "Process design manual for suspended solids removal", EPA 625/1-75-003a, Office of Technology Transfer, USEPA, Washington DC, (1975)

Vesilind P.A., Discussion of "Evaluation of activated sludge thickening theories", by Dick R.I. and B.B. Ewing, J Sanit Engng Div Am Soc Civ Engrs, 94, pp 185-191, (1968)

Vesilind P.A., "Design of prototype thickeners from batch settling tests", Water and Sewage Works, 15, 302, (1968)

White M.J.D., "Settling of activated sludge", Technical Report TR11, Water Research Centre, England, (1975)

Wilson T.E.,"Application of ISV test to the operation of activated sludge plants", Technical Note, Water Res, Vol 17, No. 6, pp 707-714, (1983)

Yoshioka N., Hotta Y., Naito S., Tanaka S. and S. Tsugami, "Continuous thickening of homogenous flocculated suspension", Chem Eng Tokyo, 21, 66, (1957)

CHAPTER 3
AVAILABLE DATA FOR ASSESSING THE SIMULATION MODEL

3.1 INTRODUCTION

In order to fulfil one of the major objectives of this investigation, which is the development of a simulation computer program to model the dynamic behaviour of secondary settling tanks, extensive data for calibration and verification of the program is required. The intention was to start the development of such a program by reconstituting the secondary settling tank segment of Anderson's program into a self contained, dedicated secondary settling tank simulation program. In order to ensure that the dedicated program was an accurate reconstruction of the secondary settling tank part of Anderson's program, the program would firstly be required to reproduce Anderson's own calibration test results.

The next step would be to check that the program was an accurate embodiment of the flux theory by checking that it generated results that conform to idealised flux theory calculations. Once this had been achieved, and confidence gained in the program's ability to predict the theoretical results correctly, calibration and verification with measured data could commence.

This was envisaged to proceed in two stages:

1. comparing the program predictions to laboratory scale data from tall, thin continuous settling column tests to ensure that the program is valid for the one dimensional case with negligible diffusivity and

2. comparing the program predictions to full scale data from large diameter (30 to 50m) settling tanks and, with appropriate modifications, such as the inclusion of

diffusivity, developing a program that is valid for simulating full scale settling tanks.

To satisfy the above two steps in developing the simulation program, both laboratory column and full scale data are required. The laboratory and full scale data used in executing the two steps are described in detail in this chapter.

3.2 LABORATORY DATA

The laboratory data consists of results collected by the Water Research Group on a laboratory scale settling tank - a tall (2m), small diameter (0.075m) column. The small diameter to depth ratio of the laboratory column ensured that horizontal movement of sludge and liquid was negligible, with the result that the major processes happened mainly in the vertical direction. In other words, the tall thin column offers the closest possible physical representation of the principles embodied in the flux theory i.e. movement of solid and liquid phases in the vertical direction only and uniformly distributed over the cross sectional area.

The settling column formed part of a continuously fed, anoxic/aerobic reactor activated sludge system operated at 25 days sludge age. The feed flow was constant and set at $35ld^{-1}$ at a COD concentration of $500mgCOD1^{-1}$. The sludge age of 25 days was set hydraulically by wasting sludge from the aerobic reactor daily. Although the mass of sludge in the settling column varied depending on the operating conditions and resulting concentration profile, it was generally between 25 to 50% of the mass of sludge in the biological reactor.

In order to vary the solids loading conditions on the settling column, the underflow recycle ratio and influent flow rate were varied. Although the influent sewage flow was kept constant at $35ld^{-1}$ to maintain a constant daily COD level, an additional "influent" flow (to the biological reactor) of recycled clarified effluent was imposed to increase the influent flow above $35ld^{-1}$. In this way, effective influent flows from 35 to

120ld^{-1} could be imposed on the system giving an overflow rate range of the settling column of 0.33 to 1.13mh^{-1}. The overflow from the settling column (or effluent) was collected in a large (150l) drum, from which effluent was decanted from time to time. In the case where the settling column was overloaded, and solids escaped with the effluent, these "lost" solids were settled out and collected from the effluent drum and returned to the biological reactor.

Slow and gentle stirring (1 to 2 rpm) was provided in the column in the same way as in the SSVI settleometer column. Thirty three-way stopcock sample points for drawing sludge concentration samples were placed along the length of the settling column and relatively small samples of 25ml were drawn via these stop cocks with a graduated syringe. The influent and underflow recycle sludge return flows were measured with a graduated measuring cylinder and stopwatch over several minutes. Influent and underflow rates were set at appropriate desired values determined by the solids loading rate desired in the settling column. These flows were then left unchanged for a number of days to allow the system to reach steady state.

After the system had been operated for a start up period of about a month and the sludge mass in the system appeared to have reached a steady state, 9 settling column loading tests were conducted over a period of 5 weeks (August and September 1980). During these loading test cases, one or more sludge concentration - depth profiles were measured but in many cases it was difficult to establish the time these profiles were taken in relation to the commencement of the loading conditions imposed. During the two month period, ZSV-X tests were carried out periodically and three groups of data were defined from which the V_o and n values could be determined (see Table 3.1). Unfortunately, due to the early date of this work, the alternative sludge settleability parameters like SVI, $SSVI_{3.5}$ and DSVI were not measured.

The nine tests are set out in Table 3.2. The most appropriate V_o and n values measured were allocated to each of the nine loading test cases, as set out in Table 3.2. According to these calculations, four of the test cases were found to be overloaded and

Table 3.1 Three sets of V_0 and n values for the labwork experiments

DATA SET	V_0 (mh^{-1})	n (m^3kg^{-3})
12/9/80	6.287	0.391
All September data	6.358	0.354
All data	7.558	0.366

Table 3.2 Summary of labwork cases

CASE	DATE OF TEST	V_0 AND n VALUES	UNDERLOADED	OVERLOADED
1	11/9/80	12/9		X
2	13/9/80	12/9	X	
5	14/9/80	12/9		X
6	8/9/80	Sept data		X
7	14/9/80	12/9	X	
8	15/9/80	12/9	X	
9	17/9/80	Sept data	X	
A	25/8/80	All data	X	
B	26/8/80	All data		X

five underloaded.

For each of the test cases, the laboratory data detailed the final sludge concentration depth profile, the influent and recycle flow rates, feed and underflow concentrations, applied flux, mass of sludge in the column and the percent difference between the masses of sludge in and out of the column (i.e. error in the mass balance), the last mentioned being an indication of whether or not the column had achieved steady state.

However, no initial conditions were detailed in the labwork report. This means that, in order to carry out a simulation of the labwork data: firstly, an arbitrary set of initial conditions must be assumed to exist in the settling column in order to initiate the simulation; and secondly, the simulation should be allowed to run for a sufficient length of time so that the influence of these initial conditions have died away. In addition, no information was available as to how long it had taken each experiment to reach a steady state condition. Thus, it was not possible to select the duration of the simulation such that it matched that of the labwork tests.

These limitations of the data introduce two additional unknowns into the simulation. Hence, it is difficult to identify whether the cause of errors (if these occur) in the final predictions of the simulation program is due to errors in the initial conditions, incorrect duration of the simulation or deficiencies in the model itself. These questions are dealt with in more detail later in Chapter 7.

3.3 FULL SCALE DATA

STORA (1981) (see also Stofkoper and Trentelman (1982)) undertook an extensive investigation into full scale settling tank behaviour in which they analysed 44 test cases of solids loading on secondary settling tanks at 22 different sewage treatment plants in Holland. Of these 44 test cases, 14 and 10 were conducted on the Rijen and Oss plant settling tanks respectively and one each on the settling tanks at 20 other different plants. The settling tanks at these plants all conformed to the following specifications:

1. circular with diameters between 30m and 48m,
2. side wall depths 1.5m to 2.5m,
3. conical bottoms with a floor slope of 1 in 12 towards the centre,
4. peripheral double sided effluent overflow launders set 0.5m to 1m from the edge,
5. centre feed arrangement,
6. scraper sludge collection systems to central collection hoppers,
7. volumes ranging from 17 to 170% of the aeration basin.

Each test was conducted as follows:

Influent to the plant was shut off and allowed to accumulate in the sewer. At the same time, the underflow recycle was set to the required rate and, while the influent was withheld, the settling tank emptied itself of sludge until it reached a steady state with the set recycle flow. The test began at the moment the influent pumps were started. The influent was set at a specified flow rate to give the required overflow rate. The influent and recycle flows were kept constant until the test led to:

1. a continuously rising sludge blanket which eventually caused sludge loss over the effluent weirs, in which case the test ended in a failed (overloaded) state,

2. a steady state in which the sludge blanket remained at a constant level in the settling tank, in which case the test ended in a safe (underloaded) state,

3. an inability to maintain the influent flow at the specified rate due to a shortage of sewage, in which case the final over- or underloaded state was inferred from sludge blanket height measurements. If this was not possible with reasonable accuracy, the test was deemed inconclusive.

During each test, the following were measured at regular intervals:

1. influent and recycle flow,
2. sludge settleability in terms of the $SSVI_{3.5}$, DSVI and flux V_o and n,
3. sludge blanket level and rise rate,
4. feed and underflow concentrations.
5. In some tests, the effluent solids concentrations with time and
6. sludge concentration-depth profiles in the tank at various radial distances from the centre and at various times in the test were also measured.

The measured raw data cited above can be found in STORA's (1981) comprehensive and detailed reports. A summary of the 44 tests carried out by STORA is set out in Table 3.3.

Table 3.3 Summary of tests carried out by STORA

TEST	FAIL/SAFE/ NO EQUILIBRIUM	REMARKS
RIJEN 1	F	No concentration profiles
RIJEN 2	F	SSVI test inconclusive
RIJEN 3	NE	No concentration profiles
RIJEN 4	F	
RIJEN 5	F	
RIJEN 6a	NE	No concentration profiles
RIJEN 6b	NE	
RIJEN 7	F	
RIJEN 8	F	
RIJEN 9	S	
RIJEN 10	S	No concentration profiles
RIJEN 11	S	
RIJEN 12	S	
RIJEN 13	S	
OSS 1	F	No effluent concentrations No concentration profiles
OSS 2	S	
OSS 3	S	No concentration profiles
OSS 4	S	
OSS 5	S	No concentration profiles
OSS 6	S	No concentration profiles
OSS 7	F	No effluent concentrations No concentration profiles
OSS 8	F	No effluent concentrations No concentration profiles
OSS 9	S	
OSS 10	S	No concentration profiles
ALMELO	S	No concentration profiles
APELDOORN 1	S	
BEVERWIJK	S	
DEVENTER 4	S	
ECHTEN	S	No concentration profiles
GIETEN	S	
GOOR	F	SSVI very high (= 260ml/g)
HAARLEM	S	No concentration profiles
HAPERT	S	No concentration profiles
HARDERWIJK (groot)	NE	
HARDERWIJK (klein)	NE	
HELMOND	NE	
HOENSBROEK	NE	No concentration profiles
HUIZEN	S	
HULST	S	No concentration profiles
JOURE	NE	
RAALTE	S	No concentration profiles
RIJSSEN	F	55% of maximum solids loading
UDEN-VEGHEL	F	
WIJK BIJ DUURSTEDE	F	No concentration profiles

F = fail, S = safe, NE = no equilibrium (i.e. inconclusive)

3.3.1 QUALITATIVE DESCRIPTION OF SETTLING TANK PERFORMANCE DURING SOLIDS LOADING TESTS CONDUCTED BY STORA

In order to provide further clarity on the behaviour of the full scale settling tanks observed during the tests conducted by STORA (1981), the following description outlining the principal four aspects of settling tank behaviour is presented. Because these parameters are to be used for assessing the predictive capacity of the settling tank model, a description of the general settling tank behaviour gives insight into the test methodology and progress. The four principal aspects are:

1. the feed concentration,

2. the underflow concentration and volumetric flow rate,

3. the sludge blanket behaviour and

4. concentration profiles in the sludge blanket.

1. The feed concentration

Just before the start of a test, practically all of the sludge is in the biological reactor because the underflow recycle pumping has emptied the settling tank of sludge due to the withholding of the influent flow. When the influent flow is commenced, sludge begins to be transferred to the settling tank by the influent and recycle flows together and more sludge enters the settling tank than is returned to the biological reactor. This transfer of sludge causes a decrease in reactor concentration. The decrease progresses at a relatively constant rate during the test. In the plants with a large settling tank volume compared to reactor volume, the decrease in reactor concentration can be quite rapid. Once steady state is achieved between the mass of solids transported to the tank and that returned to the biological reactor, the reactor concentration ceases to decrease

and remains constant. In some cases, the decrease in reactor concentration could only in part be explained by sludge build up in the settling tank; in these cases the poor solids balance probably was due to improper mixing in the reactor.

2. The underflow concentration and volumetric flow rate

Immediately after the commencement of the influent flow, there is a decrease in the underflow concentration; the minimum concentration observed in the underflow during this time is approximately equal to the reactor concentration. After about an hour, the underflow concentration begins to increase. This increase goes together with an increase in sludge blanket level. In those cases where the test ended in solids underload, the sludge blanket reached a certain level which remained constant for the remainder of the test. The underflow concentration increased while the sludge blanket level was rising, and ceased increasing at approximately the same time as the sludge blanket level ceased to rise. Once the sludge blanket level stabilised, the underflow concentration also remained unchanged. For cases which ended in solids overload, the sludge blanket level increased continuously but at a decreasing rate as the blanket level rose higher in the tank, until it reached the effluent overflow level. Concomitantly with the rising of the sludge blanket, the underflow concentration increased and in some cases continued increasing even while solids were being lost with the effluent.

3. The sludge blanket behaviour

At the start of the test, the sludge blanket level (sludge blanket-clear water interface) is right in the bottom of the tank and the sludge occupies only a minor part of the tank's bottom cone. Immediately after commencing the influent flow, the blanket level begins to rise. While the bottom cone is filling up, the sludge is not uniformly distributed over the tank area - near the centre of the tank the concentration tends to be higher than that further away from the centre. Also, the sludge blanket level is not horizontal, but tends to follow the sloping bottom of the tank. By the time the sludge blanket reaches the bottom of the side wall, the sludge blanket level adopts a horizontal

position (see Figure 3.1). Maintaining its horizontal position, the sludge blanket level continues to rise above the bottom of the side wall.

4. Concentration profiles in the sludge blanket

Sludge concentration profiles were measured at various intervals and different distances from the centre of the tank during the tests. From these profiles, a picture can be built up as to how the sludge mass distributes itself in the settling tank at the various stages of loading. Figure 3.1 shows three sludge concentration depth profiles measured at various radial distances from the centre for the Rijen 11 test.

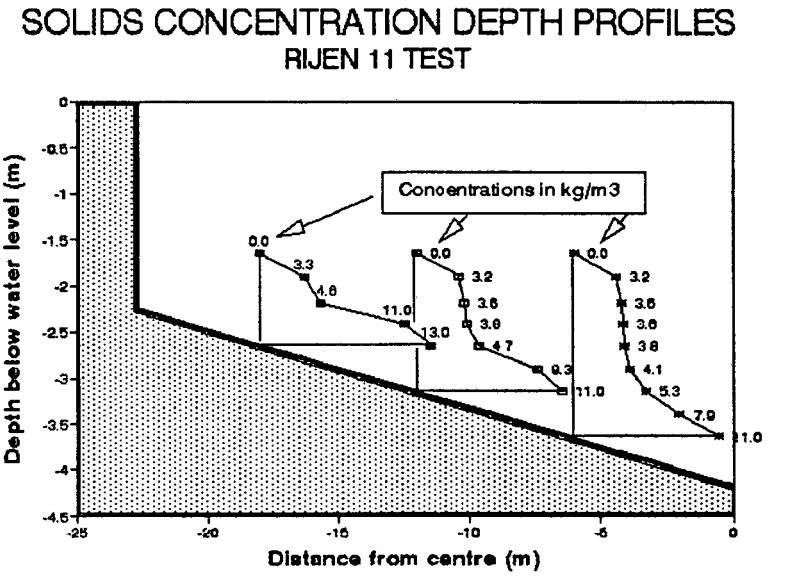

Figure 3.1 Sludge concentration depth profiles for the Rijen 11 test

From Figure 3.1, it can be seen that the sludge blanket is horizontal in the settling tank, as it has already reached the side wall and risen above the conical section of the tank. In conformity with Billmeier's (1978) observations, four sludge layers can be identified. These are, from the top down:

a. the clear water zone
b. the separation zone
c. the storage zone and

d. the thickening zone.

Above the horizontal sludge blanket level is the clear water zone in which the solids concentration is very low. The effluent emerges from this zone and the clear water in it and the effluent have essentially the same quality. From the sludge blanket level, the solids concentration increases from the very low concentration of the clear water zone to several grams per litre. This layer of increasing concentration is the separation zone and its thickness was generally <0.3m in all the tests. Below the separation zone is the storage zone. In this zone, the solids concentration is essentially constant and, with rising sludge blanket level, the thickness of this zone increases. The storage zone is present only when the sludge blanket level has risen relatively high above the bottom of the side wall. When the sludge blanket level is in the region of the bottom of the side wall, then the storage zone does not exist and the separation zone lies directly above the bottommost thickening zone. In this event, the solids concentration increases continuously through the separation and thickening zones. When the storage zone is present, its solids concentration is constant throughout the zone and remains constant with time during a test.

The bottommost zone is the thickening zone and in it the solids concentration increases sharply with depth. The thickness of this zone is virtually constant over the tank area and therefore this zone lies parallel to the tank's sloping floor. The highest concentration is always the concentration on the floor and this concentration is always higher than that in the underflow. During a test, the thickness of the thickening zone increases only marginally whereas the floor solids concentration increases markedly.

In so far as modelling the sludge concentration depth profiles, cognisance will need to be taken of the sloping floor of the settling tank because, while the sludge concentration depth profiles are similar at different radial distances from the centre, they extend over different depths. This can be dealt with by assigning the depth of the settling tank as the depth at which the concentration profile was measured. In all cases,

the concentration profiles measured closest to the centre (generally at 1/4 radius) would be selected for simulation because these give the greatest settling tank depths.

Another important aspect to be considered in simulating the sludge concentration depth profiles is the specification of the sludge concentration representing the top of the sludge blanket. In their investigation, STORA measured the sludge concentrations at 0.3m depth intervals. From an examination of the concentration depth profiles of which Figure 3.1 is typical, it can be seen that the concentration changes from 0 to $>3kgm^{-3}$ within a single depth interval of 0.3m. Therefore the sludge blanket level is somewhere between the two concentration measurements. The specification of the sludge concentration of the top of the sludge blanket is therefore not critical provided it is $<3kgm^{-3}$.

The aspects of settling tank depth and top of sludge blanket concentration specifications for the simulation model are dealt with in greater detail in Chapter 8, Section 8.2.1.

3.3.2 VERIFICATION OF THE ATV DESIGN PROCEDURE BY STORA

One of the important functions of the full scale investigation conducted by STORA (1981) was to independently verify the ATV design procedure. Because the ATV procedure is an empirical approach to design that is based on experimental observations by various research workers, it is essentially a structured representation of the important observations of these workers. Consequently, the procedure was calibrated in its development so that strictly it should not require verification. However, STORA did conduct an independent full scale verification of the procedure, the results of which are briefly presented here as motivation of the reliability of the ATV design procedure.

There are four principal parts that constitute the ATV design procedure and, if these four parts can be verified to be accurate, the procedure can be deemed reliable. These four parts are:

1. the overflow rate - sludge volume expression i.e.

$$q_A = 2400(VS_V)^{-1.34}$$

subject to (3.1)

$$q_A < 1.6mh^{-1}$$

where q_A = overflow rate (mh^{-1})

VS_V = specific sludge volume ($ml l^{-1}$)

2. the sludge storage concentration,

$$X_c = \frac{500}{I_{sv}} \quad (3.2)$$

where X_c = Merkel's critical transition concentration (kgm^{-3})

I_{sv} = DSVI (mlg^{-1})

3. the concentration in the underflow at average dry weather flow (ADWF) and peak wet weather flow (PWWF) i.e.

$$G_{rs\ dwf} = \frac{1200}{I_{sv}}$$

and (3.3)

$$G_{rs\ wwf} = \frac{1200}{I_{sv}} + 2$$

and

4. the depth of the thickening zone.

1. Verification of the overflow rate - sludge volume expression

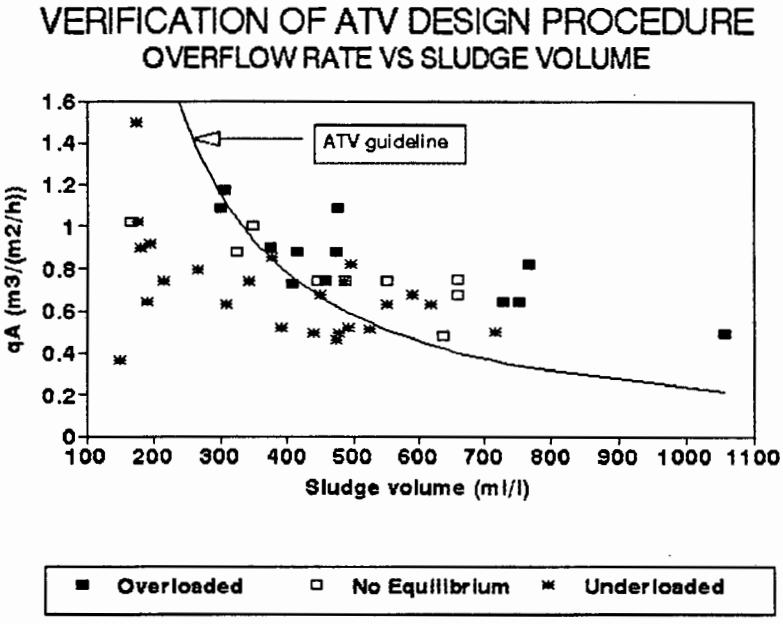

Figure 3.2 Verification of the ATV overflow rate vs sludge volume guideline

STORA (1981) used their full scale data to check the empirical ATV overflow rate (q_A) - sludge volume (VS_V) expression. For each of the 45 solids loading cases, the VS_V was calculated from the DSVI and the reactor sludge concentration G_a at the end of the test to take account of the reduction in G_a which is allowed by the ATV guideline. The applied overflow rate (excluding underflow) was plotted vs the calculated VS_V (see Figure 3.2). For perfect prediction, all the overloaded cases should fall above the line and all the underloaded cases below. Figure 3.2 shows this to be the case generally for $VS_V < 500 ml l^{-1}$. However, for $VS_V > 500 ml l^{-1}$, which are the usual design conditions, there are a group of underloaded cases that fall above the line, indicating that, for these VS_V values, the ATV procedure tends to be too conservative. This conservativeness of the ATV guideline prompted STORA to modify the empirical guideline distinguishing between safe and failure load cases as follows:

$$q_A = \frac{1}{3} + \frac{200}{VS_V} \quad (m h^{-1}) \qquad (3.4)$$

where $VS_V = G_a * I_{SV}$ ($ml l^{-1}$)

G_a = biological reactor sludge concentration ($g l^{-1}$)

I_{SV} = DSVI (mlg^{-1})

Equation (3.4) is subject to the constraint that the Sludge Volume Loading, VS_A, which is the product of VS_V and q_A, lies between 300 and 400 $lm^{-2}h^{-1}$ i.e.

$$VS_A = q_A \, VS_V \quad (lm^{-2}h^{-1}) \tag{3.5}$$

If Equation (3.5) gives $VS_A < 300$ or > 400, then VS_A is set equal to 300 or 400 respectively and the overflow rate q_A is given by:

$$q_A = \frac{VS_A}{VS_V} \quad (mh^{-1}) \tag{3.6}$$

For VS_A between 300 and 400 $lm^{-2}h^{-1}$, the overflow rate q_A is given by Equation (3.4) directly. Because settling tank failure cannot be allowed at PWWF, Equation (3.4) applies for PWWF and ADWF taking due consideration that the reactor concentration G_a would decrease during wet weather flow as observed in the settling tank loading tests. Limits are set to the reduction of G_a during wet weather i.e. not less than 70% of the dry weather value (empty settling tank) or $2kgm^{-3}$.

2. Verification of the sludge storage concentration

With the aid of the measurements of the solids concentration depth profiles, STORA, using two approaches, compared the measured solids concentration in the storage zone with that calculated by the ATV procedure i.e. the greater of the feed concentration G_a or the critical concentration $X_c = 500/I_{SV}$.

In the first approach, the measured solids concentration in the storage zone was plotted vs that calculated. The results are shown in Figure 3.3. Figure 3.3 shows that the measured concentration varies much less than the calculated concentrations in that for a measured value of, for example, $4kgm^{-3}$, the calculated value ranges between 2.5 and $4.0kgm^{-3}$. Also, the measured value is about 1.2 times higher than the calculated value.

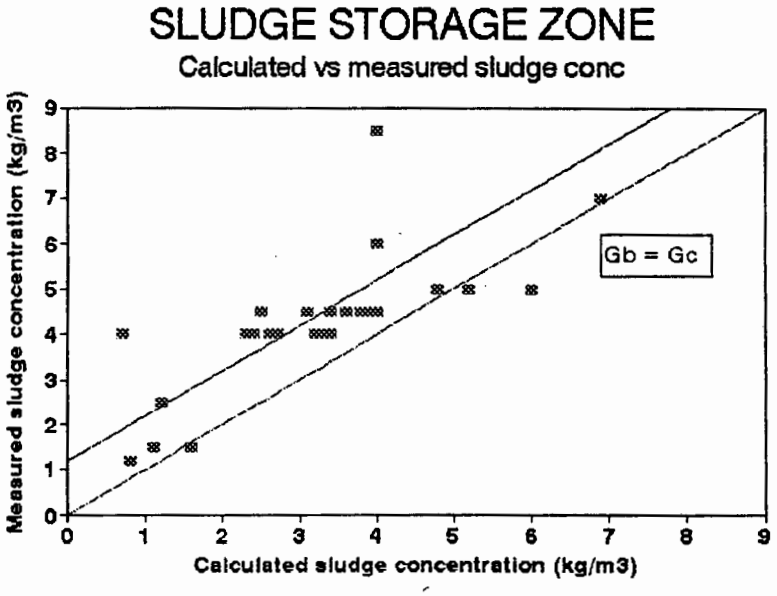

Figure 3.3 Calculated vs measured sludge concentration in the sludge storage zone

In the second approach, STORA calculated the sludge storage concentration from the change in the reactor solids mass over a period of time and the increase in the sludge blanket depth over the same time interval. They found that, for the loading cases where the sludge blanket depth increased quickly, the calculated concentration compared favourably with that measured, but when it increased slowly, the correlation was rather poor, with the measured concentrations being higher than the calculated. For low sludge blanket rise rates they speculated that, because the sludge has more time to compact, it collects in the thickening zone below rather than in the storage zone.

They concluded from their data that the calculated concentration in the storage zone is generally a low estimate with the result that the actual storage zone depth would be shallower than the calculated depth by a factor of 1.2. In this regard, the ATV procedure errs on the conservative side by approximately 20%.

3. Verification of the maximum underflow concentration

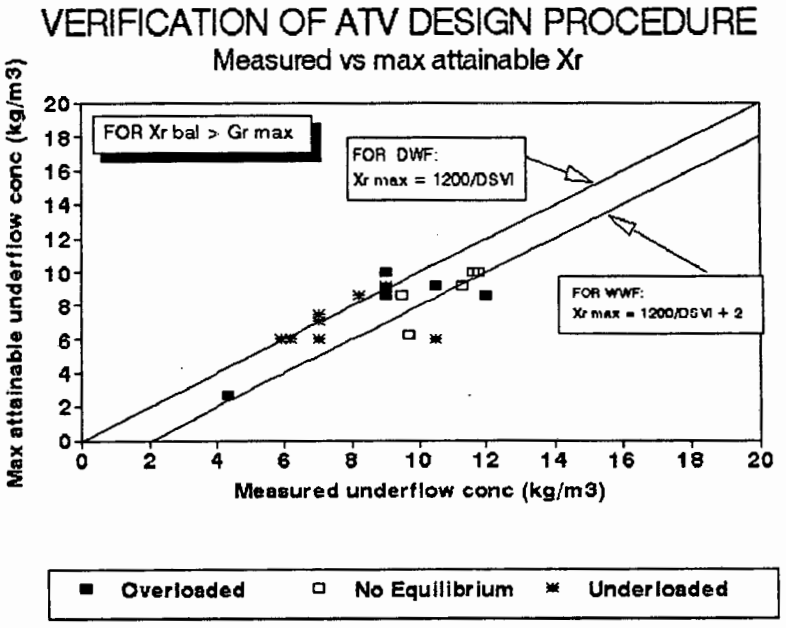

Figure 3.4 Calculated maximum attainable underflow concentration vs measured underflow concentration for data where calculated mass balance underflow concentration exceeded the calculated maximum attainable

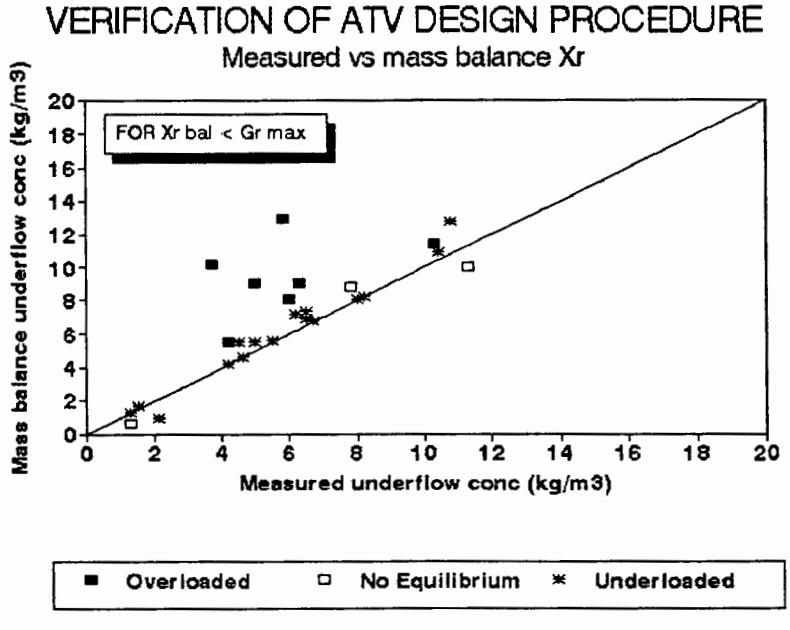

Figure 3.5 Calculated mass balance underflow concentration vs measured underflow concentration for data where calculated mass balance underflow concentration is less than the calculated maximum attainable

The maximum underflow concentration specified by the ATV procedure for DWF conditions was calculated from:

$$G_{rs,max} = \frac{1200}{I_{sv}} \quad (kgm^{-3}) \qquad (3.7)$$

where $G_{rs,max}$ = maximum attainable underflow concentration (kgm^{-3})
I_{sv} = DSVI (mlg^{-1})

It can be seen from Equation (3.7) that $G_{rs,max}$ is a function only of the DSVI and indicates that, with increasing DSVI, the compactability of the sludge decreases. In order to use measured underflow concentrations to verify Equation (3.7), STORA separated the data into two groups: those underflow concentrations which were likely to have been limited by the

a. compactability of the sludge i.e. those with mass balance underflow concentrations higher than the maximum attainable (see Figure 3.4) and

b. the underflow rate i.e those with mass balance underflow concentrations lower than the maximum attainable (see Figure 3.5).

In Figure 3.4, it can be seen that for the tests ending in solids underload, the calculated maximum attainable values for DWF conditions compare very well with those measured. For the tests that ended in solids overload or inconclusively, the calculated values are considerably less than those measured. By adding the permissable $2kgm^{-3}$ to the calculated DWF values, the maximum attainable underflow concentration for PWWF is obtained, and these values compare very well with most of the measured underflow concentrations in the tests that ended in solids overload or inconclusively. It is not unrealistic to accept that the tests that ended in solids underload are comparable to DWF conditions and those that ended in solids overload or inconclusively to WWF conditions because of the larger quantities of sludge in the settling tank in the latter

cases than in the former cases. On this basis, Figure 3.4 shows that the ATV procedure for estimating the maximum attainable underflow concentration is sufficiently accurate for calculating minimum underflow pumping rates.

In Figure 3.5, the mass balance underflow concentration is plotted vs that measured for mass balance values less than the maximum attainable given by 1200/DSVI. The comparison can be seen to be very good especially for the cases ending in solids underload. The solids overload and inconclusive cases that fall far above the diagonal may be cases where the duration of the test was insufficient to attain steady state.

When the data is plotted without separating it into two groups, far less consistency is brought to the data. From this it can be concluded that a limitation on the underflow concentration due to its compactability characteristics is a feature that cannot be ignored in settling tank design. One of the shortcomings of the flux theory based procedures is that they do not recognise this limitation. This is discussed further in, Chapter 8, Section 8.18. From Figure 3.5, it can be concluded that, provided the underflow concentration is not limited by its compactability, the steady state underflow concentration as calculated by a mass balance gives a very accurate estimate of the underflow concentration that is obtained, provided there is sufficient time for it to be achieved. This is especially so in underloaded cases, which is the desired situation for design.

4. Verification of the depth of the thickening zone

The thickening zone was not separately identified in the sludge concentration depth profile by the STORA investigators. Consequently, the depth of the thickening zone as specified by the ATV procedure was accepted without verification.

5. Conclusions

The four principal parts of the ATV procedure were shown to be accurate empirical expressions when compared with the full scale data measured by STORA. The only significant deviation is that at high Sludge Volumes ($> 500\ lm^{-3}$), which are the usual design situations, the maximum permissable overflow rate is unnecessarily conservative. Consequently, the ATV procedure can be safely used for design and will lead to conservative area provision at Sludge Volumes $> 500\ lm^{-3}$. This conservativeness is eliminated in the STORA procedure.

3.3.3 SELECTION OF SUITABLE STORA CASES FOR MODEL VERIFICATION

For the purposes of simulation, the following STORA tests were regarded as unsuitable:

1. 19 of the 23 underloaded cases except four (Rijen 9, Oss 2 and 6 and Gieten). These 19 cases, although interesting to model, are not severe tests. Because the main purpose of the simulation would be to predict the point of and the nature of failure of a settling tank, the underloaded tests were not considered to be relevant. The four underloaded test cases simulated are those that were close to the dividing line between under and overloaded conditions and were chosen specifically as a means of checking that the simulation program was able to correctly distinguish between failed and safe cases.

2. all eight inconclusive cases,

3. failed tests for which insufficient data was provided to satisfactorily asses the performance of the program (i.e Oss 1, 7 and 8),

4. two failed tests where the SSVI measurement was inconclusive or unrealistically high (Rijen 2 and Goor),

5. one failed test where the applied solids loading was less than 55% of the maximum permissable solids flux according to the flux theory i.e the failed situation is unexpected (Rijssen).

The remaining 11 cases, of which seven are failed (overloaded) and four are safe (underloaded) were used for calibration and verification of the simulation program.

3.4 ASSESSMENT OF THE DATA

The labwork data offers a useful basis for comparison and testing of the predictions made by a simulation model for the vertical direction (one dimensional) flows only. One of the major advantages of this data is that the ZSV-X tests for the sludge in the column were performed at regular intervals over the test period. With the measured ZSV-X data, the V_o and n values necessary for the flux theory may be determined directly, eliminating the necessity to estimate them from any of the other sludge settleability measures (SVI, SSVI or DSVI). This is a significant factor in favour of this data set, as generally accepted functional relationships for the determination of V_o and n values from other sludge settleability measures are not available. However, the labwork data set is limited by the lack of information regarding initial concentration profiles and test lengths. These limitations will be dealt with when the data is used in the evaluation of the simulation model in Chapter 7.

The STORA data described above represents an extremely comprehensive set of data for full scale settling tanks as regards both the broad range of underloaded and overloaded situations reported as well as the extensive measurements of operating conditions and settling tank behaviour parameters at regular intervals during the tests. It is to the knowledge of the writer the most comprehensive data set on full scale secondary settling tank performance and behaviour available in the literature. With the

aid of this data, it should be possible to thoroughly test and assess the predictions made by a secondary settling tank model. However, there is one major deficiency in the data set in so far as its usefulness for calibration and verification of a simulation model based on the flux theory is concerned. Although the sludge settleability was measured with the $SSVI_{3.5}$, DSVI and ZSV-X tests, the ZSV-X tests were not correctly performed. Although the test was carried out by STORA at four to five concentrations, the range of concentrations was much too narrow (1-5kgm^{-3}) compared to the recommended range for accurate V_o and n values (1.5-10kgm^{-3}). On the basis of the V_o and n values that were obtained from the ZSV-X measurements, STORA tested the flux theory for its ability to predict the maximum solids loading rate and concluded that the flux theory, although a good conceptual model for the settling tank, was completely inadequate quantitatively for predicting the solids loading capacity of settling tanks. Unfortunately, this conclusion contributes to the existing negative impressions of the flux theory amongst design engineers and exacerbates the lack of confidence in the theory as a design procedure of practical relevance. However, STORA's conclusion is not correct, because it is based on poor ZSV-X measurements.

The absence of reliable ZSV-X measurements and corresponding V_o and n values in the STORA data set means that if the data was to be useful for calibrating and verifying a computer simulation model based on the flux theory, some other way of estimating the V_o and n values needed to be developed. This was done by means of developing empirical relationships linking the V_o and n values and the other sludge settleability parameters $SSVI_{3.5}$ and DSVI. In Chapter 4, the statistical evaluation that was undertaken to determine empirical relationships between the conventional sludge settleability parameters (SVI, $SSVI_{3.5}$ and DSVI) and V_o and n is described.

In addition, the development of functional relationships that can be used to calculate the flux theory constants, V_o and n, from SVI, $SSVI_{3.5}$ or DSVI measurements would be useful for much more than the purposes of this study. A functional relationship of this sort, besides being able to transform the STORA settleability measurements into a

form useful for the flux theory based simulation model, could also be used in the future by other workers in the field to save the tedious ZSV-X measurement currently required for the determination of V_o and n.

REFERENCES

Billmeier E., "Verbesserte bemessungsvorschlage fur horizontal durchstromte nachklarbecken von belebungsanlagen", Berichte aus Wasserguterwirtschaft und Gesundheitdsingenieurwesen, T.U. Munchen, Band 21, (1978)

STORA (Stichting Toegepast Onderzoek Reiniging Afvalwater), "Hydraulische en technologische aspecten van het nabezink-process", Rapport 1-Literatuur, Rapport 2-Ronde nabezinktanks (Praktijkonderzoek), (1981)

Stofkoper J.A. and C.C.M. Trentelman, "Richtlijen voor het dimensioneren van ronde nabezinktanks voor aktiefslibinstallaties", H_2O, 15, 14, pp 344-354, (1982)

CHAPTER 4
DEVELOPING A RELATIONSHIP BETWEEN SLUDGE SETTLEABILITY PARAMETERS

4.1 INTRODUCTION

As discussed earlier in Chapter 2, secondary settling tank design methods at present either do not explicitly incorporate the sludge settling settleability (e.g hydraulic design criteria) or else incorporate it in the form of different simplified sludge settleability parameters (e.g.the design procedures based on SVI, $SSVI_{3.5}$ or DSVI). Although it is recognised that the zone settling velocity (ZSV or V_s) is the best measure for sludge settleability and that the flux theory based on it is the best model for secondary settling tank behaviour, these have not been accepted principally due to the tediousness of the multiple batch ZSV-concentration (X) tests, which characterise the changing settling velocity (V_s) of a sludge with concentration (X). To overcome this problem, various researchers have sought to establish empirical relationships between the different sludge settleability measures and the constants in the relationship linking the ZSV to X (e.g. V_o and n in the semilog function $V_s = V_o e^{-nX}$ after Vesilind (1968)). With the aid of these empirical relationships, the appropriate flux theory constants (e.g V_o and n) can be calculated from the simpler settleability measures (SVI, $SSVI_{3.5}$ or DSVI). In this chapter, earlier work on these empirical relationships is reviewed and, where necessary, evaluated and refined. The objective of this is twofold: firstly, and most importantly for this secondary settling tank simulation study, to obtain the most reliable possible flux theory constants from STORA's measured $SSVI_{3.5}$ or DSVI to simulate their full scale results; and secondly, to provide a link between the empirical design procedures reviewed in Chapter 2 and the flux theory so that these can be compared and integrated if possible.

4.2 REVIEW OF PREVIOUS WORK

The general acceptance of a single parameter that defines the settleability of a sludge is a source of much controversy in the field. As many as four different settleability parameters are in current use (SVI, $SSVI_{3.5}$, DSVI and ZSV-X), and there is disagreement as to their relative merits. A description of each of these parameters has been covered earlier in Chapter 2. In addition, there are no generally accepted functional relationships linking one settleability parameter to another, although various empirical relationships have been proposed (see Table 4.1). This means that, at present, if data is available which specifies only one of the settleability parameters, the other settleability parameters cannot be confidently derived. Usually it is recommended that further settleability measurements be carried out to determine the particular settleability parameter of interest. A summary of the existing relationships between sludge settleability parameters which have been proposed are presented in Table 4.1. Before commenting on Table 4.1, it needs to be pointed out that the flux theory constants defining the ZSV-X function that appears to have been adopted by all researchers are the V_o and n in Vesilind's (1968) semilog model $V_s=V_oe^{-nX}$. Other functions linking V_s and X have been in use in the past, the logarithmic function $V_s=aX^{-b}$ after Dick and Young (1972) being the most common, but power and hyperbolic functions have also been tested (Rachwal *et al* (1982)). Smollen and Ekama (1984) showed from their own and a large set of literature data (most of which is included in Table 4.1) that the semilog function not only fitted the ZSV-X data better but also leads to a more satisfactory flux model. Since 1983, most of the work published in this area has adopted the semilog function. Therefore this function will be accepted in the evaluation that follows where V_o and n are the two constants of interest in the semilog function $V_s=V_oe^{-nX}$. Because of the wide acceptance of the semilog function, no further analysis of the function between V_s and X is made in this investigation.

Table 4.1 (cont) Summary of contributions made by previous researchers in the field

RESEARCHER(S)	DATA SOURCE AND TYPE	MEASURED PARAMETER	EQUATIONS	COMMENTS
Ekama and Marais (1986)	A. Pitman (1980, 1984) White (1975) Rachwal *et al* (1982) Koopman & Cadee (1983)	SSVI	$V_s/n = 67.9\exp(-0.0016SSVI_{3.5})$ ($r^2=0.968$) $n = 0.88-0.393\log(V_o/n)$ ($r^2=0.976$)	* Confirmed Pitman's relationship with White and Rachwal *et al* data * Koopman & Kadee data did not conform
	B. * 13 Western Cape plants	SVI SSVI DSVI	SSVI = 0.67*DSVI	* Wide scatter in data
	* Stofkoper & Trentelman (1982)	DSVI SSVI	SSVI = 0.65*DSVI	* Wide scatter in data
Hartley (1985)	Literature data	SVI SSVI		* Small data set * Method lacks statistical rigour
Koopman & Cadee (1983)	Literature data * Sezgin (1980) * Palm *et al* (1981) * Jenkins *et al* (1981) * Lee *et al* (1981)	DSVI	$n = 0.249 + 0.002191*DSVI$ ($r^2=0.99$) $\ln V_o = 2.605-0.00365*DSVI$ ($r^2=0.735$)	* Data collected over a very narrow range of concentrations
Merkel (1971)	Large no. of measurements	DSVI SVI	$DSVI = SVI*(300/SV_{30})^{0.6}$ where SV_{30} = settled volume at 30min in the SVI test	* Applies to $300 < SV_{30} < 850$ ml

In establishing the relationships between the sludge settleability parameters SVI, $SSVI_{3.5}$ or DSVI (generically called the sludge settleability parameter (SSP)) and the flux constants V_o and n, two approaches have been adopted:

1. a stepwise correlation where first the V_o and n values for a particular group of ZSV-X data (with an associated SVI, $SSVI_{3.5}$ or DSVI) is found by a linear regression on $\ln V_s = \ln V_o - nX$ and then, in a second step, the V_o and n values of the data groups are correlated to the set of SVI, $SSVI_{3.5}$ or DSVI data in terms of some relationship describing the form of the V_o-SSP and n-SSP data. Wahlberg and Keinath (1988) criticised this approach and proposed the second approach.

2. In the second approach, the correlation of ZSV (or V_s) on concentration (X) and SSP is done in a single step, taking all the V_s, X and SSP data of the set together without first determining V_o and n of the groups making up the set. However, to do this requires a knowledge of the form of the function between the V_o and n values and the SSP. From their own data, Wahlberg and Keinath established the form of the V_o-SSP and n-SSP functions to be semilog and linear respectively i.e $V_o = \alpha \exp(-\beta * SSP)$ and $n = \gamma + \delta * SSP$ but only for the SVI and $SSVI_{3.5}$ parameters, and confirmed these forms with data from the literature.

   Furthermore, Wahlberg and Keinath adopted the semilog ZSV-X function so that in one step the constants α, β, γ and δ were calculated by multiple least squares correlation on the function ln V_s in terms of X and SSP i.e.

$$V_o = \alpha \exp(-\beta * SSP) \tag{4.1}$$

$$n = \gamma + \delta * SSP \tag{4.2}$$

$$\begin{aligned} V_s &= V_o \exp(-nX) \\ &= \alpha \exp(-\beta * SSP) \exp(-(\gamma+\delta * SSP)X) \end{aligned} \tag{4.3}$$

$$\ln V_s = \ln\alpha - \beta * SSP - \gamma * X - \delta * SSP * X \tag{4.4}$$

All the researchers in Table 4.1 except Wahlberg and Keinath (1988) and Hartel and Popel (1992) adopted the two step approach to establish the relationship between V_s and the X and SSP. However, before the merits of doing the correlation in one or two steps can be compared, it is necessary to confirm the semilog and linear form of the V_o-SSP and n-SSP functions (Equations (4.1) and (4.2)) implied in Equation (4.4). This is done by graphically examining the functions that various researchers have developed in Figure 4.1 to Figure 4.22. Where possible, a number of researchers' data of V_o and n are plotted versus SVI, $SSVI_{3.5}$ and DSVI in the figures. For ease of visual comparison, all the data and functions of V_o and n vs a particular SSP are plotted to the same scale.

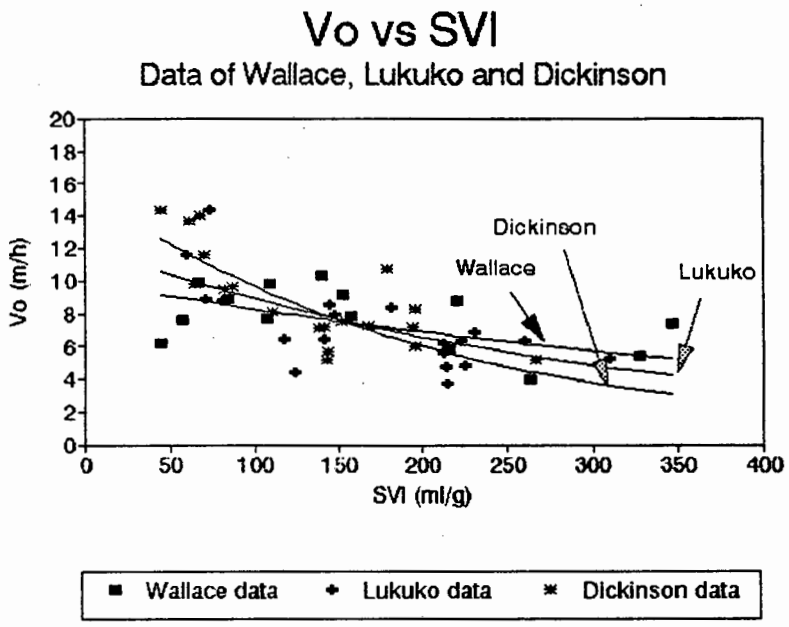

Figure 4.1 V_o **vs SVI data of Wallace, Lukuko and Dickinson**

Wallace: $V_o = 9.394e^{(-0.00134*SVI)}$ $(r^2 = 0.241)$
Lukuko: $V_o = 11.345e^{(-0.00304*SVI)}$ $(r^2 = 0.451)$
Dickinson: $V_o = 18.453e^{(-0.00550*SVI)}$ $(r^2 = 0.473)$

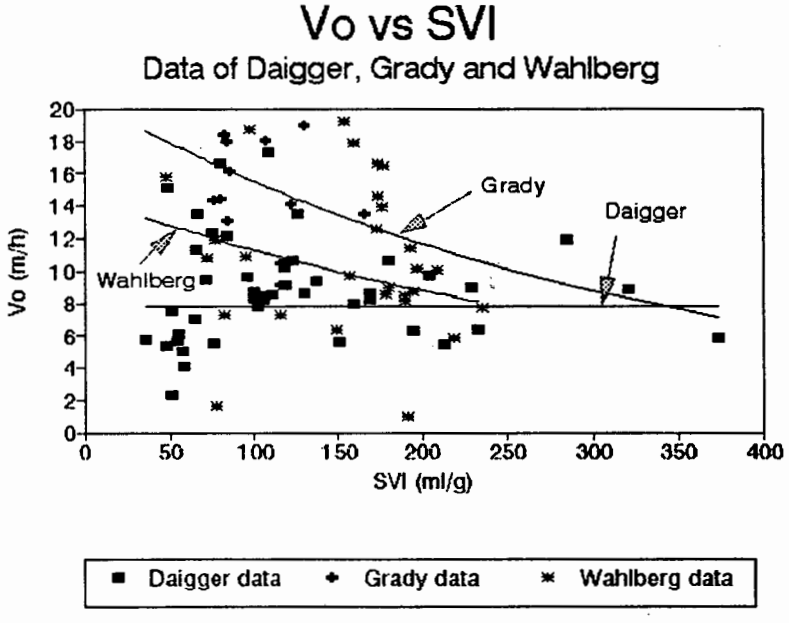

Figure 4.2 V_o **vs SVI data of Daigger, Grady and Wahlberg**

Daigger: $V_o = 7.80$ $(r^2 = \pm 0.89)$ **(after Daigger & Roper (1985))**
Grady: $V_o = 20.610e^{(-0.00285*SVI)}$ $(r^2 = 0.08)$
(after Tuntoolavest & Grady (1982))
Wahlberg: $V_o = 14.484e^{(-0.00250*SVI)}$ $(r^2 = 0.038)$

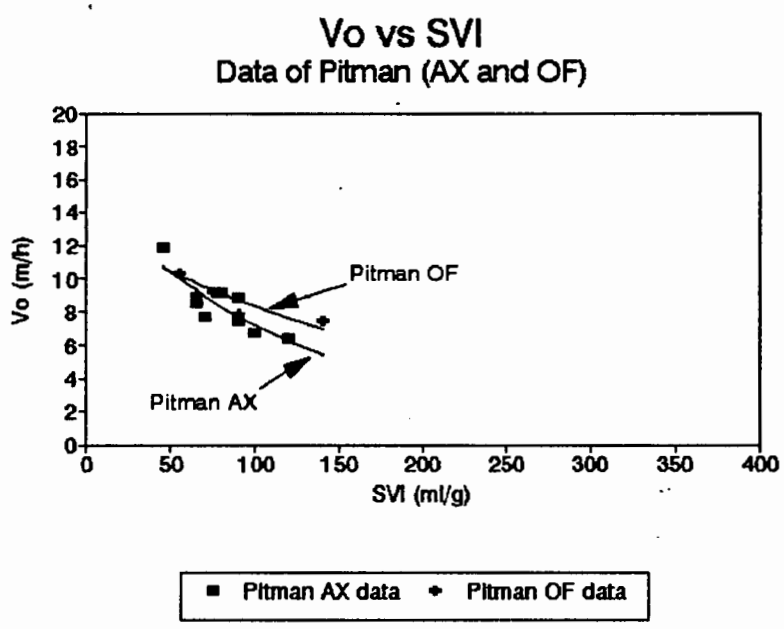

Figure 4.3 V_o vs SVI data of Pitman (AX) and (OF)

Pitman (AX): $V_o = 14.900e^{(-0.00724*SVI)}$ ($r^2 = 0.699$)
Pitman (OF): $V_o = 12.992e^{(-0.00440*SVI)}$ ($r^2 = 0.781$)

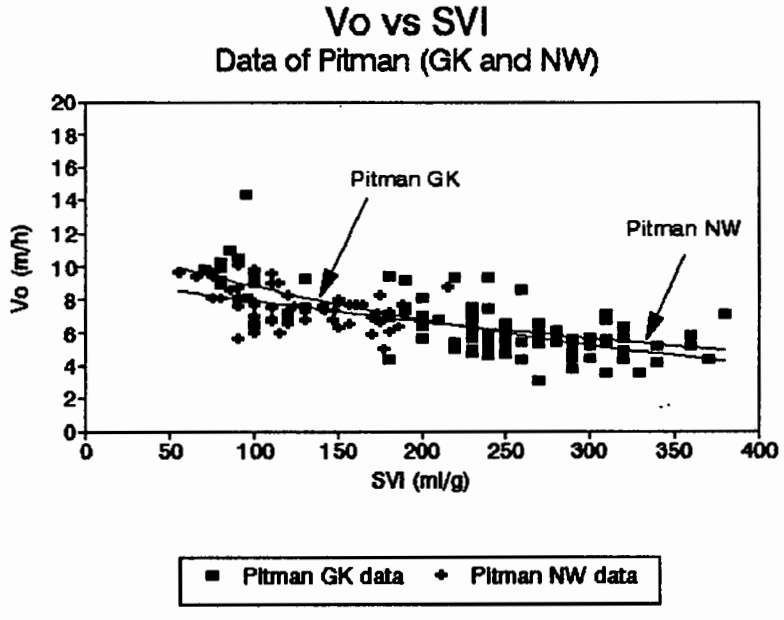

Figure 4.4 V_o vs SVI data of Pitman (GK) and (NW)

Pitman (GK): $V_o = 10.360e^{(-0.00171*SVI)}$ ($r^2 = 0.365$)
Pitman (NW): $V_o = 4.887e^{(-0.00195*SVI)}$ ($r^2 = 0.095$)

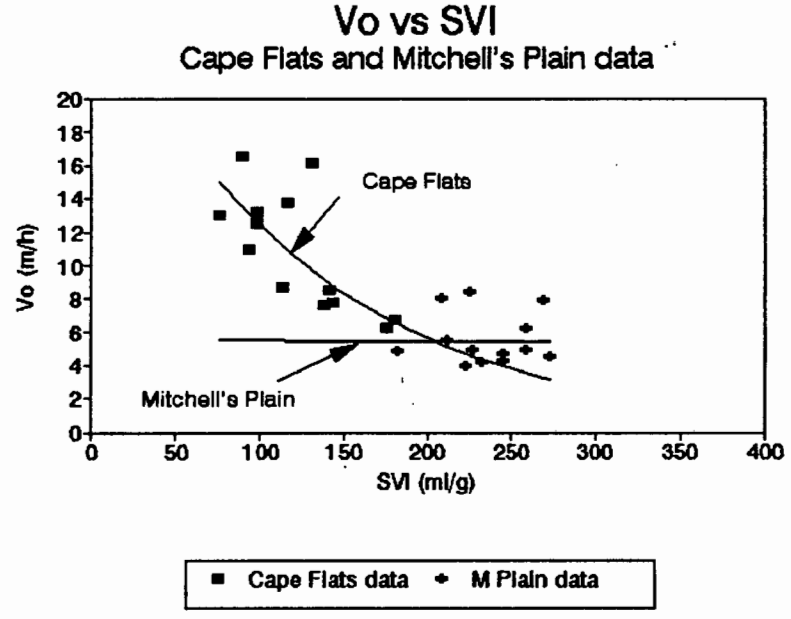

Figure 4.5 V_o vs SVI data from Cape Flats and Mitchell's Plain

Cape Flats: $V_o = 27.406e^{(-0.00791*SVI)}$ $(r^2 = 0.605)$
M Plain: $V_o = 5.557e^{(-0.00012*SVI)}$ $(r^2 = 0.0001)$

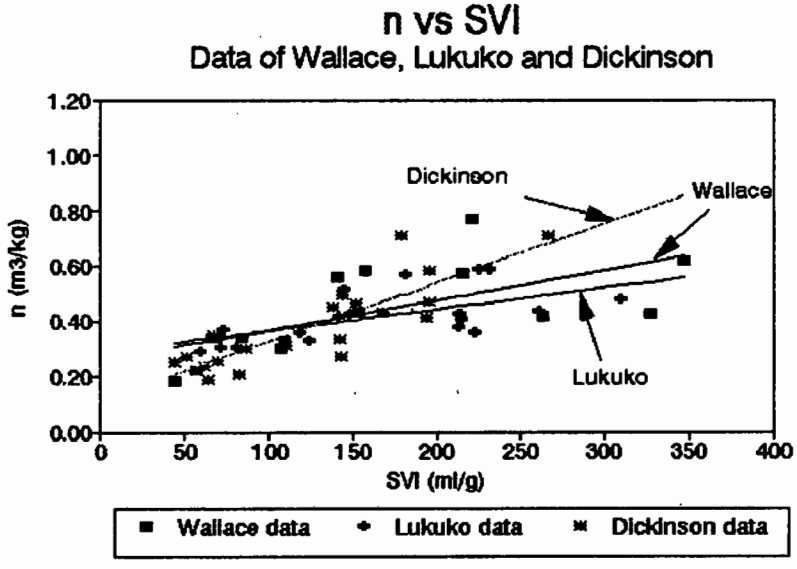

Figure 4.6 n vs SVI data of Wallace, Lukuko and Dickinson

Wallace: $n = 0.257+0.00110*SVI$ $(r^2 = 0.415)$
Lukuko: $n = 0.288+0.00079*SVI$ $(r^2 = 0.386)$
Dickinson: $n = 0.115+0.00214*SVI$ $(r^2 = 0.714)$

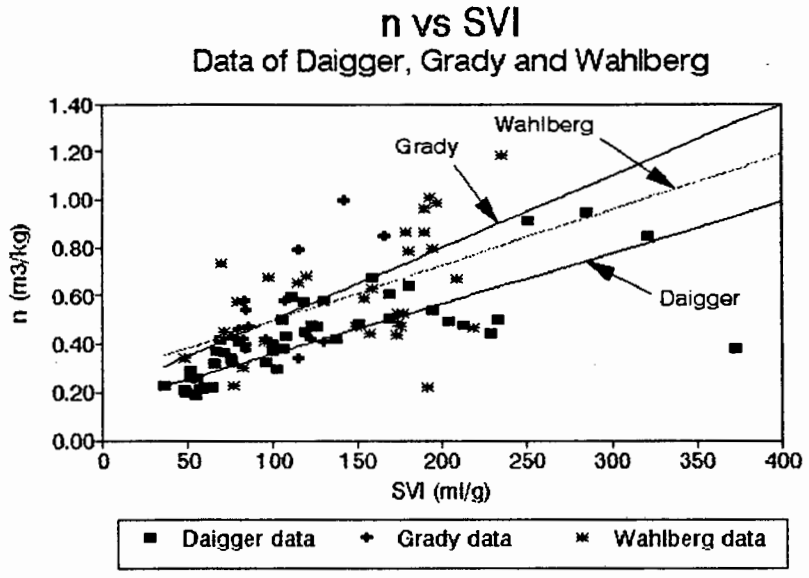

Figure 4.7 n vs SVI data of Daigger, Grady and Wahlberg

Daigger: $n = 0.148+0.00210*SVI$ (r^2 not given)
(after Daigger & Roper (1985))
Grady: $n = 0.201+0.00300*SVI$ ($r^2 = 0.260$)
(after Tuntoolavest & Grady (1982))
Wahlberg: $n = 0.267+0.00230*SVI$ ($r^2 = 0.257$)

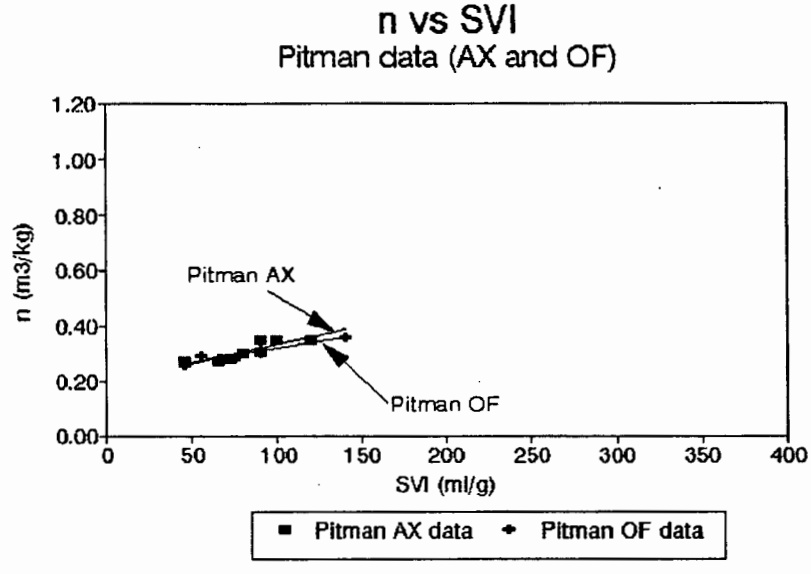

Figure 4.8 n vs SVI data of Pitman (AX) and (OF)

Pitman (AX): $n = 0.218+0.00107*SVI$ ($r^2 = 0.578$)
Pitman (OF): $n = 0.219+0.00103*SVI$ ($r^2 = 0.807$)

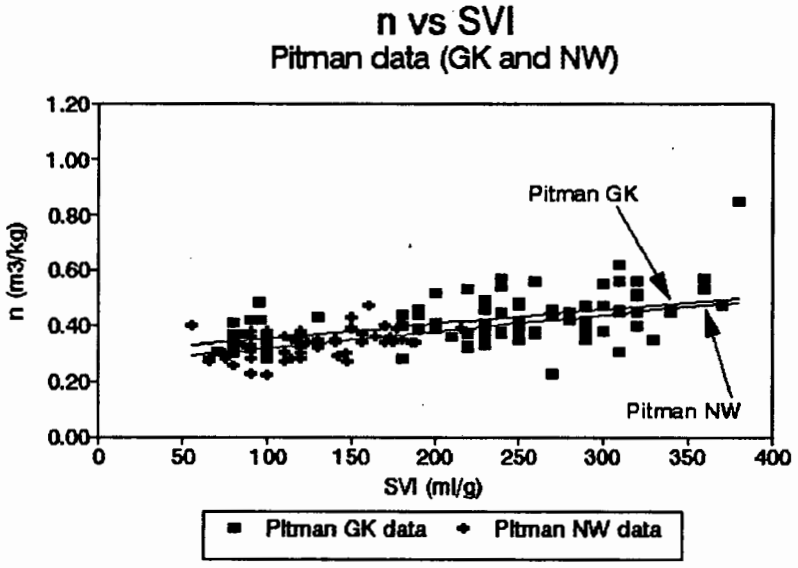

Figure 4.9 n vs SVI data of Pitman (GK) and (NW)

Pitman (GK): $n = 0.413+0.00340*SVI$ ($r^2 = 0.249$)
Pitman (NW): $n = 0.139+0.00124*SVI$ ($r^2 = 0.700$)

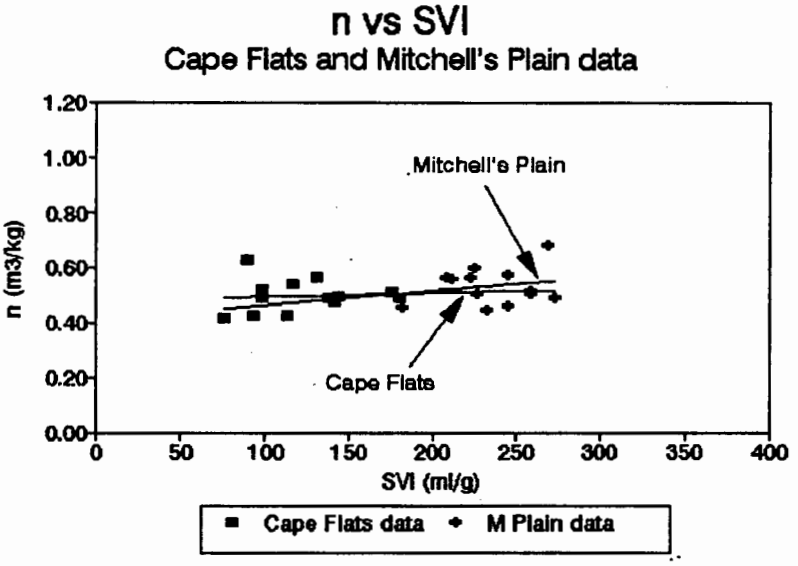

Figure 4.10 n vs SVI data from Cape Flats and Mitchell's Plain

Cape Flats: $n = 0.483+0.00014*SVI$ ($r^2 = 0.006$)
M Plain: $n = 0.403+0.00055*SVI$ ($r^2 = 0.049$)

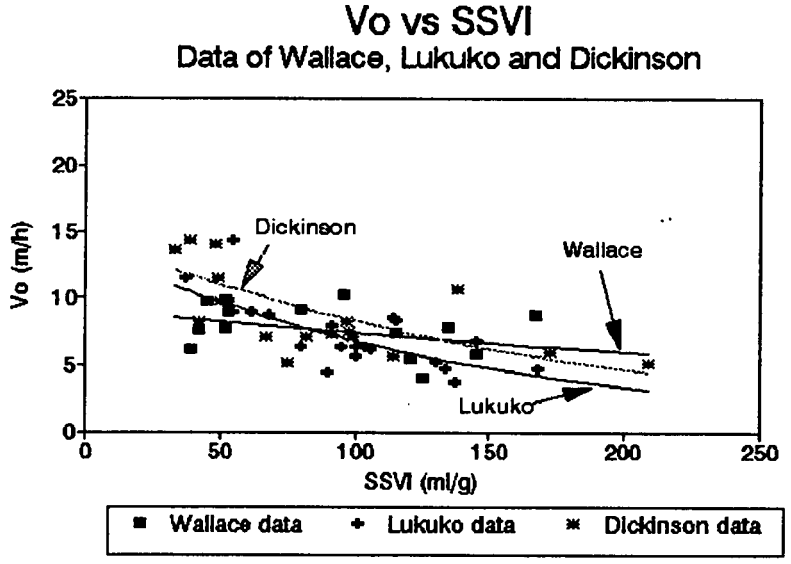

Figure 4.11 V_o vs SSVI data of Wallace, Lukuko and Dickinson

Wallace: $V_o = 9.107e^{(-0.00208*SSVI3.5)}$ $(r^2 = 0.117)$
Lukuko: $V_o = 13.761e^{(-0.00208*SSVI3.5)}$ $(r^2 = 0.524)$
Dickinson: $V_o = 14.649e^{(-0.00569*SSVI3.5)}$ $(r^2 = 0.295)$

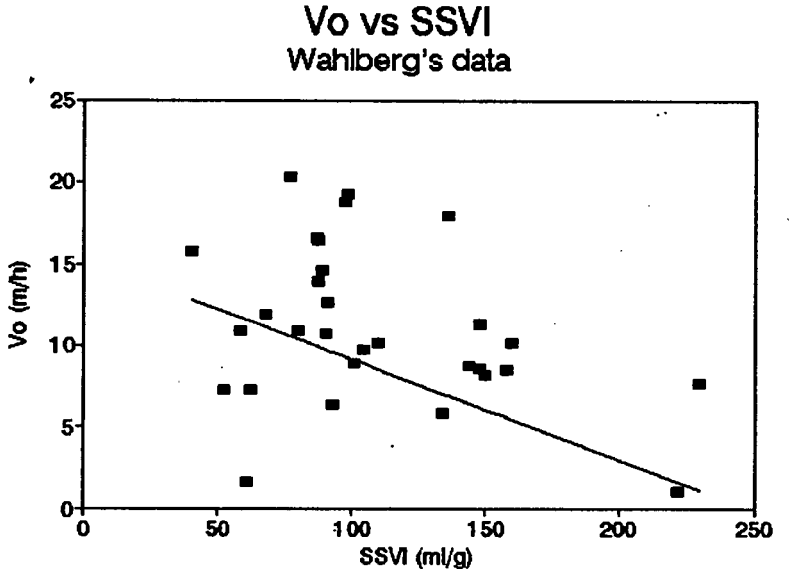

Figure 4.12 V_o vs SSVI data of Wahlberg

Wahlberg: $V_o = 15.3-0.0615*SSVI_{3.5}$
(after Wahlberg & Keinath (1988))

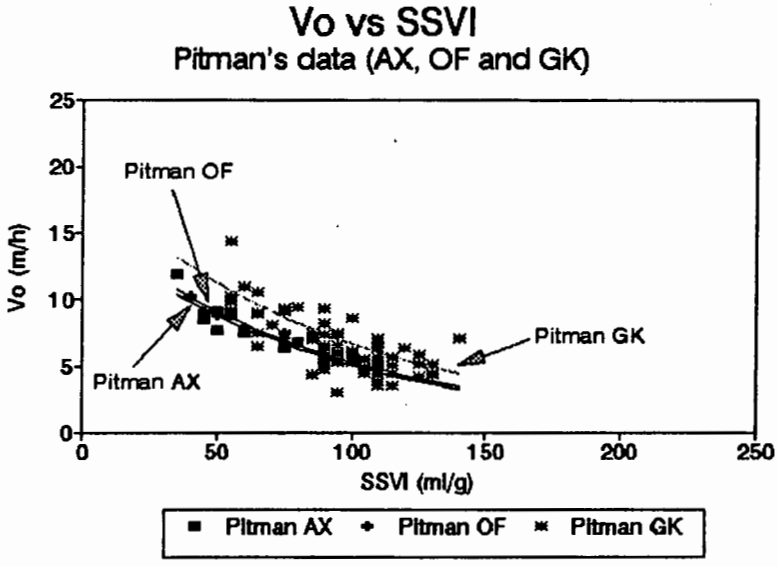

Figure 4.13 **V_o vs SSVI data of Pitman (AX), (OF) and (GK)**

Pitman (AX): $V_o = 15.405e^{(-0.01114*SSVI3.5)}$ $(r^2 = 0.778)$
Pitman (OF): $V_o = 15.695e^{(-0.01085*SSVI3.5)}$ $(r^2 = 0.846)$
Pitman (GK): $V_o = 18.936e^{(-0.01042*SSVI3.5)}$ $(r^2 = 0.713)$

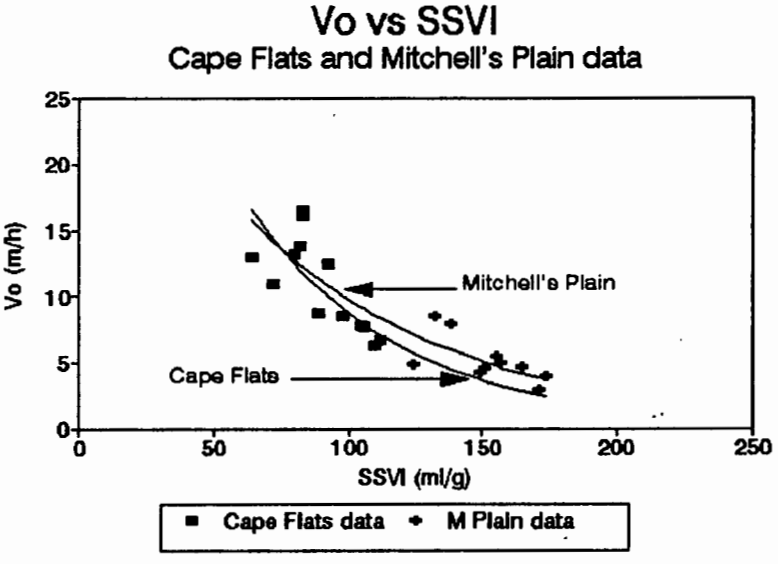

Figure 4.14 **V_o vs SSVI data from Cape Flats and Mitchell's Plain**

Cape Flats: $V_o = 51.469e^{(-0.01769*SSVI3.5)}$ $(r^2 = 0.638)$
M Plain: $V_o = 36.856e^{(-0.01322*SSVI3.5)}$ $(r^2 = 0.473)$

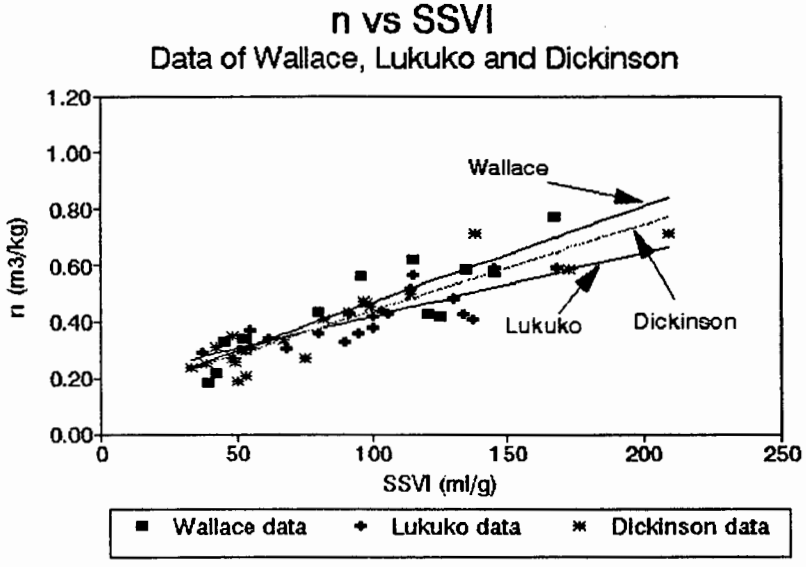

Figure 4.15 n vs SSVI data of Wallace, Lukuko and Dickinson

Wallace: $n = 0.130+0.00340*SSVI_{3.5}$ $(r^2 = 0.798)$
Lukuko: $n = 0.195+0.00225*SSVI_{3.5}$ $(r^2 = 0.686)$
Dickinson: $n = 0.136+0.00304*SSVI_{3.5}$ $(r^2 = 0.843)$

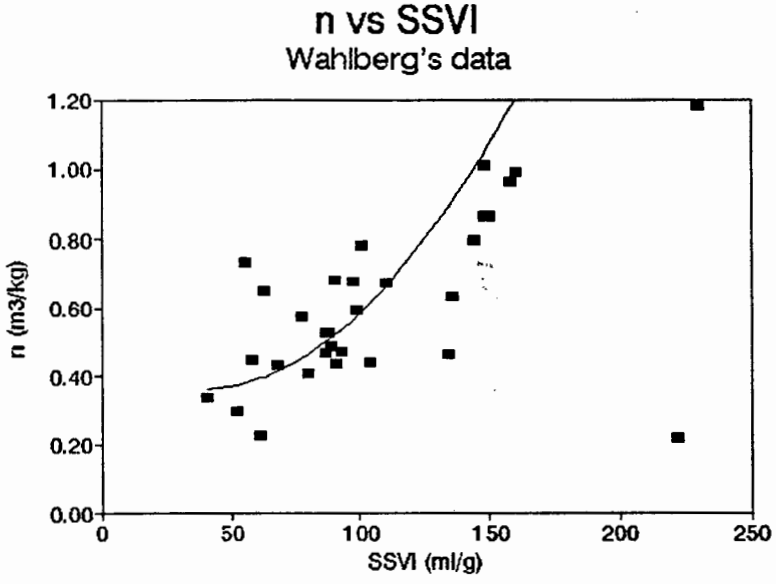

Figure 4.16 n vs SSVI data of Wahlberg

Wahlberg: $n = 0.426-0.00384*SSVI_{3.5}+0.0000543*SSVI_{3.5}^2$
(r^2 not given) (after Wahlberg & Keinath (1988))

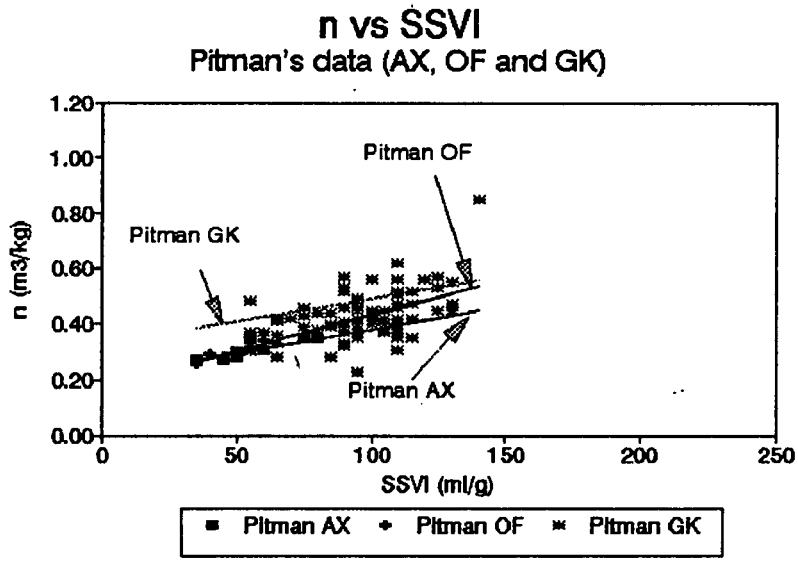

Figure 4.17 **n vs SSVI data of Pitman (AX), (OF) and (GK)**

Pitman (AX): $n = 0.213+0.00166*SSVI_{3.5}$ $(r^2 = 0.593)$
Pitman (OF): $n = 0.171+0.00261*SSVI_{3.5}$ $(r^2 = 0.931)$
Pitman (GK): $n = 0.328+0.00163*SSVI_{3.5}$ $(r^2 = 0.272)$

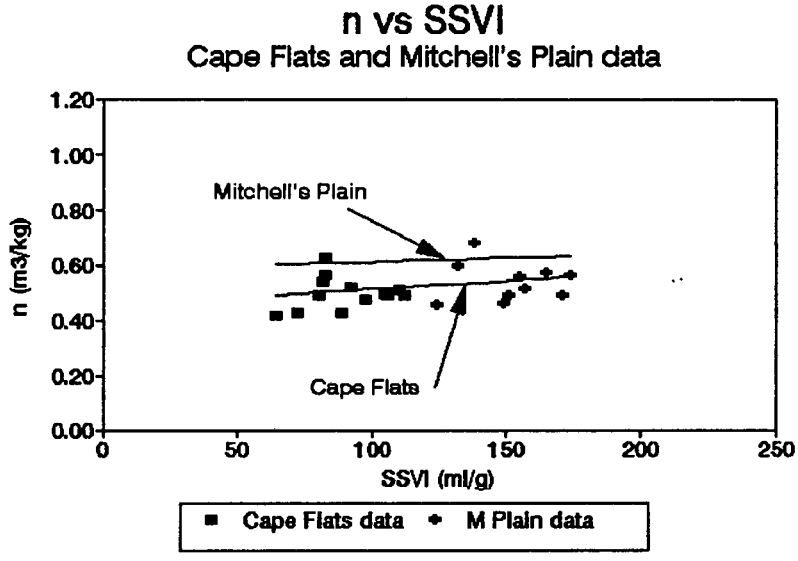

Figure 4.18 **n vs SSVI data from Cape Flats and Mitchell's Plain**

Cape Flats: $n = 0.445+0.00060*SSVI_{3.5}$ $(r^2 = 0.024)$
M Plain: $n = 0.585+0.00029*SSVI_{3.5}$ $(r^2 = 0.005)$

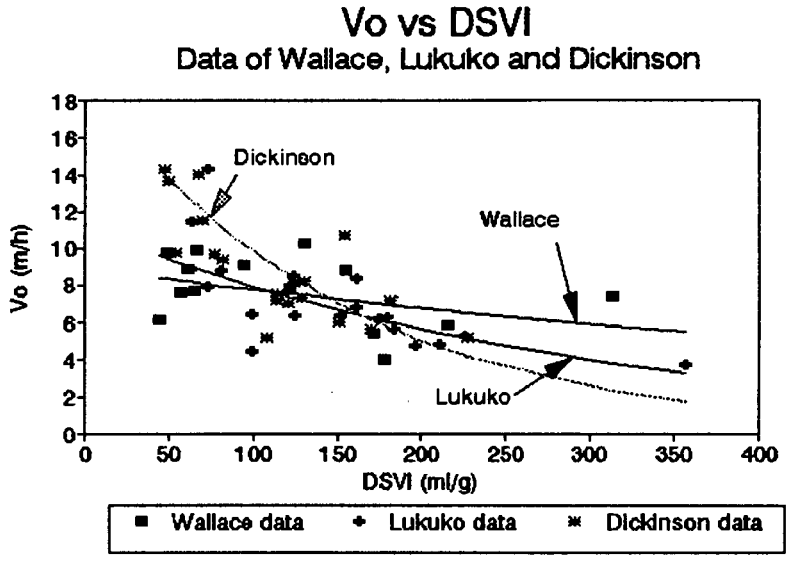

Figure 4.19 **V_o vs DSVI data of Wallace, Lukuko and Dickinson**

Wallace: $V_o = 8.918e^{(-0.00136*DSVI)}$ $(r^2 = 0.157)$
Lukuko: $V_o = 11.145e^{(-0.00339*DSVI)}$ $(r^2 = 0.573)$
Dickinson: $V_o = 19.230e^{(-0.00669*DSVI)}$ $(r^2 = 0.461)$

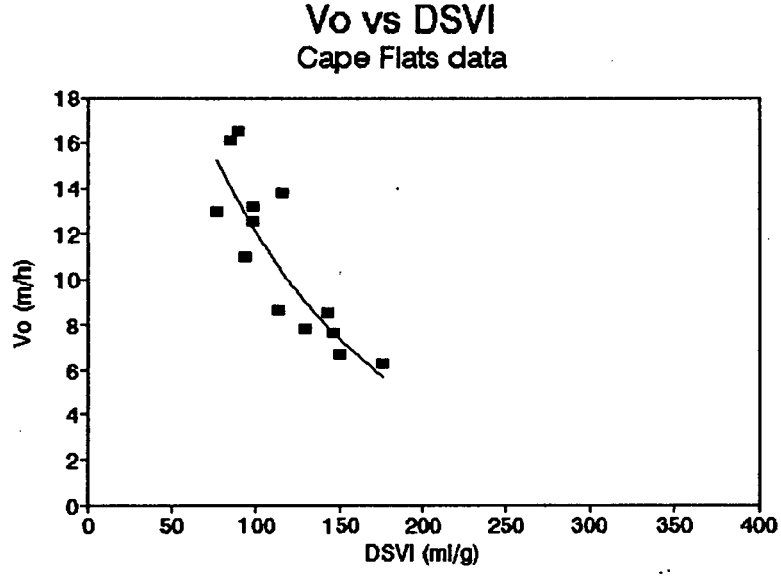

Figure 4.20 **n vs DSVI data of Wallace, Lukuko and Dickinson**

Cape Flats: $V_o = 32.249e^{(-0.00985*DSVI)}$ $(r^2 = 0.842)$

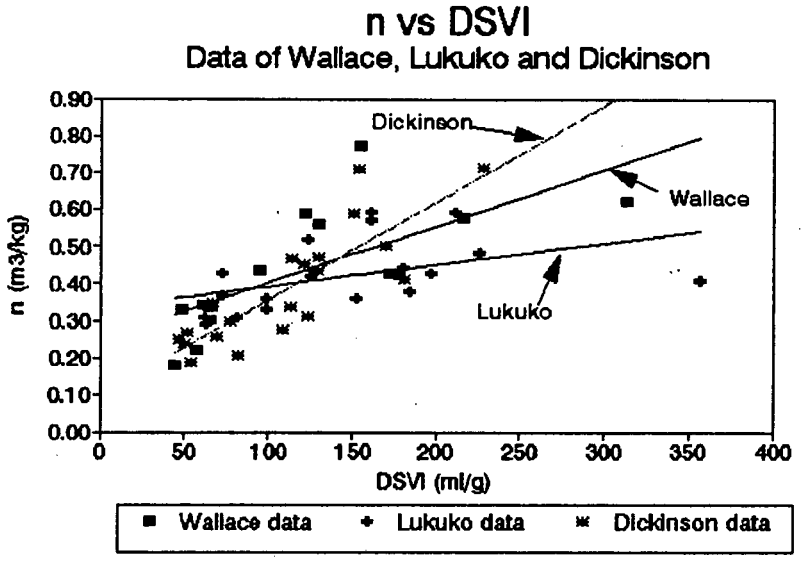

Figure 4.21 V_o **vs DSVI data from Cape Flats**

Wallace: $n = 0.250+0.00152*DSVI$ $(r^2 = 0.502)$
Lukuko: $n = 0.335+0.00058*DSVI$ $(r^2 = 0.215)$
Dickinson: $n = 0.097+0.00261*DSVI$ $(r^2 = 0.698)$

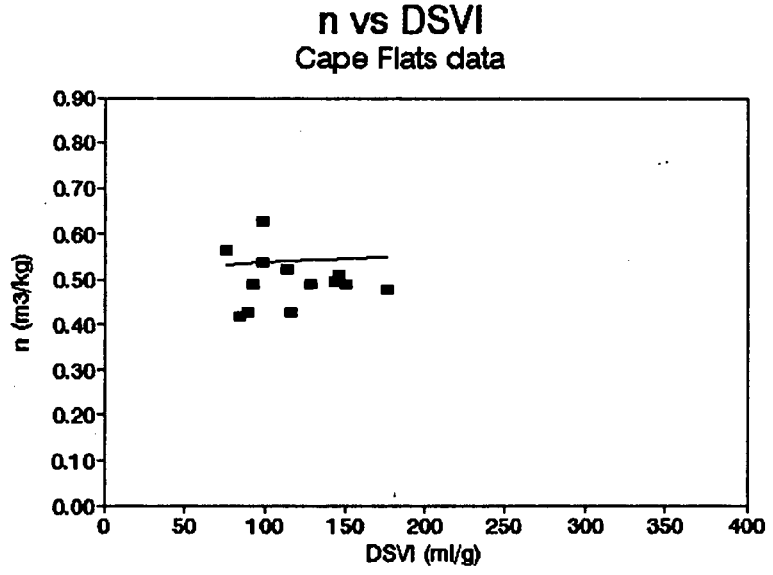

Figure 4.22 **n vs DSVI data from Cape Flats**

Cape Flats: $n = 0.520+0.00018*DSVI$ $(r^2 = 0.009)$

From Figure 4.1 to Figure 4.22, it is apparent that, although different researchers obtain different lines, in all cases the V_o - SSP data show the trend of decreasing V_o

with increasing SSP and the n - SSP trend of increasing n with increasing SSP. While in some cases the trend is a constant value of V_o or n with increasing SSP (e.g. the V_o - SVI data of Daigger), in no cases is the opposite trend apparent. With regard to the form of the trends for V_o and n respectively, it would appear that for V_o the trend is curvilinear and for n the trend is linear. It is interesting to note that, from a statistical analysis of their own data, Keinath and Wahlberg found that for the SVI, linear V_o-SVI and n-SVI functions were better than curvilinear (parabolic) ones and that an alternate parabolic form for the V_o - SVI function could not be confirmed (see Table 4.1). For the $SSVI_{3.5}$, both a linear and a parabolic form for the V_o-$SSVI_{3.5}$ function could be confirmed. Also, a curvilinear (parabolic) n-$SSVI_{3.5}$ function was confirmed but it was not stated whether a linear function also could be used. Therefore, from Wahlberg and Keinath's own $SSVI_{3.5}$ data, no positive identification of the form for the V_o-$SSVI_{3.5}$ and n-$SSVI_{3.5}$ functions could be established.

For this investigation, the $SSVI_{3.5}$ was identified as the more important settleability parameter: firstly, because it is more reliable than the SVI; and secondly because the available data set for $SSVI_{3.5}$ is much larger than that for DSVI. It was therefore considered to be most important that the correct form of the V_o-$SSVI_{3.5}$ and n-$SSVI_{3.5}$ functions be identified. From the data presented in Figure 4.1 to Figure 4.22 and statistical analysis performed on these, it was concluded that the semilog and linear forms for the two functions respectively, in conformity with Equations (4.1) and (4.2), could be accepted. These functional forms were also accepted for the SVI and DSVI. The semilog form for the V_o-SSP gives the curvilinearity required without introducing additional constants as would be the case with a parabolic function. Also, for the cases where V_o is approximately constant with increasing SSP, this could be accommodated by small to zero values of β (see Equation (4.1)). Consequently, the semilog (or exponential) form provides a large degree of flexibility with the α and β constants it introduces. With regard to the linear form for the n-SSP curve, most of the data sets gave good correlations with the linear function, and for those cases where the data appeared curvilinear in trend, the correlation coefficient was not significantly improved with a linear function (e.g. Wahlberg and Keinath $SSVI_{3.5}$ data, Figure 4.16).

However, because of the possibility that not all the data sets might conform to the form of the exponential and linear functions, it was recognised that the different data sets cannot be randomly pooled in order to determine the constants in the various functions relating the SSP to the α, β, γ and δ. Therefore, statistical tests were undertaken to examine whether or not different data sets could be legitimately pooled. However, no further statistical analysis of the semilog V_o-SSP and linear n-SSP functions were undertaken, these being accepted as the most appropriate forms for the purposes of this investigation. Once the forms of the relationships were established, the benefit of the single step correlation to determine α, β, γ and δ simultaneously in Equation (4.4) was compared to the two step correlation in which with V_o and n are calculated first.

Because, for this investigation, dynamic simulation of the settling tank based on the flux theory was the principal objective, the particular parameters of interest are V_o and n, the two flux theory constants in the semilog relationship. Thus, the overall objective of this statistical work was to collect all the available data and to create the largest possible single data set (bearing in mind the constraints on pooling mentioned below) for SVI, $SSVI_{3.5}$ and DSVI respectively. From these data sets, the objective was to develop a set of functional relationships from which the flux theory constants V_o and n can be determined with a knowledge of any one of the three settleability parameters (SVI, $SSVI_{3.5}$ and DSVI). This would enable any available data specifying only one settleability parameter to be reliably transformed by means of these functions into the form appropriate for use with the flux theory. In addition, if it is possible to establish relationships between the settleability parameters, it will be possible to use the flux theory design and operating chart with $SSVI_{3.5}$ or DSVI measurements and also to compare the various design procedures based on the different settleability parameters. Because these measurements are much simpler than the ZSV-X measurements, they are more appropriate measures for settleability in the field and would make the flux theory more accessible for use in practice. It follows that the functional relationships could also be used in reverse with the result that it is possible to choose any design

procedure and it is no longer necessary to be confined to a particular one because of the information available.

4.3 THE DATA SETS

The sludge settleability data measured by numerous researchers at a number of different wastewater treatment plants was collected either from the publication, if included, or directly from the researchers when these were not given in the published papers. Each data set comprises a group of concentration (X) and settling velocity (V_s) measurements with its associated single value for the sludge settleability parameters SVI, $SSVI_{3.5}$ and/or DSVI. For purposes of clarity, an example is illustrated below in Table 4.2. The data in the example is the SVI and $SSVI_{3.5}$ data set measured by Pitman (1984) at the Alexandra plant. The flux theory constants V_o and n can be calculated by least squares regression for each group from the V_s-X measurements (step 1 of the double step correlation) as indicated in Table 4.2. Because only one value of V_o and n is obtained for each group, the number of points in the set is reduced to the number of groups for the V_o and n on SSP correlation to obtain α, β, γ and δ (step 2 of the double step correlation). For the single step correlation, the α, β, γ and δ values are determined simultaneously using all the data points of the set at once. The single step regression yields a multiple correlation coefficient (r^2) as part of the least squares analysis. The double step method gives a multiple correlation coefficient (r^2) for each step which cannot be compared with the single step r^2 value. For comparison purposes, an equivalent single step multiple correlation coefficient (r^2) for the double step method was calculated by substituting the α, β, γ and δ values obtained via the double step method into Equation (4.4) and calculating the r^2 values as if these substituted values were obtained in a single step.

Table 4.2 The SVI and $SSVI_{3.5}$ data set collected by Pitman at the Alexandra plant (AX)

Group	Run	Data	SVI	$SSVI_{3.5}$	X	Vs	ln Vs	V_o	n	r^2
			($ml g^{-1}$)	($ml g^{-1}$)	($kg m^{-3}$)	($m h^{-1}$)	($m h^{-1}$)	($m h^{-1}$)	($m^3 kg^{-1}$)	
1	AX2	1	100	80	1.27	4.59	1.52			
	AX2	2	100	80	1.27	1.72	0.54			
	AX2	3	100	80	1.27	1.40	0.34			
	AX2	4	100	80	1.27	0.67	-0.40			
	AX2	5	100	80	1.27	0.44	-0.82			
	AX2	6	100	80	1.27	0.31	-1.17	6.74	0.35	0.941
2	AX3	1	90	55	1.03	7.66	2.04			
	AX3	2	90	55	1.97	4.93	1.60			
	AX3	3	90	55	3.35	2.34	0.85			
	AX3	4	90	55	3.74	1.89	0.64			
	AX3	5	90	55	5.00	1.45	0.37			
	AX3	6	90	55	6.33	0.73	-0.31			
	AX3	7	90	55	7.70	0.65	-0.43			
	AX3	8	90	55	8.68	0.48	-0.73			
	AX3	9	90	55	10.7	0.20	-1.61	8.84	0.35	0.942
3	AX4	1	120	75	1.43	4.84	1.58			
	AX4	2	120	75	2.73	2.33	0.85			
	AX4	3	120	75	3.83	2.25	0.81			
	AX4	4	120	75	4.06	1.38	0.32			
	AX4	5	120	75	6.04	0.71	-0.34			
	AX4	6	120	75	6.79	0.79	-0.24			
	AX4	7	120	75	7.23	0.59	-0.53			
	AX4	8	120	75	7.97	0.58	-0.54	6.44	0.32	0.943
4	AX5	1	90	60	2.05	4.68	1.54			
	AX5	2	90	60	2.79	3.30	1.19			
	AX5	3	90	60	5.38	1.19	0.17			
	AX5	4	90	60	6.72	0.79	-0.24			
	AX5	5	90	60	10.4	0.36	-1.02	7.48	0.31	0.995
5	AX6	1	45	50	1.69	7.99	2.08			
	AX6	2	45	50	2.77	5.70	1.74			
	AX6	3	45	50	3.50	4.43	1.49			
	AX6	4	45	50	6.11	2.23	0.80			
	AX6	5	45	50	6.79	1.65	0.50			
	AX6	6	45	50	10.5	0.74	-0.30			
	AX6	7	45	50	10.7	0.64	-0.45	11.89	0.27	0.960
6	AX7	1	80	45	1.35	7.73	2.05			
	AX7	2	80	45	2.08	6.11	1.81			
	AX7	3	80	45	4.86	1.90	0.64			
	AX7	4	80	45	5.02	2.14	0.76			
	AX7	5	80	45	5.42	1.80	0.59			
	AX7	6	80	45	5.70	1.26	0.23			
	AX7	7	80	45	6.86	0.81	-0.21			
	AX7	8	80	45	7.53	1.05	0.05			
	AX7	9	80	45	11.3	0.37	-0.99			
	AX7	10	80	45	11.6	0.37	-0.99	9.15	0.29	0.948
7	AX8	1	65	50	1.58	6.76	1.91			
	AX8	2	65	50	2.57	4.86	1.58			
	AX8	3	65	50	4.25	2.92	1.07			
	AX8	4	65	50	5.60	1.62	0.48			
	AX8	5	65	50	6.09	1.47	0.39			
	AX8	6	65	50	7.82	0.98	-0.02			
	AX8	7	65	50	9.28	0.61	-0.49			
	AX8	8	65	50	9.43	0.59	-0.53			
	AX8	9	65	50	11.3	0.46	-0.78			
	AX8	10	65	50	13.5	0.31	-1.17	8.54	0.27	0.965

Table 4.2 (cont) The SVI and $SSVI_{3.5}$ data set collected by Pitman at the Alexandra plant (AX)

Group	Run	Data	SVI ($ml g^{-1}$)	$SSVI_{3.5}$ ($ml g^{-1}$)	X ($kg m^{-3}$)	V_s ($m h^{-1}$)	ln Vs ($m h^{-1}$)	V_o ($m h^{-1}$)	n ($m^3 kg^{-1}$)	r^2
8	AX9	1	70	35	1.65	5.84	1.76			
	AX9	2	70	35	3.10	3.43	1.23			
	AX9	3	70	35	4.38	2.05	0.72			
	AX9	4	70	35	5.63	1.60	0.47			
	AX9	5	70	35	6.35	1.09	0.09			
	AX9	6	70	35	7.18	0.94	-0.06			
	AX9	7	70	35	8.63	0.65	-0.43			
	AX9	8	70	35	9.77	0.52	-0.65			
	AX9	9	70	35	10.9	0.47	-0.76			
	AX9	10	70	35	12.8	0.22	-1.51	7.68	0.28	0.950
Total 8		Total 65								

Note that in Table 4.2, 65 data points are available for the single step correlation (SSP and X vs V_s), but these become reduced to only 8 groups for the second step of the double step correlation (V_o and n vs SSP).

A summary of all the data that was collected is presented in Table 4.3. For reference purposes, the data sets have been labelled with the name of the researcher, or the site at which the data was collected, whichever is more convenient. Table 4.3 lists 16 data sets for which ZSV-X data was measured. Four of the sets (these are listed at the bottom of the table) were rejected because either (i) the individual ZSV-X data could not be obtained or (ii) the ZSV-X data were measured over too narrow a range. Of the remaining 12 sets, all 12 were useful for establishing the V_s relationship in terms of the SVI, but for the $SSVI_{3.5}$ and the DSVI only eight and four data sets respectively included the measurements for the $SSVI_{3.5}$ and DSVI. The data points (i.e. V_s measurements at some X and SSP) and groups (i.e. number of distinct SSP measurements) in each of the SVI, $SSVI_{3.5}$ and DSVI data sets are give in Table 4.4, Table 4.5 and Table 4.6. Considering the reliability of the different SSP's and the data available for establishing the relationship between V_s and the X and SSP, it is clear that the $SSVI_{3.5}$ is likely to give the best estimates of V_s - it is far superior to the SVI and has a far larger data set than the DSVI.

Table 4.3 Summary of all available data sets

REFERENCE	SETTLEABILITY PARAMETERS MEASURED			
	SVI	**$SSVI_{3.5}$**	**DSVI**	**ZSV-X**
UCT - Western Cape region				
* Lukuko[1]	Yes	Yes	Yes	Yes
* Wallace[1]	Yes	Yes	Yes	Yes
* Dickinson[1]	Yes	Yes	Yes	Yes
* Cape Flats (CF)[2]	Yes	No	Yes	Yes
* Mitchell's Plain (MP)[2]	Yes	Yes	No	Yes
Daigger and Roper (1985)	No	No	No	Yes
Pitman - Johannesburg Region				
* Alexandra (AX)[3]	Yes	Yes	No	Yes
* Olifantsvlei (OF)[3]	Yes	Yes	No	Yes
* Northern Works (NW)[4]	Yes	No	No	Yes
* Goudkoppies (GK)[4]	Yes	Yes	No	Yes
Wahlberg and Keinath (1988)[5]	Yes	Yes	No	Yes
Tuntoolavest and Grady (1982)[6]	Yes	No	No	Yes

1. measured at 15 different plants in the Western Cape: some with, some without primary sedimentation but all with long sludge ages (>20 days) and with N removal, none exhibiting significant P removal
2. CF: a 5 stage Bardenpho plant, not exhibiting P removal
   MP: modified Ludzack - Ettinger plant for N removal
3. AX, OF: both extended aeration (long sludge age, no primary sedimentation), modified for significant biological phosphorus removal
4. NW, GK: both 3/5 stage Bardenpho plants for N and P removal
5. 21 different treatment plants: conventional activated sludge as well as completely mixed, step aeration and contact stabilisation systems. All fully aerobic.
6. Fully aerobic, $2.8 m^{-3} day^{-1}$ pilot plant

ADDITIONAL DATA	SVI	$SSVI_{3.5}$	DSVI	ZSV-X
Koopman and Cadee (1983)[7]	No	No	Yes	Yes
Hartley (1985)[8]	No	Yes	No	Yes
Rachwal *et al* (1982)[8]	No	Yes	No	Yes
STORA (1981)[7]	No	Yes	Yes	Yes

7. ZSV-X data over a very narrow X range ($1-6 gl^{-1}$); rejected
8. No ZSV-X data given, only V_o and n vs $SSVI_{3.5}$; only useful for confirming V_o-$SSVI_{3.5}$ and n-$SSVI_{3.5}$ relationship

Table 4.4 Data sets for SVI values

SET	REFERENCE	NUMBER OF DATA POINTS	NUMBER OF GROUPS
	UCT - Western Cape region		
1	* Lukuko	124	20
2	* Wallace	72	14
3	* Dickinson	94	20
4	* Cape Flats (CF)	64	13
5	* Mitchell's Plain (MP)	76	13
6	Daigger and Roper (1985)	241	47
	Pitman - Johannesburg Region		
7	* Alexandra (AX)	65	8
8	* Olifantsvlei (OF)	248	7
9	* Northern Works (NW)	80	70
10	* Goudkoppies (GK)	249	92
11	Wahlberg and Keinath (1988)	175	31
12	Tuntoolavest and Grady (1982)	60	15

Table 4.5 Data sets for $SSVI_{3.5}$ values

SET	REFERENCE	NUMBER OF DATA POINTS	NUMBER OF GROUPS
	UCT - Western Cape region		
1	* Lukuko	124	20
2	* Wallace	72	14
3	* Dickinson	94	20
4	* Cape Flats (CF)	64	13
5	* Mitchell's Plain (MP)	56	10
	Pitman - Johannesburg Region		
6	* Alexandra (AX)	65	8
7	* Olifantsvlei (OF)	248	7
8	* Goudkoppies (GK)	225	89
9	Wahlberg and Keinath (1988)	175	31

Table 4.6 Data sets for DSVI values

SET	REFERENCE	NUMBER OF DATA POINTS	NUMBER OF GROUPS
	UCT - Western Cape region		
1	* Lukuko	124	20
2	* Wallace	72	14
3	* Dickinson	94	90
4	* Cape Flats (CF)	64	13

4.3.1 POOLING THE DATA SETS

From the data and functions given in Figure 4.1 to Figure 4.22, it can be seen that considerable differences occur between data sets for the same SSP and therefore data sets cannot be randomly pooled to create a single data set. Ideally, it would be most convenient if all 12 data sets for the SVI could be pooled, in which case the measured parameters account for all the positive variability in the V_s. However, in practice, this is unlikely because factors such as plant type, temperature, settled or unsettled influent, etc. may affect the V_s in a way not accounted for by measurements of X and SVI. The same applies to the $SSVI_{3.5}$ and the DSVI, although inter set variability should be less for these parameters because they are better measures of sludge settleability. Nevertheless, the cited factors can have an influence on the data sets such that statistically they cannot be pooled because they originate from different populations.

The statistical tests that need to be carried out to determine whether or not all the data belongs to a single population consist of establishing the answers to the following questions:

1. Can one regression line be fitted to all the data?

2. Are all the sample slopes estimates of the same true slope?

3. Would a regression fitted to the group means be linear?

4. Is the true regression coefficient of the pooled within groups of data equal to the true regression coefficient for the means?

If the answer to all of the above questions is positive, then it can be concluded that the grouped samples all originate from the same population and it is valid to perform a linear regression on the pooled data as a single sample. If not, then linear regression may only be carried out on individual samples. The order in which these tests are performed is very important since the assumptions necessary for the later tests are tested as hypotheses in the earlier tests. The necessary calculations for the above tests are presented in Appendix B. The tests for pooling the data described here do not apply to multi-linear regression and therefore can only be applied to the single step correlations. The results of the statistical pooling test are described in detail under each settleability parameter.

4.4 ESTABLISHING THE CONSTANTS BY MULTIPLE LEAST SQUARES REGRESSION

Having defined the data sets, multiple least squares regression analyses were conducted for the zone settling velocity function in terms of concentration (X) and a sludge settleability parameter (SSP) i.e. Equation (4.4). This was also performed for the double step regression procedure for the SVI, $SSVI_{3.5}$ and DSVI. The results obtained from this statistical analysis for the α, β, γ and δ constants (and therefore also V_o and n via Equations (4.1) and (4.2)) are discussed below.

4.4.1 THE ZONE SETTLING VELOCITY IN TERMS OF SVI

The results obtained by fitting the SVI data to Equation (4.4) with the single and double step methods respectively are listed in Table 4.7 and Table 4.8 respectively.

Table 4.7 Fitted constants for Equation (4.4) SVI data obtained with the single step method

REFERENCE	ln α	β	γ	δ	r^2
Lukuko	2.009951	+0.00101	0.19571	0.00122	0.7822
Wallace	1.82088	-0.00005	0.15355	0.00141	0.8240
Dickinson	2.59644	+0.00438	0.09836	0.00199	0.8409
Daigger	1.80826	-0.00021	0.18169	0.00141	0.8282
Cape Flats	3.35105	+0.00820	0.46845	0.00021	0.9668
M Plain	1.48218	-0.00076	0.35095	0.00072	0.9277
Pitman AX	2.57943	+0.00569	0.18927	0.00141	0.9579
Pitman OF	2.54639	+0.00355	0.30125	-0.00034	0.8888
Pitman GK	2.30565	+0.00160	0.35509	0.00059	0.9124
Pitman NW	1.07376	-0.00478	0.06376	0.00166	0.9563
Wahlberg	2.38040	+0.00496	0.30985	0.00036	0.6408
Grady	4.00338	+0.01641	0.59060	-0.00210	0.6602

A comparison of the two methods is given in Figure 4.23, which shows the multiple regression coefficients (r^2) obtained with the two methods plotted against each other.

From Figure 4.23, the following observations can be made:

1. The Pitman AX, NW and GK and the Mitchell's Plain and Cape Flats data give multiple correlation coefficients greater than 0.9, Pitman OF, Daigger and UCT Dickinson and Wallace data between 0.8 and 0.9 and UCT Lukuko just below 0.8. Wahlberg and Grady data sets yield correlation coefficients of about 0.65 for the single step method and between 0.4 and 0.5 for the double step method.

2. The multiple correlation coefficient (r^2) obtained using the double step method is in no case greater than the correlation coefficient obtained by the single step

Table 4.8 Fitted constants for Equation (4.4) for SVI data obtained with the double step method

REFERENCE	ln α	β	γ	δ	r^2
Lukuko	2.42876	+0.00304	0.28754	0.00079	0.7672
Wallace	2.24012	+0.00134	0.25741	0.00110	0.7707
Dickinson	2.91523	+0.00550	0.11453	0.00214	0.8286
Daigger	2.09053	-0.00062	0.22127	0.00168	0.7432
Cape Flats	3.31076	+0.00791	0.48257	0.00014	0.9658
M Plain	1.71510	+0.00012	0.40248	0.00055	0.9267
Pitman AX	2.70136	+0.00724	0.21762	0.00107	0.9571
Pitman OF	2.56433	+0.00440	0.21939	-0.00103	0.7915
Pitman GK	2.33798	+0.00171	0.41294	0.00034	0.9031
Pitman NW	1.58655	-0.00195	0.13850	0.00124	0.9554
Wahlberg	2.67305	+0.00250	0.26744	0.00230	0.4272
Grady	2.84035	+0.00070	0.09427	0.00425	0.4771

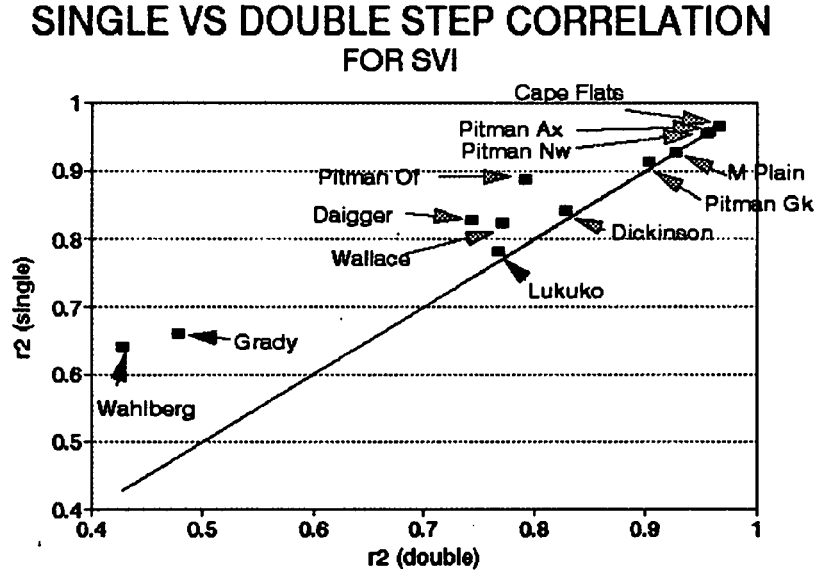

Figure 4.23 Single vs double step methods multiple correlation coefficients for the SVI data

method. This is to be expected, because the least squares fitting technique applied in one step to the data will always yield constants which give the highest possible value of r^2. i.e. it is not possible to choose another set of constants

which give a higher value of r^2. At best, a different set of constants may be found using the double step method which will give the same value of r^2.

3. The difference between the r^2 value generated by the single step correlation and the double step correlation decreases as the value of r^2 increases. In other words, the better the fit, the smaller the difference in r^2 between the single step and double step methods.

Pooling the SVI data

Because the tests for pooling the data apply only to simple linear regression equations, they cannot be applied to the regression lines obtained with the single step method. Instead, they must be carried out in two stages using the two regression lines (one for V_o and one for n) obtained in the double step method. Pooling the data was carried out by a trial and error procedure. Selected groups of samples were pooled and then the hypothesis that they originated from the same population was tested. This was achieved by calculating the F statistics for the regression line (F_1), the slope (F_2), the regression of the group means (F_3) and the within groups regression coefficient (F_4) as described in Appendix B. The critical F statistics were found from a standard table of cumulative F distribution with degrees of freedom υ_1 and υ_2, where υ_1 and υ_2 are different for each F statistic and are defined in Appendix B. If each of the calculated F statistics are less than each of the critical F statistics, then it can be concluded that each of the respective hypotheses outlined in Section 4.2.1 are valid. If not, then the hypotheses must be rejected. This process was carried out separately for the V_o data and the n data. In order for the hypothesis to be accepted i.e. the data sets may be pooled, it needed to be shown via the F statistics that both the V_o and n data groups individually complied with the F statistics for corresponding pooled sets.

On the above basis, the biggest possible sample of SVI data that could legitimately be pooled was one comprising the sets given in Table 4.9 i.e. all the Pitman data sets with the Wallace set. One of the data points in the Wallace set was rejected as an

outlier, reducing the number of data groups to 13 for this set. The pooled sample then consisted of one set containing 190 groups of SVI and V_o and n pairs from a total number of 713 V_s-X data points. The F statistics for pooling on the basis of V_o and for pooling on the basis of n were calculated separately and the results are illustrated in Table 4.9. Only those sets where both the V_o and n based F statistics satisfied the critical F statistics were pooled. The others were rejected on the basis of not satisfying the critical F statistics for either the V_o or n data groups.

Table 4.9 F factors for the pooled SVI data set

PITMAN FAMILY WALLACE PITMAN ALEXANDRA OLIFANTSVLEI GOUDKOPPIES NORTHERN WORKS			V_o		n	
	v_1	v_2	F calculated	F critical	F calculated	F critical
F_1	8	180	1.538	1.94	1.699	1.94
F_2	4	180	2.178	2.37	1.500	2.37
F_3	3	184	0.748	2.60	2.119	2.60
F_4	1	184	1.504	3.84	1.158	3.84

The trial and error pooling statistical tests showed that the data sets collected by Lukuko, Dickinson, Daigger, Wahlberg, Grady and the Cape Flats and the Mitchell's Plain data could not be pooled in any combination and it was concluded that each had to be treated individually. It was curious to note that the Wallace set could be pooled together with the four Pitman sets, while the Lukuko and Dickinson sets could not, even though the latter two sets were measured on the same 15 Western Cape Plants, although one and two years later respectively. That the other sets could not be pooled seems reasonable in that the Wahlberg and Daigger sets were measured at different plants and the Cape Flats and Mitchell's Plain sets were both measured at the same plant over a 10 week period and therefore are fairly narrow in SVI or V_o and n range.

The pooled set comprising all the data collected by Pitman at the Alexandra (AX), Olifantsvlei (OF), Goudkoppies (GK) and Northern Works (NW) plants and that collected by Wallace was called the Pitman family because it principally comprises his data and comprises a total of 713 points of SVI, V_s and X measurements. The pooled set was then subjected to a linear regression analysis (Equation (4.4)) with the single step method. The constants, multiple correlation coefficient and significance levels set out in Table 4.10 were obtained.

Table 4.10 Constants, multiple correlation coefficient and significance levels for the pooled set of SVI data

REFERENCE	ln α	β	γ	δ	r^2
Pitman Family	2.14370	0.00165	0.20036	0.00091	0.8418
Significance level*	<0.001	<0.001	<0.001	<0.001	

* where the significance levels of the intercept and each of the slopes indicates each of their contributions to the multiple correlation coefficient. A small significance level indicates a large contribution i.e. if one of these parameters was excluded from the regression, then the multiple correlation coefficient would decrease significantly.

All t values for the estimates of the fitted constants (α,β,γ and δ) were found to be greater than the critical t values, indicating that the null hypothesis (that there is no relationship between the selected variables and the settling velocity) can be rejected. These t values give significance levels that are all <0.001, indicating that at the 99.9% level, all terms in the regression are significant. The F ratio for the full regression is F = 1259.73. This indicates that, on the basis of a risk of a 5% error (i.e. in only 5% of similar cases will the conclusion be wrong), the least squares equation is a good predictor because the calculated F value is greater than the tabulated F value F(3,710,0.95) = 2.6.

The fitted constants α,β,γ and δ calculated by the single step method for the remaining data sets that could not be pooled and needed to be treated individually are detailed in

Table 4.11. Table 4.12 shows the significance levels for each of the constants α,β,γ and δ.

Table 4.11 Fitted constants for SVI obtained using the single step method for the unpooled groups

REFERENCE	ln α	β	γ	δ	r^2
Lukuko	2.009951	0.00101	0.19571	0.00122	0.782
Dickinson	2.59644	0.00438	0.09836	0.00199	0.841
Daigger	1.80826	-0.00021	0.18169	0.00141	0.828
Cape Flats	3.35105	0.00820	0.46845	0.00021	0.967
M Plain	1.48218	-0.00076	0.35095	0.00072	0.928
Wahlberg	2.38040	0.00496	0.30985	0.00036	0.641
Grady	4.00338	0.01641	0.59060	-0.00210	0.660

Table 4.12 Significance levels for the fitted constants of the unpooled SVI groups

REFERENCE	ln α SIG. LEVEL	β SIG. LEVEL	γ SIG. LEVEL	δ SIG. LEVEL	
Lukuko	<0.001	0.647	<0.001	<0.001	*
Dickinson	<0.001	<0.001	0.002	<0.001	
Daigger	<0.001	0.79	<0.001	<0.001	*
Cape Flats	<0.001	<0.001	<0.001	0.603	*
M Plain	0.046	0.799	0.055	0.656	*
Wahlberg	<0.001	0.006	<0.001	0.187	*
Grady	<0.001	0.143	<0.001	0.152	*

The data sets that have been marked by an asterix in Table 4.12 are those that have high significance levels for one or more of the fitted constants. For the Lukuko and Daigger sets, for example, the significance levels for β are 0.647 and 0.79 respectively, indicating that the β term contributes little to the multiple regression coefficient. In other words, the β term in Equation (4.4) is superfluous for these data sets, and the equation should rather be formulated as:

$$\ln V_s = \ln\alpha - \gamma * X - \delta * SVI * X \qquad (4.5)$$

From Equation (4.1), it can be seen that, with the β term removed, the V_o value is constant with increasing SVI. This outcome corresponds to that of Daigger and Roper (1985), who also found from their data that V_o is independent of SVI at $7.8mh^{-1}$. Even though the Lukuko data show the same characteristics as the Daigger data, it was found that these two data sets could not be pooled. This is because, although the form of the regression lines for the two data sets should be the same, the magnitude of the constants describing the lines are significantly different. For more obvious reasons, the remaining data sets in Table 4.12 could not be pooled because each shows different combinations of terms that are not significant in the correlation. It is interesting to note from Table 4.11 and Table 4.12 that the Mitchell's Plain data has a high multiple correlation coefficient (0.928), yet none of the terms α,β,γ and δ are significant. The reason for this is that the data, having been measured at one plant over ten weeks, has only a narrow range of SVI and V_o and n values which plot in a circular pattern. These results confirm the necessity for conducting a thorough statistical evaluation before accepting any empirically based relationship.

In conformity with the conclusions above, the reason that the Wallace and four Pitman data sets could be pooled is that each of these sets yield a high degree of significance for each of the α,β,γ and δ terms. These data sets therefore manifest not only the same trends but also the same degree in this trend.

The reasoning for the validity of this conclusion regarding degree of trend can be seen from the Dickinson data results in Table 4.12. This data set shows significance in three of the terms i.e. α,β and δ, but not γ. However, the significance level of γ (0.002) is still important, because it is only twice the value of the significance levels for the other terms. At a significance level of 0.002, if the γ term is omitted, the result is a considerable reduction in the multiple correlation coefficient, indicating that the general form of Equation (4.4) with all four terms is appropriate. Figure 4.24 to

Figure 4.27 show the ln V_o and n values vs SVI data for the 190 groups of the Pitman data family and the 20 groups of the Dickinson data set respectively.

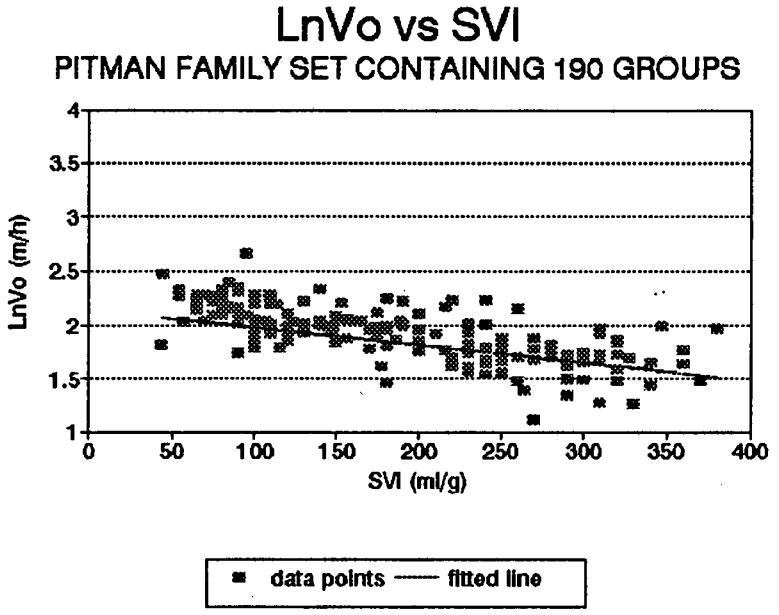

Figure 4.24 Ln V_o vs SVI for the pooled Pitman family data set

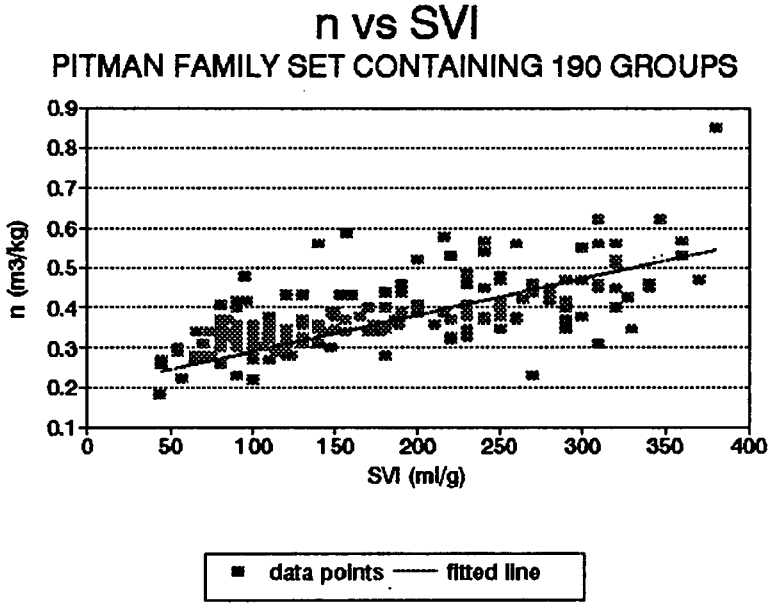

Figure 4.25 n vs SVI for the pooled Pitman family data set

Since the graphs for this data family and set are plotted to the same scale, visual comparison is valid. It can be seen that, for the Dickinson data set, the ln V_o and n vs

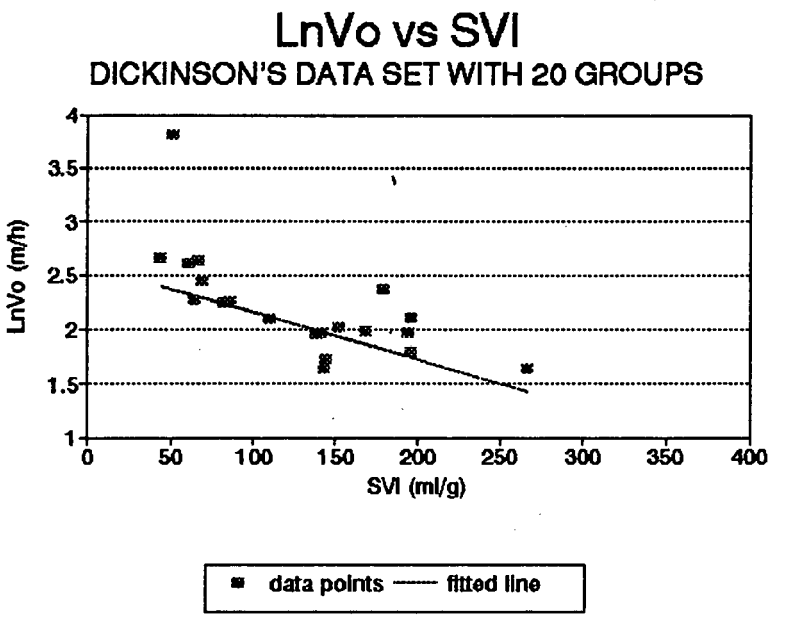

Figure 4.26 **Ln V_0 vs SVI for the data set collected by Dickinson**

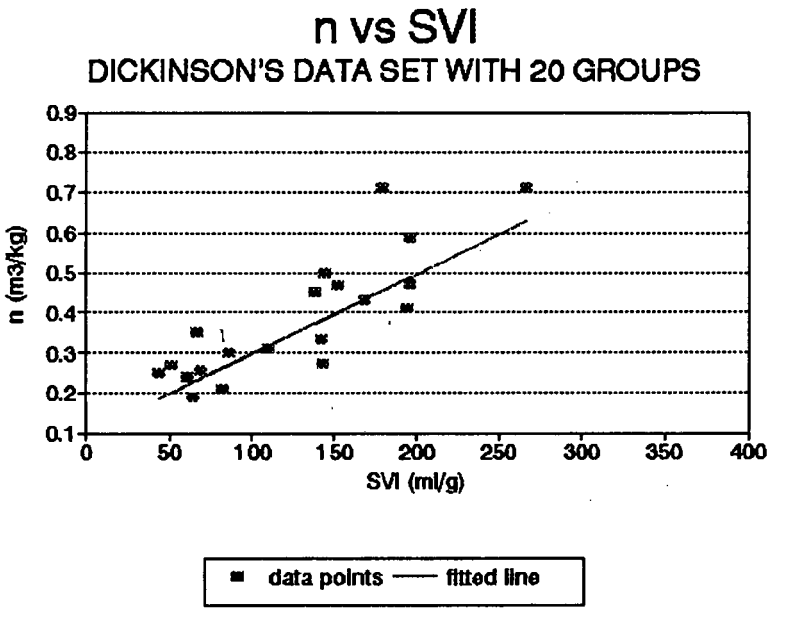

Figure 4.27 **n vs SVI for the data set collected by Dickinson**

SVI slopes are much steeper (ln V_0 decreasing and n increasing) than for the Pitman family data. This demonstrates visually the finding that the Dickinson set could not be pooled with the Pitman family. Elimination of the γ term from Equation (4.4) constrains the line for n vs SVI to pass through the origin. It can be seen in Figure 4.27 that to do this will distort the slope to a steeper value and is the reason for

the high significance level of the γ term and the reduction in multiple correlation coefficient if it is removed. From the above statistical analysis, it would appear that the largest family of data that can be pooled is the four Pitman sets with the Wallace set. This does not mean that this is the best empirical relationship between V_o and n and the SVI. The fact that the Daigger, Grady, Wahlberg and other sets could not be pooled into the Pitman family indicates that factors other than the concentration (X) and SVI measurements affect the V_o and n values. It could be the differences in the SVI test itself, but it could also be differences in sludges from which the data sets were obtained. The Wallace and four Pitman data sets were all measured on activated sludges incorporating either biological N or N and P removal whereas the Daigger, Grady and Wahlberg data sets were all measured on fully aerobic activated sludges.

4.4.2 THE ZONE SETTLING VELOCITY IN TERMS OF $SSVI_{3.5}$

The results obtained by fitting the $SSVI_{3.5}$ data to Equation (4.4) with the single step and double step methods are listed in Table 4.13 and Table 4.14 respectively.

Table 4.13 Fitted constants for Equation (4.4) for the $SSVI_{3.5}$ data obtained with the single step method

REFERENCE	ln α	β	γ	δ	r^2
Lukuko	2.742115	0.00794	0.21707	0.00204	0.936
Wallace	2.282526	0.00255	0.14210	0.00328	0.943
Dickinson	2.287320	0.00287	0.05309	0.00371	0.873
Cape Flats	4.184881	0.02020	0.46101	0.00027	0.982
M Plain	3.274657	0.13965	0.54118	-0.00008	0.960
Pitman AX	2.634586	0.00947	0.18118	0.00223	0.957
Pitman OF	2.647000	0.00941	0.30912	0.00069	0.892
Pitman GK	2.700652	0.00808	0.22632	0.00264	0.916
Wahlberg	2.418940	0.00487	0.22173	0.00236	0.744

Examining Table 4.13 and Table 4.14, it can be seen that, similarly to the SVI, the Mitchell's plain data is odd because it is the only data set that gives a negative sign on δ. Although δ is very small, its negative sign suggests that n decreases with increasing

Table 4.14 Fitted constants for Equation (4.4) for the $SSVI_{3.5}$ data obtained with the double step method

REFERENCE	ln α	β	γ	δ	r^2
Lukuko	2.621845	0.00703	0.19493	0.00225	0.935
Wallace	2.209092	0.00208	0.12975	0.00340	0.942
Dickinson	2.684350	0.00569	0.13559	0.00304	0.855
Cape Flats	3.940978	0.01769	0.44511	0.00060	0.980
M Plain	2.839322	0.00362	0.62118	-0.00055	0.955
Pitman AX	2.734662	0.01114	0.21280	0.00166	0.956
Pitman OF	2.753341	0.01085	0.17136	0.00261	0.791
Pitman GK	2.941058	0.01042	0.32764	0.00163	0.914
Wahlberg	2.919790	0.00577	0.304181	0.002847	0.666

SVI. This data set was therefore rejected even though it gives a high multiple correlation coefficient for both the single and double step correlations. A comparison of the multiple correlation coefficients (r^2) for the single and double step methods is given in Figure 4.28. From Figure 4.28, the following observations can be made:

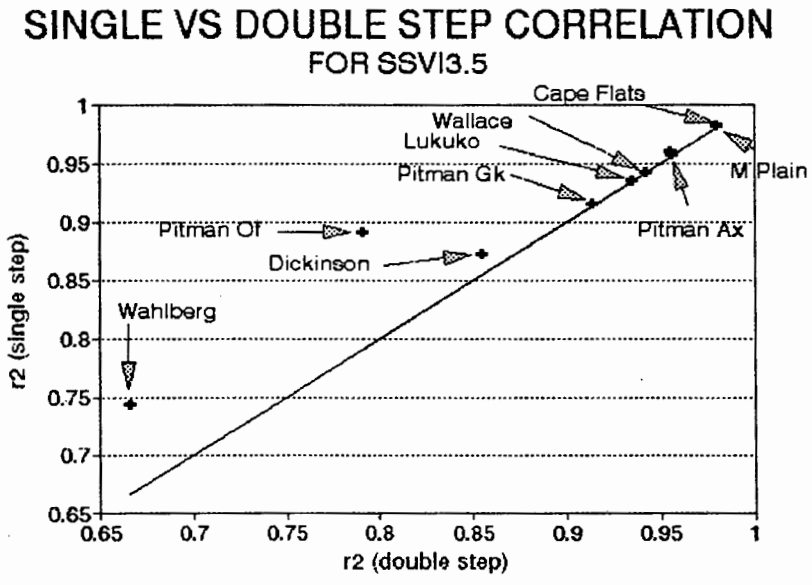

Figure 4.28 Single vs double step methods multiple correlation coefficients for the $SSVI_{3.5}$ data

1. The Cape Flats, Mitchell's Plain, Pitman GK and AX, Wallace and Lukuko sets give the best multiple correlation coefficients; in excess of 0.9 for both methods. The Dickinson and Pitman OF data sets give multiple correlation coefficients of between 0.8 and 0.9 and the Wahlberg data set 0.75 with the single step method and 0.67 with the double step method.

2. As for the SVI data, the multiple correlation coefficient (r^2) obtained using the double step method is not greater for any set than the multiple correlation coefficient obtained by the single step method.

3. The difference between the r^2 value generated by the single step correlation and the double step correlation decreases as the value of r^2 increases.

4. Generally, for the $SSVI_{3.5}$ data, the multiple correlation coefficient (r^2) is better than that for the SVI data. This indicates that the linear relationship explains more of the variation in the data for the $SSVI_{3.5}$ parameter than for the SVI parameter. This is an expected and satisfying result because the $SSVI_{3.5}$ was developed as an improvement over the SVI by reducing the influence of concentration on the measured result and indicate that, while not ideal, it is a better sludge settleability measure than SVI and therefore a more secure basis from which to estimate the ZSV (V_s).

Pooling the $SSVI_{3.5}$ data

Pooling the $SSVI_{3.5}$ data set was carried out in the same way as for the pooling of the SVI data sets.

It was found that the biggest possible sample that could legitimately be pooled was one comprising the UCT Lukuko, Wallace and Dickinson sets and the Pitman AX and OF sets (see Table 4.15). These sets together are called the UCT family, because the bulk of the data groups were measured by UCT. In the pooling analysis it was found that

the Pitman GK, Cape Flats, Mitchell's Plain and Wahlberg data sets could not be pooled in any combination and consequently are sets that need to be treated as statistically distinct. With regard to the Pitman GK set, this set was measured on a 5 stage Bardenpho biological N and P removal plant and is clearly distinct from the Pitman OF and Pitman AX nitrification denitrification plants (see Table 4.3). These differences in system design and operation would probably cause the differences in the data sets and indicate that the factors that influence ZSV are not fully described in the measurement of only X and $SSVI_{3.5}$. The Wahlberg data set, obtained from fully aerobic plants, and the Cape Flats and Mitchell's Plain data sets, obtained from nitrification-denitrification plants, were all measured over a very narrow range of $SSVI_{3.5}$, V_o and n values.

The UCT family of data comprised 68 groups of $SSVI_{3.5}$ and V_o and n pairs from a total number of 603 V_s-X data points. The F statistics for pooling on the basis of V_o and n were calculated separately and the results for the calculated and critical F statistics are listed in Table 4.15, indicating that the pooling of the five data sets is statistically permissable.

Table 4.15 F factors for the pooled $SSVI_{3.5}$ data set

UCT FAMILY LUKUKO WALLACE DICKINSON PITMAN ALEXANDRA OLIFANTSVLEI			V_o		n	
	v_1	v_2	F calculated	F critical	F calculated	F critical
F_1	8	58	1.558	2.10	1.276	2.10
F_2	4	58	1.983	2.53	1.307	2.53
F_3	3	62	0.054	2.76	1.528	2.76
F_4	1	62	0.0007	4.00	0.310	4.00

The UCT family comprising the data collected by Lukuko, Wallace, Dickinson and Pitman at the Alexandra and Olifantsvlei plants was then subjected to a linear regression analysis on Equation (4.4) with the single step method. The constants,

multiple correlation coefficient and the significance levels obtained for each term are listed in Table 4.16.

Table 4.16 Constants, multiple correlation coefficient and significance levels for the pooled set of $SSVI_{3,5}$ data denoted the UCT family on the basis of the single step correlation

REFERENCE	ln α	β	γ	δ	r^2
UCT family	2.45095	0.00636	0.16756	0.00218	0.849
Significance level	<0.001	<0.001	<0.001	<0.001	

All the t values for the estimates of the fitted constants (α,β,γ and δ) were found to be greater than the critical t values, indicating that each of the parameters makes a significant contribution to the multiple correlation coefficient. These t values give significance levels that are all <0.001, indicating that at the 99.9% level, there is a 99.9% probability of being correct in accepting that this is the correct form for the relationship between these parameters. The F ratio for the full regression was found to be F = 1124.26. This indicates that, on the basis of a risk of 0.05, the least squares equation is a good predictor because the calculated F value is greater than the tabulated F value F(3,599,0.95) = 2.60.

The fitted constants α,β,γ and δ for the remaining data sets that could not be pooled into pairs and needed to be treated individually are detailed in Table 4.17. These constants are those obtained by the single step method of regression. Table 4.18 shows the significance levels for each of the α,β,γ and δ constants for each of these individual sets.

The data sets that have been marked by an asterix are those that have high significance levels for one or more of the fitted constants. The only data set for which all four fitted constants have acceptable significance levels for the chosen form of the equation is that collected by Pitman at the Goudkoppies (GK) plant. The constants from

Table 4.17 Fitted constants for $SSVI_{3.5}$ obtained using the single step method for the unpooled groups

REFERENCE	ln α	β	γ	δ	r^2
Cape Flats	4.18488	0.02020	0.46101	0.00027	0.982
M Plain	3.27466	0.13965	0.54118	-0.00008	0.960
Wahlberg	2.41894	0.00487	0.22175	0.00236	0.744
Pitman Gk	2.70065	0.00808	0.22632	0.00264	0.916

Table 4.18 Significance levels for the fitted constants of the unpooled $SSVI_{3.5}$ groups

REFERENCE	ln α SIG. LEVEL	β SIG. LEVEL	γ SIG.LEVEL	δ SIG. LEVEL	
Cape Flats	<0.001	<0.001	<0.001	0.666	*
M Plain	<0.001	0.004	0.003	0.940	*
Wahlberg	<0.001	0.0178	<0.001	<0.001	*
Pitman Gk	<0.001	<0.001	<0.001	<0.001	

Table 4.16 are similar to those drawn from the SVI analysis. This indicates that the data sets that can be pooled manifest not only the same trends but also the same degree in trend (all the terms are significant). The fact that the Pitman GK set also has all four terms significant and yet could not be pooled into the UCT family supports the conclusion regarding the degree of the trend. The remaining three data sets (Cape Flats, Mitchell's Plain and Wahlberg) could not be pooled because each has different terms that are not significant in the correlation e.g. δ for Cape Flats, β,γ and δ for Mitchell's Plain and β for Wahlberg, similar to the SVI results.

Accepting the UCT family as the basic data set for linking the $SSVI_{3.5}$ to the V_o and n values, Figure 4.29 and Figure 4.30 show plots of Ln V_o and n against $SSVI_{3.5}$, illustrating both the data points and the fitted line.

For comparative purposes, Figure 4.31 and Figure 4.32 show to the same scale plots of Ln V_o and n against $SSVI_{3.5}$ for the data collected by Pitman at the Goudkoppies

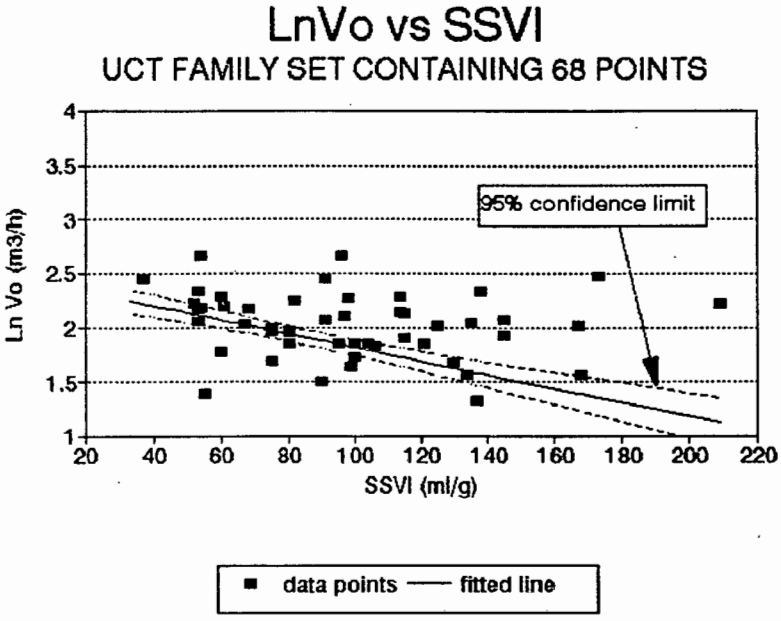

Figure 4.29 Ln V_o vs $SSVI_{3.5}$ for the UCT family data set

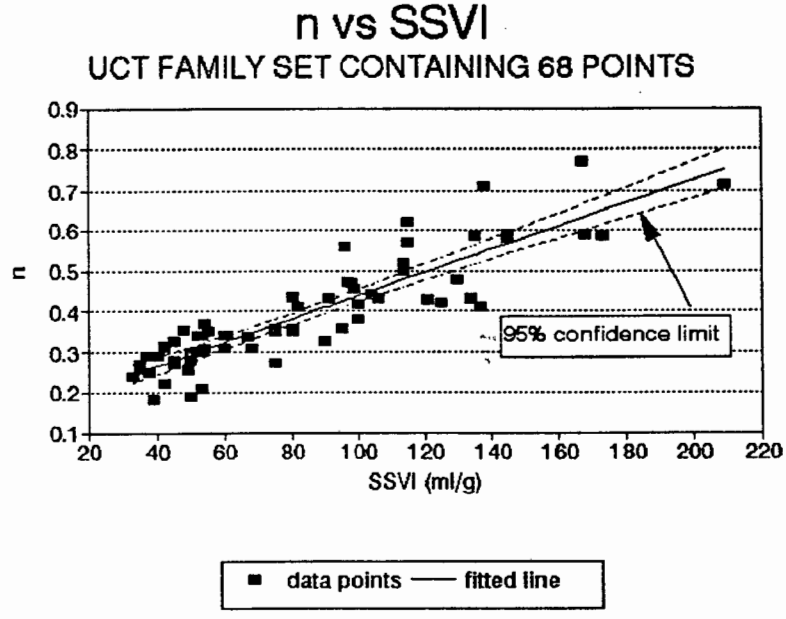

Figure 4.30 n vs $SSVI_{3.5}$ for the UCT family data set

For comparative purposes, Figure 4.31 and Figure 4.32 show to the same scale plots of Ln V_o and n against $SSVI_{3.5}$ for the data collected by Pitman at the Goudkoppies plant which, as stated before, has all four terms significant but must be treated individually.

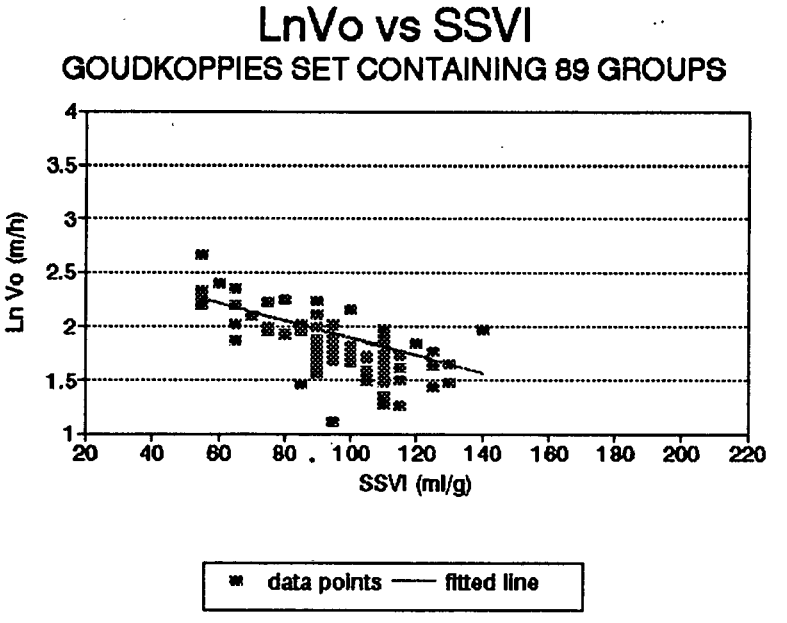

Figure 4.31 **Ln V_o vs $SSVI_{3.5}$ for the data set collected by Pitman at the Goudkoppies plant**

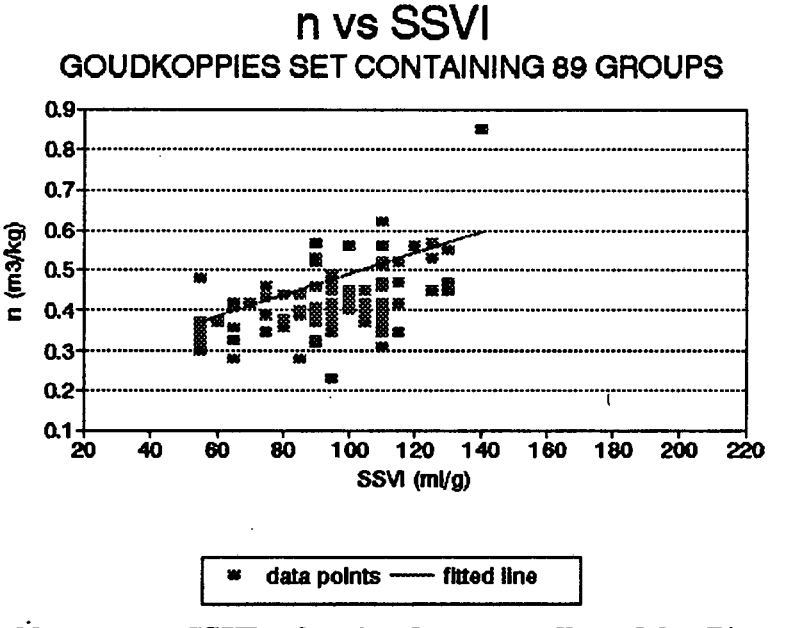

Figure 4.32 **n vs $SSVI_{3.5}$ for the data set collected by Pitman at the Goudkoppies plant**

than that for the UCT family. This is apparent from the γ values which define the intercept of the n line on the vertical axis. For the Pitman data GK set, the γ value is greater than the γ value for the UCT family.

4.4.2 THE ZONE SETTLING VELOCITY IN TERMS OF DSVI

The results obtained by fitting the DSVI data to Equation (4.4) with the single step and double step methods are illustrated in Table 4.19 and Table 4.20 respectively.

Table 4.19 Fitted constants for Equation (4.4) for the DSVI data obtained with the single step method

REFERENCE	ln α	β	γ	δ	r^2
Lukuko	1.89373	0.00176	0.22665	0.00083	0.743
Wallace	1.82304	-0.00100	0.13825	0.00235	0.840
Dickinson	2.57638	0.00395	0.04934	0.00304	0.841
Cape Flats	3.35136	0.00887	0.45652	0.00029	0.974

Table 4.20 Fitted constants for Equation (4.4) for the DSVI data obtained with the double step method

REFERENCE	ln α	β	γ	δ	r^2
Lukuko	2.41101	0.00339	0.33477	0.00058	0.697
Wallace	2.18812	0.00136	0.25016	0.00152	0.797
Dickinson	2.95646	0.00669	0.97180	0.00261	0.832
Cape Flats	3.47348	0.00985	0.51993	0.00018	0.973

A comparison of the two methods is given in Figure 4.33 which shows the multiple regression coefficients (r^2) obtained with the two methods plotted against each other. It is difficult to identify general trends from Figure 4.33 because of the few data points recorded. However, the following observations can be made:

1. only the Cape Flats data gives a multiple correlation coefficient of greater than 0.9, the Dickinson and Wallace sets give multiple correlation coefficients of between 0.8 and 0.9 and the Lukuko set gives a multiple correlation coefficient of around 0.75,

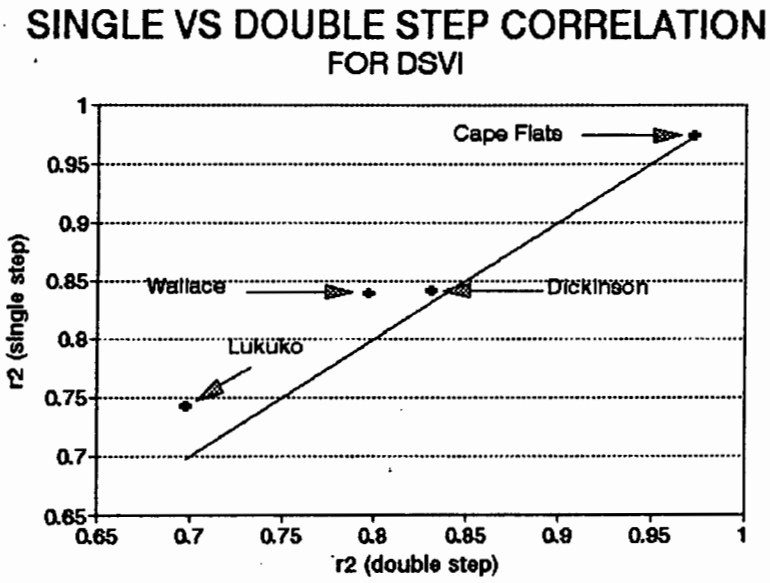

Figure 4.33 Single vs double step methods multiple correlation coefficients for the DSVI data

2. as for the previous data sets, the multiple correlation coefficient (r^2) obtained using the double step method is in no case greater than the multiple correlation coefficient obtained by the single step method.

Pooling the DSVI data

Pooling the DSVI data set was carried out in the same way as for the pooling of the SVI and $SSVI_{3.5}$ data sets.

It was found that the biggest possible sample that could legitimately be pooled was one comprising the UCT Lukuko and Wallace data sets (see Table 4.21). The pooled sample then consisted of 34 groups of DSVI and V_o and n pairs from a total number of 239 V_t-X data points. The F statistics for pooling on the basis of V_o and n were calculated separately and the results for those that satisfied the critical F statistics are illustrated in Table 4.21.

Table 4.21 F factors for the pooled DSVI data set

POOLED DATA SETS Lukuko Wallace			V_o		n	
	v_1	v_2	F calculated	F critical	F calculated	F critical
F_1	2	30	1.806	3.32	2.528	3.32
F_2	1	30	3.317	4.17	3.838	4.17

The pooling tests showed that the Dickinson and Cape Flats data sets could not be pooled together into a separate family and had to be treated individually.

The pooled set containing the Lukuko and Wallace data was then subjected to a linear regression analysis on Equation (4.4) with the single step method. The constants, multiple correlation coefficient and the significance levels obtained are listed Table 4.22.

Table 4.22 Constants, multiple correlation coefficient and significance levels for the pooled set of DSVI data

REFERENCE	ln α	β	γ	δ	r^2
Pooled DSVI group	2.30854	0.00297	0.29721	0.00095	0.776
Significance level	<0.001	<0.001	<0.001	<0.001	

All t values for the estimates of the fitted constants (α,β,γ and δ) were found to be greater than the critical t values, indicating that each of the terms is significant in contributing to the multiple correlation coefficient. These t values give significance levels that are all <0.001, indicating that at the 99.9% level, there is a 99.9% probability of being correct in accepting that this is the correct form for the relationship between these parameters. The F ratio for the full regression was found to be F = 221.925. This indicates that, on the basis of a risk of 0.05, the least squares

equation is a good predictor because the calculated F statistic is greater than the tabulated F statistic F(3,195,0.95) = 2.6.

The fitted constants α,β,γ and δ for the remaining data sets that could not be pooled into one group are detailed in Table 4.23. These constants are those obtained by the single step method of regression. Table 4.24 shows the significance levels for each of the α,β,γ and δ constants.

Table 4.23 Fitted constants for DSVI obtained using the single step method for the unpooled groups

REFERENCE	ln α	β	γ	δ	r^2
Dickinson	2.57637	0.00395	0.04934	0.00304	0.841
Cape Flats	3.35136	0.00088	0.45652	0.00029	0.974

Table 4.24 Significance levels for the fitted constants of the unpooled DSVI groups

REFERENCE	ln α SIG. LEVEL	β SIG. LEVEL	γ SIG. LEVEL	δ SIG. LEVEL	
Dickinson	<0.001	0.012	0.139	<0.001	*
Cape Flats	<0.001	<0.001	<0.001	0.557	*

The high significance levels for β and γ for the Dickinson data and δ for the Cape Flats data support the finding that these data sets could not be pooled with the rest of the DSVI group.

Figure 4.34 shows a plot of Ln V_o against DSVI for the pooled data set. Figure 4.35 shows a similar plot for n vs DSVI.

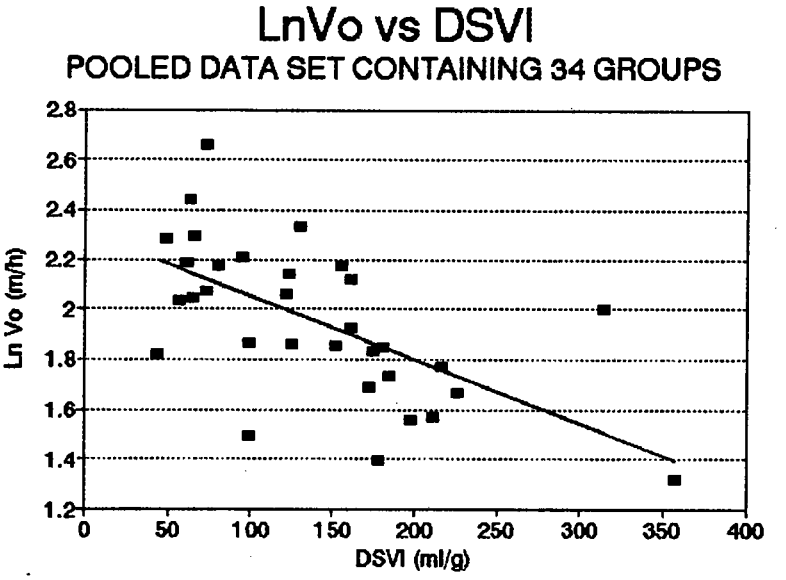

Figure 4.34 **Ln V_o vs DSVI for the pooled data set**

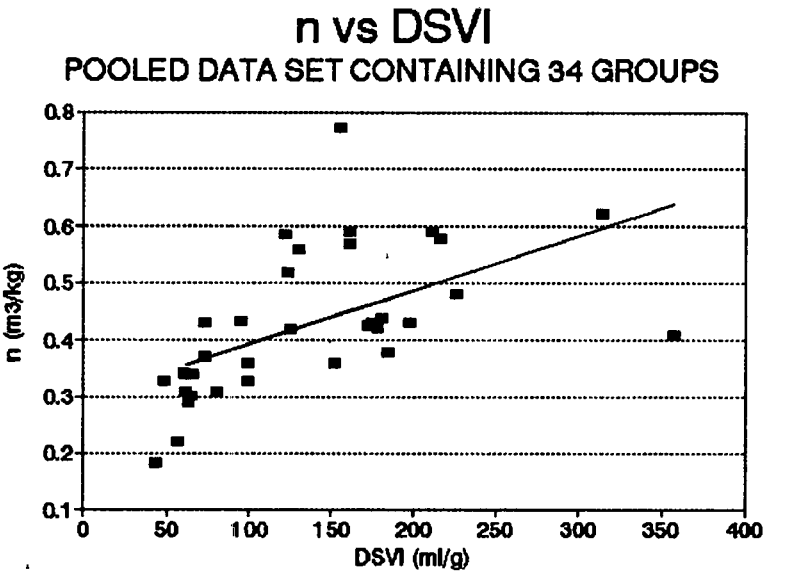

Figure 4.35 **n vs DSVI for the pooled data set**

4.5 CONCLUSIONS

The principal objective of the statistical evaluation was to derive an empirical relationship linking the zone settling velocity, V_s, and V_o and n values in the $V_s=V_oe^{-nX}$ function to the $SSVI_{3.5}$ or DSVI sludge settleability parameters. This

relationship would enable the V_o and n values to be calculated from the measured $SSVI_{3.5}$ or DSVI so that the full scale settling tank tests undertaken by STORA could be simulated with a flux theory based dynamic simulation model. In this respect, the $SSVI_{3.5}$ relationship is superior because (i) it is a better measure for sludge settleability than the SVI and (ii) it is based on a larger data set than the DSVI relationship. Consequently, in the simulation of the STORA data described in Chapter 8, the V_o and n values were calculated with the aid of Equations (4.1) and (4.2) where the α,β,γ and δ values are those given for the pooled UCT data family given in Table 4.16. This family comprises 603 individual V_s, X and $SSVI_{3.5}$ data and 68 groups of V_o, n and $SSVI_{3.5}$ data giving an average of eight to nine V_s-X data pairs per group. The multiple correlation coefficient (r^2) for this family on the basis of the single step correlation method is 0.85, indicating that the empirical relationship (Equation (4.4)) in terms of $SSVI_{3.5}$ explains 85% of the variance in the data. Although the double step correlation method gives different α,β,γ and δ values, the multiple correlation coefficient corresponds well to that of the single step method. To show the trend of this relationship, a graph of the V_s vs $SSVI_{3.5}$ for different sludge concentrations (X) of 3, 4 and 5kgm^{-3} is given in Figure 4.36.

Also, a graph of the V_o and n values versus $SSVI_{3.5}$ obtained from Equation (4.1) and (4.2) with α,β,γ and δ values from Table 4.16 is given in Figure 4.37.

For the calculation of the V_o and n values for the STORA simulations, the single step correlation α,β,γ and δ values were adopted because these gave the best multiple correlation coefficient (i.e. the values given in Table 4.16).

Because the various data sets could not all be pooled into a single family, it was concluded that differences exist in the data sets which are not accounted for in the measured parameters X and SSP. It is interesting to note that, for the SVI, all the Pitman data could be pooled but, for the $SSVI_{3.5}$, the Goudkoppies (GK) data set could not be pooled with the Alexandra (AX) and Olifantsvlei (OF) sets of Pitman. Because the latter two plants are extended aeration with N removal and the former a

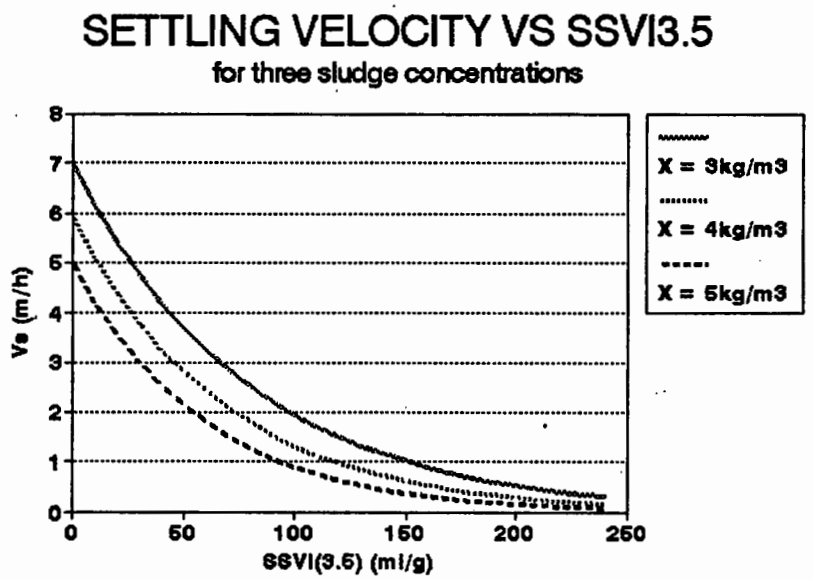

Figure 4.36 **Settling velocity vs $SSVI_{3.5}$ for three different sludge concentrations**

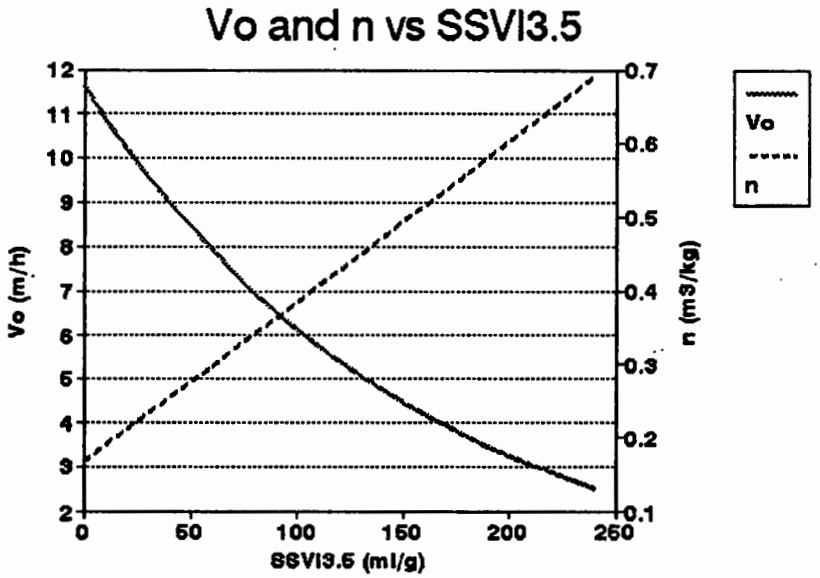

Figure 4.37 **V_o and n vs $SSVI_{3.5}$**

biological N and P removal plant, the $SSVI_{3.5}$ appears sufficiently sensitive in distinguishing these two plant operating conditions whereas the SVI is not. Also, the UCT data sets measured on 15 Western Cape plants (all long sludge age, biological N removal, no P removal) could be pooled with the Pitman OF and AX plants. Since all

these plants are similar in design (but not in size) i.e. long sludge age nitrification-denitrification, it seems reasonable that their data sets could be pooled. In contrast, for the SVI, while all the Pitman data sets could be pooled, (even though these are from two different plant types), the UCT Western Cape plant SVI data could neither be pooled into a family of their own nor with Pitman's.

The above discussion serves to demonstrate that a consistent pattern with regard to plant type for the $SSVI_{3.5}$ emerges, which gives confidence to the empirical relationship developed. Furthermore, because the relationship was developed on the basis of the UCT Western Cape Plant and Pitman AX and OF data, all of which are long sludge age nitrification-denitrification plants, the developed relationship is particularly suited to the STORA data because these plants also were mainly long sludge age nitrification plants (with some denitrification inevitably taking place in the poorer aerated and mixed zones). It was felt, therefore, that the flux theory constants V_o and n could be confidently calculated from the measured $SSVI_{3.5}$ data for the simulation study. Even though the DSVI also is a good sludge settleability parameter, because the empirical relationship based on it was established on a restricted data set and has a lower multiple correlation coefficient than the $SSVI_{3.5}$, it was not regarded as sufficiently reliable to estimate the V_o and n for the STORA data simulation.

In conclusion, even though the empirical relationships developed in this chapter are based on a large data set obtained from different countries, these relationships should be used with caution for a particular application. The fact that not all the data sets could be pooled into one family indicates that the zone settling velocity V_s is influenced by factors not incorporated in the X and SSP measurements. The statistical analysis in this chapter indicates that plant type possibly affects the results. In this regard, the $SSVI_{3.5}$ proved more discerning than the SVI, which appeared to allow and disallow pooling of data sets more randomly. This possibly arises in part from the weakness of the SVI as a sludge settleability measure.

Considerably more information can be gleaned from the statistical evaluation presented in this chapter. For example, how do the different empirical relationships for V_o and n in terms of the SVI, $SSVI_{3.5}$ and DSVI, and relationships between the SVI, $SSVI_{3.5}$ and DSVI themselves, affect the design of the settling tank area and compare with the empirical design procedures? However, because these aspects were not regarded as directly relevant to the objective at hand i.e. dynamic simulation of secondary settling tanks, they are not dealt with in this thesis. These aspects should be pursued in further research to integrate and compare the various settling tank design procedures.

REFERENCES

Daigger G.T. and R.E. Roper., "The relationship between SVI and activated sludge settling characteristics", JWPCF, Vol 57, No 8, pp 859-866, (1985)

Dick R.I and K.W. Young, "Analysis of thickening performance of final settling tanks", Procs 27th Purdue International Waste Conf, Lafayette, Indiana, (1972)

Ekama G.A. and G.v.R. Marais, "Improved parameters for measuring activated sludge settleability", IMIESA, 9, (6), 20, (1984)

Ekama G.A. and G.v.R. Marais, "Sludge settleability and secondary settling tank design procedures", Wat Pollut Control, Vol 5, No. 1, (1986)

Hartel L. and H.J. Popel, "A dynamic secondary clarifier model including processes of sludge thickening", Wat Sci Tech, Vol 25, No. 6. pp 267-284 (1992)

Hartley K.J., "Operating the activated sludge process", Gutteridge, Haskins and Davey Pty Ltd, Brisbane, Qld., Australia, (1985)

Koopman B. and K. Cadee, "Prediction of thickening capacity using diluted sludge volume index", Water Research, 17, 10, pp 1427-1431, (1983)

Merkel W., "Untersuchungen u das verhalten des belebten schlammes im system belebungsbeken - nachklarbecken", Gewasserschutz, Wasser-Abwasser, Aachen, (1971)

Pitman A.R., "Settling of nutrient removal activated sludges", Procs of 12th IAWPRC Conference, Amsterdam, Wat Sci Tech, 17, 493, (1984)

Rachwal A.J., Johnstone D.W.M., Hanbury M.J. and D.J. Critchard, "The application of settleability tests for control of activated sludge plants", Chapter 13 in "Bulking of Activated Sludge - preventatives and remedial methods", Eds. Chamber B. and E.J. Tomlinson, Ellis-Hopwood Publishers, Chichister, (1982)

Smollen M. and G.A. Ekama. "Comparison of empirical settling velocity equations in flux theory for secondary settling tanks", Water S.A., 10, (4), 175, (1984)

Stofkoper J.A. and C.C.M. Trentelman, "Richtlijen voor het dimensioneren van ronde nabezinktanks voor aktiefslibinstallaties", $HO6_2O$, 15, 14, pp 344-354, (1982)

STORA (Stichting Toegepast Onderzoek Reiniging Afvalwater), "Hydraulische en technologische aspecten van het nabezink-process", Rapport 1-Literatuur, Rapport 2-Ronde nabezinktanks (Praktijkonderzoek), (1981)

Tuntoolavest M. and C.P.L. Grady Jr., "Effect of activated sludge operational conditions on sludge thickening characteristics", JWPCF, 54, 1112, (1982)

Vesilind P.A., "Design of prototype thickeners from batch settling tests", Water and Sewage Works, 115, 302, (1968)

Wahlberg E.J. and T.M. Keinath, "Development of settling flux curves using SVI", JWPCF, Vol 60, No 12, pp 2095-2100, (1988)

CHAPTER 5
ANDERSON'S WORK

5.1 INTRODUCTION

In the review of secondary settling tank simulation models in Chapter 2, it was concluded that at the time of commencement of this research, the most refined and true application of the flux theory in a computer model was that of Anderson (1981) (see also Anderson and Edwards (1980, 1981)). In this chapter, details of his model and the purposes for which it was developed are presented. This is necessary because many aspects of Anderson's computer model required modification in order to meet the objectives of this investigation, and in order to appreciate the significance of these modifications, the objectives and salient features of Anderson's model need to be described.

5.2 ANDERSON'S OBJECTIVES

Anderson's (1981) dynamic computer simulation model was developed in order to simulate the Detroit Wastewater Treatment Plant and is a portion of a comprehensive computer simulation model of the entire wastewater renovation system for metropolitan Detroit called the Detroit Water and Sewage Department (DWSD) system model. This overall model was expected to predict the effect of discharging untreated wastes to receiving waters during wet weather when the volumetric capacity of the sewerage transport network and treatment plant, which incorporated an activated sludge process for secondary treatment, was exceeded.

Anderson's model of the activated sludge treatment plant, which is a subset of the DWSD system model, was expected to simulate short and long term responses to influent perturbations to the plant and to give output for eight effluent quality parameters for transfer to the Detroit Water and Sewage Department system model.

The activated sludge plant subset model is specific to the type of treatment practised at the Detroit Wastewater Treatment Plant (DWWTP).

Anderson's secondary settling tank model, which in turn is a subset of the activated sludge treatment plant model, was expected to predict the suspended solids concentrations in the final effluent, in the return sludge and in the settling tank itself at different depths during diurnal and seasonal transient operation.

Anderson concluded that his program was adequately able to simulate dynamic fluctuations in plant performance during wet weather periods. He concluded that, with respect to the suspended solids, the secondary settling tank is the most critical step in the wastewater treatment plant because it most significantly affects the effluent suspended solids discharged to the receiving waters, much more so than the activated sludge biological reactor. As a result, he made considerable effort to refine the application of the flux theory to dynamic simulation by dividing the settling tank depth into many layers and to define the behaviour and characteristics of the settling tank by including considerations such as diffusion. Unfortunately, important quantitative information relating to parameters such as eddy diffusivity effects and turbulence in secondary settling tanks was unavailable. Anderson overcame this problem by calibrating his model very specifically for the geometric configuration of the DWWTP secondary settling tanks. This enabled Anderson to meet his objectives, which were specifically to simulate the Detroit Wastewater Treatment Plant but resulted in a model that may not be generally applicable. Nevertheless, both his method and his algorithm are the most advanced for settling tank modelling using the flux theory as a theoretical basis.

5.3 DESCRIPTION OF ANDERSON'S ALGORITHM

Anderson and Edwards (1980) developed an implicit, second-order, non-iterative finite difference algorithm which solves the set of equations describing the dynamic

behaviour of settling sludge in secondary settling tanks. A general outline of the algorithm is as follows:

In a single (vertical) dimension, the continuity equation in conservation law form for the continuous sedimentation process is a hyperbolic partial differential equation which states that the rate of change of concentration with time is equal to the rate of change of flux with depth:

$$\frac{\delta X}{\delta t} = \frac{\delta G}{\delta z} \tag{5.1}$$

where $X = X(z,t)$ = concentration of mixed liquor suspended solids (M/L^3)

z = distance in the vertical direction (L)

$G = G(z,t)$ = solids flux in the z direction ($M/L^2/T$)

where

$$G = (V_b + V_g)X \tag{5.2}$$

where V_g = settling velocity of the particles due to gravitational acceleration i.e. gravity zone settling velocity (L/T)

V_b = particle velocity due to the bulk motion of the fluid i.e. bulk movement (L/T)

The governing differential equations are **partial** differential equations (PDE's) because the concentration field under consideration depends on both depth (z) and time (t).

The presence of the flux law in the equation renders the equation both non-linear and non-convex. The non-linearity arises from the fact that the flux law is itself a function of concentration, the variable for which we are trying to solve. The shape of the flux function is non-convex because it does not lie above all its tangents. i.e.

$$-\frac{\delta^2 G}{\delta X^2} \text{ not } > 0 \text{ over the whole domain} \qquad (5.3)$$

Practically, this means that, in certain regions of the flux curve, tangents drawn to the curve lie above it i.e. in the region where $X < 2/n$ or to the left of the inflection point. See Figure A.9 in Appendix A.

Because of the convective nature of the sludge settling behaviour, the governing equations for settling are **hyperbolic** partial differential equations. Problems of hyperbolic character occur in processes like convection-diffusion with small or vanishing diffusion such as those encountered in heat conduction, gas dynamics, wave propagation and electro-magnetism. The hyperbolic nature of the equations originates from vibration problems, or problems where discontinuities persist in time, such as with shock waves. These shocks manifest themselves mathematically as surfaces on which density, pressure, temperature, concentration and the like have discontinuities, which propagate through the system without becoming smoothed out over time. In the settling tank, the shocks are manifested as abrupt changes in concentration with depth as one moves from one settling region to another (see Figure A.10 to Figure A.12 in Appendix A). As time passes, these discontinuities (i.e. sudden concentration changes) may move up and down in the tank, but remain sharply defined.

Unfortunately, the presence of shocks in a hyperbolic system can cause problems when using finite difference methods to solve hyperbolic partial differential equations, as some solutions of hyperbolic conservation laws are not uniquely determined by their initial conditions. This means that multiple solutions may be generated for the same initial conditions, only one of which has physical significance. A number of different strategies have been proposed to ensure that the solution generated by the numerical method or algorithm for the hyperbolic partial differential equations is the correct (physically realistic) one.

1. Lax's Entropy Rule (1957). This requires that the second law of thermodynamics is not violated when crossing over a shock front.

2. The Rankine-Hugoniot boundary conditions. Since the shocks in the system manifest themselves as discontinuities, the partial differential equations governing the motion require boundary conditions connecting the values of the discontinuous parameters on the two sides of the shock surface. The necessary boundary conditions are supplied by the Rankine-Hugoniot equations. However, their application is complicated because the shock surfaces are in motion relative to the network of points in space-time used for the numerical finite difference method and the differential equations and boundary conditions are non linear. Furthermore, the motion of the surfaces is not known in advance, but is governed by the differential equations and boundary conditions themselves. As a result, the Rankine-Hugoniot treatment of shocks requires lengthy computations at each step of the calculation.

3. Von Neumann and Richtmyer (1950) have proposed a method for the automatic treatment of shocks which avoids the necessity for application of any such boundary conditions. Their method of dealing with shocks uses a dissipative mechanism (such as viscosity or heat conduction) to smooth out the shock, so that the mathematical surfaces of discontinuity are replaced by thin layers in which the relevant parameters vary rapidly but continuously. The introduction of an (artificial) dissipative term into the equations enables the partial differential equations (and the corresponding difference equations) to be used for the entire calculation, just as though there were no shocks at all. Thus, the dissipative term effectively renders the equations parabolic (the solutions of which are uniquely determined by their initial values) and thereby not subject to the same multiple solution difficulties as hyperbolic equations. Von Neumann and Richtmyer also note that the inclusion of a dissipation term still allows the Rankine-Hugoniot boundary conditions to be satisfied, provided the thickness of the shock layers is small in comparison with other physically relevant dimensions of the system.

Anderson's algorithm makes use of the proposal made by Von Neumann and Richtmyer by introducing a diffusivity term that smooths out the shocks in the system. In practice, Anderson argued, abrupt discontinuities in the system are smoothed out by various diffusive effects which include eddy effects, density currents, changes in temperature and turbulence in the settling tank due to the wind and the action of the feed and recycle flows. Thus, the scheme proposed by Von Neumann and Richtmyer is physically appropriate. These diffusive effects were all combined into a single turbulent diffusion term (denoted E).

By adding a small amount of diffusivity to the hyperbolic conservation law (Equation (5.1)), and thus smoothing out the concentration profile discontinuities over several grid cells of the finite difference network, the shape of the flux curve is smoothed out in the region of the shock. The diffusivity ensures that strict convexity (see Equation (5.3)) is preserved in the non-linear flux curve, and thus no entropy law violations are possible.

The result is a parabolic convective diffusion equation with a diffusivity coefficient (E) to account for the cumulative effects of turbulence mentioned above i.e.

$$\frac{\delta X}{\delta t} = \frac{\delta G}{\delta z} + \frac{\delta}{\delta z}\left(E.\frac{\delta X}{\delta z}\right)+G_s \qquad (5.4)$$

where $E = E(z,t)$ = turbulent diffusion coefficient in the z direction (L^2/T)

G_s = source or sink terms present as boundary condition ($M/L^3/T$)

Although the mathematical description appears more complex, the parabolic equation avoids some of the difficulties associated with the solution of hyperbolic equations. Most importantly, as already mentioned, unlike the hyperbolic partial differential equations, the solution of a parabolic partial differential equation is uniquely determined by its initial conditions.

Because the dispersive effects have a large influence in the region of the feed point and diminish to zero in the more quiescent zones, the diffusivity coefficient must be allowed to approach zero away from the feed point. This means that the classification of the differential equation (hyperbolic or parabolic) changes according to settling tank depth. The solution algorithm developed by Anderson and Edwards takes this into account. Thus Anderson argued that the algorithm is valid for both the hyperbolic (Equation (5.1)) (no diffusion) and parabolic (Equation (5.4)) (with diffusion) cases. This assertion, however, needs to be accepted with some reservations. Anderson proposed no method to deal with the multiple solutions generated by the hyperbolic equations. In the lower regions of the tank, where the diffusivity is low to negligible, the equations will be hyperbolic, and the finite difference method might generate physically meaningless solutions. This is especially possible as it is in the lower regions of the tank that the solution for the limiting concentration (X_L) is sought for overloaded conditions. Anderson's algorithm does not take this into account.

Anderson further improved his algorithm by the inclusion of a spatially switched scheme for shock resolution. This scheme was proposed by Beam and Warming (1976). Beam and Warming showed that, although the addition of the dissipative term to the hyperbolic scheme reduces post shock oscillations, which are a problem when solving hyperbolic systems containing shocks, it does not provide an adequate resolution of the discontinuity. They found that, for a second order scheme (which was the one developed by Anderson), the judicious use of central, forward and backward difference operators across a discontinuity greatly reduces the spurious oscillations usually associated with shock capturing techniques in finite difference numerical solution procedures. With a knowledge of the allowable direction in which the shocks travel, the appropriate difference operator can be selected to ensure that any oscillation that develops is forced backwards or forwards into the shock, thereby concentrating the oscillation into the shock and improving the shock resolution, or shock capturing. In addition, they proposed special transition operators which ensure mass conservation and correct shock speeds. A more detailed discussion of their technique can be found in their paper.

Another significant improvement in Anderson's model compared to early layer based sedimentation models is that the settling tank was divided into many (40) fixed depth layers within which the concentration was calculated. Consequently, the depths of the thickening and the various zone settling regions are not fixed as in the earlier models, but are calculated as part of the numerical algorithm.

Anderson's model is also superior to more recent layer based sedimentation models (see Section 2.4.1 in Chapter 2) in that these and previous sedimentation models did not incorporate hydraulic effects and considered sedimentation to be the only process occurring in the tank. Anderson's technique of including diffusivity in the model has the fortuitous effect of accounting for various hydraulic phenomena such as turbulence, density currents, weir effects, wind and temperature disturbances, scraper action, etc that occur in the tank.

From the above brief description of the features of Anderson's settling tank model and numerical algorithm, it can be seen that, compared to earlier and later layer based models, Anderson's model is one of the most sophisticated models based on the flux theory developed to date. Consequently, it was considered the most promising means by which to verify the flux theory and to use as a basis for dynamic modelling of secondary settling tanks.

5.4 DESCRIPTION OF THE SECONDARY SETTLING TANK SECTION OF ANDERSON'S PROGRAM

Because Anderson's program (STPSIM2) was intended to simulate the entire Detroit Wastewater Treatment Plant, only a few of the subroutines in the program are relevant to the secondary settling tank simulation. The relevant section of the program consists of three subroutines which simulate, for a user-defined time period, the change in concentration in each of 40 layers of the tank, with user defined initial conditions for the concentration profile.

The first subroutine, DETSTP, reads the data from data files and initialises the concentration profile in the settling tank.

The subroutine reads the following input variables (using Anderson's symbols) from a data file at the beginning of the simulation. The values of these variables remain unchanged throughout the simulation which comprises a defined number of time intervals.

V_o, n = sludge settling characteristics (L/T), (L^3/M) i.e. constants in the semi-log exponential function relating concentration (X) to sludge zone settling velocity (V_s): $V_s = V_o e^{-nX}$.

nfq = feed point position

A = cross sectional area of the settling tank (L^2)

dx = depth of each modelling layer (L)

diftop = diffusivity coefficient for the tank above the feed point (L^2/T)

conc = initial concentrations at all depths (M/L^3)

dt = length of time interval (T)

For each time interval, the following variables are read from a data file.

cas0 = feed concentration at the start of the interval (M/L^3)

cast = feed concentration at the end of the interval (M/L^3)

q0 = feed rate at the beginning of the interval (L^3/T)

qt = feed rate at the end of the interval (L^3/T)

qdown = volumetric underflow rate during the time interval (L^3/T)

The second subroutine, DIFFUS, sets up the diffusivity vs depth distribution in the settling tank.

The third subroutine, CLAR2, uses the flux equations for each layer and the boundary conditions for the settling tank to set up the matrix of equations for solution. The boundary conditions are as follows:

1. the concentration in the bottommost layer (layer 40) is equal to the underflow or return sludge concentration,

2. the concentration in the topmost layer (layer 1) is equal to the overflow or effluent concentration,

3. the influent flow to the clarifier is the sum of the biological reactor influent flow (Q_i) and the volumetric underflow rate (Q_r). At the feed point Q_i is directed vertically upwards and Q_r vertically downwards, both uniformly distributed over the clarifier area producing an overflow rate u_0 ($= Q_i/A$) and an underflow rate u_u ($= Q_r/A$).

In CLAR2, appropriate switching functions are allocated to each layer in the settling tank, depending on the direction in which the shocks are travelling (up or down).

In practice, the shock direction is established by calculating an approximation to the velocity of the shock and noting its sign i.e.

$$\frac{\delta G}{\delta X} = S \qquad (5.5)$$

Where S = shock velocity (L/T)

δG = flux entering layer - flux leaving layer ($M/L^2/T$)

δX = concentration entering layer - concentration leaving layer (M/L^3)

If the flux entering a layer is greater than that leaving a layer, then the concentration in that layer is increased until it reaches the limiting flux concentration. When this limiting concentration is reached, it is not possible for that layer to accumulate any

more material by convective transport. The accumulating material is then "pushed" to the next layer in the appropriate direction using a knowledge of the shock velocity to select the correct switching functions. In this fashion, the shock is propagated through the system.

Once all the equations with their appropriate switching functions have been set up, CLAR2 solves the matrix using a Gaussian elimination procedure.

Upon careful examination of Anderson's algorithm and computer coding abstracted from his PhD thesis, it was found that a few inconsistencies and unsubstantiated equations exist in the three subroutines:

1. Although Anderson stated that the magnitude of the diffusivity coefficient is dependent on both the distance from the feed point and on the volumetric feed flow to the settling tank, the program fails to take this into account.

   The form of the equation presented in the text of the thesis is as follows:

$$E_i = \text{diftop}.(Q_i+Q_r).e^{+\alpha_1(i-i_{feed})} \text{ for } i<i_{feed} \quad (5.6)$$

$$E_i = \text{diftop}.(Q_i+Q_r).e^{-\alpha_2(i-i_{feed})} \text{ for } i>i_{feed} \quad (5.7)$$

   Where E_i = diffusivity in the ith layer (m^2h^{-1})

   Q_i+Q_r = feed flow rate to the settling tank (m^3h^{-1})

   diftop, α_1, α_2 = constants determined by calibration, which, for the DWWTP settling tanks he gave as:

   diftop = $4ft^2h^{-1}mgd^{-1}$ (= $0.002355m^{-1}$)

   α_1 = $0.075h^{-1}$

   α_2 = $0.8h^{-1}$

   i_{feed} = feed point depth layer number (0-40)

   i = number of the layer referring to the depth in the tank (0-40)

The variation of E with depth in accordance with Equations (5.6) and (5.7) for an arbitrary feed flow rate of $Q_i+Q_r = 2785ft^3h^{-1}$ is presented in Figure 5.1.

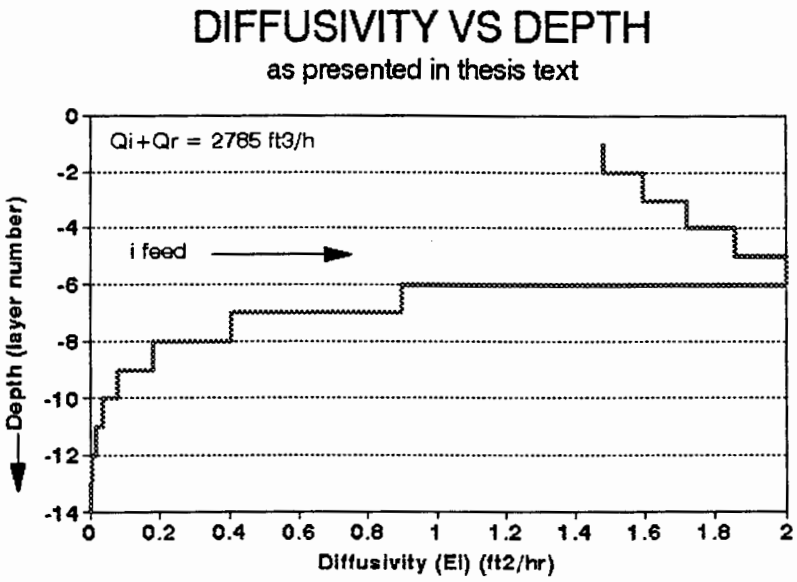

Figure 5.1 Diffusivity vs depth as presented in Anderson's thesis text

In the program, however, it was found that the diffusivity coefficient (E_i) is independent of the influent feed rate, and takes the following form:

$$E_i = \text{diftop}.e^{+\alpha_1(i-(i_{feed-1}))} \text{ for } i<i_{feed} \quad (5.8)$$

$$E_i = \text{diftop}.e^{-\alpha_2(i-i_{feed})} \text{ for } i_{feed} \leq i \leq i_{feed+4} \quad (5.9)$$

$$E_i = \text{difbot for } i>i_{feed+4} \quad (5.10)$$

The variation of E_i with depth in accordance with Equations (5.8) to (5.10) (independent of influent flow rate) is presented in Figure 5.2.

It would therefore seem that, in the practice of calibrating his program, Anderson concluded that the diffusivity was more a function of settling tank depth than of influent flow rate. Anderson gave no estimate for the magnitude of diftop (see Equations (5.8) and (5.9)). Although Anderson included a graph illustrating the shape of the variation of diffusivity (E_i) with depth, no units were given on the

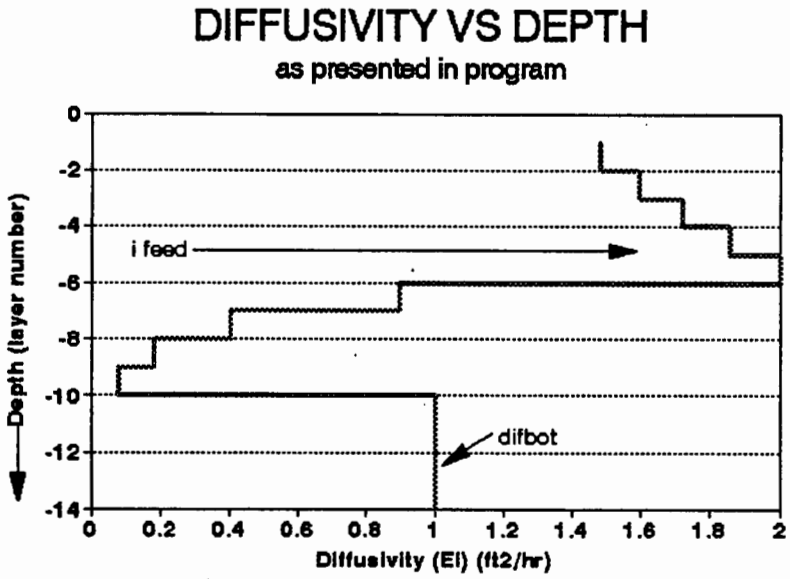

Figure 5.2 Diffusivity vs depth as presented in Anderson's program

graph. Anderson also included a graph showing the variation of his value of E_i with time when simulating a stepped change influent flow situation. Since the function for E_i in the program is independent of flow, it seems that the graph represents an adhoc arrangement to take flow into account as is suggested in the text. However, the depth to which the graph refers is not specified. Since E_i is, by Anderson's assertion, depth dependent, the graph presented lacks essential information to make it meaningful. It is thus not possible to determine the magnitude of the diffusivity term with the information given.

Anderson's program sets difbot (see Equation (5.10)) at a constant value for all layers from the fifth layer below the feed point to the bottom of the tank. This is contrary to the assertions made in the body of his thesis i.e. that diffusivity varies with depth. The value of difbot is set at $1ft^2h^{-1}$ ($0.09295m^2h^{-1}$) for all cases except:

a. if the feed point is at layer 15 and the feed rate is greater than $3715ft^3s^{-1}$ ($378759m^3h^{-1}$),

b. if the feed point is at layer 20 and the feed rate is greater than $2135ft^3s^{-1}$ ($217672m^3h^{-1}$),

in which cases difbot is set equal to $25ft^2h^{-1}$ ($2.323m^2h^{-1}$).

The above strategy in the program clearly indicates that specific settling tank characteristics (such as feed point height) determine the magnitude of the diffusivity, and that the constants in the program were calculated for the particular settling tanks at the DWWTP. This suggests that the general case was not considered by Anderson, and that the program is specific to the DWWTP settling tanks.

The diffusivity in layer 1 (i.e. effluent flow) is set equal to that in layer 2 and the diffusivity in layer 41 is set equal to that in layer 40. Layer 41 does not physically exist in the tank, but is necessary to complete the terms in the matrix for the Gaussian solution procedure. Thus a value for the diffusivity coefficient is required in this layer. Not only are the form and magnitude of the diffusivity function implemented differently in the program to that outlined in the text, but Anderson also applied an averaging scheme for the E values at adjacent layers, which was not explained. Once the diffusivity in each layer is calculated, it is averaged with that in the previous layer to give the final value of the diffusivity coefficient. No reasons were given for including this averaging step.

2. The influent flow enters the settling tank at the feed point, which is a specified layer at the feed point depth in the clarifier - not at a boundary between two layers. Above this layer, the water velocity is upwards (Q_f/A) and below this layer the water velocity is downwards (Q_r/A). The water velocity in the feed point layer does not physically exist, but the program algorithm needs a velocity term for this layer. Anderson specified that the velocity in the feed point layer (V_3) should be set equal to ($3V_1 + V_2$) where
V_1 = downward velocity (Q_r/A) (M/T)

V_2 = upward velocity (Q_i/A) (M/T)

in order for the resultant flux to have the correct sign. There was no explanation as to how he arrived at this function or why this strategy is necessary.

3. The switching functions in Anderson's program are overwritten at two layers in the settling tank depth. The program sets the shock velocity in the layer immediately below the feed point equal to the shock velocity in the layer immediately below that. The reason for this was also not given.

4. Anderson's program uses an artificial condition at the feed point. This condition sets the concentration at the feed point always equal to the concentration in the layer immediately above it. The reason for this became apparent in the process of checking the program (see Section 6.2 in Chapter 6). Later a different strategy was adopted.

5. Anderson specified in his program that, if any of the concentrations produced by the Gaussian solution procedure is negative, then they should be replaced by a small positive concentration ($4mgl^{-1}$). The reason for this strategy is clear in that it avoids negative concentrations in the solution because even small negative concentrations could seriously adversely affect the algorithm stability and hence the final solution.

5.5 EVALUATION OF ANDERSON'S PROGRAM

To implement Anderson's program the three relevant subroutines (DETSTP, DIFFUS and CLAR2) were combined into a specific Fortran program called SETTLER (revision 1). The program was progressively tested and modified as necessary. This constitutes the major work of this investigation. SETTLER was tested in four stages against three different data sets i.e.

1. the data collected at the DWWTP, which was used by Anderson to calibrate his own program,
2. idealised flux theory calculations,
3. laboratory scale data obtained by the Water Research group at UCT and
4. the full scale data collected by STORA described in Chapter 3.

At each stage of the evaluation, the program was critically examined and assessed for its ability to predict:

1. concentration profiles that are in reasonable accordance with those given in the data,

2. underflow concentration values that follow the general trend of those given in the data,

3. for underloaded cases: the absence of failure in the tank as measured by
   a. lack of significant solids loss with the effluent,
   b. constant or falling sludge blanket levels

   in accordance with the values given by the data,

4. for overloaded cases: the onset of failure in the tank as measured by
   a. sludge blanket rise rate resulting in
   b. effluent solids loss

   in accordance with the values given by the data.

5.5.1 REPRODUCING ANDERSON'S OWN DATA WITH SETTLER (revision 1)

Anderson tested his program by simulating an observed upset event which occurred on one of the settling tanks at the DWWTP. It appears that the intention of the simulation was primarily to ascertain the value of the diffusivity coefficient (E_t) and thus to

calibrate the settling tank subset of the DWSD system model. It is the only calibration test of his settling tank program given in his thesis and publications. The DWWTP upset event lasted for a 16-hour period and during this time a number of different influent rates, feed concentrations and underflow rates were imposed on the settling tank by means of step changes. The operating parameters during the 16h period are presented in Table 5.1.

The initial conditions i.e. the concentration profile in the tank at time = zero, are presented in Figure 5.3.

During the 16h period, sludge concentration profiles were measured on four occasions, four hours apart, i.e. at 1, 5, 9 and 13 hours after the start. To measure the profiles, sludge samples were taken at 2ft depth intervals over the settling tank depth. The measured results are shown in Figure 5.4 to Figure 5.7 inclusive.

In the simulation program, it is possible to monitor parameters such as sludge concentration depth profiles at any time in the simulation. Anderson presented his simulation results at 2 hourly intervals i.e. at 1, 3, 5, 7, 9, 11, 13 and 15 hours after the start of the simulation. However, for purposes of comparison, only the concentration profiles at the same times as the experimental observations are given in Figure 5.4 to Figure 5.7 inclusive.

Table 5.1 Operating parameters for the DWWTP upset

LABEL	PARAMETER	VALUE	CHANGE
SETTLING TANK	AREA	2920.9m^2	
	FEED LEVEL	2.287m (7.5ft)	
	OVERALL DEPTH	5.95m (20ft)	
INITIAL CONDITIONS	FEED FLOW RATE	7099m^3h^{-1}	
	OVERFLOW RATE	4890m^3h^{-1}	
	UNDERFLOW RATE	2208m^3h^{-1}	
	FEED CONCENTRATION	2.5gl^{-1}	
CONDITIONS FROM 4 - 10 HOURS	FEED FLOW RATE	10096m^3h^{-1}	+30%
	OVERFLOW RATE	7887m^3h^{-1}	+38%
	UNDERFLOW RATE	2208m^3h^{-1}	same
	FEED CONCENTRATION	2.3gl^{-1}	-8%
CONDITIONS FROM 10- 16 HOURS	FEED FLOW RATE	8992m^3h^{-1}	-11%
	OVERFLOW RATE	7099m^3h^{-1}	-10%
	UNDERFLOW RATE	1893m^3h^{-1}	-14%
	FEED CONCENTRATION	1.9gl^{-1}	-17%

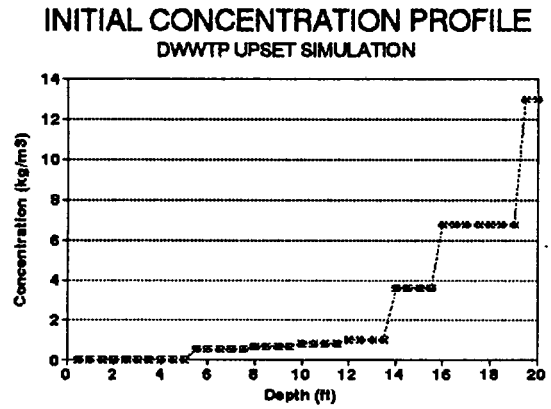

Figure 5.3 Initial concentration profile for the DWWTP upset simulation

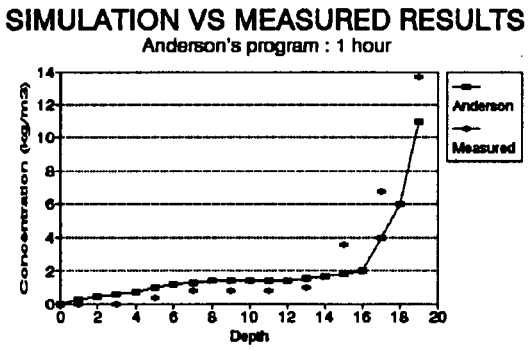

Figure 5.4 DWWTP simulation vs measured results: 1 hour

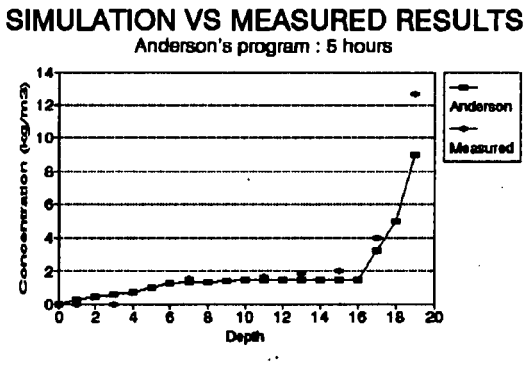

Figure 5.5 DWWTP simulation vs measured results: 5 hours

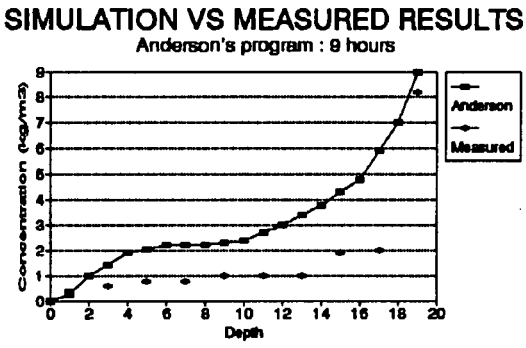

Figure 5.6 DWWTP simulation vs measured results: 9 hours

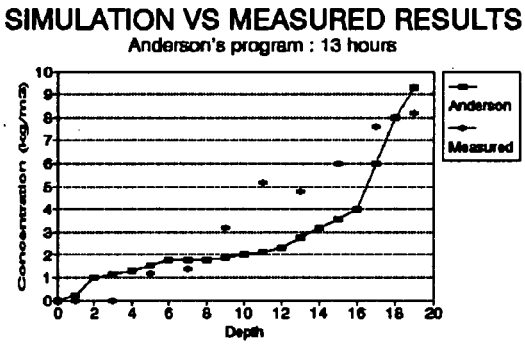

Figure 5.7 DWWTP simulation vs measured results: 13 hours

It should be noted that the simulated data in Figure 5.4 to Figure 5.7 were generated by SETTLER, the self contained settling tank program extracted from the listings in the back of Anderson's thesis.

5.5.2 SPECIFICATIONS OF THE SETTLING TANK SIMULATION PROGRAM

Before it was possible to run SETTLER, it was necessary to resolve some of the problems resulting from the discrepancies and inconsistencies outlined in Section 5.4, the major problem of which was resolving the discrepancy between the diffusivity functions given in the body of the thesis and those given in the program listings at the back. Because the object of this first test was to try and reproduce Anderson's results as he had generated them, it was decided to use the diffusivity functions given in the listings, which were presumed to be a more accurate reflection of the program actually run by Anderson.

These functions were flow independent, and are given in Equations (5.8) to (5.10). The unknown constant in the equations, diftop, was selected to be $0.02534 ft^2 h^{-1}$ ($0.002355 m2h^{-1}$), partly because this was the value given for the constant diftop in the body of the thesis (with adjustment of units, due to it no longer being flow dependent) (Equations (5.6) and (5.7)), and partly because this value was found to accurately reproduce the results presented by Anderson. Difbot was set at $1 ft^2/h$ ($0.0930 m^2/h$), as given in Anderson's listing.

The velocity at the feed point layer, the switching functions, the artificial concentration condition at the feed point and the condition to prevent negative concentrations (see Section 5.3 above) were all retained as specified in Anderson's program.

5.5.3 FLUX THEORY ANALYSIS OF THE SIMULATION CONDITIONS

According to the flux theory, using the sludge settleability constants specified by Anderson, (V_o = 13.776mh^{-1}, n = 0.579m^{3}kg^{-1}), the settling tank was underloaded for the first phase of operation (from 0 to 4 hours), overloaded for the second phase (from 4 to 10 hours), and underloaded again for the third phase (from 10 to 16 hours). The gravity flux curve showing the overflow line, underflow line and the state point (indicated by their intersection) for the first phase of the operation is illustrated in Figure 5.8, for the second phase of the operation in Figure 5.9, and for the third phase of the operation in Figure 5.10.

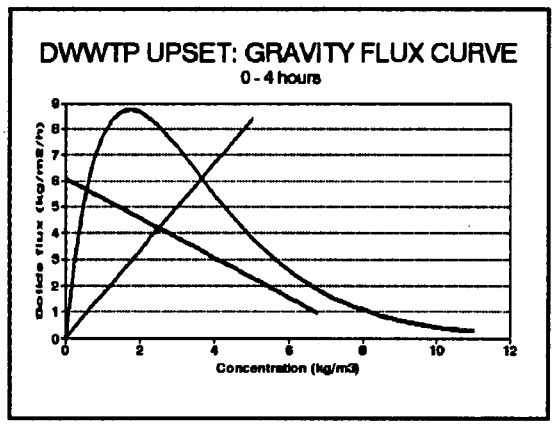

Figure 5.8 Gravity flux curve for phase 1

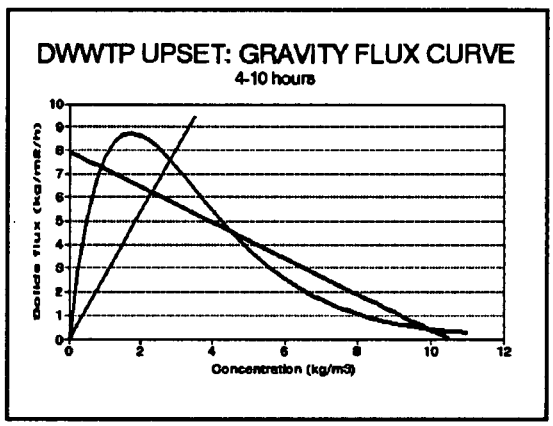

Figure 5.9 Gravity flux curve for phase 2

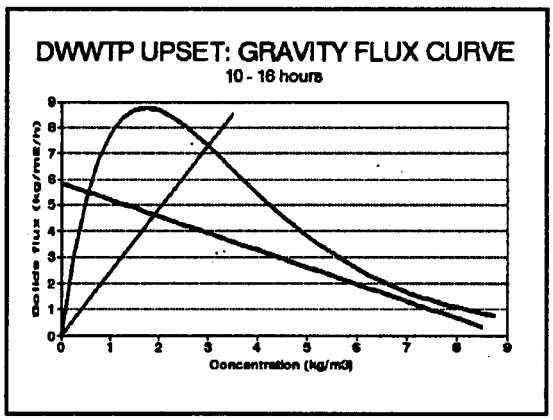

Figure 5.10 Gravity flux curve for phase 3

For the first phase of operation, the state point is within the envelope of the flux curve i.e. solids flux limit A criterion is met and, because the underflow line does not touch or cut the gravity flux curve in more than one place, the settling tank was underloaded (see discussion of flux theory in Appendix A). On the design and operating chart (Figure 5.11), this is confirmed by observing that the state point for phase 1 (X_o = 2.5kgm^{-3}) lies below the hyperbola marking the underflow line tangent limit and inside (to the right of) the solids flux

limit A line X_o = 2.5kgm^{-3} (solid line). Similarly to phase 1, phases 2 and 3 are illustrated on the gravity flux curves and on the design and operating chart in Figure 5.11 with dotted and dashed lines respectively. Note that the solids flux limit A line is feed concentration specific i.e. the three different solids flux limit A lines correspond to the three different feed concentrations during the operation.

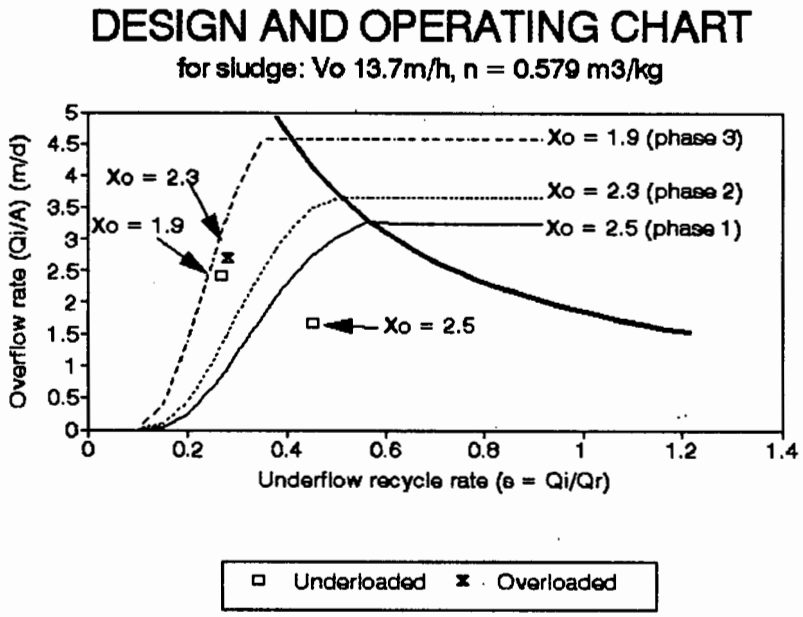

Figure 5.11 Design and operating chart for the DWWTP upset

For the second phase of the operation, although the state point lies within the envelope of the flux curve, the underflow line cuts the flux curve in three places, indicating that the settling tank was overloaded (Figure 5.9). This is confirmed on the design and operating chart (Figure 5.11) by observing that the state point for X_o = 2.3kgm^{-3} lies below the hyperbola marking the underflow line tangent limit but above (to the left of) the solids flux limit A line for this feed concentration (dotted line).

For the third phase of the operation, similar conditions to phase 1 apply and the settling tank was once again underloaded (Figure 5.10). This is confirmed on the design and operating chart (Figure 5.11) by the position of the operating point for X_o = 1.9kgm^{-3}. This point lies below the hyperbola marking the underflow line tangent limit and below (to the right of) the solids flux limit A line (dashed line).

5.5.4 DISCUSSION OF THE PROGRAM RESULTS

1 hour after start (phase 1, Figure 5.8 and Figure 5.11)

The experimental results for the concentration profile at 1 hour (Figure 5.4), show that the measured concentration profile has remained virtually unchanged from the initial conditions, with the sludge blanket still at 13.5ft below the surface. There is no solids loss measured in the effluent and the underflow concentration remains at $\pm 14 kgm^{-3}$. In contrast, the program predicts a considerable change in the concentration profile during the first hour. The simulation results (Figure 5.4) show that the sludge blanket has fallen markedly (from 13.5ft to 17ft below the surface of the tank). However, the program predictions of no solids loss in the effluent and the underflow concentration of $\pm 14 kgm^{-3}$ match the measured results quite closely.

5 hours after start (phase 2, Figure 5.9 and Figure 5.11)

Figure 5.5, which illustrates the concentration profile after 5 hours of operation, shows a close correspondence between the measured results and those predicted by the program. The measured results show that the sludge blanket has virtually disappeared and is at approximately 16ft below the surface of the settling tank. The underflow concentration has decreased to $13 kgm^{-3}$, and there is no solids loss observed in the effluent. The simulation program predicts a slightly lower sludge blanket level (± 17ft), and an underflow concentration of $\pm 12 kgm^{-3}$. The program correctly predicts no solids loss in the effluent.

Although, according to the flux theory, the settling tank begins to experience overloaded conditions at 4 hours, after 5 hours this is clearly not apparent in the measured and simulated concentration profiles. However, this is not unexpected because it takes some time for the characteristic concentration profile for overloaded conditions to develop in the tank, the time interval being dependent on the magnitude of the solids overload and the difference between the applied and limiting fluxes. From

Figure 5.9 and Figure 5.11 it can be seen that the settling tank is only about 15% overloaded.

9 hours after start (phase 2, Figure 5.9 and Figure 5.11)

The measured concentration profile (Figure 5.6) shows that there has been little change in the total mass of sludge in the settling tank since the start of the test as well as an insignificant change in the sludge blanket level below the surface. However, 9h after the start of the test there is a solids loss with the effluent at a measured concentration of $180mgl^{-1}$. The underflow concentration has decreased from $12kgm^{-3}$ to $10kgm^{-3}$.

The simulated results show a marked increase in the mass of sludge in the tank. This does not occur in the form of a well defined and raised sludge blanket, but rather as a dispersed layer that progressively increases in concentration down the tank depth from $130mgl^{-1}$ at the overflow level (layer 1) to $\pm 10kgm^{-3}$ in the underflow level (layer 40). The sludge mass in the tank at 9 hours is 66364kg compared to the initial mass of 44516kg, an increase of 49%. The simulation program correctly predicts solids loss with the effluent but at a lower concentration of $130mgl^{-1}$ instead of the measured $180mgl^{-1}$.

From the above, it is clear that there is a significant difference between the results measured and those predicted by the simulation program.

It appears that there is a "lag" time for the concentration profile typical of overloaded conditions to become manifest in the tank, a lag that is not apparent in the simulation program predictions. In addition, it seems that the effect of the diffusivity function in the simulation program is to smooth out the profile of the rising sludge blanket to the point that it is difficult to identify the position of the sludge blanket in the settling tank.

established that the total mass balance around the system (i.e. inflow - outflow = accumulation) was not preserved for both the measured and predicted results. The error in the mass balance for the measured results was found to be 59% at 13 hours, whilst the mass balance error in the simulated results was found to be 82% at 15 hours. This is a problem of some concern that is examined later in greater depth.

In commenting on his own results, Anderson stated that the applied flux on the settling tank was at no stage of the test higher than the theoretical limiting flux. Therefore he concluded that a dynamic model based solely on flux theory considerations would have identified the entire test period as underloaded and thus failed to predict a rising sludge blanket resulting effluent solids loss during the second phase of the test. However, calculating the theoretical limiting flux from the flux theory constants V_o and n supplied by Anderson and comparing it to the applied flux, it was found that the second phase of the operation (4-10 hours) was in fact overloaded (albeit small i.e. 114% of limiting flux). It is therefore possible that a much simpler settling tank model e.g. that of Tracy and Keinath (1974) without the inclusion of turbulent diffusion and the sophisticated shock capturing and numerical integration techniques, might also have adequately predicted a solids overloaded condition for phase 2.

Although SETTLER, like Anderson's own program, seems to perform quite adequately in predicting the results for the DWWTP example, it appears that this may be due to Anderson's tailoring his diffusivity functions to the specific configuration of the DWWTP with the result that the model may not be applicable to the general case. The reason for concluding this arises mainly from the discrepancies between the equations given for the diffusivity functions in the body of the thesis and the actual equations included in the program (see Figure 5.1 and Figure 5.2). The main difference is the program's relatively high and constant value of the diffusivity in the tank from the fifth layer below the feed point to the bottom of the tank. From experience with the program, it was found that the accuracy of the simulation results are very sensitive to the magnitude of the diffusivity in the lower layers of the tank and therefore Anderson probably determined the diffusivity equation and values by trial and error to obtain

favourable comparison with the measured results. While this is an acceptable engineering approach, it may indicate that the form and value of the diffusivity is more a function of the tank specific geometry and hydraulics than a function of turbulence, eddy effects, density currents and diffusion in general taking place in all settling tanks. Clearly, while including turbulent diffusion in the flux model allows the development of simpler and more efficient algorithms, it also has a major impact on the simulation results. The significance of this aspect in the program needs to be carefully examined.

5.5.6 CONCLUSIONS

In view of the above, the application of the program to other test cases at this stage will be confounded by the lack of clarity as regards the form and magnitude of the diffusivity function. Consequently, if inaccurate or unexpected results are generated, it is not possible to establish whether this is because of incorrect application of the diffusivity term, or due to other possible deficiencies in the program. However, because the program simulations with SETTLER compared reasonably favourably with the DWWTP measured data, at least as favourably as Anderson's own simulation results, it was concluded that SETTLER was an accurate reconstitution of the appropriate section of Anderson's own program, at least as accurate as could be determined. Therefore the above simulations should not be regarded as verification of the program, rather as confirmation that Anderson's program was accurately reconstituted in the form of SETTLER. With this confirmation, it was concluded that general verification work on the program could be commenced.

In order to try and resolve the confusion introduced by the lack of clarity about the diffusivity functions and possible other deficiencies in the program, it was decided to select a test case where it would be possible to almost entirely eliminate the effects of diffusivity. This would reduce the program to a form where other deficiencies in the program, should they exist, will become apparent and can be dealt with. For small diameter to depth ratios, (i.e. small diameter, tall columns as encountered in the labwork data) vertical flow (only up and down) dominates the settling behaviour and

horizontal effects are negligible. Thus, diffusivity effects in the column can be assumed to be very small and the diffusivity coefficient can be set to zero. By this action, the partial differential equations governing the settling motion are rendered hyperbolic and the need to know the form and magnitude of the diffusivity function is obviated.

Unfortunately, all of the labwork data available falls into only two of four regions on the design and operating chart (see Figure 5.12), and therefore in testing the ability of the program to perform under a representative selection of operating conditions it was meaningful to select only one case from each region. This means that, using only the labwork data for comparison, the program is not rigorously verified for all areas of the design and operating chart. In addition, the limitations of the labwork data which does not specify initial conditions or test duration means that it is useful only for approximately verifying the predictions of the model.

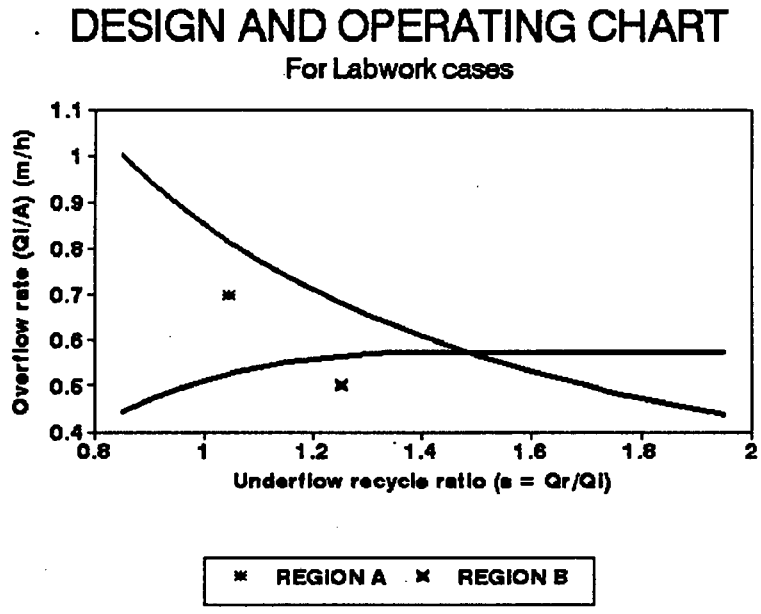

Figure 5.12 **Design and operating chart showing categories of all labwork cases.**

In view of the above, verification of the model was undertaken in three steps

1. Using theoretical cases (no diffusivity) i.e. comparison against idealized flux theory concentration profile solutions,
2. semi-idealized cases with no diffusivity i.e. laboratory data from tall slender continuous settling columns,
3. real cases from full scale large diameter settling tanks (with diffusivity).

The outcome of each of these three stages is discussed in detail in Chapters 6, 7 and 8 respectively.

REFERENCES

Anderson H.M. and R.V. Edwards, "Combined sewer overflow modelling: STPSIM2, A dynamic model of the wastewater treatment plant", Paper presented at the 91st National Meeting of the AIChE, Detroit, Michigan, (1981)

Anderson H.M. and R.V Edwards, "A finite differencing scheme for the dynamic simulation of continuous sedimentation", AIChE Symposium Series, Water, (1980)

Anderson H.M., "A dynamic simulation model for wastewater renovation systems", PhD thesis, Wayne State University, Detroit, Michigan, (1981)

Beam, R.M. and R.F Warming, "An implicit finite-difference algorithm for hyperbolic systems in conservation law form", Journal of Computational Physics, Vol 22, No 1, pp 87-110, (1976)

Lax, P.D., "Hyperbolic systems of conservation laws II", Comm Pure Appl Math, Vol 10, No 2 , pp 537-566, (1957)

Tracy, K.D. and T.M. Keinath, "Dynamic model for thickening of activated sludge", AIChE Symposium Series, Vol 70, No. 136, p 291, (1974)

Von Neumann, J. and R.D. Richtmyer, "A method for the numerical calculation of hydrodynamic shocks", Jour Appl Phys, Vol 21, No 1, pp 232-237, (1950)

CHAPTER 6
SETTLER APPLIED TO THEORETICAL CASES

6.1 INTRODUCTION

In this chapter, SETTLER is applied to four idealised theoretical test cases with the diffusivity coefficient set to zero. This enables other (non-diffusivity related) deficiencies in the program to be identified and resolved. Once this has been achieved, it will be possible to reintroduce the diffusivity coefficient into the program and to apply SETTLER to real settling tanks. The outcome of the reintroduction of diffusivity into the program for the simulation of full scale settling tanks is discussed in detail in Chapter 8.

Although Anderson stated that his solution algorithm is valid for both the hyperbolic and the parabolic cases, the previous description of the behaviour of hyperbolic equations and their tendency to generate physically meaningless solutions suggests that some modifications will need to be made to the program SETTLER before applying it to the hyperbolic theoretical test cases (no diffusivity).

For the underloaded case, no modification is needed as the underflow line cuts the gravity flux curve in one place only with the result that only one possible solution exists in the dilute concentration region (X_{dz}). For the overloaded case, however, the underflow line cuts or touches the gravity flux curve in more than one place and multiple solutions are possible - both X_{dz} and X_L. In this case, the solution that is being sought is that for X_L, the limiting concentration, which is found where the underflow line makes a tangent to the gravity flux curve to the right of the inflexion point (see Figure 6.1.)

In the concentration field of the partial differential equations, the region of influence of the dilute zone concentration (X_{dz}) is larger and more powerful than that for the

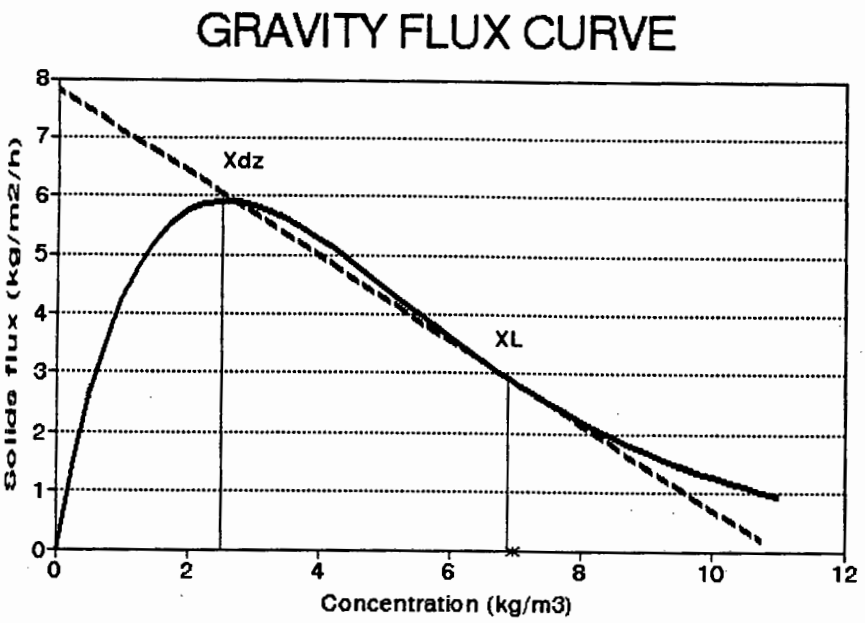

Figure 6.1 The gravity flux curve showing the two possible solutions for concentration.

limiting concentration X_L. Thus, in the absence of any additional criterion, the numerical method for the hyperbolic case (no diffusivity) will invariably converge onto X_{dz} in preference to X_L, and predict this as the concentration for the sludge blanket in the overloaded case. In order to induce the numerical method for the hyperbolic case to search for a solution in the region of X_L, some additional criterion needs to be activated for the overloaded case. This is accomplished by using a "seeding" procedure when overloaded conditions prevail. It should be noted that, for the parabolic case i.e. the form in which Anderson implemented his model, such seeding is not necessary because the parabolic equations (with diffusivity) automatically generate a steady state solution for X_L which is uniquely defined by the initial conditions.

Analysis of the loading situation in the settling tank using flux theory at each time step of the simulation enables the correct value of X_L to be determined. This externally calculated value can then be used to "seed" the hyperbolic equations to ensure that the solution is initiated in the correct region of the concentration range. A seeding procedure was developed and included in the program SETTLER. It operates in the following manner:

concentration value. However, for the case where only one solution is possible, if incorrect values were used for seeding, the correct solution was nevertheless generated for all layers from 37 upwards (because correct values for layers 38 and 39 were overwritten with incorrect seed values, the predicted values for these two layers remained incorrect). Thus, although the seeding technique could be seen as a "brute force" method of imposing theoretically calculated values onto the solution, this is only true for the overloaded cases where two solutions are possible (region A in Figure 6.2). In other cases (region D in Figure 6.2), the program converges to the correct solution for X_L without the seeding procedure.

In order to rigorously test the ability of the program to predict accurate (as defined by the flux theory) concentration profiles for the hyperbolic equations, it was decided to select four different theoretical test cases, each one falling into a different region of the design and operating chart. The design and operating chart showing the position of each of the four theoretical test cases is illustrated in Figure 6.2.

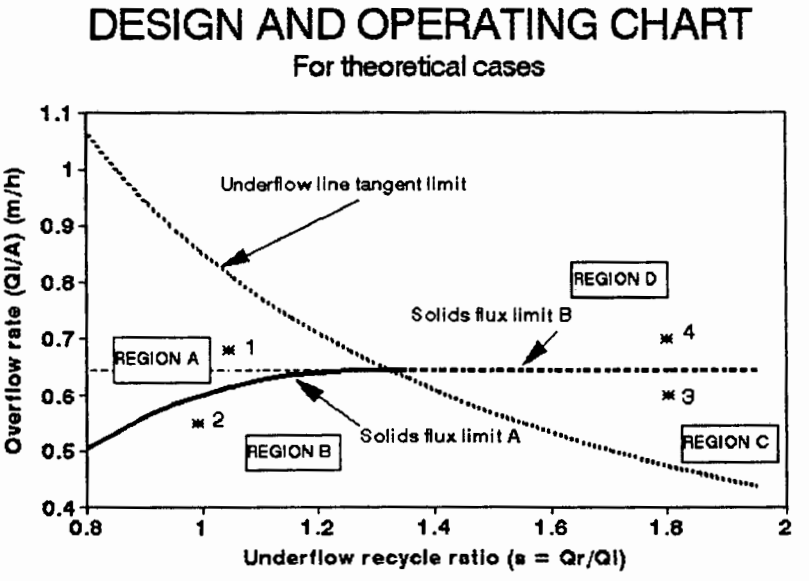

Figure 6.2 Design and operating chart showing four different possible regions of operation

The defining characteristics and flux curves for each of the four different regions are illustrated in Figure 6.3 and are described below.

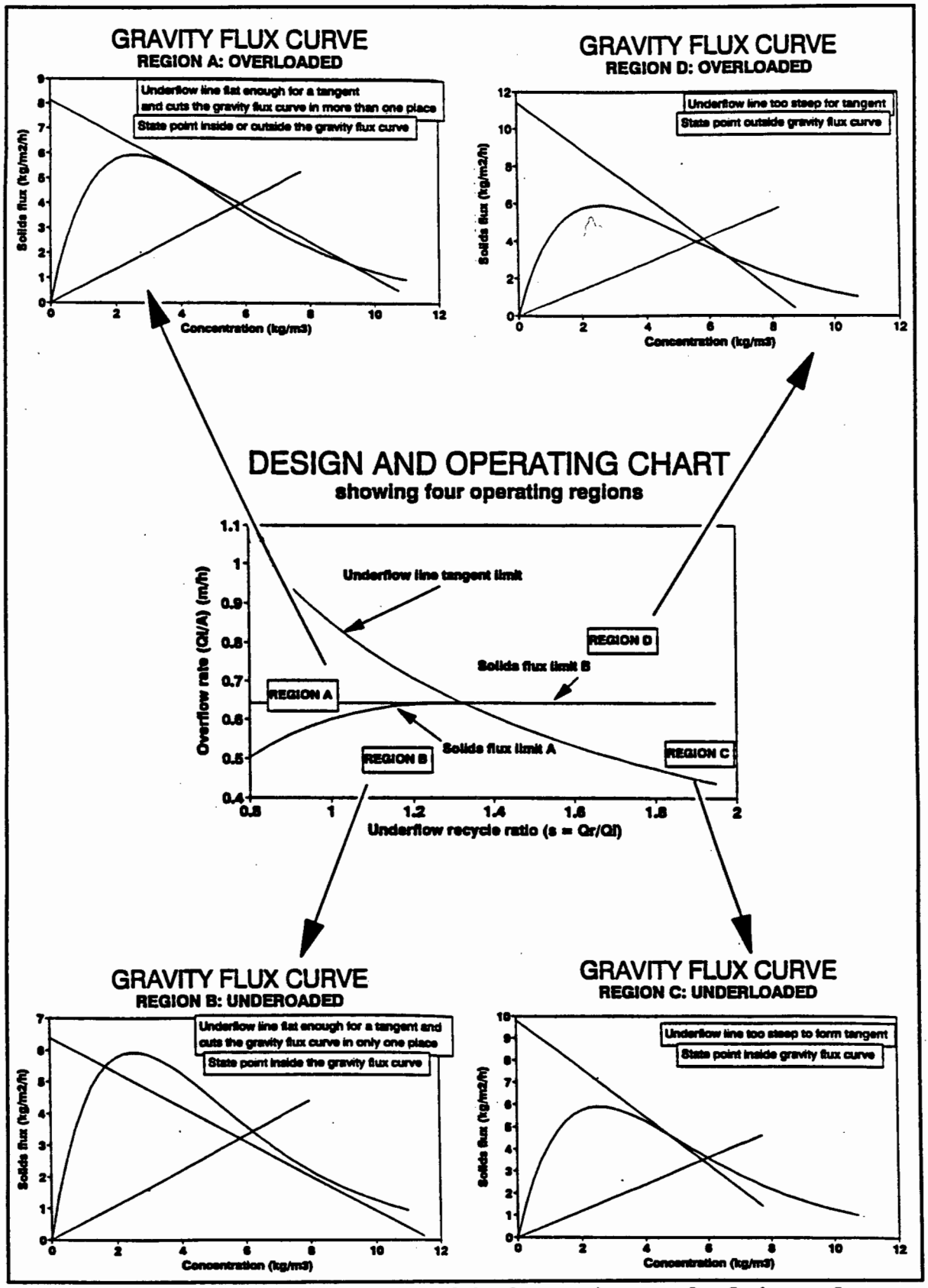

Figure 6.3 Flux curves for each of the four regions on the design and operating chart

POINT 1 IN REGION A

On the design and operating chart, it can be seen that this is an overloaded situation with the solids flux limit A criterion not being met (the operating point falls above the solids flux limit A line) but with the underflow line being sufficiently flat to enable a tangent to be drawn to the gravity flux curve (the operating point falls to the left of the underflow line tangent limit). On the gravity flux curve, for point 1, the state point is outside the envelope of the gravity flux curve and the underflow line (i) cuts the gravity flux curve in more than one place and (ii) is sufficiently flat to enable a tangent to be drawn to the gravity flux curve to the right of the inflexion point. This point 1 is representative of all the failure cases by this mode, i.e. in region A (See Figure 6.2).

Region A comprises two subregions:

a. cases where the state point is within the envelope of the gravity flux curve (operating point falls below the extension of the solids flux limit B line to the vertical axis) and

b. cases where the state point falls outside the envelope of the gravity flux curve, (operating point falls above the solids flux limit B extension as in the case of point 1).

For both subregions, the underflow line is sufficiently flat to make a tangent to the gravity flux curve to the right of the inflexion point (i.e. $U_u \leq V_o/e^2$).

POINT 2 IN REGION B

This is an underloaded situation with the operating point on the design and operating chart falling below the solids flux limit A curve (solids flux limit A

criterion satisfied), and to the left of the underflow line tangent limit. On the gravity flux curve, the state point falls within the envelope of the gravity flux curve (solids flux limit criterion A is met) and the underflow line is sufficiently flat to enable a tangent to be drawn to the gravity flux curve. This point 2 is representative of all the safe cases in region B (see Figure 6.2).

POINT 3 IN REGION C

This is an underloaded situation with the operating point on the design and operating chart falling below the solids flux limit B criterion line (solids flux limit B criterion is met) but to the right of the underflow line tangent limit. On the gravity flux curve, this situation is characterised by the underflow line being too steep to enable a tangent to be drawn to the gravity flux curve (i.e. $U_u > V_o/e^2$) but with the state point being within the envelope of the gravity flux curve, indicating that solids flux limit B is met. This point 3 is representative of all the underloaded cases in region C (see Figure 6.2).

POINT 4 IN REGION D

This is an overloaded situation with the operating point on the design and operating chart falling above the horizontal line representing the solids flux limit B criterion and to the right of the underflow line tangent limit. On the gravity flux curve, the state point is outside the envelope of the gravity flux curve (solids flux limit B not met) and the underflow line is too steep to enable a tangent to be drawn to the gravity flux curve (i.e. $U_u > V_o/e^2$). This point 4 is representative of all the failure cases in region D (see Figure 6.2).

In general, for each of the cases above, the program is expected to be able to predict correctly whether or not the system is underloaded or overloaded as well as the correspondingly correct concentration profile as defined by flux theory calculations. In particular, for the underloaded cases, the program is expected to be able to predict:

1. the absence of a sludge blanket,
2. the correct concentration in the dilute zone (X_{dz}),
3. the correct underflow concentration (X_r),

and for the overloaded cases:

1. eventual solids loss with the effluent at the correct solids concentration (X_{ef}),
2. the correct concentration in the zone above the feed point (X_{af}),
3. the presence of a rising sludge blanket below the feed point at a concentration of X_L,
4. the correct underflow concentration (X_{rL}).

The relevant parameters common to all the theoretical cases tested are presented in Table 6.1. The physical dimensions of the settling tank were taken to be the same as those of the laboratory scale settling column and the settling characteristics of the sludge were chosen to be the same as those for labwork cases 2 and 5.

Table 6.1 Operating parameters that are common to all theoretical test cases.

PARAMETER	VALUE
AREA	$0.00442m^2$
DEPTH	2m
FEED POINT LAYER	7
V_o	$6.287mh^{-1}$
n	$0.391m^3kg^{-1}$

6.2 SETTLER APPLIED TO THE OVERLOADED CASE: POINT 1 IN REGION A

The onset of solids flux limit A failure in the column takes place when the conditions are such that the underflow rate line touches as a tangent on the gravity flux curve. Therefore, in order to test the discernment of the program in identifying failure, the first theoretical overloaded test case selected was close to flux limit A failure, and only just overloaded (G_{ap} = 104% of G_L). If the program can successfully identify this as an overloaded case, then it will be capable of fulfilling one of its critically important requirements.

The relevant parameters which are specific to test case A are detailed in Table 6.2 and the gravity flux curve for test case A is presented in Figure 6.4.

Table 6.2 Operating parameters for test case A.

PARAMETER	VALUE	ALTERNATIVE UNITS
Q_i	$0.003008m^3h^{-1}$	$(3.008lh^{-1})$
Q_r	$0.003141m^3h^{-1}$	$(3.141lh^{-1})$
X_o	$5.85kgm^{-3}$	

In Figure 6.4 the dotted line is the underflow line for the case of the limiting flux (G_L) and the solid line is the underflow line for the applied flux (G_{ap}). The graph shows that the state point is outside the envelope of the gravity flux curve and that the underflow line for the applied flux cuts the gravity flux curve in more than one place, indicating that solids flux limit A is not met and that this is an overloaded situation. From manual flux theory calculations (i.e. ideal conditions, no diffusivity) the following results are expected (for details of the method for these calculations, see Appendix A):

1. an underflow concentration of approximately $X_{rL} = 11.01kgm^{-3}$,

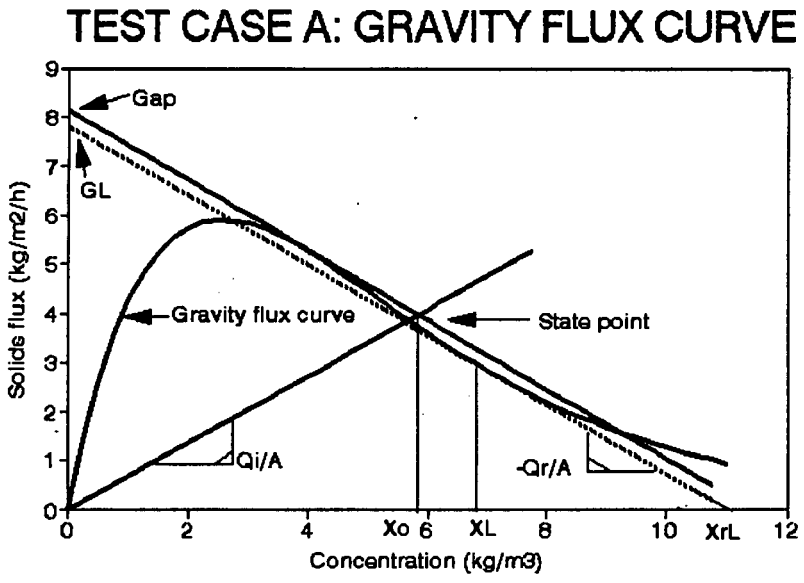

Figure 6.4 Gravity flux curve for test case A.

2. the formation of a sludge blanket of concentration of approximately $X_L = 6.97 kgm^{-3}$,
3. a region above the feed point of concentration approximately $X_{af} = 5.89 kgm^{-3}$,
4. solids loss with the effluent at a concentration of approximately $X_{ef} = 0.46 kgm^{-3}$.

An arbitrary initial concentration profile relatively different to the expected solution was selected to initiate the simulation. This was intended to test the ability of the program and seeding strategy to initiate the correct limiting concentration X_L and to overcome the area of influence of X_{dz}. The initial concentration profile is illustrated in Figure 6.5.

The simulation for test case A was run for an arbitrary time period of 80 hours which was deemed sufficient for steady state conditions to be established in the settling column. This would ensure that, were the expected sludge blanket to form, there would be sufficient time for it to build up in the column and to rise above the feed point, thereby allowing the expected solids loss to occur in the effluent.

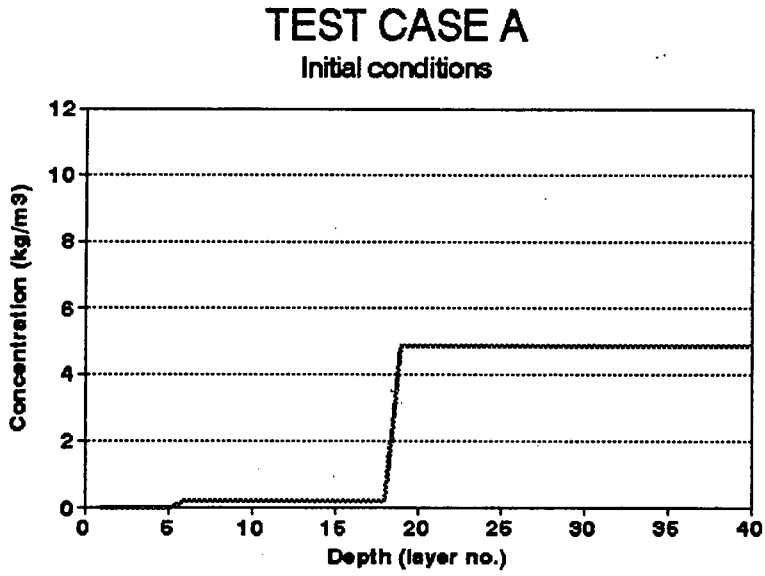

Figure 6.5 Initial concentration profile for test case A

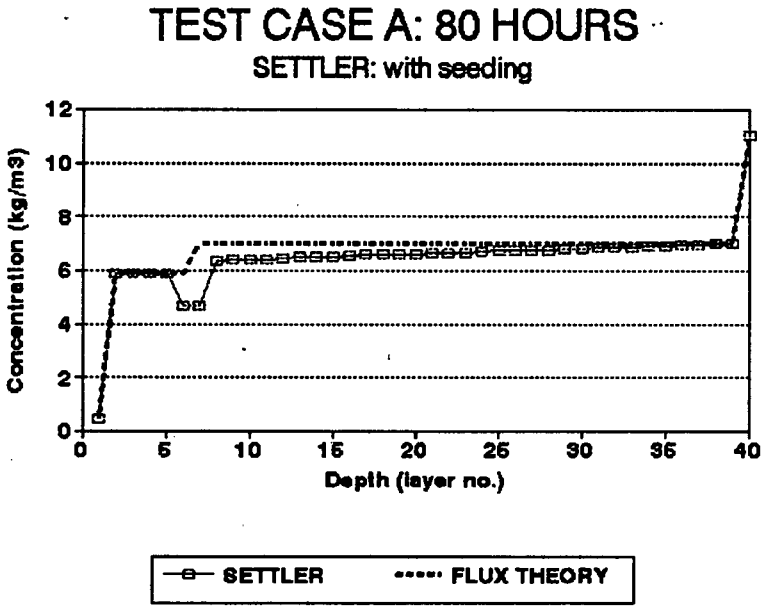

Figure 6.6 Test case A: predicted and theoretical concentration profile at 80 hours

The concentration versus depth profile generated by SETTLER after 80 hours is compared with the theoretical concentration profile obtained from the flux theory in Figure 6.6. From Figure 6.6 it can be seen that the values obtained by SETTLER correspond almost exactly to the theoretical ones. However, the predicted

concentration profile (SETTLER) exhibits two layers at the feed point (layers 6 and 7) in which the concentrations are not as expected. In these layers, the predicted concentrations, besides being much lower than expected, also represent an entropy rule violation, as it is not physically possible to achieve a concentration increase from layer 6 to layer 5 without a change in gravity or bulk flux.

The reason for this entropy rule violation is Anderson's condition in the program that the concentration in the layer directly above the feed point (6) be set equal to the concentration in the layer at the feed point (7). This is one of the points of concern raised in Chapter 5, Section 5.4. This condition overwrites the values for the concentrations in these two layers calculated by the Gaussian procedure by averaging the calculated concentrations in layers 6 and 7 and inserting this average value in both layers as follows:

$$conc(6)_{NEW} = \frac{conc(6)_{OLD} + conc(7)_{OLD}}{2} \qquad (6.1)$$

$$conc(7)_{NEW} = conc(6)_{NEW} \qquad (6.2)$$

where $conc(6)_{OLD}$ = the concentration in layer 6 as calculated by the Gaussian solution procedure

$conc(7)_{OLD}$ = the concentration in layer 7 as calculated by the Gaussian solution procedure

However, it was found that, without this condition, the concentration in the feed point layer (7) increased indefinitely while the concentrations in the layers above the feed point (6 upwards) remained low and no solids loss in the effluent took place i.e. instead of the solids propagating upwards above the feed point, they accumulated in the feed point layer. This is illustrated in Figure 6.7. Thus, it appears that Anderson found it necessary to insert the averaging condition in order to force the sludge blanket to move above the feed point layer for the overloaded case.

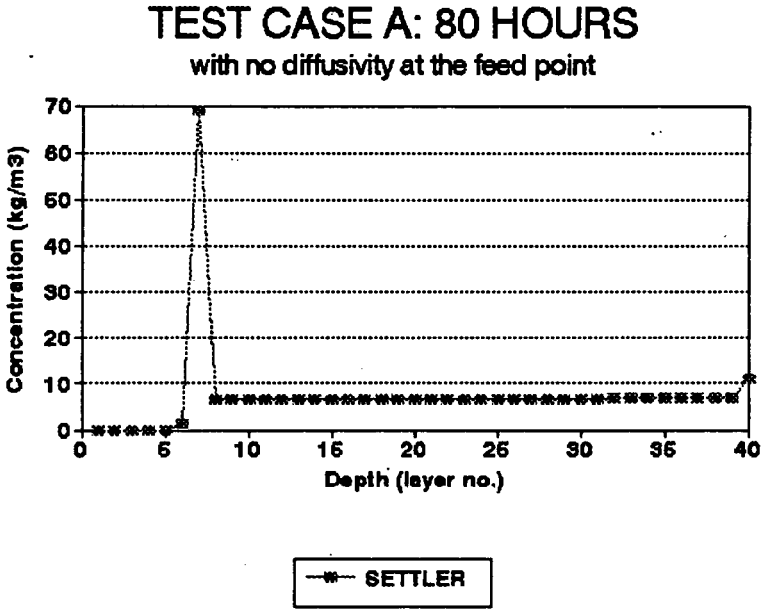

Figure 6.7 Test case A: the effect of eliminating the feed point conditions in SETTLER

After examining the problem, it became apparent that the necessity for Anderson's averaging condition results from the change in flux directions at the feed point. Between the feed point layer (7) and the layer above (6), there is a change in the direction of the bulk flux as well as in the gravity flux. In layer 7, both the bulk flux and the gravity flux are downwards, whereas in layer 6, the bulk flux is upwards whilst the gravity flux is downwards. These step changes in bulk and gravity fluxes cause a disturbance in the switching functions which control the propagation of a rising sludge blanket past the feed point layer. A more detailed explanation of the mechanism of the switching function operation can be found in Appendix B.

In the program, control over whether either the concentration in a layer changes or the sludge blanket moves to the next layer is maintained by a switching function. For example, when a layer is at the limiting concentration (X_L or X_{af}), the switching function prevents the concentration in this layer from increasing further and instead forces the accumulating sludge in the layer to be passed onto the next layer above it, thus causing the sludge blanket to rise. In order for the switching functions to be correctly activated, either the concentrations in adjacent layers need to be equal, or a

decrease in concentration from one layer to the next above it must always be associated with a corresponding increase in flux between the two layers. This is the case for all adjacent sludge layers below the feed point (7 to 39) but not for layers 6 and 7. Because of the change in flux direction between layers 6 and 7, the total flux decreases with decreasing concentration between the layers, and consequently the switching function is not correctly activated to propagate the accumulating material into the layer above the feed point layer. Anderson's averaging condition, by ensuring that the concentrations in layers 6 and 7 are equal, artificially overcomes this problem with the switching functions, thereby enabling the sludge blanket to move above the feed point.

The program SETTLER was revised (revision 1) in order to avoid the necessity to overwrite the calculated concentrations in the feed point layer (7) and the one above it (6). This overwriting, although enabling the sludge blanket to move above the feed point for the overloaded case, also causes an entropy violation at the feed point in the predicted concentration profile. Because the feed enters the column in a horizontal stream at the feed point layer, it can be assumed that if there is any turbulence causing horizontal flow components in the column, it will be greatest at this layer. It was thus decided to investigate including a diffusivity term at the feed point layer as an alternative method of overcoming the switching function problem at the feed point. The diffusivity of all the other layers would remain at zero.

It was found that the effect of introducing a diffusivity term at the feed point layer (7) was to "mix" the contents of the feed point layer with the one directly above it i.e layer 6. This eliminated the concentration discontinuity that was previously encountered between layers 6 and 7 as the diffusivity distributed the total sludge available to the two layers between them. This had the desired effect of overcoming the discontinuity in the total flux curve and ensured that a decrease in concentration (from layer 7 to layer 6) was associated with an increase in flux. Hence, the switching functions were correctly activated, enabling the sludge blanket to propagate above the feed point.

Various values of the diffusivity coefficient for test case A were evaluated on the basis of their ability to (i) allow the sludge blanket to propagate above the feed point and (ii) produce a concentration profile free of entropy rule violations i.e. a concentration profile of continually increasing concentration from top to bottom of the settling tank. It was found that any value of $E \geq 0 m^2h^{-1}$ would allow the sludge blanket to propagate above the feed point for the overloaded case but a small value (e.g. $E = 20m^2h^{-1}$) produced a concentration profile containing an entropy rule violation at the feed point. This is illustrated in Figure 6.8.

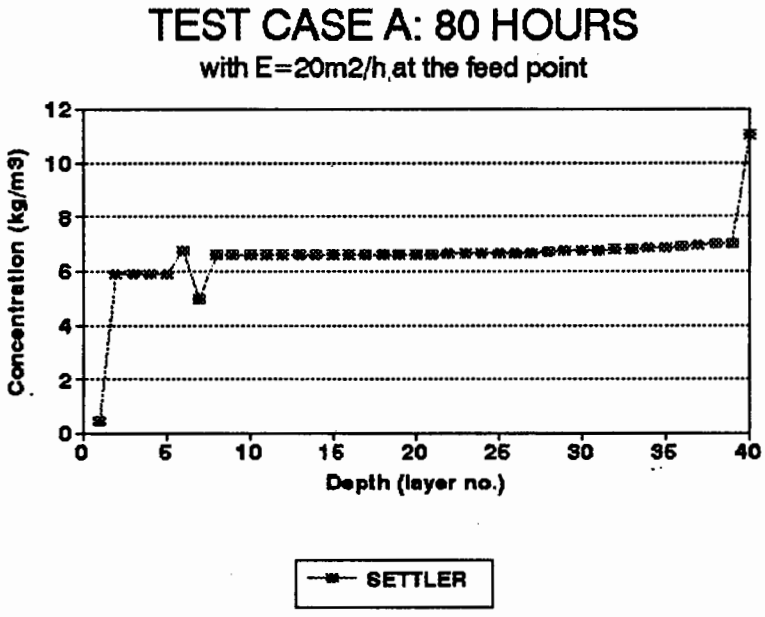

Figure 6.8 Test case A: the effect of $E = 20m^2h^{-1}$ on the concentration profile

Progressively higher values of E gradually smoothed out the concentration profile. The values of E for which no entropy rule violation occurs at the feed point are $E \geq 20000m^2h^{-1}$. Thus, it was found that the introduction of diffusivity at the feed point both allows the sludge blanket to propagate past the feed point for the overloaded case and eliminates the entropy rule violation associated with the averaging approach. In addition, since a high degree of diffusivity in the form of turbulence and horizontal movement has been shown to be physically evident at the feed point (Ranger and Christie (1978)) (Giffels/Black and Veatch (1978)) (Williams and Works (1979)), this

strategy has the advantage of being physically more realistic than the averaging approach.

The concentration profile predicted by SETTLER with E = 20000m^2h^{-1} in the feed point layer (revision 1) after 80 hours is illustrated in Figure 6.9.

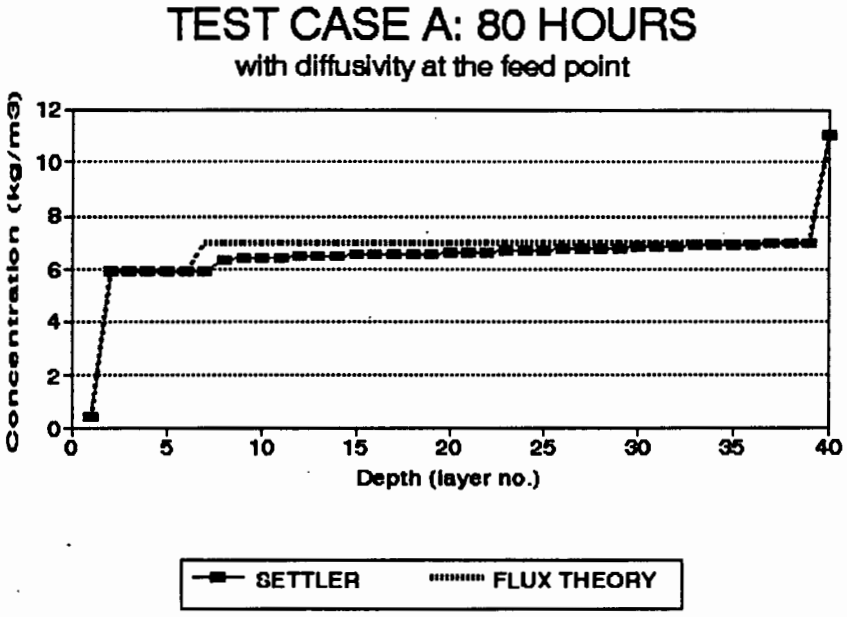

Figure 6.9 Test case A : concentration profile at 80 hours with E=20000m^2h^{-1} at the feed point

It can be observed that the major concentration regions predicted correspond almost exactly to those predicted by the flux theory i.e.

1. an underflow concentration of 11.01kgm^{-3},
2. a sludge blanket zone of concentration $\pm$6.6kgm^{-3},
3. a region above the feed point of concentration 5.88kgm^{-3},
4. solids loss with the effluent at a concentration of 0.43kgm^{-3}.

The entropy rule violation between the feed point layer (7) and the layer above it (6) no longer occurs. It can be concluded that SETTLER (revision 1) accurately predicts the theoretically expected concentration profile for the overloaded test case A.

6.3 SETTLER APPLIED TO THE UNDERLOADED CASE: POINT 2 IN REGION B

The second test carried out on the program SETTLER was in region B (See Figure 6.2). Once again, in order to test the discernment of the program in identifying failure conditions, the theoretical test case in region B was chosen to be very close to failure and only just underloaded (G_{ap} = 97% of G_L).

The relevant parameters which are specific to test case B are presented in Table 6.3. The sludge settling characteristics V_o and n are the same as for the first test (see Table 6.1).

Table 6.3 Operating parameters for test case B.

PARAMETER	VALUE	ALTERNATIVE UNITS
Q_i	$0.00243m^3h^{-1}$	$(2.43lh^{-1})$
Q_r	$0.00241m^3h^{-1}$	$(2.41lh^{-1})$
X_o	$5.83kgm^{-3}$	

The gravity flux curve for test case B is presented in Figure 6.10, which shows underloaded conditions, i.e, the state point is within the envelope of the gravity flux curve and the underflow line cuts the gravity flux curve in one place only. However, the underflow line is close to the potential tangent point on the gravity flux curve, indicating that the applied flux is close to the theoretical limiting flux.
From flux theory calculations (i.e. ideal conditions, no diffusivity) (for details of the method for these calculations, see Appendix A), the following results are expected:

1. no sludge blanket,
2. only two major regions of concentration: the dilute zone settling region of concentration X_{dz} = $1.68kgm^{-3}$ and the underflow concentration region of

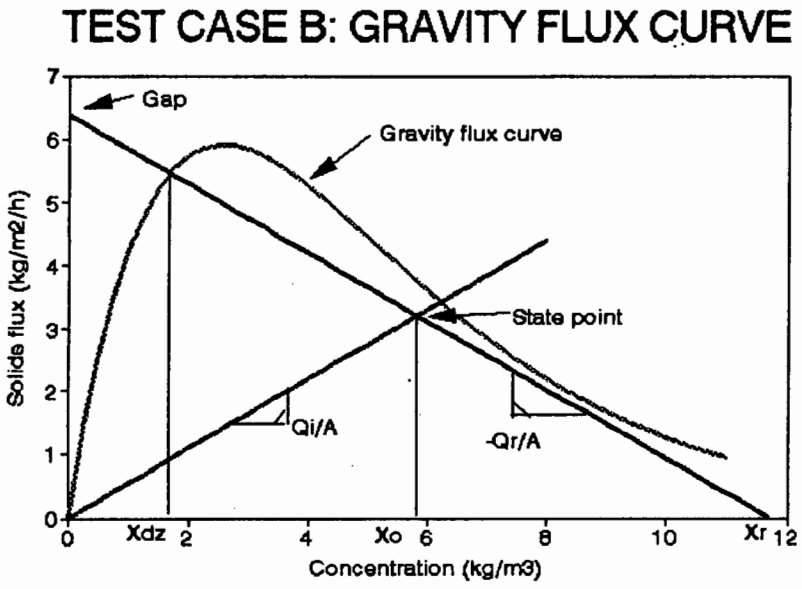

Figure 6.10 Gravity flux curve for test case B.

concentration X_r = 11.72kgm^{-3} and

3. no solids loss associated with the effluent.

The initial conditions used for test case B were those generated by test case A after 80 hours i.e. the concentration profile illustrated in Figure 6.9. These initial conditions were selected to check SETTLER's ability to move from an overloaded to an underloaded situation - the opposite to that of test case A.

The diffusivity value at the feed point layer was adjusted to account for the reduced feed flow rate to the column in test case B. For Q_f = 0.006149m^{3}h^{-1} (test case A) the minimum value of the diffusivity coefficient was found to be E = 20000m^{2}h^{-1}. Thus for Q_f= 0.004840m^{3}h^{-1} (test case B) the diffusivity at the feed point was adjusted proportionally and set at E = 15742m^{2}h^{-1}. However, this is theoretically an unnecessary adjustment because for the underloaded case, the sludge blanket is not expected to rise to the feed point. The diffusivity coefficient was nonetheless included in the event that SETTLER found the case to be overloaded.

The test case was run for an arbitrary time period of 120 hours in order to ensure that, should SETTLER correctly identify the test case as underloaded, the sludge blanket would have ample time to fully propagate out of the system. In Figure 6.11, the concentration profile generated by SETTLER for test case B after 120 hours of operation is compared with the theoretically expected concentration values from the flux theory.

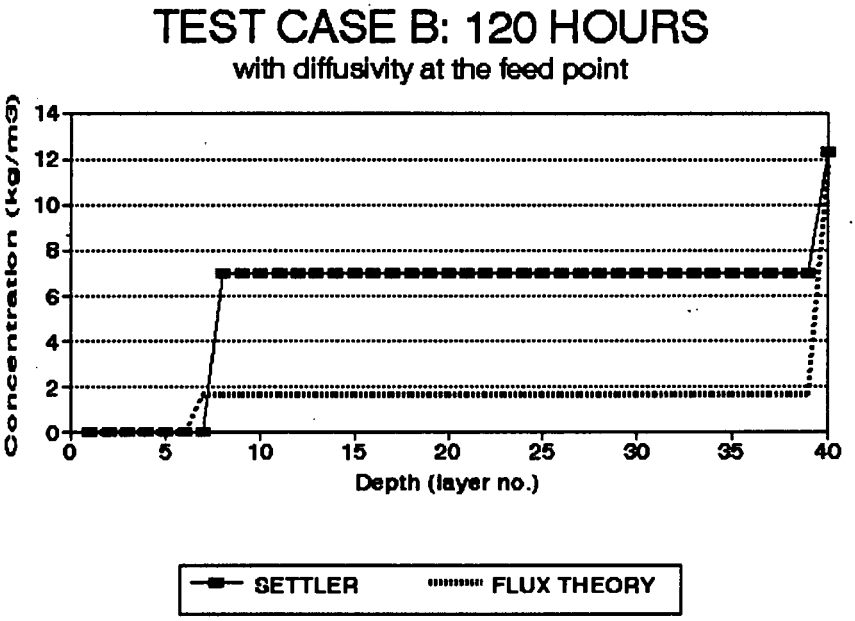

Figure 6.11 **Test case B: predicted and theoretical concentration profiles at 120 hours**

In Figure 6.11, it can be seen that the sludge blanket above the feed point has correctly disappeared, but, contrary to expectations, the sludge blanket below the feed point has not propagated out of the tank and appears to be "stuck" at the feed point. The cause of this unexpected result was identified as an incorrect switching function specification for the two layers immediately below the feed point i.e. layers 8 and 9. As mentioned earlier (see Section 5.4 above), these switching functions were overwritten in Anderson's program. In overwriting these switching functions, the program specifies that the shock directions in these two layers, which are controlled by the switching functions, should always be set equal to each other and ignores the directions calculated by the algorithm itself. For a detailed explanation of the switching function operation, see Appendix B.

The statements overwriting the two switching functions were removed from SETTLER. Repeating the simulation of test case B with the revised SETTLER program (revision 2) produced the concentration profile after 120 hours illustrated in Figure 6.12.

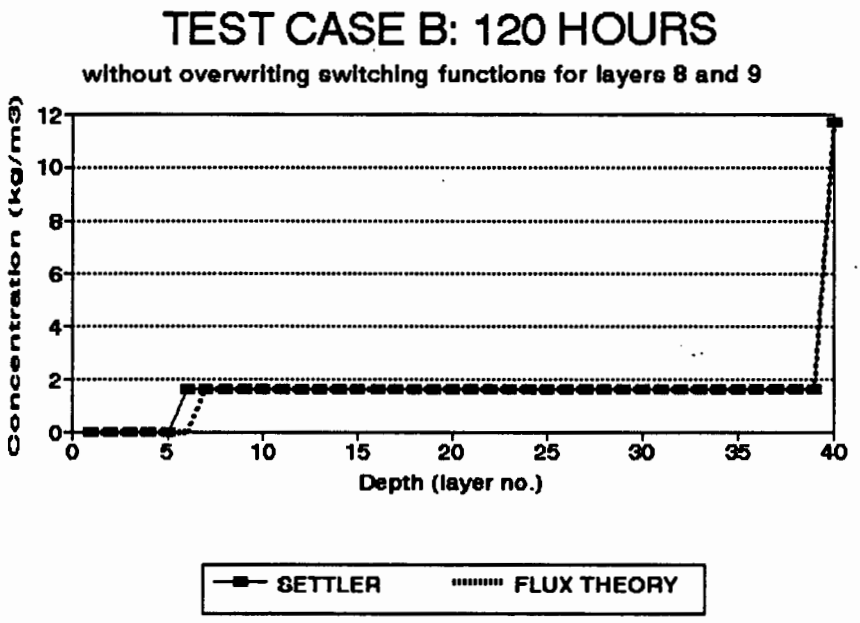

Figure 6.12 **Test case B: predicted and theoretical concentration profiles at 120 hours with the switching function overwriting condition removed**

Comparing SETTLER's predictions with the flux theory calculations, it can be seen that now SETTLER's predictions correspond almost exactly with those calculated the flux theory i.e.

1. zero effluent solids concentration,
2. a dilute zone settling region of concentration $X_{dz} = 1.68 kgm^{-3}$,
3. no sludge blanket formation and
4. an underflow concentration of $X_r = 11.72 kgm^{-3}$.

6.4 SETTLER APPLIED TO THE UNDERLOADED CASE: POINT 3 IN REGION C

The conditions imposed on SETTLER for the third test were those representative of region C and were once again selected to be close to the boundary between underloaded and overloaded conditions on the design and operating chart (See Figure 6.2), in this case, slightly underloaded (G_{ap} = 97% of G_L).

The operating parameters for test case C are given in Table 6.4. The V_o and n values remained unchanged from previous cases.

Table 6.4 Operating parameters for test case C.

PARAMETER	VALUE	ALTERNATIVE UNITS
Q_i	$0.002652m^3h^{-1}$	$(2.65lh^{-1})$
Q_r	$0.004774m^3h^{-1}$	$(4.77lh^{-1})$
X_o	$5.83kgm^{-3}$	

The gravity flux curve for test case C (Figure 6.13) shows that the state point is within the envelope of the gravity flux curve and that the underflow line cuts the curve in one place only, indicating that this is an underloaded situation. In this instance, the underflow line is too steep to form a tangent to the gravity flux curve (i.e. $U_u > V_o/e^2$), which means that the solids flux limit B criterion governs the settling tank behaviour. For this case, according to the flux theory, one would expect (for details of the method for these calculations, see Appendix A):

1. no sludge blanket,
2. only two major regions of concentration: the dilute zone settling region of concentration $X_{dz} = 4.76kgm^{-3}$; and the underflow concentration region of concentration $X_r = 9.07kgm^{-3}$ and

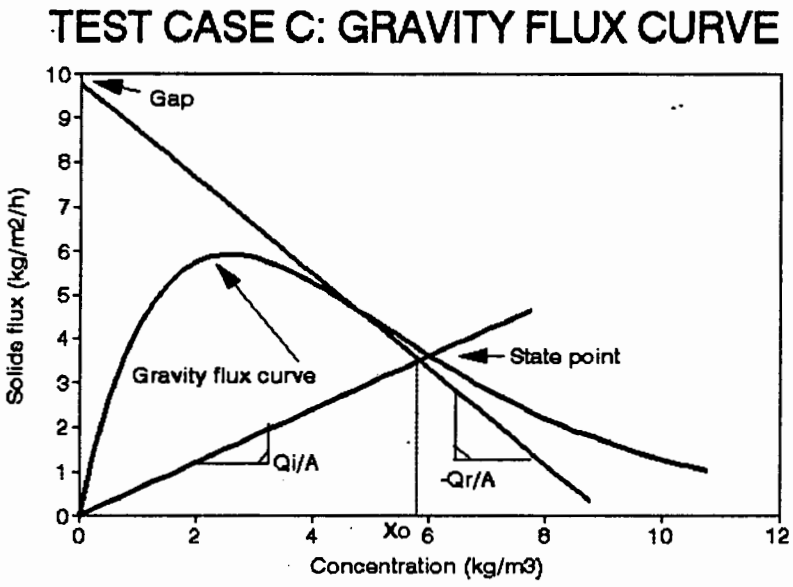

Figure 6.13 Gravity flux curve for test case C

3. no solids loss associated with the effluent.

The initial conditions for test case C were those generated by test case B after 120 hours i.e. the concentration profile labelled SETTLER in Figure 6.12. The diffusivity value at the feed point layer was adjusted proportionally (as before) to account for the increase in feed flow rate for test case C i.e. E was increased to $24152 m^2 h^{-1}$.

The simulation for test case C was run for an arbitrary time period of 40 hours which was deemed sufficient for steady state conditions to be established in the settling column as it moved from one underloaded state to another. In Figure 6.14, the concentration profile generated after 40 hours is compared with the theoretically expected concentration values obtained from the flux theory.

The results predicted by the program SETTLER show

1. no solids loss with the effluent, as expected,
2. a dilute zone concentration of $X_{dz} = 4.76 kgm^{-3}$, as expected from the flux theory,

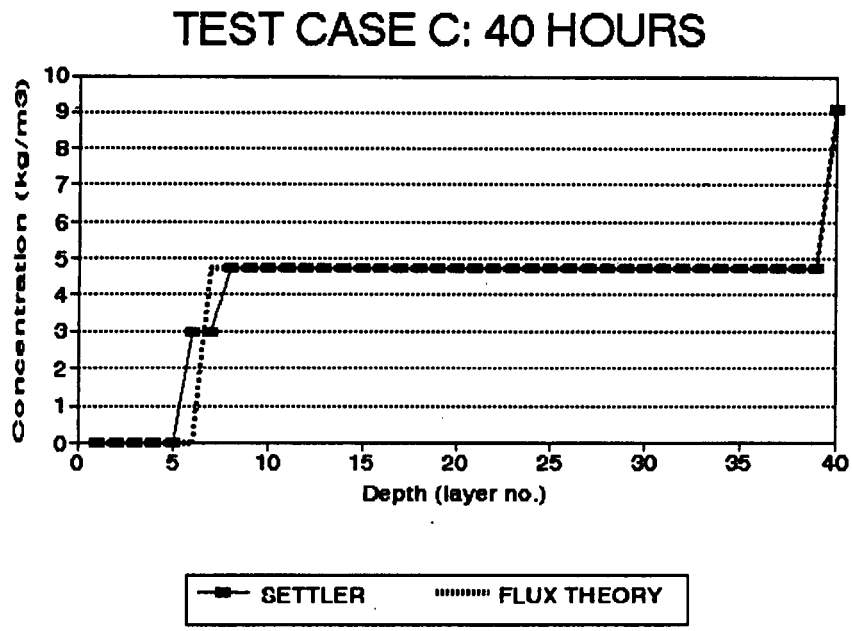

Figure 6.14 Test case C: concentration profile at 40 hours

3. no sludge blanket,
4. an underflow concentration of $X_r = 9.07 kgm^{-3}$ as expected from the flux theory.

From the above, it was concluded SETTLER (revision 2) accurately predicts the theoretically expected concentration profile for the underloaded test case C.

6.5 SETTLER APPLIED TO THE OVERLOADED CASE: POINT 4 IN REGION D

The conditions imposed on SETTLER for the fourth test case (point 4) were representative of region D and were again selected to be close to the boundary between underloaded and overloaded conditions on the design and operating chart (Figure 6.2), in this case, slightly overloaded (G_{ap} = 103% of G_L). The operating parameters for test case D are detailed in Table 6.5. The feed concentration (X_o) and V_o and n values were the same as for the previous tests.

The gravity flux curve for test case D (Figure 6.15) shows that the state point is outside the envelope of the gravity flux curve, indicating overloaded conditions. In this

Table 6.5 Operating parameters for test case D.

PARAMETER	VALUE	ALTERNATIVE UNITS
Q_i	$0.003094 m^3h^{-1}$	$(3.09 lh^{-1})$
Q_r	$0.005569 m^3h^{-1}$	$(5.57 lh^{-1})$
X_o	$5.83 kgm^{-3}$	

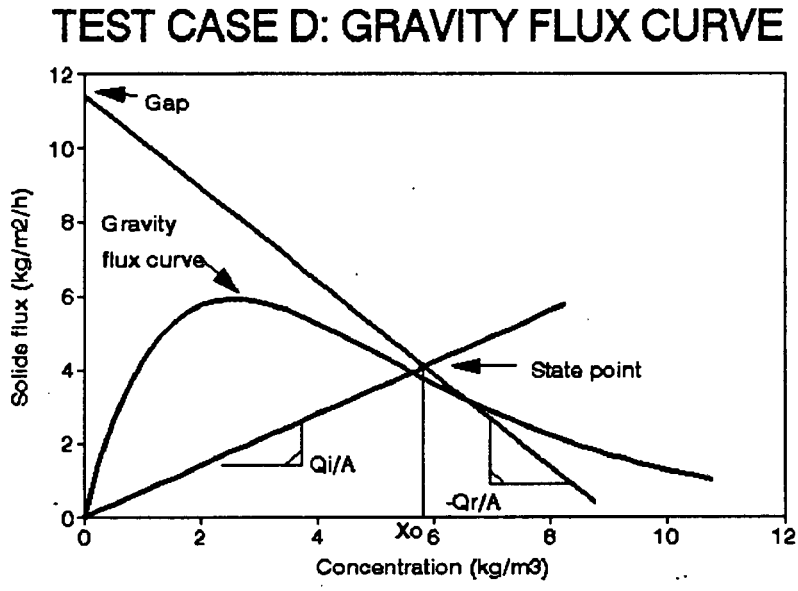

Figure 6.15 Gravity flux curve for test case D.

instance, the underflow line is too steep to form a tangent to the gravity flux curve (i.e. $U_u > V_o/e^2$), which means that flux limit B governs the operation of the settling column.

From the flux theory calculations, the following results are expected (see Appendix A for details of the method for these calculations):

1. an underflow concentration of approximately $X_{rL} = 8.81 kgm^{-3}$,

2. the formation of a sludge blanket of concentration approximately $X_L = 5.83 kgm^{-3}$,
3. a region above the feed point of concentration approximately $X_{af} = 5.83 kgm^{-3}$,
4. Solids loss with the effluent at a concentration of approximately $X_{ef} = 0.47 kgm^{-3}$.

Note that the concentrations above and below the feed point are equal to the feed concentration. This will always be the case as the critical condition for this form of failure occurs when the state point is on the gravity flux curve.

The initial conditions for test case D were those generated by test case C after 40 hours i.e. the concentration profile labelled SETTLER in Figure 6.14.

The diffusivity value at the feed point layer was adjusted proportionally to account for the increase in feed flow rate i.e. E was increased to $28178 m^2h^{-1}$.

Test case D was run for an arbitrary time period of 40 hours which was deemed sufficient for steady state conditions to be established in the settling column as it moved from a slightly underloaded to a slightly overloaded state. The concentration profile predicted by SETTLER for test case D is shown in Figure 6.16 together with the theoretically expected concentration values calculated from the flux theory.

Comparing the results predicted by SETTLER with the flux theory calculations shows that

1. the predicted underflow concentration of $8.98 kgm^{-3}$ is somewhat greater than the theoretical value of $8.81 kgm^{-3}$.
2. the predicted sludge blanket concentration of $6.30 kgm^{-3}$ is somewhat greater than the theoretical value of $5.83 kgm^{-3}$.
3. the predicted concentration above the feed point of $5.69 kgm^{-3}$ is somewhat lower than the theoretical value of $5.83 kgm^{-3}$.

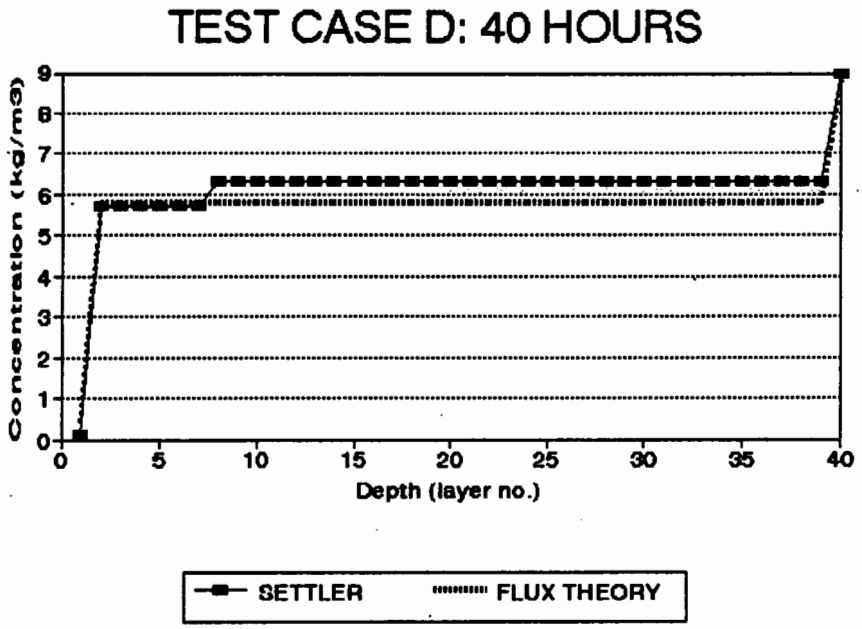

Figure 6.16 Test case D: concentration profile at 40 hours

4. the predicted effluent concentration of 0.17kgm^{-3} is lower than the theoretical value of 0.47kgm^{-3}.

Although the predicted concentration profile generated by SETTLER (revision 2) do match the theoretically expected concentration profile fairly closely, it was not regarded as sufficiently accurate to be confident that it is correct. The different concentrations in the effluent, underflow and region above the feed point are not as much a cause for concern as the concentration below the feed point because this concentration governs the other three. Consequently, the reason was sought as to why SETTLER predicted 6.30kgm^{-3} for the concentration below the feed point rather than the expected 5.83kgm^{-3}. The cause was found in the specification of the bulk velocity for the feed point layer, one of the points of concern raised earlier when describing Anderson's program (see Chapter 5, Section 5.4).

In SETTLER, as in Anderson's program, the bulk velocity in the feed point layer was specified as $V_3 = (3V_1+V_2)/2$, where V_1 and V_2 are the bulk velocities downwards (Q_r/A) and upwards (Q_i/A) respectively. The purpose of this equation seems to be to create an intermediate value for the (theoretical) velocity in the feed point layer and

smooth out the sharp change in the direction of the water flow in the settler from upwards (above the feed point) to downwards (below the feed point). Besides causing the inaccurate values in the concentration profile described above, this averaging technique was considered another interference with the "independence" of the algorithm. Consequently, the bulk velocity in the feed point layer was set equal to the downwards bulk velocity ($V_1 = Q_r/A$) with the result that all the layers from layer 40 (bottom layer) up to and including the feed point layer (7) had the same bulk velocity equal to Q_r/A.

SETTLER was revised (revision 3) to incorporate the above modifications and the simulation of test case D repeated. The predicted concentration profile (after 40 hours) is presented in Figure 6.17.

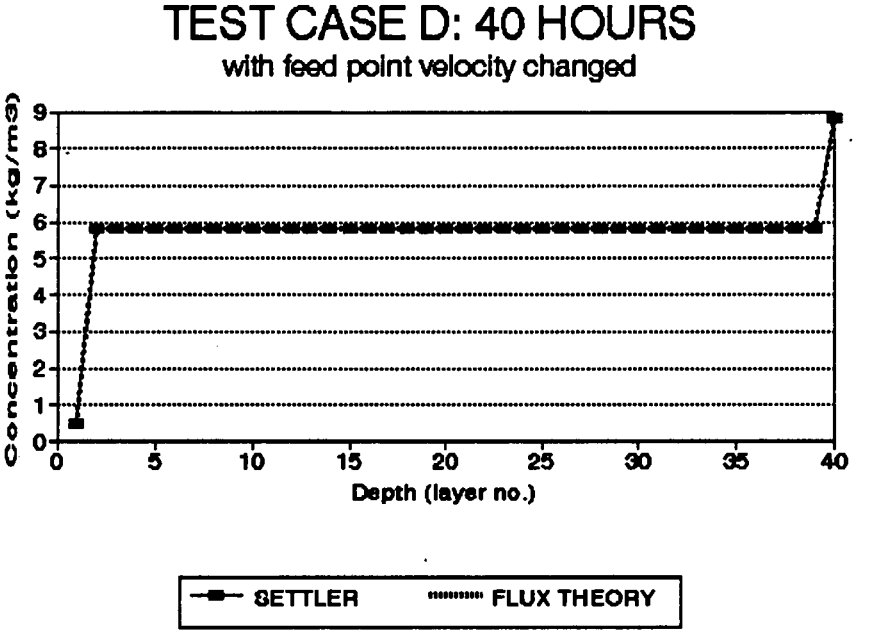

Figure 6.17 **Test case D: concentration profile at 40 hours with a modified feed point velocity**

The predicted results are now identical to the flux theory calculations i.e.

1. the underflow concentration is the same at 8.81kgm^{-3},
2. the sludge blanket zone of concentration 5.83kgm-3 is the same,
3. the concentration above the feed point is the same at 5.83kgm^{-3},

4. the effluent concentration is the same at 0.47kgm^{-3}.

The incorrect feed point bulk velocity specification led to a sludge blanket concentration error because, for this particular mode of failure (region D), the shock originates at the feed point and propagates both upwards and downwards. (In contrast, for Region A failure (Figure 6.2), the shock originates in the bottom of the tank and propagates upwards. For test case D, the correct concentration prediction for the feed point is thus critical, because the switching functions identify the feed point as the origin of the limiting concentration propagation both upwards and downwards. Hence, an incorrect feed point concentration propagates the incorrect concentration throughout the tank.

From the identical results obtained, it was concluded that SETTLER (revision 3) accurately predicted the theoretically expected concentration profile for test case D.

6.6 CONCLUSIONS

Once test case D was satisfactorily simulated, the program SETTLER (revision 3) was retested on the earlier test cases (A to C) and found to still produce identical results in conformity with flux theory calculations. Accordingly, it was concluded that the revised SETTLER program (revision 3) accurately predicted the idealized flux theory concentration profile for the four test cases representing the four different modes of settling tank operation. To confirm the reliability of the program in exactly reproducing the idealized flux theory concentration profiles, not only were the above four test cases tested in reverse order, but also other cases randomly selected within the four failure/safe operating regions in the design and operating chart. The former tests were deemed important because they tested the ability of SETTLER to move correctly between different types of underloaded and overloaded conditions. For all types of transitions from underloaded to overloaded states tested, SETTLER was found to correctly predict the expected results from the flux theory.

A summary of the modifications made to SETTLER (and incorporated into revision 3) that enabled it to exactly reproduce the idealized flux theory concentration profiles is:

Revision 1 - the condition setting the concentration in the feed point layer always equal to the concentration in the layer above it was removed and, in its place, a high value of diffusivity was introduced at the feed point layer to allow the sludge blanket to propagate above the feed point for overloaded conditions when the shock (or sludge blanket) originates in the bottom of the tank and to eliminate the entropy rule violation across the feed point;

Revision 2 - the condition setting the shock directions in the two layers below the feed point layer (layers 8 and 9) always equal was removed, thus allowing a sludge blanket that has filled the entire tank depth to propagate downwards past the feed point and out of the tank for underloaded conditions;

Revision 3 - the bulk velocity at the feed point was changed so that it is always equal to the underflow rate i.e. $V_3 = Q_r/A$, rather than an empirical function of the overflow and underflow bulk velocities.

6.7 MATERIAL BALANCE CHECKS FOR THE PROGRAM SETTLER

In reproducing Anderson's calibration runs with the Detroit Wastewater Treatment Plant data (Chapter 5), it was found that the sludge mass balance was not preserved by either the experimental data or the program SETTLER. Preservation of the material balance is an important requirement of the program. The law of material or mass conservation states that "mass can neither be created or destroyed" or "the mass of an isolated system is constant". To take into account the flow of material into and out of a

system, the generalised law of mass conservation is expressed as a material balance in the following way (Himmelblau (1974)):

$$\left[\begin{array}{c}\text{Input}\\ \text{through}\\ \text{system}\\ \text{boundaries}\end{array}\right] - \left[\begin{array}{c}\text{Output}\\ \text{through}\\ \text{system}\\ \text{boundaries}\end{array}\right] + \left[\begin{array}{c}\text{Generation}\\ \text{by}\\ \text{chemical}\\ \text{reaction}\end{array}\right] - \left[\begin{array}{c}\text{Consumption}\\ \text{by}\\ \text{chemical}\\ \text{reaction}\end{array}\right] = \left[\begin{array}{c}\text{Accumulation}\\ \text{within}\\ \text{the}\\ \text{system}\end{array}\right] \quad (6.3)$$

Equation (6.3) refers to a time interval of any specified length. In the case of a material balance for SETTLER, the generation and consumption by chemical reaction terms in Equation (6.3) are zero and will fall away. In the real settling tank this is not strictly so because an active biological mass is passing through it. However, the mass changes from biochemical reaction are considered to be small enough with respect to the overall mass so as to be negligible and Equation (6.3) thus reduces to Equation (6.4).

$$[\text{Input}] - [\text{Output}] = [\text{Accumulation}] \quad (6.4)$$

The system boundary defines the part of the system being considered for the material balance. Since the conservation law holds for the complete system and any subdivision of it, the system can be the whole system or any portion of it that is identified specifically for analysis (Coulson and Richardson (1983)). The flows into and out of the system (or subsystem) are those crossing the boundary and must balance with material accumulated within the boundary. The system can be subdivided in any convenient way to facilitate the material balance calculations.

For the specific example of the settling tank, two of the possible systems for the material balance checks are:

1. one that excludes the aerobic reactor and comprises only the settling tank or
2. one that includes both the aerobic reactor and the settling tank i.e. the biological reactor-settling tank system.

1. Settling tank only

When the aerobic reactor is excluded, the system to be analysed is as illustrated in Figure 6.18.

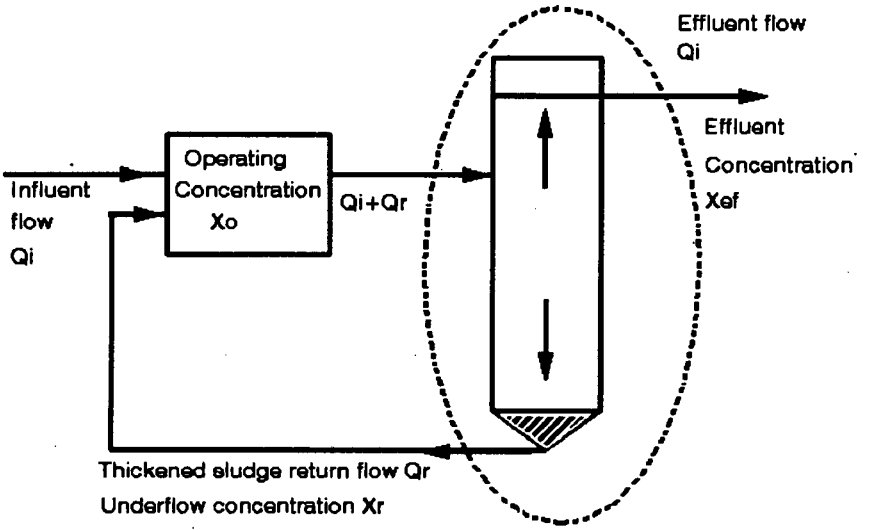

Figure 6.18 System boundary for the material balance excluding the aerobic reactor

The streams crossing the system boundary are the feed flow (input), the effluent flow (output) and the underflow recycle (output). The input mass is the product of the feed flow (Q_i+Q_r) and its concentration (X_o), and the output mass is the product of the effluent flow (Q_i) and its concentration (X_{ef}) plus the product of underflow recycle (Q_r) and its concentration (X_r). The accumulation term is the difference between the masses of sludge contained in the settling tank at time t=t and at time t=0, where t is the specified time interval. This is expressed as a material balance in Equation (6.5):

$$[\text{Input}] - [\text{Output}] = [\text{Accumulation}]$$

$$X_o(Q_i+Q_r)t - Q_i\sum_{t=0}^{t} X_{ef} - Q_r\sum_{t=0}^{t} X_r = V\left[\sum_{i=1}^{40} X_i\right]_{t=t} - V\left[\sum_{i=1}^{40} X_i\right]_{t=0} \qquad (6.5)$$

Where X_o = operating concentration of the aerobic reactor (kgm^{-3})

Q_i+Q_r = feed flow to the settling tank (m^3h^{-1})

t = specified time interval (h)

Q_i = effluent flow (m^3h^{-1})

X_{ef} = concentration of solids in the effluent (kgm^{-3})

Q_r = underflow recycle (m^3h^{-1})

X_r = underflow concentration (kgm^{-3})

X_i = concentration of sludge in the settling tank at layer i (kgm^{-3})

V = volume of the settling tank (m^3)

2. Aerobic reactor-settling tank system

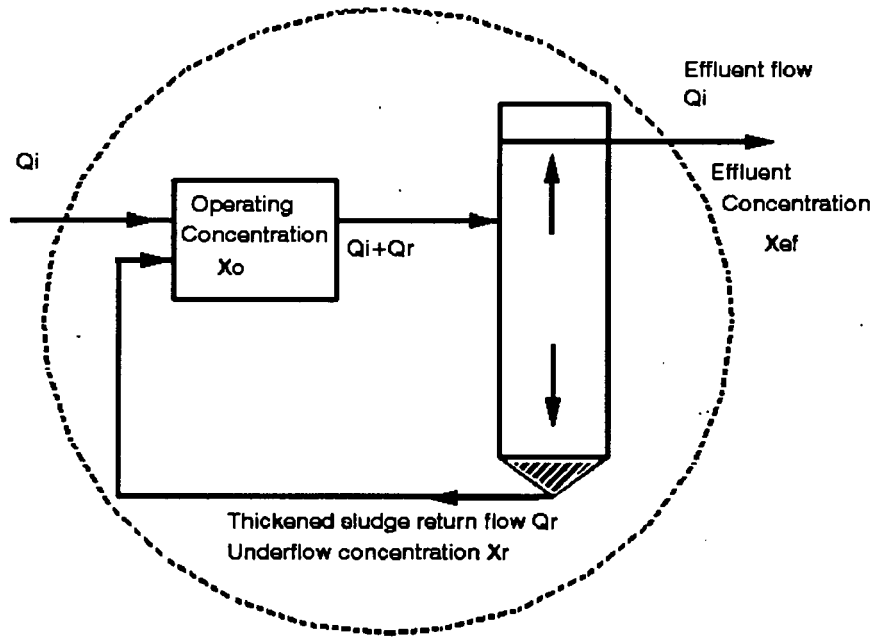

Figure 6.19 System boundary for the material balance including the aerobic reactor

When the aerobic reactor is included, the system to be analysed is illustrated in Figure 6.19. The streams crossing the system boundary are the influent flow (Q_i) to the reactor (input stream) and the effluent flow (Q_i) (output stream). The input mass to the system is the product of the influent flow entering the aerobic reactor (Q_i) and its concentration (X_a). Because it is assumed that all the sludge is generated in the biological reactor, this term is zero. The output mass is the product of the effluent flow (Q_i) and its concentration (X_{ef}). The accumulation term is the difference between

the total masses of sludge contained in the aerobic reactor and the settling tank at time t=t and time t=0, where t is the specified time interval. Equation (6.6) expresses the above in mathematical form.

[Input] - [Output] = [Accumulation]

$$X_a Q_i t - Q_i \sum_{t=0}^{t} X_{ef} = V \left[\sum_{i=1}^{40} X_i \right]_{t=t} - V \left[\sum_{i=1}^{40} X_i \right]_{t=0} + [V_R X_o]_{t=t} - [V_R X_o]_{t=0} \quad (6.6)$$

Where
- X_a = concentration in the influent to the aerobic reactor (kgm^{-3})
- Q_i = influent flow to the aerobic reactor (m^3h^{-1})
- t = specified time interval (h)
- Q_i = effluent flow (m^3h^{-1})
- X_{ef} = concentration of solids in the effluent (kgm^{-3})
- X_i = concentration of sludge in the settling tank at layer i (kgm^{-3})
- X_o = operating concentration of the aerobic reactor (kgm^{-3})
- V = volume of the settling tank (m^3)
- V_R = volume of the aerobic reactor (m^3)

The relative merits of choosing either of these two system boundaries is described in their application to the material balance.

6.7.1 MATERIAL BALANCE CHECK OF SETTLER - THEORETICAL TEST CASE A

In order to check that the program SETTLER (revision 3) is internally consistent i.e. that it neither consumes nor generates mass during the simulations, it was decided to initially carry out a material balance on theoretical test case A. It should be noted that the results obtained for test case A with SETTLER (revision 3) are identical to the results discussed for test case A with SETTLER (revision 2) (see Section 6.2).

Test case A was run in the same manner as described previously (see Section 6.2). The operating parameters remained unchanged and took the form of a step change imposed on the initial conditions. This step change was maintained for 80h. The effluent concentration and the underflow concentration were noted every 15 minutes during this period. The sludge concentration depth profile was only examined at the end of the 80h period. Initially, the material balance on test case A was carried out on the settling tank only. Both initial (t = 0h) and final (t = 80h) sludge concentration depth profiles for the simulation are illustrated in Figure 6.20.

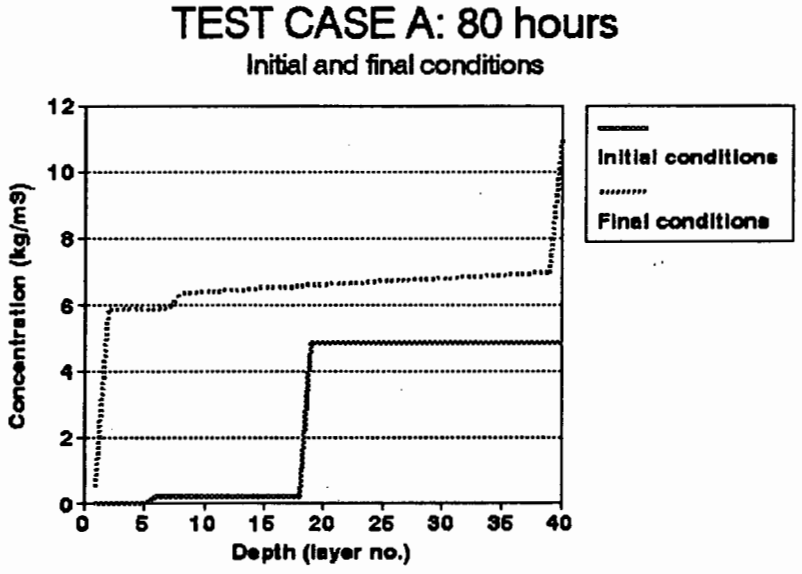

Figure 6.20 Initial and final concentration profiles for test case A

The initial and final masses of sludge in the column were 0.02408kg and 0.05750kg respectively. The difference between the two masses is 0.033421kg, indicating that 0.033421kg of sludge accumulated in the column during the 80h simulation. This accumulated mass was compared with the difference between the calculated input and output masses. The results obtained are set out in Table 6.6.

It is clear that this method of comparing the sludge mass accumulation in the column gives a poor result for the material balance. The reason for this is that during the long time interval chosen for the test, a relatively large mass of sludge passes through the

Table 6.6 Material balance for test case A for the system including the settling tank only

PARAMETER	MASS (KG)
Initial mass of sludge in the column	0.02408
Final mass of sludge in the column	0.05750
Accumulation of sludge in the column	**0.03342**
Total mass entering the column in 80h	2.8777
Total mass leaving the column in 80h (a) in the effluent	0.0196
(b) in the underflow	2.7687
Mass in - mass out (accumulation)	**0.09006**
% difference	**169%**

column. When the order of magnitude of the input mass (2.8777kg) is compared to the order of magnitude of the accumulated mass of sludge (0.03342kg), it can be seen that the input mass is approximately 2 orders of magnitude higher. In this case, a 1% error in the calculation of the input mass ($\pm$0.03kg) is the same as the accumulated mass. This will lead to a 100% error in the material balance based on accumulated (or lost) mass. Confining the material balance to the last 15min of the test i.e. between 79.75h and 80h, when the column is almost at steady state does not solve the problem, because the same difference in orders of magnitude difference between sludge mass accumulated and passing through remains. The results obtained for the 15min material balance are set out in Table 6.7.

Because it is unrealistic to expect small rounding errors in the calculation of mass entering and leaving the tank to be avoided, the method of defining the system boundary around the settling tank only is not helpful in ascertaining whether or not SETTLER preserves the material balance. Any errors in the preservation of the material balance will be obscured by the magnification of the rounding error in the

Table 6.7 Mass accumulation in the column for the last 15min of test case A (settling tank only)

PARAMETER	MASS (KG)
Mass of sludge in the column at 79.75h	0.05749
Mass of sludge in the column at 80h	0.05750
Accumulation of sludge in the column	**0.00001**
Total mass entering the column in 15min	0.008993
Total mass leaving the column in 15min (a) in the effluent	0.000322
(b) in the underflow	0.008646
Mass in - mass out (accumulation)	**0.000347**
% difference	**97.12%**

final result. The problem was resolved by extending the system boundary to include the aerobic reactor. This ensures that the orders of magnitude of the calculated masses that are compared for the material balance are the same, thereby allowing a realistic estimate of the accuracy of the material balance.

When the aerobic reactor is included in the system boundary, the feed concentration to the settling column can no longer be directly controlled as it is now determined by the operating concentration in the aerobic reactor. Although the initial feed concentration to the settling column was set at 5.85kgm^{-3}, the concentration at subsequent time steps is calculated from the volume of the aerobic reactor and the mass of sludge it contains. If the settling column accumulates sludge mass during the simulation, then the operating concentration of the aerobic reactor will decrease. Conversely, if the settling column releases sludge via the underflow during the simulation, then the operating concentration of the aerobic reactor will increase. The volume of the aerobic reactor was chosen to be 1000 times greater than the laboratory column i.e. 8.844m^3. This

large volume was selected to ensure that the concentration of the feed flow to the column was not significantly altered during the test.

As earlier, the simulation was run for 80 hours and at each hour the total mass of sludge in the aerobic reactor was calculated. The operating concentration of the aerobic reactor was then adjusted and this new concentration fed to the settling column. In addition, the total mass lost in the effluent was calculated by monitoring the effluent solids concentration at each hour during the simulation. The material balance was evaluated by comparing the total initial mass of sludge in the system (mass in the aerobic reactor + mass in the settling column) with the total final mass in the system (mass in the aerobic reactor + mass in the settling column + mass lost in the effluent). The results of these calculations are presented in Table 6.8.

Table 6.8 Comparison of initial and final masses for the 80h test case A simulation (including aerobic reactor)

PARAMETER	MASS (KG)
INITIAL CONDITIONS	
Mass in aerobic reactor	.51.737
Mass in settling column	0.024
Total initial mass	**51.761**
CONDITIONS AT 80H	
Mass in aerobic reactor	51.680
Mass in settling column	0.058
Mass loss in effluent during 80h	0.023
Total final mass	**51.761**
% difference	**0**

It can be seen that defining the system boundary to include the aerobic reactor yields a

by two orders of magnitude for the material balance check. Now a 1% error in the calculation of the effluent mass lost will lead to a 0.0004% error in the final material balance and a 1% error in the calculation of the total mass in the aerobic reactor will lead to a 1% error in the final material balance. Smaller (and more realistic) reactor volumes will naturally change the relative percentage errors. However, material balance checks with aerobic reactors of 1:1 and 10:1 aerobic volume to settling tank volume still yielded 100% material balances. In these cases, it was necessary to use more time steps over the 80h period in order to take into account the more rapidly changing reactor concentration and thus achieve accurate results for the material balance. Overall, the aerobic reactor-settling tank system enables the error in the material balance to be accurately assessed without the interference of other sources of error such as rounding error, and demonstrates that SETTLER conforms to the law of mass conservation and therefore that its algorithm is internally consistent.

6.8 CONCLUSIONS

After making the following modifications to SETTLER:

1. A seeding procedure was introduced - this was to ensure that the solution to the hyperbolic equations was initiated in the correct region of the concentration range;

2. Revision 1 - the condition setting the concentration in the feed point layer always equal to the concentration in the layer above it was removed, and in its place, a high value of diffusivity was introduced at the feed point layer to allow the sludge blanket to propagate above the feed point for overloaded conditions when the shock (or sludge blanket) originates in the bottom of the tank and to eliminate the entropy rule violation across the feed point;

3. Revision 2 - the condition setting the shock directions in the two layers below the feed point layer (layers 8 and 9) always equal was removed, allowing a sludge

3. Revision 2 - the condition setting the shock directions in the two layers below the feed point layer (layers 8 and 9) always equal was removed, allowing a sludge blanket that has filled the entire tank depth to propagate downwards past the feed point and out of the tank for underloaded conditions;

4. Revision 3 - the bulk velocity at the feed point was changed so that it is always equal to the underflow rate i.e. $V_3 = Q_r/A$, rather than an empirical function of the overflow and underflow bulk velocities;

it was found to accurately predict the idealised (hyperbolic) sludge concentration profiles calculated from the flux theory for different forms of underloaded and overloaded conditions irrespective of the initial conditions. It was also found to conform to material balance checks.

The above simulation tests and material balance checks indicated that SETTLER (revision 3) conformed to the flux theory and mass conservation principles and therefore was ready for calibration and testing of the full scale data (diffusivity included). Any difficulties encountered with regard to simulation accuracy are likely to be caused by the form and magnitude of the diffusivity function itself and unlikely to be a flux theory or material balance problem. However, before SETTLER was applied to the dynamic modelling of full scale settling tanks, (with diffusivity) (see Chapter 8), it was first checked against the laboratory settling column data (no diffusivity) in Chapter 7.

REFERENCES

Coulson J.M. and J.F. Richardson, "Chemical Engineering", Vol 6, Pergamon Press, (1983)

Giffels/Black and Veatch, "Existing waste collection and treatment facilities - Detroit Water and Sewerage Department", Segmented Facilities Plan, Book 8, Detroit, Michigan, (1978)

Himmelblau D.M., "Basic principles and calculations in chemical engineering", 3rd Edition, Prentice Hall, Englewood Cliffs, New Jersey, ((1974)

Ranger C. and D. Christie, "Modified final clarifier evaluation", City of Detroit Water and Sewerage Department Report, Detroit, Michigan, (1978)

Williams and Works Inc., "Final clarifier studies: Detroit Wastewater Treatment Plant", Phosphorus Removal and Related Facilities Segmented Step 1 - Studies Phase, DWSD Contract Report CS-822, Grand Rapids, Michigan, (1979)

CHAPTER 7
SETTLER (REVISION 3) APPLIED TO THE LABWORK CASES

7.1 INTRODUCTION

Having established the accuracy of SETTLER (revision 3) in reproducing the idealised (hyperbolic case, no diffusivity) concentration profiles, it remains to compare the predicted concentration profiles with the experimentally measured ones in the laboratory settling column. Because all of the labwork data fell into either region A (overloaded) or region B (underloaded) on the design and operating chart (see Figure 5.12), it was decided to use SETTLER (revision 3) to simulate only two laboratory cases i.e. Labwork 2 (region B) and Labwork 5 (region A). Simulation of all of the labwork cases would have been merely repetitious and two cases were deemed to be a sufficiently representative selection to judge the ability of the program to reproduce the laboratory column concentration profiles. The design and operating parameters for both Labwork 2 and Labwork 5 are presented in Table 7.1.

7.2 SETTLER (REVISION 3) APPLIED TO LABWORK 2

Because the design and operating parameters for Labwork 2 are the same as those for the theoretical test case in region B (underloaded) (point 2 in Figure 6.2), the description of the system as defined by the flux theory is not repeated. This can be found in Chapter 6 above. The diffusivity value for the feed point layer was selected to be the same as that for test case B i.e. $E = 15742 m^2 h^{-1}$. Because both the initial concentration profile and the length of operation for the laboratory system were unknown, it was necessary to assume an arbitrary initial concentration profile for the simulation and to select a sufficiently long simulation time for the effect of the initial conditions to propagate out of the system and for a steady state to be reached. The arbitrary initial concentration profile selected is illustrated in Figure 7.1 (wavy line).

Table 7.1 Laboratory settling column design and operating parameters for Labwork 2 and Labwork 5 cases.

PARAMETER	LABWORK 2 & LABWORK 5	
AREA	$0.00442m^2$	
DEPTH	2m	
FEED POINT LAYER	7	
V_o	$6.287mh^{-1}$	
n	$0.391m^3kg^{-1}$	
	LABWORK 2	**LABWORK 5**
Q_i	$2.43lh^{-1}$	$3.008lh^{-1}$
Q_r	$2.41lh^{-1}$	$3.141lh^{-1}$
X_o	$5.83kgm^{-3}$	$5.85kgm^{-3}$

The operation time was selected to be 10 hours, which was confirmed to be sufficient for the column to reach a steady state, as no further changes in the concentration profile occurred after this time.

The concentration profile generated by SETTLER after 10 hours of operation under the conditions outlined in Table 7.1 is shown in Figure 7.1 (10 hours) and compared with the measured concentration profile (dotted line).

The predicted concentration profile shows two concentration regions:

1. a dilute zone settling region of concentration $X_{dz} = 1.68kgm^{-3}$ and
2. an underflow concentration of $X_r = 11.71kgm^{-3}$.

No solids loss in the effluent is predicted.

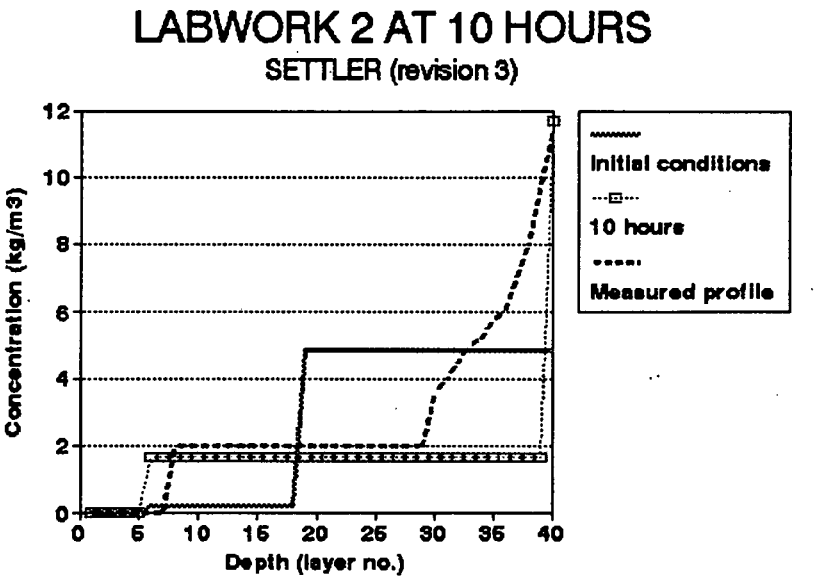

Figure 7.1 Initial concentration profile and measured and predicted concentration profiles for Labwork 2 at 10 hours.

These predictions correspond exactly with those predicted by the flux theory for ideal (hyperbolic) conditions and they match the measured concentration profile reasonably well. The measured results show a region of low concentration corresponding approximately to the dilute zone settling region concentration (X_{dz} = 2kgm^{-3}), which exists from the feed layer to the 29th layer in the column (where the first layer is the topmost layer and the 40th layer is the bottommost layer). Below the 29th layer, the measured concentration increases gradually until layer 40, where the concentration corresponds to the underflow concentration (X_r = 11.41kgm^{-3}). The measured concentration profile shows no solids loss in the effluent.

The existence of the region of gradual concentration increase in the measured results from layer 29 to layer 40 deviates from predictions made by the flux theory and SETTLER and in all likelihood is because the time required for sludge thickening is not accounted for in the program i.e. no compression zone exists and the column is treated as if zone settling behaviour is dominant throughout the entire depth of the column. The inclusion of diffusivity at all layers in the column would, to some extent, address this problem, as diffusivity has the effect of smoothing out the step changes in

the concentration profile predicted by the hyperbolic equations. The resulting concentration profile predicted by SETTLER (modified to include diffusivity at all layers) might be expected to increase gradually from top to bottom of the tank, thereby more closely matching the measured profile. In the absence of a diffusivity function, it was felt at this stage that a comparison between the measured and predicted concentration profiles in the lower layers of the column would not be valid at this stage.

7.3 SETTLER (REVISION 3) APPLIED TO LABWORK 5

The operating parameters specific to the Labwork 5 case were given in Table 7.1 and are the same as those for the theoretical test case A (overloaded). Hence, the description of the system in terms of the flux theory will not be repeated as this can be found in Chapter 6 above.

The initial concentration profile selected for the simulation was, as with Labwork 2, arbitrary and is illustrated in Figure 7.2 (wavy line). The time of operation was selected to be 80 hours in order to allow the expected sludge blanket to build up in the column and for the system to reach steady state. The diffusivity coefficient for the feed point layer was selected to be the same as that for test case A i.e. $E = 20000 m^2h^{-1}$.

The predicted concentration profile after 80 hours (Figure 7.2; 80 hours) shows the following:

1. an underflow concentration of $X_{rL} = 11.01 kgm^{-3}$,
2. a sludge blanket zone of concentration $X_L = \pm 6.6 kgm^{-3}$,
3. a region above the feed point of concentration $X_{af} = 5.88 kgm^{-3}$ and
4. solids loss with the effluent at a concentration of $X_{ef} = 0.43 kgm^{-3}$.

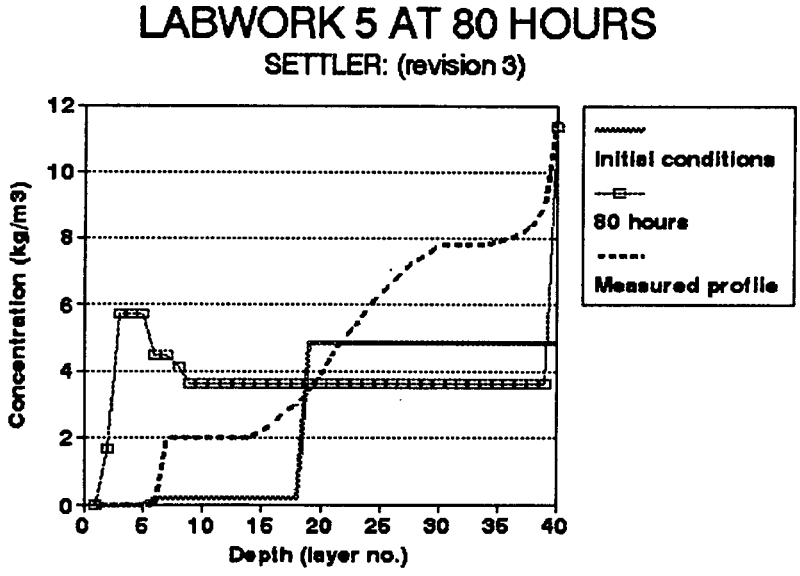

Figure 7.2 Initial conditions and measured and predicted concentration profiles for Labwork 5 at 80 hours

The measured concentration profile shows the following:

1. an underflow concentration of $X_{rL} = 11.67 kgm^{-3}$,
2. a region of constant concentration ($\pm$ $8 kgm^{-3}$) from layer 30 to layer 37,
3. a second region of constant concentration ($\pm$ $2 kgm^{-3}$) between the feed point layer (7) and layer 14 and
4. no solids loss with the effluent.

From Figure 7.2, it is clear that there is little similarity between the measured and predicted concentration profiles. The reason for this is most likely that the measured data does not represent a steady state but rather the intermediate concentration profile occurring before the sludge blanket has risen sufficiently to cause solids loss in the effluent. Thus, the two zones of constant concentration below the feed point layer correspond approximately to (i) the limiting concentration zone ($\pm 8 kgm^{-3}$) and (ii) the dilute concentration zone ($\pm 2 kgm^{-3}$).

Accepting that the measured data do not reflect steady state conditions in the column for the input parameters, the predicted and measured results were examined at an earlier time period. At 30h, before the predicted sludge blanket has risen above the feed point layer, and therefore before solids loss occurs in the effluent, the concentration profile as illustrated in Figure 7.3 is obtained.

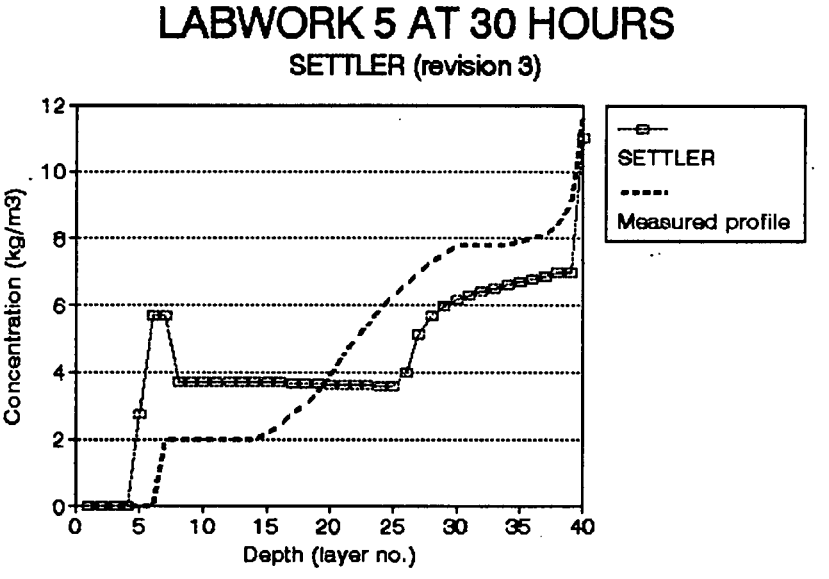

Figure 7.3 Predicted concentration profile at 30 hours for Labwork 5

The concentration profile shows the following:

1. an underflow concentration of 11.01kgm^{-3},
2. a sludge blanket of concentration $\pm$6.8kgm^{-3} between layers 26 and 39,
3. a region of constant, low concentration ($\pm$ 3.6kgm^{-3}) between the sludge blanket level and the feed point layer (7), which corresponds to the dilute zone concentration,
4. a region of unexpectedly high concentration at the feed point layer (7) and the one above it (6),
5. no solids loss with the effluent.

The predicted transient concentration profile matches the measured concentration profile much more closely than the steady state profile. Both the predicted and

measured effluent solids concentrations are zero, and there is close correspondence between the predicted and measured underflow concentrations. In addition, the two zones of constant concentration predicted by SETTLER correspond approximately to the two zones in the measured concentration profile.

The unexpectedly high concentrations predicted at layers 6 and 7 are due to the diffusivity at the feed point for the hyperbolic case i.e. a single, very high value which enables the sludge blanket to move above the feed point layer and prevents an entropy rule violation in the final (steady state) concentration profile. This high value of diffusivity at the feed point causes a "surge" in concentration at the feed point layer which, although creating a disturbance in the concentration profile during transient operation, is eventually smoothed out once steady state is achieved. This "surge" behaviour at the feed point was examined more closely and it was found that it does not occur in progressively changing dynamic input conditions, only in step change conditions where the magnitude of the "surge" is related to the magnitude of the step change.

It would appear that the measured concentration profile does not represent a steady state situation, but rather a transient state of the overloaded conditions which will ultimately result in solids loss with the effluent. Hence, if SETTLER (revision 3) is used to simulate a transient of the Labwork 5 conditions, the predicted concentration profile matches approximately the significant features of the measured concentration profile.

7.4 CONCLUSIONS

From the simulations of the labwork data, it was concluded that, besides the behaviour at the feed point, which seems to take place only with step changes in input parameters, SETTLER (revision 3) simulates the concentration profiles measured in the tall slender laboratory column reasonably accurately for the hyperbolic (no diffusivity) case.

CHAPTER 8
SETTLER APPLIED TO THE STORA DATA

8.1 INTRODUCTION

Checking the program against the theoretical cases and the labwork data enabled the non-diffusivity related deficiencies in SETTLER to be identified and resolved and SETTLER to be verified for the hyperbolic case. The next step in the development of the dynamic simulation model for secondary settling tanks was to check the program against the full scale data collected by STORA. Because this data was collected at full scale, large diameter to depth ratio tanks, it was no longer valid to assume that diffusivity effects throughout the tank would be small or negligible and thus it was necessary to develop a diffusivity function and introduce it into the program. The STORA data was found to be sufficiently comprehensive for both development and calibration of a general diffusivity function and for subsequent verification with other settling tank tests. Consequently, the diffusivity function developed is not specific to a particular settling tank, but can be implemented over a wide range of applications because it is set in terms of settling tank design and operating parameters.

The application of SETTLER to the STORA full scale settling tank data and the development of a general diffusivity function is presented in this chapter. The STORA investigation and experimental data were described in Chapter 3. The STORA data does not give sludge settleability in terms of the flux theory constants V_o and n so the V_o and n values were calculated from the measured $SSVI_{3.5}$ with the relationship developed in Chapter 4 for extended aeration plants i.e.

$$\ln V_o = 2.45095 - 0.00636 * SSVI_{3.5} \qquad (8.1)$$

$$n = 0.16756 + 0.00218 * SSVI_{3.5} \qquad (8.2)$$

8.2 SIMULATING THE RIJEN 1 TEST WITH SETTLER (revision 3)

The first settling tank test carried out at Rijen (hereafter referred to as Rijen 1) conducted by STORA was chosen as the first case for the testing of SETTLER (revision 3). General descriptive parameters of all the settling tanks included in the STORA investigation were given in Chapter 3. The settling tank at Rijen has a diameter of 45.5m which gives a surface area of $1625m^2$, a side wall depth of 2.25m with a 1:12 sloping bottom, and a volume of 42% of the aeration basin.

The Rijen 1 test was run for a total of 6h, with the influent flow being shut off twice, the first time for 0.75h from 3.5h to 4.25h after the start, and the second time for 1h from 5h to 6h after the start. The $SSVI_{3.5}$ was measured to be $90mlg^{-1}$ which leads to V_o and n values of $7.543mh^{-1}$ and $0.409m^3kg^{-1}$ respectively.

From these values of V_o and n, it was calculated with the flux theory that the settling tank was overloaded only during the first 2.5h of the test because of the progressively decreasing reactor concentration as the settling tank accumulated sludge. Thereafter, it was underloaded for the remainder of the test, irrespective of whether the feed was on or off. The data measured by STORA for Rijen 1 is given in Table 8.1.

A summary of the operating parameters imposed on the settling tank during the 6 hour period is presented in Table 8.2. During this time, although the feed concentration varied continuously, it remained within the limits specified in Table 8.2.

Because a complete initial concentration profile for Rijen 1 was not measured by STORA (only the underflow concentration and the sludge blanket level), it was necessary to generate a starting profile for SETTLER (revision 3). This was achieved by using an arbitrary set of initial conditions and simulating the same input conditions as used by STORA before the start of each test i.e. setting the influent flow to zero and the underflow at the required rate ($531m^3h^{-1}$). These operating conditions were maintained until conditions in the tank remained stable and unchanging i.e. a steady

Table 8.1 Data measured by STORA for the Rijen 1 test

Test Rijen 1 Begin test: 9:15h
Date: 7 November 1978 End test: 13:30h

Q_i = 1780m^3h^{-1} Q_r = 531m^3h^{-1}

Time (h)	Feed conc (kg/m3)	Underflow conc (kg/m3)	Effluent conc (mg/l)	Sludge blanket height (m)	Remarks
09:15					start influent
09:25	4.12	4.84			
09:30			< 0.1		
09:35	4.35	3.32			
09:45				2.30	
09:50	3.83	3.49			
10:00	4.08	3.55	5.00	2.25	
10:10		3.61			
10:20	3.72	3.37			
10:30		3.64	< 0.1	1.90	
10:40	2.78	3.51			
10:45				1.60	
10:50		4.60			
11:00	3.57	3.83	< 0.1	1.45	
11:10		4.98			
11:20	3.33	7.41		1.10	
11:30		5.53	< 0.1		
11:40	3.08	5.60			
11:45				1.00	
11:50		5.53			
12:00	3.00	5.31	< 0.1	0.95	
12:10		6.51			
12:15				0.90	
12:20	2.72	6.91			
12:30		6.60	8.30	0.70	solids loss
12:35			405.00		
12:40	2.81	7.64	698.00		
12:43					influent stopped
12:50		8.27	628.00	0.60	
12:55					
13:00	2.76	10.56	152.00		
13:05				0.80	
13:10		10.49	< 0.1		
13:15				0.95	
13:20	2.64	10.40		1.00	
13:30		10.22		1.20	influent restarted
13:40	2.79	10.09			
13:45				1.25	
13:50		7.22			
13:55				1.25	
14:00	3.06	6.25	< 0.1		
14:05				1.10	
14:10		6.78			
14:20	3.09	6.98		0.96	influent stopped
14:30		7.33	< 0.1	0.95	
14:40	2.84	9.80			
14:45				0.90	
14:50		10.78			
15:00	2.87	10.70	< 0.1	1.00	
15:10				0.95	

necessary to generate a starting profile for SETTLER (revision 4). This was achieved by using an arbitrary set of initial conditions and simulating the same input conditions as used by STORA before the start of each test i.e. setting the influent flow to zero

Table 8.2 Summary of operating parameters for the Rijen 1 test.

PARAMETER	VALUE
Q_i	$1780m^3h^{-1}$
Q_r	$531m^3h^{-1}$
X_o (max)	$4.35kgm^{-3}$
X_o (min)	$2.64kgm^{-3}$
Area	$1625m^2$
Depth (from overflow weir to bottom of tank)	3.35m
Feed point layer	5
$SSVI_{3.5}$	$90mlg^{-1}$
DSVI	$110mlg^{-1}$
Duration of test	6 hours
V_o	$6.544mh^{-1}$
n	$0.363m^3kg^{-1}$

and the underflow at the required rate ($531m^3h^{-1}$). These operating conditions were maintained until conditions in the tank remained stable and unchanging i.e. a steady state had been reached. The predicted concentration of X_{dz} achieved at steady state was used in the initial concentration profile for the test; the sludge blanket level was positioned at the measured value at a concentration of X_r (also as measured by STORA). The initial concentration profile generated in this fashion for Rijen 1 is illustrated in Figure 8.1.

Although the intention of simulating the STORA data was primarily to develop a general diffusivity function for the program, it was decided as a first step to use SETTLER (revision 4) (the hyperbolic version with diffusivity at the feed point level only) in order to ascertain the extent to which the absence of diffusivity in the tank led

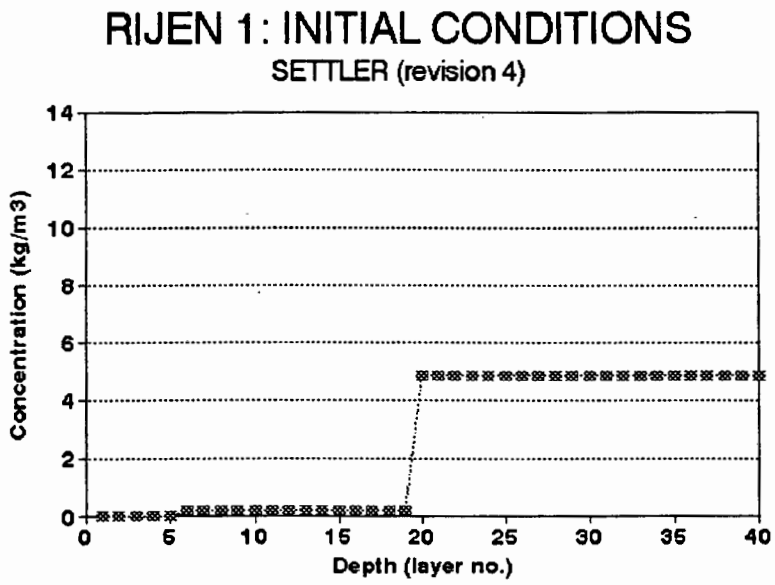

Figure 8.1 Initial concentration profile for Rijen 1.

With this in mind, the magnitude of the diffusivity coefficient for the feed point was adjusted using the diffusivity value from theoretical test case A as a basis and increasing the value to be proportional to the influent flow rate i.e. E increased to 7.52×10^9 m^2h^{-1}. The diffusivity at all other layers in the tank was set to zero. The diffusivity for the feed point layer was calculated as a simple linear scale up of the minimum value for the laboratory scale column, which is the reason for its very high value. The program was tested (in hyperbolic form) with a number of reduced E values for the feed point and it was found that, as for the hyperbolic test cases (case A), a minimum value of E for the sludge blanket to successfully rise above the feed point was $E > 0 m^2h^{-1}$, whereas the minimum value of E in order to prevent an entropy rule violation at the feed point once the sludge blanket has risen above the feed point was $E > \sim 8000 m^2h^{-1}$ compared to $20000 m^2h^{-1}$ for the settling column test cases (See Chapter 6). Values below $8000 m^2h^{-1}$ caused an entropy rule violation (concentration decrease) at the feed point (see Figure 6.7 in Chapter 6). This indicates that the diffusivity at the feed point is not a simple linear scale up phenomenon.

Because of the nature of the STORA data and the relative brevity of the Rijen 1 test (6h) SETTLER (revision 3) was modified to read the input variables Q_i, Q_r, and X_o

point (see Figure 6.8 in Chapter 6). This indicates that the diffusivity at the feed point is not a simple linear scale up phenomenon.

In the absence of a diffusivity function for SETTLER, a quantitative analysis of the results was not expected to be meaningful, therefore the results were evaluated only qualitatively, based on an evaluation of the following parameters extracted from the measured and predicted results:

1. Sludge blanket level and rise rate
2. Underflow concentration with time
3. Effluent concentration with time

8.2.1 RESULTS OF THE RIJEN 1 SIMULATION

1. Sludge blanket level

The sludge blanket level is defined as the depth below the top of the tank (overflow weir) at which the concentration in the tank exceeds $3kgm^{-3}$. This is consistent with the definitions of Vitasovic (1986) and Takacs *et al* (1991). The STORA (1981) publication describes the sludge blanket level as the interface between the observed sludge blanket and the clear water. According to the raw STORA data, this interface consistently occurs at a sludge concentration of $>3kgm^{-3}$ and lies in a horizontal plane once the sludge blanket level rises past the conical section of the tank (see Figure 3.1). In all the STORA profiles, the sludge concentration increases from $0kgm^{-3}$ to $>3kgm^{-3}$ over a depth of $<0.3m$, which is the depth interval at which the concentration measurements were taken. Consequently, the definition of the sludge blanket level at any concentration up to $3kgm^{-3}$ is not critical to the predictions of the program, as in all cases the sludge blanket level occurs at a concentration of $>3kgm^{-3}$. The measured sludge blanket level has been adjusted to account for the fact that the Rijen tank has a double sided effluent launder. STORA found that with double sided effluent launders, solids escape with the effluent, indicating failure, when the sludge blanket reaches

0.2m below the bottom of the launder. With a 0.6m launder depth, the sludge blanket level effectively reaches the top of the Rijen tank at a depth of 0.8m below the water surface level. This reduces the effective height of the settling tank from 4.15m to 3.35m. Because the sludge blanket is horizontal once it rises past the conical section of the tank (see Figure 3.1), it was deemed valid to assume a flat bottomed tank for modelling purposes. All sludge concentration depth profiles examined in this investigation are those measured as close to the centre of the tank as possible (6m for the Rijen tank), and thus the depth of the assumed flat bottomed tank is the same as that at which the central sludge concentration depth profile was measured. In addition, because SETTLER defines layer 1 as the effluent flow, layer 2 is the maximum possible height that the sludge blanket can attain. Hence, when the sludge blanket level is at layer 2 (0.16m below the surface of the tank, each layer being 0.0836m high), the sludge blanket is effectively at the top of the tank. The measured results have been adjusted in order to reflect this. In terms of this definition, the predicted and measured sludge blanket levels are compared in Figure 8.2.

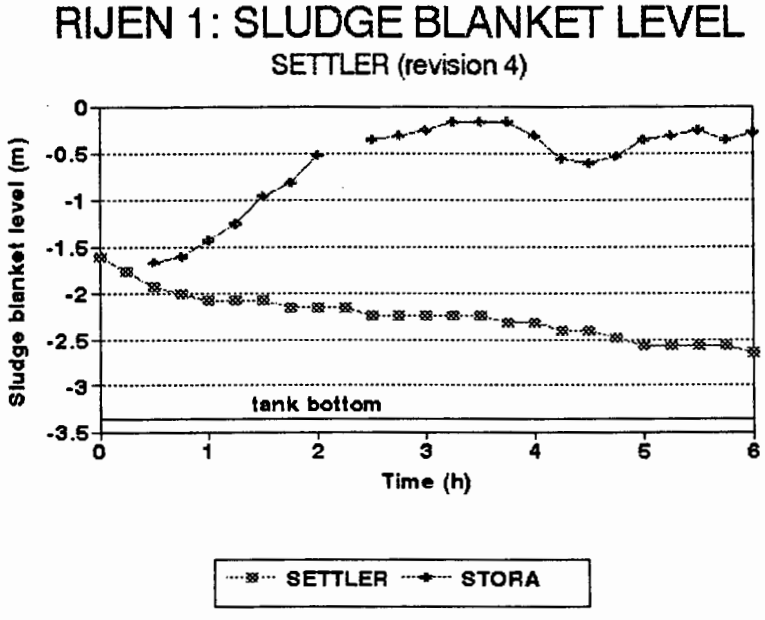

Figure 8.2 Predicted and measured sludge blanket levels for Rijen 1 with SETTLER (revision 4)

The predicted sludge blanket level falls continuously during the test from 1.6m below the surface (the tank being 3.35m deep) at the start of the test to 2.64m below the

surface at the end of the test. In contrast, the measured sludge blanket level rises almost constantly from 1.66m below the surface at the start of the test to 0.16m (effectively the top of the tank) at 3.25h. At the end of the test, the measured sludge blanket level is at 0.285m.

Although the predicted sludge blanket level falls during the test, it was observed that the total predicted mass of sludge in the settling tank increases from 14177kg at the start of the test to 18000kg one hour after the start. During this hour, the material in the tank is being redistributed, with the concentration in the lower layers increasing which necessitates a decrease in the layers higher up in the tank. Figure 8.3 shows the predicted concentration profiles at 15 minute intervals during the first hour of the test.

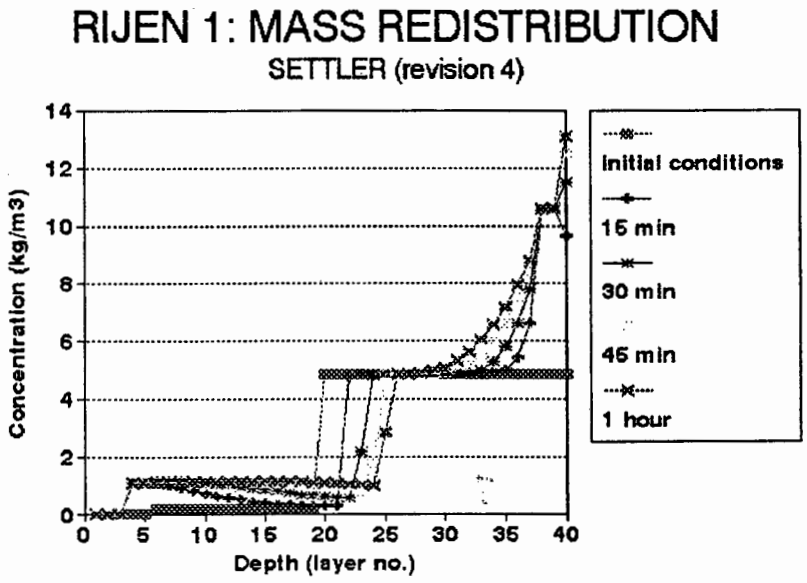

Figure 8.3 Mass redistribution in the settling tank during the first hour of the Rijen 1 test

It is the redistribution of the sludge that causes the drop in the predicted sludge blanket level. However, the fact that the mass of sludge in the tank increases continuously for the first 2.5h of the test indicates that, in time, had the feed sludge concentration not decreased, settling tank failure would have taken place. The decrease in sludge blanket level therefore arises as an artefact of sludge redistribution in the tank at the

commencement of the influent flow (Q_i), and is not an indication that the settling tank is underloaded.

The reason for the discrepancy between predicted and measured results was identified as being an absence of diffusivity in all but the feed point layer of the settling tank. Although under prolonged overload, SETTLER does correctly predict a gradually increasing sludge blanket level and ultimately settling tank failure, the period of overload in Rijen 1 (only 2.75h) is too brief relative to the response time of the hyperbolic form of the equations to reflect a measurable rise in sludge blanket level. This is because, for the hyperbolic equations under overloaded conditions, the layers behave discretely, and the concentration in each one must first increase to approximately the limiting concentration (X_L) before the accumulating material is permitted to be passed upwards into the next layer. In small diameter columns, this does not have a major influence, but in a large diameter tank such as Rijen, the slow response time causes a significant delay in the rise rate of the sludge blanket level. If, however, a degree of diffusivity is introduced into all the layers of the tank, creating a "mixing" effect between the layers, the sharp concentration discontinuities are smoothed out and the discrete behaviour of the layers is averaged out. This allows the sludge blanket (shock front) to propagate more rapidly up the tank, increasing the sensitivity of the tank to changing loading conditions.

2. Underflow concentration

Figure 8.4 compares the predicted and measured underflow concentrations for Rijen 1. The predicted underflow concentration increases very quickly from the start of the test and attains the maximum theoretical value of 13.77kgm^{-3} only three hours after the start of the test. In contrast, the measured underflow concentration is erratic throughout the test, but shows a gradual and slow increase over the six hour period. It is only at 3.75h that the value first approaches its greatest measured value of 10.58kgm^{-3}.

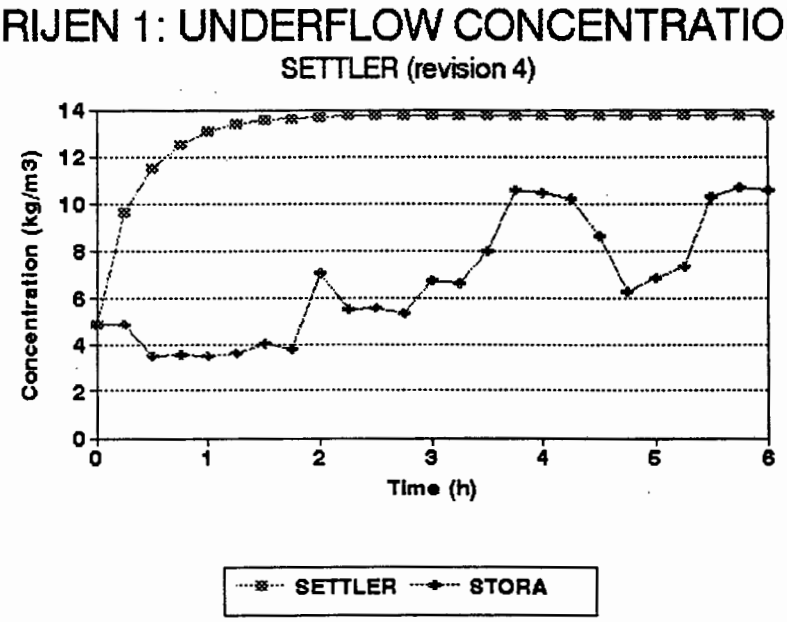

Figure 8.4 Predicted and measured underflow concentrations for Rijen 1 with SETTLER (revision 4)

The reason for the extremely rapid rise in the predicted underflow concentration is that SETTLER does not take into account the time required for thickening to take place in the bottom of the settling tank, and treats the system as if zone settling is dominant throughout. In order for SETTLER to correctly predict the slow increase in underflow concentration, a modification that simulates the time lag introduced by the thickening process in the bottom of the tank is necessary.

3. Effluent concentration

The measured and predicted effluent concentrations over the 6h test are compared in Figure 8.5.

The measured concentrations are very low ($<0.1 mgl^{-1}$) until 3.25h, when a sudden loss of solids ($400 mgl^{-1}$ to $700 mgl^{-1}$) was measured. Considering that the flux theory indicates that the settling tank is only overloaded for the first 2.5h of the test, effluent solids loss occurring during an underloaded period might appear to be an unlikely result. However, as mentioned in Chapter 2, it has been shown by Ekama and Marais

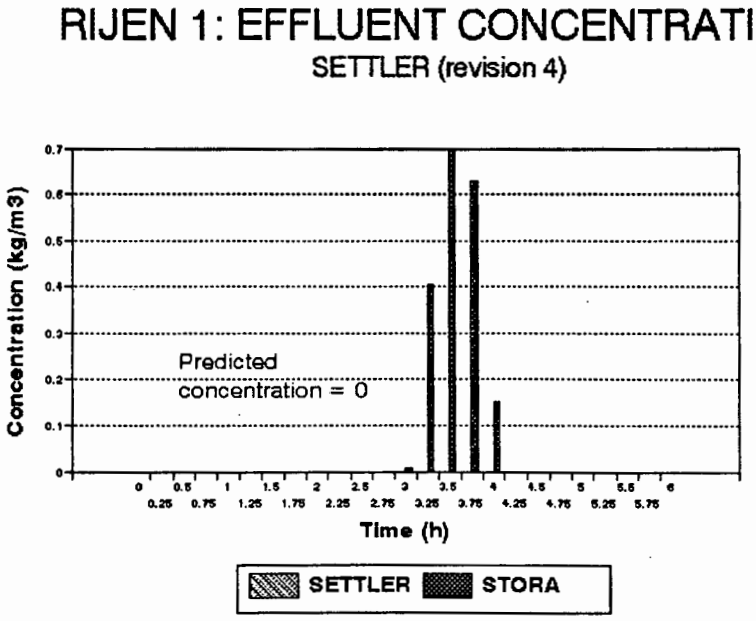

Figure 8.5 Predicted and measured effluent concentrations for Rijen 1 with SETTLER (revision 4)

(1986) that the flux theory tends to overpredict the limiting solids flux by 20%. If the recommendation of Ekama and Marais is followed, and the limiting flux reduced to 80% of that predicted by the flux theory, then the settling tank is found to be overloaded for the first 3.75h of the test. In this light, effluent solids loss at 3.25h is not unexpected, as it occurs at a time when the tank is still overloaded. The total measured mass loss in the effluent is 773kg. Throughout the 6h test, the predicted effluent solids concentration is zero, and no loss of solids is predicted in the effluent at any stage. This result is directly related to the predicted slow rise rate of the sludge blanket.

4. Concentration profile

The measured data does not include a concentration profile in the settling tank for Rijen 1. It was therefore decided to repeat the simulation using Rijen 4 as a basis for comparison, because in this case the measured data does include sludge concentration depth profiles at various stages of the test.

8.3 SIMULATING THE RIJEN 4 TEST WITH SETTLER (revision 4)

The fourth settling tank test carried out at Rijen (hereafter referred to as Rijen 4) was run for a total of seven hours, with the influent flow being shut off for 1.5h from 5.5h after the start of the test until the end of the test. The flux theory constants, V_o and n, were calculated from the measured $SSVI_{3.5}$ of $120mlg^{-1}$, to be $V_o = 5.188mh^{-1}$ and $n = 0.429m^3kg^{-1}$ using the relationship for extended aeration plants derived in Chapter 4. With these values of V_o and n, the flux theory indicated that the settling tank was overloaded for the first 5.5h of the test. Once the feed was shut off, the system became underloaded and remained so until the end of the test. The data measured by STORA for the Rijen 4 test is given in Table 8.3 and a summary of the operating parameters for the test is presented in Table 8.4.

Table 8.3 Data measured by STORA for the Rijen 4 test

Test Rijen 4 Begin test: 9:15h
Date: 23 November 1978 End test: 14:00h

Q_i = 1425m^3h^{-1} Q_r = 531m^3h^{-1}

Time (h)	Feed conc (kg/m3)	Underflow conc (kg/m3)	Effluent conc (mg/l)	Sludge blanket height (m)	Remarks
09:00	??	7.01	< 0.1	2.75	start influent
09:15	??	6.53		2.75	
09:30	??	6.86			influent sample disturbed
09:45		6.60			
10:00	??		< 1		
10:05		4.25		2.40	
10:15		4.06		2.15	
10:30	3.81	3.92			
10:45		4.32		2.00	
11:00	4.39	4.18	??	1.90	
11:15		5.82			
11:20				1.70	
11:30	4.04	5.84		1.60	
11:45		6.90		1.45	
12:00	3.85	7.23	< 0.1		
12:10				1.40	
12:15		7.10			
12:20				1.25	
12:30	3.41	7.47			
12:45		8.40		1.15	
13:00	3.47	8.15	< 0.1	1.05	
13:15		7.50		0.95	
13:30	3.25	8.18		0.90	
13:45		8.83			
13:50				0.80	
14:00	3.20	7.92	< 0.1		flocks over weir
14:05				0.70	
14:10			34.00		
14:15		7.69			solids loss
14:20			101.00		
14:30	3.32	8.94	558.00		influent stopped
14:40			700.00		
14:45		10.04			
14:55				0.70	
15:00	2.87	10.56	65.00		
15:15		11.57			
15:20			< 0.1	1.05	
15:30	3.29	9.77		1.15	
15:45	3.06	9.67		1.40	

The initial conditions for Rijen 4 are illustrated in Figure 8.6. These were generated in the same manner as for Rijen 1 i.e. SETTLER (revision 4) was used to establish the concentration of X_{dz} but the sludge blanket level and underflow concentration (X_r) were set at the measured values. The magnitude of the diffusivity coefficient for the feed point was left unchanged from the Rijen 1 simulation at E = 7.52x$10^9 m^2h^{-1}$. The diffusivity at all other layers in the tank was set to zero.

Table 8.4 Summary of operating parameters for the Rijen 4 test

PARAMETER	VALUE
Q_i	$1425m^3h^{-1}$
Q_r	$531m^3h^{-1}$
X_o (max)	$4.39kgm^{-3}$
X_o (min)	$2.87kgm^{-3}$
Area	$1625m^2$
Depth (from overflow weir to bottom of tank)	3.35m
Feed point layer	5
Duration of test	7 hours
$SSVI_{3.5}$	$120mlg^{-1}$
DSVI	$130mlg^{-1}$
V_o	$5.188mh^{-1}$
n	$0.429m^3kg^{-1}$

The following parameters were extracted from the measured data and simulation results and compared:

1. Sludge blanket level and rise rate
2. Underflow concentration with time
3. Effluent concentration with time
4. Concentration profiles at specific times in the test

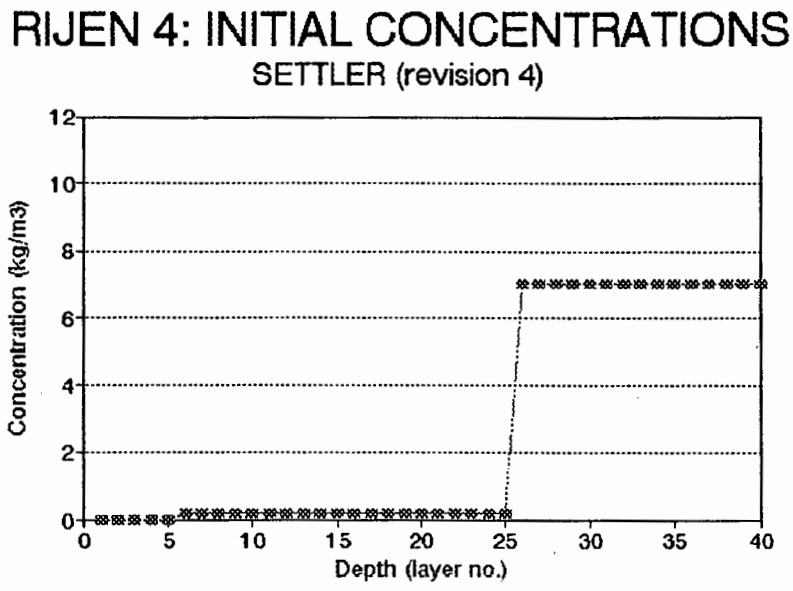

Figure 8.6 Initial concentration profile for Rijen 4

8.3.1 RESULTS OF THE RIJEN 4 SIMULATION

1. Sludge blanket level

In Figure 8.7, the measured and predicted sludge blanket levels for Rijen 4 are compared, a similar pattern being observed in the measured (STORA) and predicted (SETTLER) sludge blanket behaviour for this test to that for Rijen 1.
The measured sludge blanket level rises continuously from 2.11m below the surface at the beginning of the test to 0.16m (effectively the top of the tank) 6h after the start of the test. Thereafter, a drop in sludge blanket level from the top of the tank to 0.76m below the surface is observed. This is expected at this time because of the influent flow (Q_i) being shut off at 5.5h.

Despite the overloaded conditions, the predicted sludge blanket level falls from 2.08m below the surface at the beginning of the test to 2.24m below the surface 1.75h after the start of the test. During this time, as in Rijen 1, although the sludge blanket level falls, the mass in the settling tank increases, the decrease in sludge blanket level being the result of sludge redistribution in the tank. From 1.75h until 6h, the sludge blanket

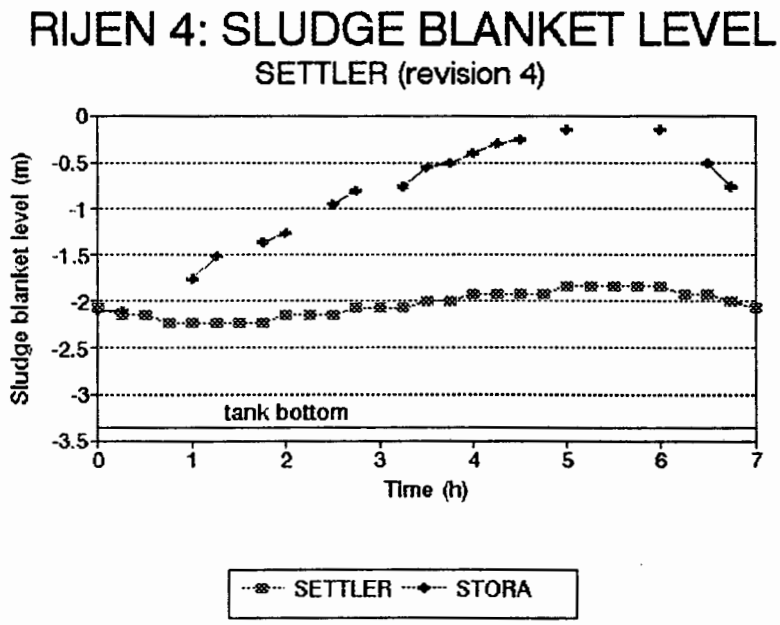

Figure 8.7 Predicted and measured sludge blanket levels for Rijen 4 with SETTLER (revision 4)

level rises very slowly from 2.24m to 1.84m below the surface of the tank. During the last hour of the test (from 6h to 7h), the sludge blanket level falls slightly from 1.84m to 2.08m as the tank becomes underloaded at 5.5h when the influent flow is shut off.

As for Rijen 1, for this test there is also a clear discrepancy between the measured and predicted results. The absence of diffusivity in all but the feed point layer of the tank is probably a contributing cause of this discrepancy for the same reasons as discussed for Rijen 1.

2. Underflow concentration

Figure 8.8 compares the measured and predicted underflow concentrations for Rijen 4. The predicted underflow concentration rises rapidly from the initial concentration of 7.01kgm^{-3} to the theoretical maximum underflow concentration of 11.02kgm^{-3} and attains this maximum value only 3h after the start of the test.

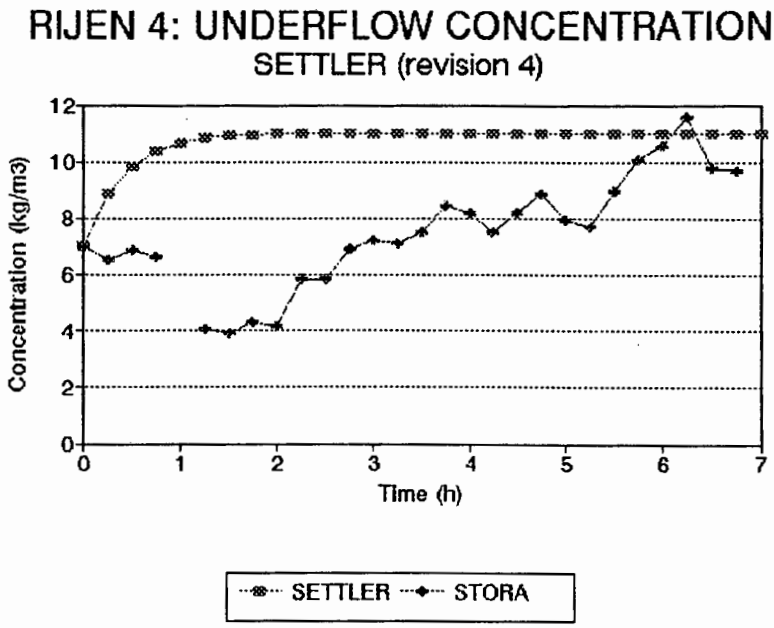

Figure 8.8 Predicted and measured underflow concentrations for Rijen 4 with SETTLER (revision 4)

In contrast, the measured results show an initial decrease in concentration from 7.01kgm^{-3} at the start of the test to 3.92kgm^{-3} at 1.5h after the start of the test. Thereafter, the underflow concentration rises continuously, although erratically, to attain its maximum value of 11.57kgm^{-3} at 6.25h after the start of the test. From 6.25h to the end of the test, the measured underflow concentration decreases from 11.57kgm^{-3} to 9.67kgm^{-3} because of the shut off of the influent flow at 5.5h.

As for Rijen 1, the discrepancy in measured and predicted underflow concentrations is ascribed to the fact that SETTLER does not take into account the time required for thickening to take place in the bottom of the tank.

3. Effluent concentration

The measured and predicted effluent concentrations over the 7h test are compared in Figure 8.9. The measured results show a negligible concentration in the effluent until 5.5h, when a sudden loss of solids (558mgl^{-1}) is measured. The total mass of solids lost measured by STORA amounts to 740kg over the 7h period. SETTLER predicts no

loss of solids at any stage of the test. As for Rijen 1, the reason for the lack of solids loss predicted in the effluent can be linked to the slow rise rate of the sludge blanket and hence to the absence of diffusivity in all but the feed point layer.

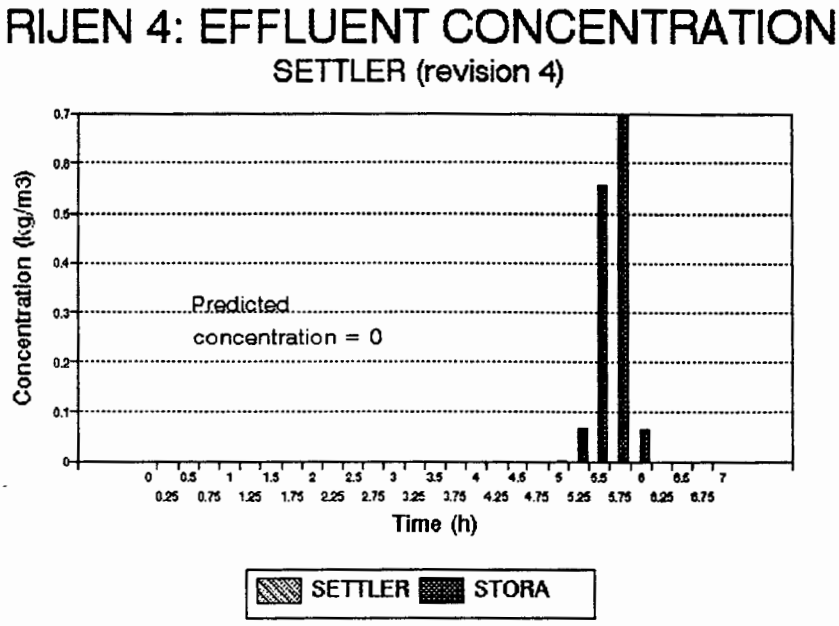

Figure 8.9 Predicted and measured effluent concentrations for Rijen 4 with SETTLER (revision 4)

4. Concentration profile

The STORA measurements show a total of nine concentration profiles at different times during the test. To avoid repetition, only two profiles at critical stages in the test were selected for comparison, the first at 5.5h, just after the influent flow has been shut off and the second at 7h, the end of the test.

Figure 8.10 compares the measured and predicted concentration profiles at 5.5h after the start of the Rijen 4 test.

The predicted underflow concentration (11.02kgm^{-3}) is higher than that measured (8.89kgm^{-3}). The predicted sludge blanket level (1.84m below the surface of the tank) is lower than the measured sludge blanket level, which extends over most of the tank depth from layer 39 to layer 9. However, the predicted sludge blanket concentration

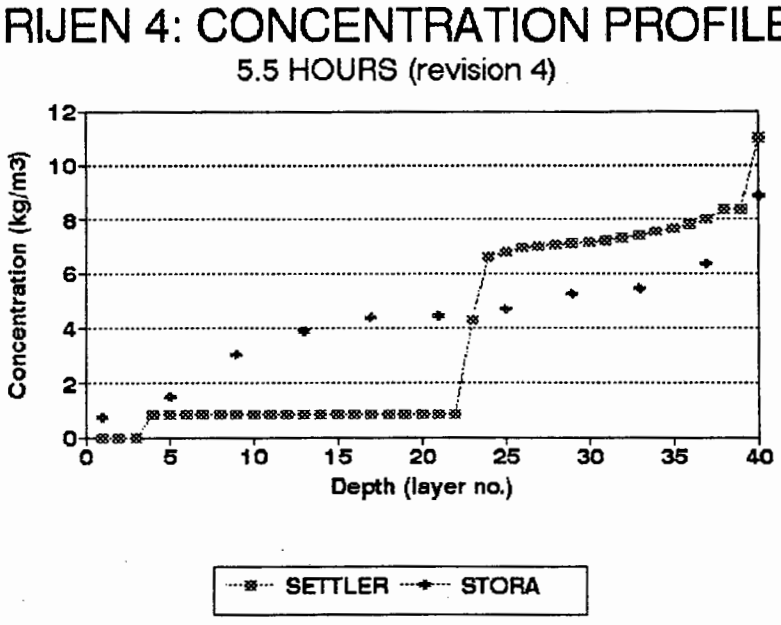

Figure 8.10 **Predicted and measured concentration profiles at 5.5h for Rijen 4 with SETTLER (revision 4)**

($\pm$7kgm^{-3}) is higher than the measured sludge blanket concentration ($\pm$5kgm^{-3}). There is no effluent solids loss predicted in the effluent, whereas the measured results show an effluent solids concentration of 0.77kgm^{-3} (770mgl^{-1}). The total mass of sludge in the tank at 5.5h has increased from an initial mass of 14808kg (presumed to be the same for the measured and predicted tests) to 21931kg (measured) and 20368kg (predicted).

Figure 8.11 compares the predicted and measured concentration profiles for Rijen 4 at 7h i.e. the end of the test.

The predicted underflow concentration (10.66kgm^{-3}) is higher than the measured underflow concentration (8.33kgm^{-3}). The predicted sludge blanket level has fallen since 5.5h to a level of 2.24m below the surface of the tank, whilst the measured results show a sludge blanket that still extends over most of the tank. No effluent solids loss is predicted, whilst the measured results show a low effluent solids loss of 40mgl^{-1}. The total mass of sludge in the tank has decreased from 21931kg (measured) and 20368kg (predicted) at 5.5h to 20989kg (measured) and 16706kg (predicted).

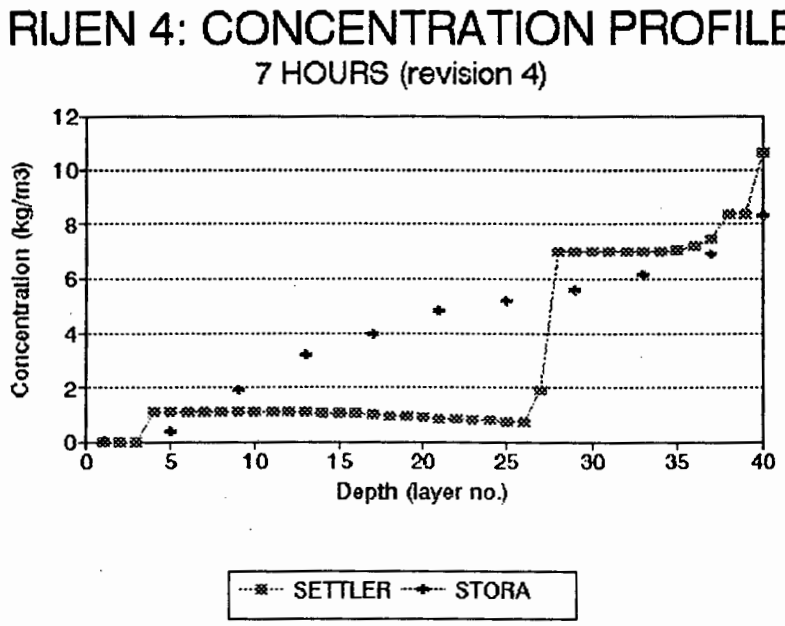

Figure 8.11 **Predicted and measured concentration profiles at 7h for Rijen 4 with SETTLER (revision 4)**

8.3.2 CONCLUSIONS

As discussed for Rijen 1, the most probable reason for the discrepancy between predicted and measured results is related to the absence of diffusivity in all but the feed point layer of the tank. Since the sludge blanket level is closely linked to the concentration profile, similar reasons to those for the problems with the sludge blanket level prediction can be cited for the erroneous predictions in the concentration profile.

8.4 MODIFICATIONS TO SETTLER

Although it was accepted that the most likely cause of the discrepancy between predicted and measured results is the absence of diffusivity in all but the feed point layer of the tank, a second possible cause of error was briefly investigated.

It is possible that the statistical procedure used to derive expressions for the calculation of the sludge settleability characteristics, V_o and n, could be inaccurate, leading to V_o and n values that give incorrect simulation results. It was found that it was possible to

artificially fix the V_o and n values such that at least the time of failure in the tank was accurately predicted. This was at the cost of accurate prediction of the other predicted parameters, so much so that the model predictions were very far from the measured results. From this investigation, it was clear that the problems with the model predictions could not only be ascribed to inaccuracies in the V_o and n values. Since the statistically derived expressions are the best available method for estimating the sludge settleability parameters, it was decided to accept these as derived and concentrate on improving SETTLER in other ways, focusing on the absence of diffusivity as the most urgent source of error.

SETTLER was modified to overcome the problems identified above by introducing:

1. diffusivity at all layers of the tank

2. a technique that simulates the required timelag in underflow concentration change in the thickening region of the settling tank.

These were found to be interlinked problems in that, because diffusivity affects the concentration profile, sludge blanket level and effluent solids concentration, it also indirectly affects the underflow concentration. Similarly, any strategy to simulate the sludge thickening delay in the bottom of the tank will influence the concentration profile and hence the form and magnitude of the diffusivity function. Consequently, it was decided to implement both strategies simultaneously and interactively.

8.4.1 THE DIFFUSIVITY FUNCTION

Although little detailed information exists about the nature of turbulence in secondary settling tanks, it is nevertheless physically apparent that turbulence does exist in full scale tanks with large diameter to depth ratios (Collins and Crosby (1980)). From the literature, Anderson made the following assumptions as regards the nature of turbulence in a settling tank:

1. the intensity of the turbulence and thus the diffusivity coefficient decreases as the distance from the feed point increases (up and down)
2. the diffusivity increases everywhere when the feed rate to the settling tank ($Q_i + Q_r$) increases.

From these assumptions, Anderson proposed a function (See Chapter 5: Equations 5.6 and 5.7) which modelled the diffusivity for the tank as an exponential function having its greatest value at the feed point layer and dying away exponentially with distance from the feed point. The function was dependent on the feed rate ($Q_i + Q_r$) to the settling tank.

While the form of the diffusivity function was soundly conceived, for some unknown reason Anderson did not implement it in his program in this form. The form of the diffusivity function chosen by Anderson in his program was not dependent on the feed rate and, from the fifth layer below the feed point to the bottom of the tank, was not dependent on depth i.e. it was constant (see Figure 5.2). In addition, in implementing

the diffusivity function in the program, Anderson incorporated an averaging procedure whereby, at each layer, i, the calculated value of diffusivity is averaged with that in the layer above it (i-1). This average value of diffusivity is then accepted for the layer i (see Chapter 5, Section 5.4).

In the absence of other information regarding the nature of turbulence in a secondary settling tank, Anderson's originally conceived form for the diffusivity function was considered to be the most reasonable, and this was adopted in principle for the program SETTLER. In deference to Anderson's modelling experience, his strategy of averaging the calculated value of diffusivity in each layer with that in the one above it to give the final value of diffusivity was initially also retained.

Having defined the form of the diffusivity function, the next step was to examine its sensitivity to the values of the three constants (diftop, α_1 and α_2). The effect on the diffusivity function of changes in these three parameters is illustrated in Figure 8.12. Note that in these equations, the α_1 and α_2 values representing the diffusivity die off rate have units of layer^{-1}. To obtain the die off rates in units of m^{-1}, the layer^{-1} values need to be divided by the layer depth which, for the Rijen tank, is 0.0836mlayer^{-1}.

The sensitivity of the settling tank to changes in the values of the three constants was determined by monitoring the effect on the total mass of sludge lost with the effluent during the Rijen 1 test when varying the value of one of the parameters whilst holding the other two constant.

In the process of investigating the sensitivity of SETTLER to the values of α_1, α_2 and diftop, it was observed that an increase in the value of diftop did not result in a monotonic increase in the mass lost with the effluent. A gradual increase in the value of this parameter resulted in an erratic and non-monotonic increase in the mass lost with the effluent. This is illustrated in Figure 8.13 for the case of the Rijen 1 test with α_1 and α_2 held constant at 0.075layer^{-1} and 0.008layer^{-1} respectively. In 23 separate simulations carried out for each different value of diftop, the total mass lost during the

$$E_i = \text{diftop}\ (Q_i + Q_r)e^{\alpha_1(i-i_{feed})} \text{ for } i<i_{feed} \qquad (8.3)$$

$$E_i = \text{diftop}\ (Q_i + Q_r)e^{-\alpha_2(i-i_{feed})} \text{ for } i>i_{feed} \qquad (8.4)$$

(see Equations (5.6) and (5.7) in Chapter 5 for details)

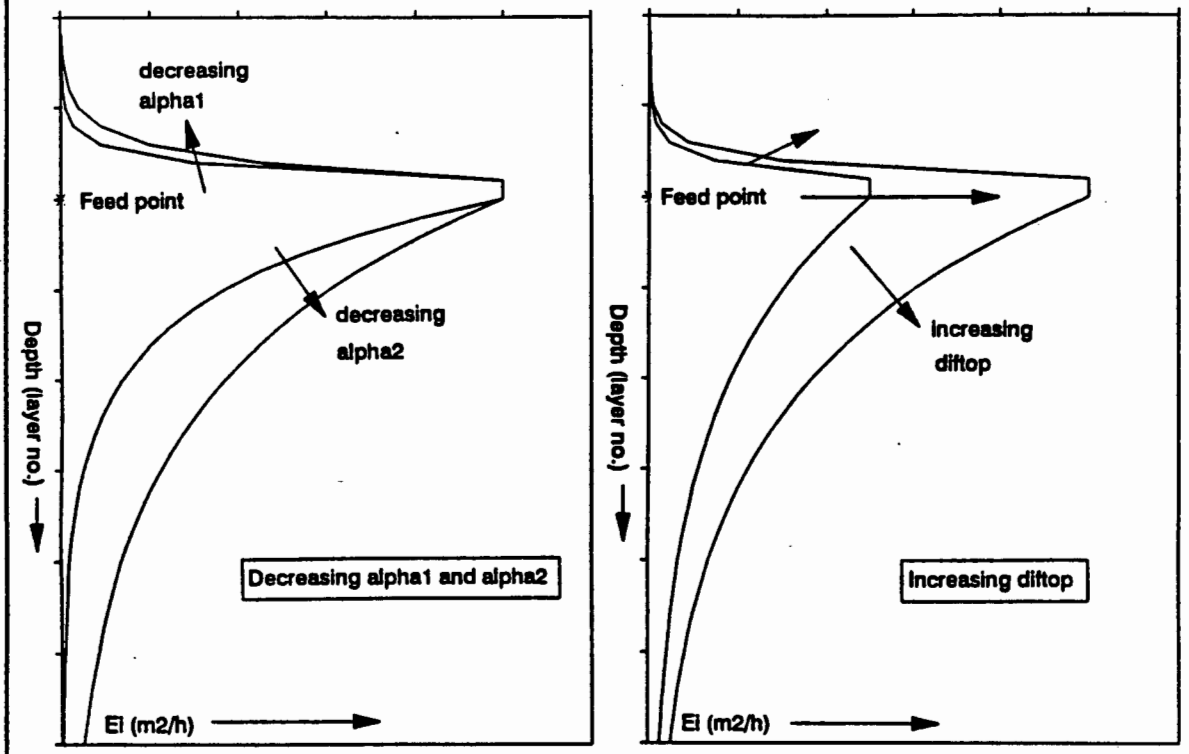

Figure 8.12 The effect of varying diftop, α_1 and α_2.

six hour test period was recorded. Because the overall diffusivity in the tank (area between the curve and the vertical axes) was monotonically increased, which increases the mixing between the layers in the tank, it was expected that the mass of solids in the effluent would also increase monotonically. The fact that this was not the case indicated that there may be some problem in the form and implementation of the diffusivity function. In investigating this problem, it was found that the averaging procedure used by Anderson was responsible. The averaging procedure was therefore eliminated from the program and this eliminated the problem. Without the averaging

procedure, the mass of solids in the effluent increased monotonically with increasing diftop.

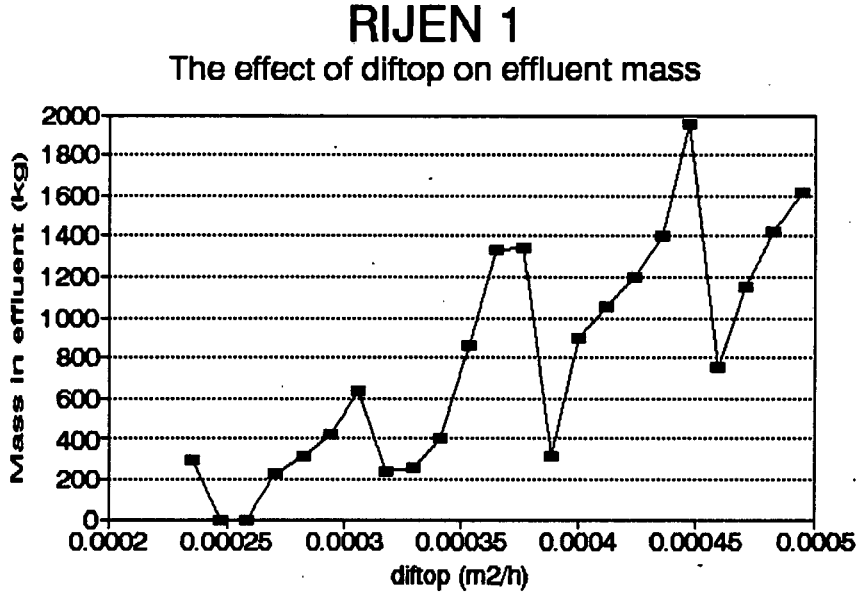

Figure 8.13 **The effect of diftop on effluent mass for the Rijen 1 test**

The effect of α_1 on mass lost with the effluent with the averaging removed

The effect of varying α_1 (the rate at which the diffusivity dies off above the feed point) was investigated, and the mass lost with the effluent was found to be insensitive to this parameter. Consequently, an arbitrary value of 10.00layer^{-1} (or equivalently 119.6m^{-1} for the 0.0836m layers of the Rijen tank) was selected for α_1 for all the STORA tests.

The effect of α_2 and diftop on mass lost with the effluent

The mass of sludge lost with the effluent was found to be fairly sensitive to the values of these two parameters. An increase in diftop (with α_2 held constant) resulted in an increase in mass lost with the effluent, as was expected. When α_2 was increased i.e. the exponential function died away more quickly with depth of the tank, (with diftop held constant) a corresponding decrease in mass lost with the effluent was observed, also as expected. Generally, it appears that the greater the amount of "total diffusivity"

(area between vertical axes and the diffusivity curve) in the tank (i.e. small α_2, large diftop), the greater the amount of mass lost with the effluent. Clearly these two parameters are related, as a high value of diftop coupled with a high value of α_2 (i.e high diffusivity at the feed point, but dying away rapidly with distance from the feed point), was found to produce the same mass in the effluent as a low value of diftop coupled with a low value of α_2 (i.e low diffusivity at the feed point, but dying away slowly with distance from the feed point).

Unfortunately, this flexibility in the choice of diftop and α_2 was not sufficient to model the diffusivity using the exponential function alone for the lower layers of the tank. Certain choices for the diftop and α_2 combination resulted in problems with the simulation results. It was observed that, although the mass lost with the effluent generally increased with decreasing magnitude of α_2, low values of α_2 caused the exponential function to die away too slowly, resulting in diffusivity values in the lower regions of the tank being too high. These high diffusivity values caused an excessive mixing effect in the lower layers of the tank and resulted in entropy rule violations in the predicted concentration profile. This is illustrated in Figure 8.14 for the case of the Rijen 1 test at 6h with diftop = 2596.28m^{-1}, α_1 = 10.00$layer^{-1}$ (119.6m^{-1}) and α_2 = 0.506$layer^{-1}$ (6.05m^{-1}).

On the other hand, higher values of α_2 caused the exponential function to die away too quickly, resulting in very low diffusivities in the bottom layers of the tank. This causes the equations in this region to become essentially hyperbolic, which creates problems with the upward propagation of the sludge blanket, as already discussed earlier in simulating Rijen 1 and Rijen 4 with SETTLER (revision 4) i.e. diffusivity at the feed point only (see Chapter 8, Sections 8.2 and 8.3) Thus, for high values of α_2, very little or no mass loss in the effluent is predicted for the Rijen tests.

From the above discussion, it is clear that both high and low values of α_2 lead to poor simulation results. It was therefore hoped that between the two extremes a narrow range of α_2 values existed that would lead to accurate simulations for the effluent

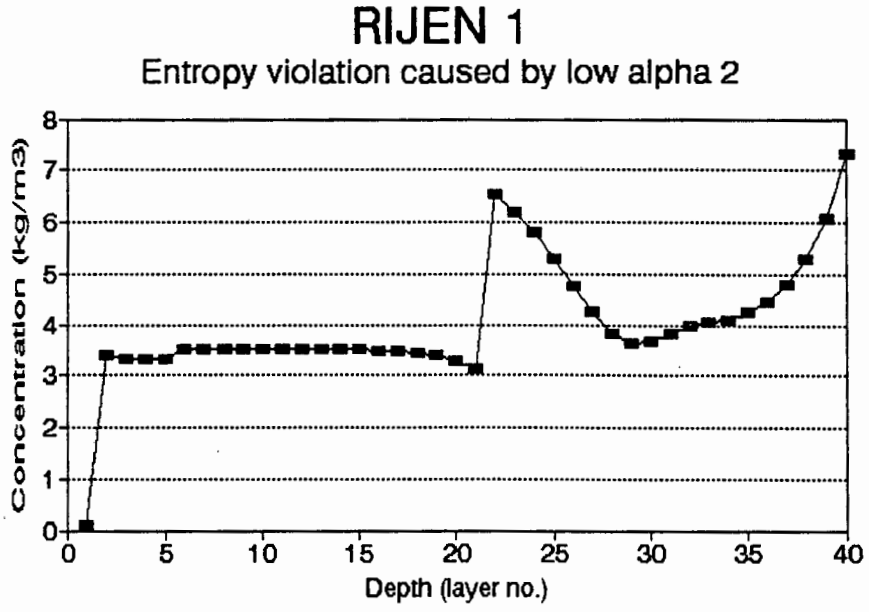

Figure 8.14 The effect of a low value of α_2 on the concentration profile

solids mass and the concentration profile. However, this was found not to be the case because the errors arising from too high (poor concentration profile) and too low (no effluent solids mass lost) α_2 values overlapped.

Therefore, it was concluded that, as no single value of α_2 could be selected to avoid both these problems, modification to the form of the diffusivity function was necessary to ensure that with a high value of α_2 some diffusivity remained in the bottom regions of the tank. This was achieved by accepting a constant value of diffusivity in the bottom layers of the tank (called difbot) and modifying the diffusivity function for the tank as follows:

$$E_i = \text{diftop}.(Q_i+Q_r).e^{+\alpha_1(i-i_{feed-1})} \text{ for } i<i_{feed} \quad (8.5)$$

$$E_i = \text{diftop}.(Q_i+Q_r).e^{-\alpha_2(i-i_{feed})} \text{ for } i \geq i_{feed} \quad (8.6)$$

The criterion for the selection of the constant value for diffusivity (difbot) in the bottom layers of the tank was formulated as follows:

$$\text{IF}(E_i < \text{difbot}) \text{ THEN } E_i = \text{difbot} \quad \text{for } i > i_{feed} \text{ only} \tag{8.7}$$

The problem with accepting that a constant value of diffusivity was necessary in the bottom of the tank was that this introduced an extra variable into the diffusivity function determination. This meant that defining the diffusivity at each layer in the tank became more complex as it was not possible to determine the magnitude of each of the diffusivity constants in a stepwise manner due to the highly interactive nature of the constants. By trial and error, however, approximate ranges for the three diffusivity constants were determined, their specific values being subsequently refined by an iterative search procedure.

Determining the values of α_2, diftop and difbot

Using a trial and error search, it was found for the Rijen 1 test that α_2 and diftop should be approximately in the range 1.2layer^{-1} (14.35m^{-1}) < α_2 < 2layer^{-1} (23.92m^{-1}) and 3.9m^{-1} < diftop < 21300m^{-1}. For α_2 > 2layer^{-1} and diftop < 21300m^{-1}, i.e. total diffusivity small, no single value of difbot could be found that was large enough to propagate the sludge blanket and cause solids loss in the effluent without also causing an entropy rule violation in the predicted concentration profile. Conversely, when α_2 < 1.2layer^{-1} and diftop > 21300m^{-1}, no single value of difbot could be found that was low enough to prevent excessive mass loss in the effluent. However, once α_2 and diftop were set in the ranges mentioned above, it was possible to experiment with various values of difbot.

The effect of difbot on the mass lost with the effluent and the concentration profile

In investigating the effect of difbot on the mass lost with the effluent and the concentration profile in the tank, it was found that difbot had a significant influence on the behaviour of these parameters, although they were also found to be sensitive to the

values of α_2 and diftop. The effect of difbot on the mass lost in the effluent is illustrated in Figure 8.15.

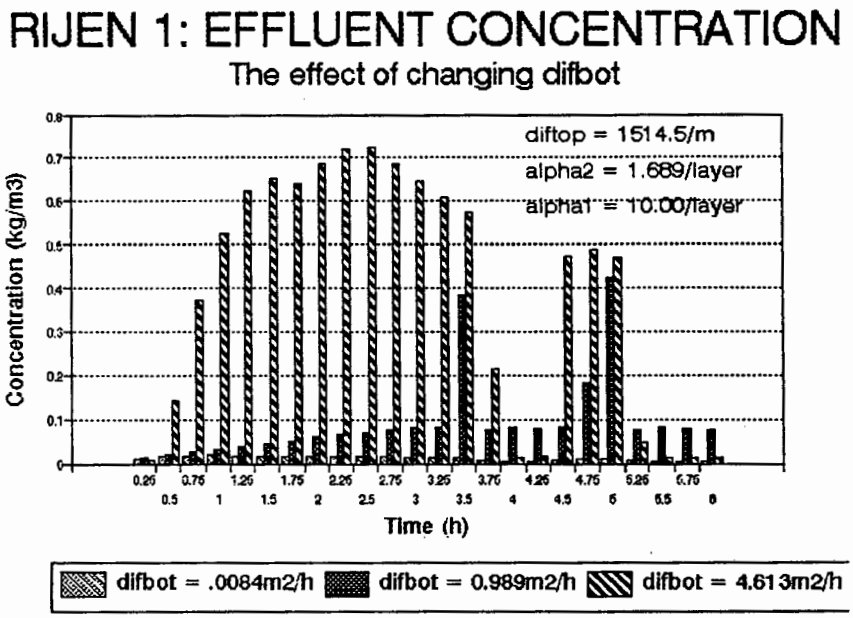

Figure 8.15 The effect of difbot on effluent mass for Rijen 1

When difbot is low ($0.0084m^2h^{-1}$), the predicted mass lost in the effluent remains negligible throughout the test. No failure is predicted by SETTLER during the 6h test period. When difbot is high ($4.613m^2h^{-1}$), the sludge blanket rises too quickly and the predicted mass lost in the effluent is high from the start of the test almost throughout the entire 6h period. For this value of difbot, the settling tank becomes oversensitive to the overloaded situation and failure is predicted only 15min into the test. For difbot = $0.989m^2h^{-1}$, the predicted pattern of failure corresponds with that expected i.e. a negligible solids concentration in the effluent for the first few hours of the test while the sludge blanket builds up in the tank followed by a sudden increase in the effluent solids concentration at the time of failure. This "peak" of effluent solids concentration corresponds to that observed in practice. This suggests that a value of difbot in the region of $0.989m^2h^{-1}$ accurately represents the diffusivity in the bottom layers of the settling tank and therefore accurately predicts not only the time of failure but also the observed manner of failure.

The effect of difbot on the concentration profile is illustrated in Figure 8.16.

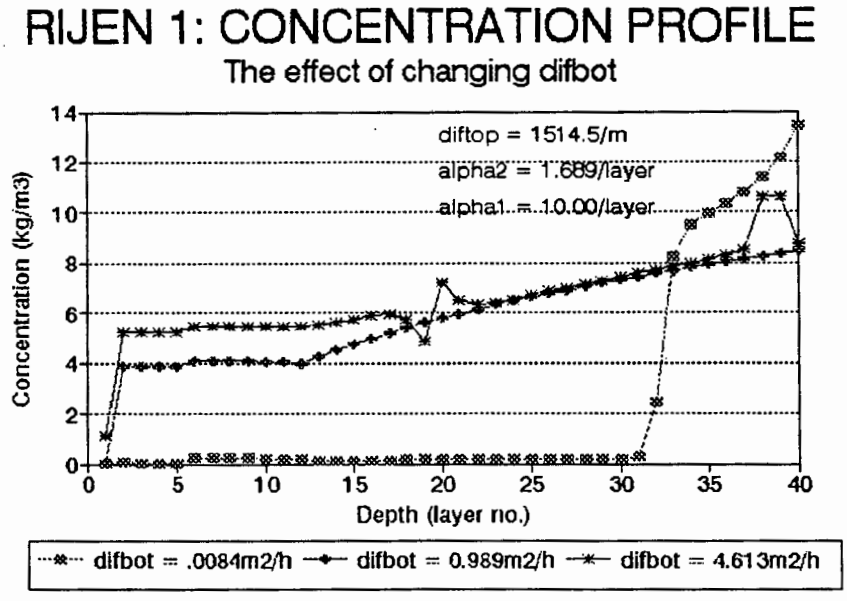

Figure 8.16 The effect of difbot on the concentration profile

When difbot is low ($0.0084 m^2h^{-1}$), the predicted concentration profile for the Rijen 1 test shows a poorly developed sludge blanket which has fallen continuously since the start of the test. Above the sludge blanket, the concentration is very low throughout the remaining upper layers of the tank. When difbot is high ($4.613 m^2h^{-1}$), the sludge blanket rise rate is extremely rapid (predicted failure occurs 15min into the test), and the high diffusivity causes the middle layers of the tank (from 17 to 24) to become excessively mixed, resulting in an entropy rule violation (layers of low concentration below layers of high concentration) in the concentration profile in this region of the tank. For difbot = $0.989 m^2h^{-1}$, the concentration profile is as expected, with a discernable sludge blanket extending through most of the tank, decreasing slightly in concentration near the feed point. No entropy rule violations occur in the concentration profile. This test confirms that an approximate value of difbot for the Rijen 1 test would be in the region of $0.989 m^2h^{-1}$.

Further experiments carried out on the Rijen 1 tank confirmed that the value of difbot should not be greater than $2.5 m^2h^{-1}$ to prevent entropy rule violations in the final concentration profile. For Rijen 1, the following criteria were used in selecting the α_2, diftop and difbot values:

1. the total mass of solids lost with the effluent over the six hour test should correspond to that measured by STORA (773kg),

2. the manner in which the mass was lost with the effluent should be as a negligible solids concentration in the effluent for the first few hours of the test followed by a peak in effluent solids concentration at the time of failure,

3. the concentration profile generated by the program after six hours should have an identifiable sludge blanket and concentration values that increases approximately monotonically from top to bottom of the tank.

It was established that the four groups of diffusivity function constants (amongst others) given in Table 8.5 all satisfy the specified criteria above:

Table 8.5 Four possible groups of diffusivity constants for the Rijen 1 test.

	GROUP			
	1	2	3	4
α_2 (layer^{-1})	1.8	1.689	1.5	1.4
difbot (m^2h^{-1})	0.914	0.989	1.115	1.375
diftop (m^{-1})	2596.31	1514.52	51.93	17.30
diftop.$(Q_i+Q_r)^*$ (m^2h^{-1})	6000000	3500000	120000	40000

* Note that the factor before the exponent in the diffusivity function at the feed point (Equations (5.6) and (5.7)) contains diftop*(Q_i+Q_r), making diftop only a part of this factor and is the reason for the units of diftop being m^{-1} rather than those of diffusivity (m^2h^{-1}).

Next, the sensitivity of the settling tank to changes in all three parameters α_2, diftop and difbot was examined. Initially disregarding the effluent solids concentration (i.e. the manner in which solids are lost from the settling tank) and focusing only on the sensitivity of the total mass lost in the effluent to changes in α_2, diftop and difbot it was found that:

1. a 10% increase in α_2 from 1.689layer^{-1} to 1.858layer^{-1} (20.2 to 22.2m^{-1}) (i.e. lower total diffusivity) resulted in a 7.8% decrease in mass lost i.e. from 778kg to 718kg,

2. a 10% decrease in diftop from 1514.5m^{-1} to 1363m^{-1} (i.e lower total diffusivity) resulted in a 13.5% decrease in mass lost i.e. From 778kg to 673kg,

3. a 10% decrease in difbot from 0.989m^{2}h^{-1} to 0.891m^{2}h^{-1} (i.e. lower total diffusivity) resulted in a 47% decrease in mass lost i.e. from 778kg to 411kg.

Clearly, the mass lost in the effluent is far more sensitive to the magnitude of difbot than to the other two parameters. i.e. difbot was found to be the single most important parameter in determining the total mass of sludge lost with the effluent. When all other parameters were held constant (α_1, α_2, diftop), very small changes in the value of difbot resulted in significant changes in the sludge mass lost.

Because many possible "groups" of constants for the diffusivity function can satisfy the specified criteria, some additional criterion for selecting a specific α_2 and diftop pair must be defined. Once the α_2 and diftop pair has been selected, only one value of difbot will uniquely predict the correct effluent solids mass lost. Because the effluent mass lost was so much more sensitive to the value of difbot than to the value of the other three parameters (α_1, α_2 and diftop), it was hypothesised that α_2 and diftop are dependent more on the geometry of the tank (area, depth) than on the hydraulic operating parameters (Q_i, Q_r and X_o). This hypothesis appears to correspond to the implementation of the final diffusivity function developed by Anderson and included in

his program. In the process of calibration, Anderson's function appeared to have had its dependence on hydraulic parameters eliminated, thereby making it dependent on tank geometry factors rather than on hydraulic parameters. Because of the high sensitivity of the tank response to the value of difbot, it was hypothesised that instead of diftop, difbot should be dependent on the feed flow rate ($Q_i + Q_r$) so that the feed flow term should appear in a function for estimating difbot rather than in the function defining diffusivity in the upper layers of the tank (α_2 and diftop). (Equation (8.5) and Equation (8.6)). The inclusion of the feed flow in the diffusivity equations for the upper layers was thus removed, and the factor before the exponent in the equations transformed as follows:

$$E_i = \text{diftop}.e^{+\alpha_1(i-i_{feed-1})} \text{ for } i<i_{feed} \tag{8.8}$$

$$E_i = \text{diftop}.e^{-\alpha_2(i-i_{feed})} \text{ for } i\geq i_{feed} \tag{8.9}$$

$$\text{IF } (E_i<\text{difbot}) \text{ THEN } E_i = \text{difbot} \quad \text{for } i > i_{feed} \text{ only} \tag{8.10}$$

where diftop in Equation (8.8) = diftop * (Q_i+Q_r) in Equation (8.5) and
diftop in Equation (8.9) = diftop * (Q_i+Q_r) in Equation (8.6)
= $51.93m^{-1} * 2311m^3h^{-1}$
= $120000m^2h^{-1}$ for Group 3 in Table 8.5.

Thus, the only criterion specified in choosing the α_2 and diftop pair was that it should be possible (without violating the constraint on difbot that it should not be greater than $2.5m^2h^{-1}$) to use the same pair of α_2 and transformed diftop (in terms of m^2h^{-1}) for all the overloaded Rijen tests (of which there are five i.e. Rijen 1, 4, 5, 7 and 8) because all these tests were carried out on the same settling tank. A trial and error search was carried out for all the Rijen tests to determine valid pairs for α_2 and diftop. From this search, the α_2 and diftop values from Group 1 and Group 4 in Table 8.5 were found to be unsuitable. For the Rijen 7 test, the values of α_2 and diftop in Group 1 introduced excessive total diffusivity (the area between the vertical axis and the diffusivity curve)

into the tank. This meant that, even with difbot set to zero, the predicted effluent solids mass lost was greater than the measured results. Since difbot could not be set to anything less than zero, it was concluded that the α_2 and diftop values in Group 1 were unsuitable for the Rijen tank. At the other extreme, for the Rijen 5 test it was found that the α_2 and diftop values in Group 4 provided insufficient total diffusivity in the tank. Even with difbot set equal to its maximum value of $2.5m^2h^{-1}$, the predicted effluent solids mass lost was less than the measured value. Since difbot cannot be set greater than $2.5m^2h^{-1}$ without causing entropy rule violations in the predicted sludge concentration depth profile, it was concluded that the values of α_2 and diftop in Group 4 were unsuitable for the Rijen tank. Both the α_2 and diftop values from Group 2 and Group 3 were acceptable in that valid difbot values could be selected for all the Rijen tests that predicted the correct effluent solids mass lost, but it was found that the Group 3 values of α_2 and diftop produced a more accurate pattern of effluent solids mass lost with time. The Group 3 values were thus selected as being the more realistic ones. Thus, the final values for the tank geometry dependent variables α_2 and diftop that were found to be the best for the Rijen settling tank were:

α_2 = $1.5layer^{-1}$ ($17.94m^{-1}$)

diftop = $120000m^2h^{-1}$

Having fixed α_2 and diftop, the value of difbot was simultaneously fixed for the Rijen 1 test at $1.115m^2h^{-1}$. The final form of the diffusivity function for Rijen 1 is illustrated in Figure 8.17.

In summary, the constants in the diffusivity function have so far been determined to be as follows:

1. the parameter α_1 = $10.00layer^{-1}$ ($119.6m^{-1}$) and is fixed for all settling tanks and tests,

2. the parameters α_2 = $1.5layer^{-1}$ ($17.94m^{-1}$) and diftop = $120000m^2h^{-1}$ are fixed for the Rijen settling tank but will be different for different tanks,

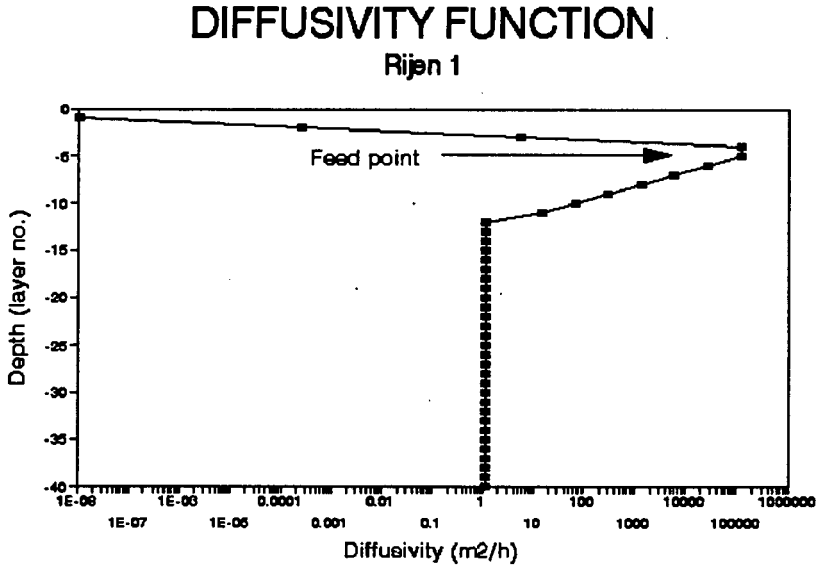

Figure 8.17 The diffusivity function as used for the Rijen 1 test

3. the parameter difbot = $1.115 m^2h^{-1}$ is fixed for the Rijen 1 test but will be different for a different $(Q_i + Q_r)$.

Having examined as a first step the factors that influence the effluent solids concentration and the concentration profile in the settling tank, attention was focused on resolving the problem regarding the absence of a time lag in the predicted underflow concentration. This involved incorporating an appropriate procedure that takes the timelag into account by simulating the thickening region and then examining the effect of this procedure on the selected values of diftop, α_2 and difbot. Because difbot mainly affects the bottom layers of the tank, and diftop and α_2 mainly the upper layers of the tank, it was realised that the introduction of a thickening region would influence the determined value of difbot more than the determined values of the other two variables i.e. once the timelag is incorporated, it would be necessary to recalibrate the diffusivity function, in particular, the value of difbot.

8.4.2 TIME LAG FOR THE THICKENING REGION

The time lag for the thickening region was simulated using a single CSTR (completely mixed stirred tank reactor) at the bottommost layer of the tank. This CSTR simulated the changing underflow concentration in the thickening zone by treating it as an unreactive tracer in a pure liquid, thereby damping the rapid response of the underflow concentration to overloaded conditions in the settling tank. Alkema (1971) investigated the effect of using between one and four CSTR's in series and concluded that the number of CSTR's in series made little difference to the unsteady state underflow concentration although the total volume of the CSTR had a major effect. In the light of this conclusion, it was decided to use only one CSTR reactor for the thickening zone simulation. A diagrammatic representation of the thickening zone CSTR is illustrated below in Figure 8.18.

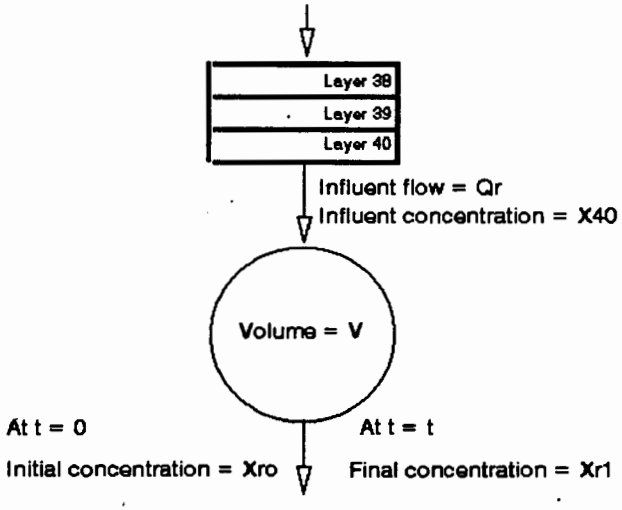

Figure 8.18 The single CSTR used to model compression time delay response of the underflow concentration

In the figure,

X_{ro} = the initial concentration in the CSTR (and thus in the exit stream) (kgm^{-3}) i.e. the underflow concentration emerging from the compression zone at the previous time step

X_{r1} = the final concentration in the CSTR (and thus in the exit stream) (kgm^{-3}) i.e. the underflow concentration emerging from the compression zone at the present time step

X_{40} = the underflow concentration introduced into the CSTR at time t=0 (kgm^{-3}) i.e. the underflow concentration as calculated by the Gaussian solution procedure at the present time step

Q_r = the flow rate through the CSTR (m^3h^{-1}) i.e the underflow rate

V = the volume of the CSTR (m^3)

= $A.d_{CSTR}$

where

A = the cross sectional area of the CSTR which is the same as that for the settling tank (A) (m^2)

d_{CSTR} = the depth of the CSTR (m)

Applying a material balance to the solids concentration (X) (considered here to be an inert tracer), and noting that, as far as solids concentration is concerned, the system is not in a steady state and solving for the underflow concentration in terms of the layer 40 concentration (X_{40}) yields:

$$\begin{aligned}
\text{Accumulation} &= \text{inflow} - \text{outflow} \\
\Delta X_r V &= Q_r X_{40}\Delta t - Q_r X_r \Delta t \\
\frac{dX_r}{dt} &= \frac{Q_r}{V}(X_{40}-X_r) \\
\int_{X_{ro}}^{X_{r1}} \frac{dX_r}{(X_{40}-X_r)} &= \int_0^t \frac{Q_r}{V}dt \qquad (8.11) \\
\frac{X_{40} - X_{ro}}{X_{40} - X_{r1}} &= e^{\frac{Q_r}{V}t} \\
X_{40} - X_{r1} &= (X_{40} - X_{ro})\, e^{-\frac{Q_r}{V}t}
\end{aligned}$$

$$X_{r1} = X_{40} - (X_{40} - X_{ro})\, e^{-\frac{Q_r}{A \cdot d_{CSTR}}t} \qquad (8.12)$$

Equation (8.12) gives the underflow concentration at the new time step (X_{r1}) in terms of the underflow concentration at the previous time step (X_{ro}) and the concentration of

solids entering the thickening region (X_{40}). The volume of the thickening region is V (m^3) and the flow through rate is Q_r (m^3h^{-1}) which is the underflow rate. The term Q_r/V is the reciprocal of the retention time in the thickening region and t is the time interval over which the concentration change is calculated. The volume of the thickening zone is dependent on the depth (d_{CSTR}) of the region because the area of the thickening region of the settling tank was assumed the same as the surface area of the settling tank i.e. a cylindrical shape for the settling tank was assumed.

The procedure for simulating the thickening region was incorporated into the program SETTLER (now revision 5). Without changing the previously established values of diftop, α_2 and difbot, the results for the predicted underflow concentration are shown in Figure 8.19 for different thickening region depths (d_{CSTR} of 0.5m, 1.0m and 5.0m) and compared with the measured underflow concentration in the Rijen 1 test. The 0.5m, 1.0m and 5.0m depths yield retention times of 1.53h, 3.06h and 15.31h respectively.

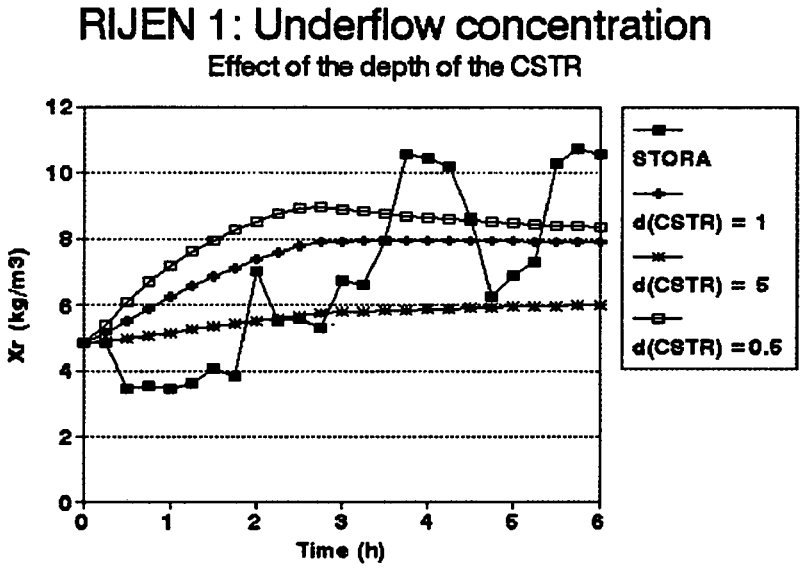

Figure 8.19 The effect of the depth of the CSTR on underflow concentration

It can be seen from Figure 8.19 that an increase in depth of the CSTR is associated with a more severe damping effect on the underflow concentration, as would be

expected. A depth of 5m for the CSTR produced a damping effect that was too severe, preventing the underflow concentration from increasing sufficiently, whereas a depth of 0.5m produced an insufficient degree of damping in underflow concentration. A depth of 1m was selected for the CSTR, as this produced an underflow concentration that reflected a gradual but pronounced increase, best reflecting the general trend of the measured results.

Once the depth of the thickening zone had been selected, the Rijen 1 test simulation was repeated with the previously determined α_2 and diftop values i.e. $\alpha_2 = 1.5 layer^{-1}$ and diftop = $120000 m^2h^{-1}$ which are the Group 3 values that gave the best results before the inclusion of the thickening zone. It was found that the value of difbot needed to be increased from its previous value ($1.115 m^2h^{-1}$ to $1.367 m^2h^{-1}$) in order that the total predicted mass lost with the effluent matched the measured results. This is to be expected, as the effect of including a thickening zone is to dampen the response of the equations in the bottom layer of the tank and thus difbot would need to be increased to compensate for this effect if the correct solids mass lost in the effluent is to be predicted. The effect of increasing difbot by this small amount on the effluent solids concentration pattern and the concentration profile was found to be negligible. Thus the final value of difbot selected for the Rijen 1 test was difbot = $1.367 m^2h^{-1}$.

8.4.3 DETERMINING THE VALUE OF DIFBOT FOR THE REMAINING RIJEN TESTS

During the process of simulating the Rijen 1 test and determining the values of the four diffusivity constants (α_1, α_2, diftop and difbot), it was found that, because the mass lost in the effluent and the concentration profile in the tank are relatively insensitive to changes in the values of α_2 and diftop, these two parameters were accepted to be functions of the geometry of the tank (area and depth) rather than of the operating parameters (Q_i, Q_r and X_o). Supporting this finding was the fact that it was possible to find a pair of α_2 and diftop values that could be used to simulate all five overloaded Rijen tests giving the correct mass lost in the effluent and a reasonable

solids concentration depth profile. These results were obtained without necessitating difbot values that are either too high, causing entropy rule violations in the predicted concentration profile, or too low, where α_2 and diftop by themselves provide greater than the required diffusivity consequently causing excessive solids mass loss in the effluent even if difbot is set to zero. In contrast, it was found that both the mass lost in the effluent and the sludge concentration depth profile in the tank are very sensitive to the value of difbot and that it is not possible to use the same value of difbot for all the Rijen tests. From this, it was concluded that difbot is dependent on some function of the operating parameters (Q_i, Q_r and X_o) as well as possibly the tank geometry. However, because the prediction of the correct mass loss in the effluent was influenced by the total diffusivity in the tank (α_1, α_2, diftop and difbot), it became evident that the values of difbot, α_2 and diftop operate interactively on each other. Thus it was accepted that α_2 and diftop are fixed by the geometry of the settling tank and that difbot, being dependent on the total diffusivity in the tank, is a function of α_2 and diftop as well as some function of the settling tank operating parameters.

In terms of the above conclusions, the α_1, α_2 and diftop values are fixed at α_1 = 10.00layer^{-1} (119.6m^{-1}), α_2 = 1.5layer^{-1} (17.94m^{-1}) and diftop = 120000m^{2}h^{-1} for the Rijen tank by its geometry. The next step was to establish the manner in which difbot changes as a function of the feed flow rate and the feed concentration (and possibly some other operating parameters), which was done by evaluating the remainder of the Rijen tests. However, because only one particular tank was being evaluated at this first step, it was not possible to determine the difbot dependency on the α_2 and diftop values. This will be examined later with other settling tanks.

The remaining overloaded Rijen tests (4, 5, 7, and 8) were simulated with SETTLER (revision 5) (with diffusivity function and thickening zone), and a unique value for difbot for each test was determined by a successive search such that the predicted effluent mass lost matched the measured value. During the process of determining the difbot values for these tests, the sensitivity of the solids mass lost in the effluent to the magnitude of the value of difbot was confirmed. The change in the predicted solids

Table 8.6 The effect of difbot on the mass lost in the effluent for the Rijen 4 test.

DIFBOT (m^2h^{-1})	MASS LOST (kg)
0.495	48.93
0.579	751.53
0.663	1837.99

mass lost in the effluent for the Rijen test 4 for three different values of difbot is illustrated in Table 8.6. The manner (i.e. effluent solids concentration vs time profile) in which the solids loss occurs is the same for all three cases because this is governed by the choice of the α_2 and diftop values. Whilst simulating the Rijen tests, the effluent solids concentrations and the sludge concentration depth profiles were examined to confirm that the selected values of difbot generated reasonable simulation results. The fact that reasonable simulation results were obtained (see Sections 8.5 to 8.9 below), without the need for fine tuning α_2 and diftop, indicated that the approach to defining the values of the diffusivity function was appropriate i.e. α_2 and diftop are geometry dependent alone and difbot is dependent on some function of the operating parameters as well as possibly the tank geometry.

Once the difbot values for the Rijen 4, 5, 7 and 8 tests had been determined, the next step was to develop a functional relationship between selected operating parameters and the value of difbot. A summary of the difbot values and the feed flow rates (Q_i+Q_r) for all the Rijen tests is presented in Table 8.7.

Although it became apparent during the investigation that many factors influenced the value of difbot, because the simplest and most general possible functional relationship was being sought it was not considered appropriate to include every possible factor as this would have resulted in a complicated function that would also be less broadly applicable. Thus, only those factors that appeared to influence the value of difbot were

Table 8.7 Feed flow rates and difbot values for the Rijen tests.

TEST	$(Q_i + Q_r)$ (m^3h^{-1})	DIFBOT (m^2h^{-1})
Rijen 7	1731	0.423
Rijen 4	1956	0.579
Rijen 8	2206.5	1.476
Rijen 1	2311	1.367
Rijen 5	2431.5	1.687

included in the function. The factors that influence the value of difbot include total feed flow to the settling tank (Q_i+Q_r), $SSVI_{3.5}$ measurement, feed flow concentration (X_o), applied flux (G_{ap}), average % solids overload ($100*(G_{ap}-G_L)/G_{ap}$) and the inverse of the initial sludge blanket level (from the bottom of the tank) as a percentage of the total depth of the tank (100*(1-sbl/depth)). Each of these factors was regressed individually against difbot to determine whether or not a significant functional relationship existed between the two. Various combinations of the factors such as $(Q_i+Q_r)/X_o$ and $(Q_i+Q_r)/(100*(1-sbl/depth))$ were also regressed against difbot and the multiple correlation coefficient (r^2) determined. Many of the combinations of factors gave significant linear correlations, a sample of the most promising being illustrated in Table 8.8.

Although the multiple correlation coefficient for the total feed flow (Q_i+Q_r) to the settling tank vs difbot was significant ($r^2 = 0.921$), the combination of (Q_i+Q_r) and the factor incorporating the inverse of the initial sludge blanket level as a percentage of the total depth dramatically improved the multiple correlation coefficient ($r^2 = 0.999$). However, during the investigation on the Rijen 1 tank, it was found that an increase in initial sludge blanket level (i.e. beginning the test with more sludge in the tank) necessitated an increase in the value of difbot. From this, it should follow that a decrease in the term 100*(1-sbl/depth) (resulting from an increase in the initial sludge

Table 8.8 A sample of the multiple correlation coefficients obtained for difbot against selected combinations of factors

FACTOR	r^2
$(Q_i+Q_r)/(100*(1-sbl/depth))$	0.999
(Q_i+Q_r)	0.921
Average % solids overload	0.905
$(Q_i+Q_r)/X_o$	0.853

blanket level) should cause a decrease in the difbot value. However, because the term 100*(1-sbl/depth) is on the denominator of the term $(Q_i+Q_r)/100*(1-sbl/depth)$ in the regression equation, an increase in initial sludge blanket level (causing the term 100*(1-sbl/depth) to decrease) will result in an increase in the calculated value of difbot. This is contrary to the findings made during the investigations into the behaviour of the settling tank at Rijen. In addition, the sludge blanket level is in any case related to the term (Q_i+Q_r) in the "history" of the operation of the settling tank, as high values of (Q_i+Q_r) will cause a high sludge blanket level in time and *vice versa*. Therefore, including both the flow and the sludge blanket level terms would be statistically suspect, as they are not independent and are significantly cross-correlated. Thus, it was concluded that the improvement in the multiple correlation coefficient caused by the inclusion of the initial sludge blanket level term is not causal and that it would not be correct to incorporate it in the function for difbot. It was therefore decided to select only (Q_i+Q_r) as the single most powerful factor that influences the value of difbot, and to initially use only this factor in the function for difbot. Intuitively also, this is most satisfying, as it has been shown that the diffusivity in the tank is closely linked to (Q_i+Q_r). If, in the process of further testing and calibration, it was found that this function is an oversimplification, then it would still be possible to modify it by including other contributory factors.

The multiple correlation coefficient (r^2) for difbot as a linear function of (Q_i+Q_r) indicates that the regression equation explains 92.1% of the total variation (see Table 8.8) with the best fit linear relationship for difbot being:

$$\text{difbot (in } m^2h^{-1}) = -2.995 + 0.0019 * (Q_i+Q_r)(\text{in } m^3h^{-1}) \qquad (8.13)$$

The t statistic for the estimate of the slope of the regression line of (Q_i+Q_r) against difbot was found to be 5.926, compared to a critical t-statistic of t(3,0.975) = 3.182 at the 95% confidence interval, indicating that the null hypothesis (that there is no relationship between (Q_i+Q_r) and difbot) can be rejected in 7 cases out of 100 without making an incorrect decision. This t statistic gives a probability level of 0.01049, indicating that there is a 99% probability of being correct in accepting that there is a linear relationship between (Q_i+Q_r) and difbot. Figure 8.20 shows the best fit linear regression line of difbot as a function of (Q_i+Q_r) with the 95% confidence limits indicated. The difbot values giving the best simulation results for the five Rijen tests are also shown. The simulation results are evaluated in detail in Sections 8.5 to 8.9 below.

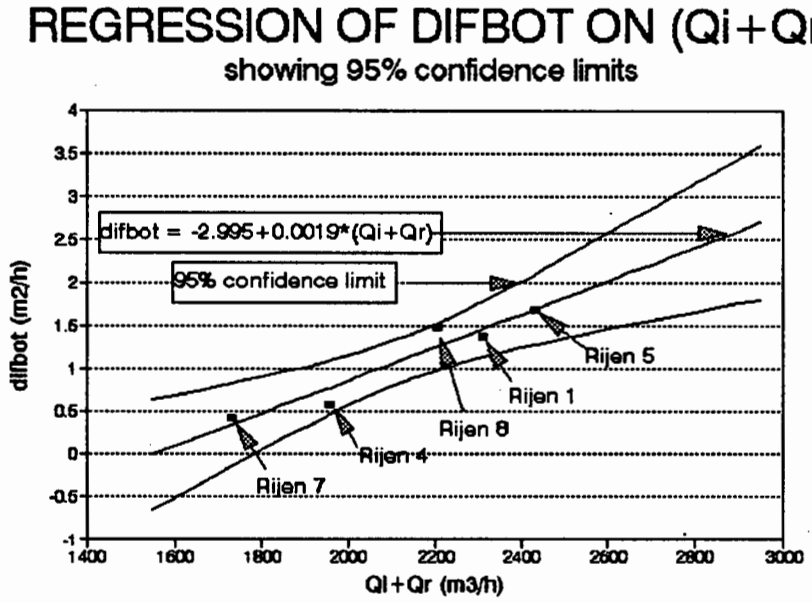

Figure 8.20 Regression of difbot on Q_i+Q_r

It should be noted that Equation (8.13) only applies for α_2 = 1.5layer^{-1} (17.94m^{-1}) and diftop = 120000m^{2}h^{-1} i.e. it is specific to the geometry of the settling tank at Rijen.

Calculating the values of difbot on the basis of the feed flow to the settling tank for all the Rijen tests with Equation (8.13) resulted in the calculated values given in Table 8.9. For comparison, the "real" difbot values giving the best simulation results are also given.

Table 8.9 Calculated and "real" difbot values for the Rijen tests in increasing order of feed flow (Q_i+Q_r) (see Figure 8.20)

TEST	(Q_i + Q_r) (m^3h^{-1})	CALCULATED DIFBOT (m^2h^{-1})	"REAL" DIFBOT (m^2h^{-1})
Rijen 7	1731	0.342	0.423
Rijen 4	1956	0.776	0.579
Rijen 8	2206.5	1.259	1.476
Rijen 1	2311	1.461	1.367
Rijen 5	2431.5	1.693	1.693

In order to confirm that the calculated values of difbot gave reasonable simulations for all the relevant measured parameters governing the settling tank behaviour, the Rijen tests (1, 4, 5, 7 and 8) were simulated with SETTLER (revision 5) using the calculated difbot values and comparing the results with both the measured results and those obtained using the "real" difbot values in terms of the following parameters:

a. sludge blanket level and rise rate
b. underflow concentration
c. effluent solids concentration and mass lost
d. concentration profile for at least one critical time in the simulation (where measured results are available).

For all these tests, the α_1, α_2 and diftop values were the same and were fixed at the previously determined values: α_1 = 10.0layer^{-1} (119.6m^{-1}), α_2 = 1.5layer^{-1} (17.94m^{-1})

and diftop = 120000m^2h^{-1}. The depth of the CSTR for the thickening zone was also the same for all the tests and was set at 1m for the Rijen tank. The difbot value, however, was different for each test depending on the feed flow and was the "real" or calculated value from Equation (8.13) (see Table 8.9).

8.5 SIMULATING THE RIJEN 1 TEST WITH SETTLER (revision 5)

The calculated value of difbot for the Rijen 1 test was found from Equation (8.13) to be difbot = 1.461m^2h^{-1} compared to the "real" difbot value of 1.367m^2h^{-1}. Simulations carried out with both these difbot values are compared with the measured results below. Details of the operating parameters for the Rijen 1 test are given in Section 8.2.

1. Sludge blanket level

Figure 8.21 compares the predicted sludge blanket levels using both the calculated and the real values of difbot with the measured results for the Rijen 1 test.

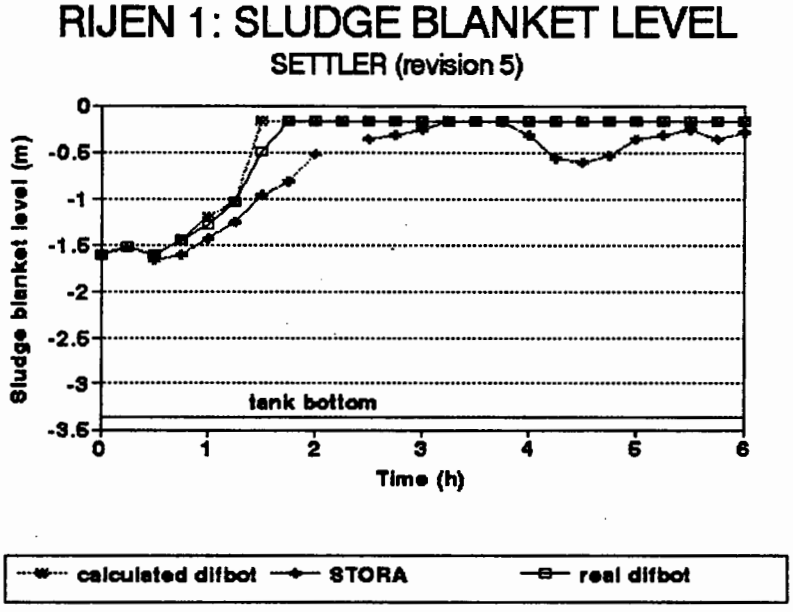

Figure 8.21 Predicted and measured sludge blanket levels for the Rijen 1 test with SETTLER (revision 5)

For both sets of predicted results, the inclusion of diffusivity at all layers in the tank makes the response of the sludge blanket much more sensitive to overloaded conditions, with the consequence that both sets of predicted results show a rapid rise of the sludge blanket from 1.6m below the surface at the start of the test to 1.04m below the surface 1.25h after the start of the test. Between 1.25h and 1.5h, the sludge blanket

level rises rapidly to 0.16m (which is effectively the top of the tank at layer 2) by 1.5h for the calculated difbot value and by 1.75h for the real difbot value. Thereafter, the sludge blanket level remains at 0.16m until the end of the test. The only difference between the two sets of predicted results is that the calculated value of difbot, being higher, causes a more rapid rise rate of the sludge blanket level in the tank and thus the sludge blanket reaches the top of the tank 15min earlier.

The measured sludge blanket level also rises rapidly from approximately 1.6m below the surface at the start of the test to 0.16m (the top of the tank) 3.25h into the test. At 3.75h, the measured sludge blanket level begins to fall in response to the shut off of the influent flow (see Table 8.1), and drops to 0.61m below the top of the tank at 4.5h. It then rises again in response to the restarting of the influent flow at 4.25h and reaches 0.16m (effectively the top of the tank) at 5h, where it remains constant until the end of the test. It should be noted that influent flow means influent sewage to the activated sludge plant - not the feed flow to the settling tank i.e. when the influent flow was shut off, the underflow Q_r was constant at the set rate throughout the test.

Both predicted rise rates of the sludge blanket closely match the measured data for the first part of the test, although after 1h they both rise more rapidly than the measured sludge blanket level. This more rapid predicted rise rate does not signify a discontinuity in settling tank behaviour, as the concentration in all layers is gradually increasing as the settling tank accumulates sludge. It is a consequence of both the definition of the sludge blanket level i.e. the level in the tank at which the concentration is greater than or equal to $3kgm^{-3}$ and the increase in diffusivity in the upper layers of the tank as the sludge blanket approaches the feed point layer. The fluctuation in the measured sludge blanket height from 4h onwards in response to the influent flow being switched off and on is not reflected in the predicted results. This is because, even though the concentration in all the layers in the tank is decreasing with zero influent flow, the concentration in the second layer never falls below $3kgm^{-3}$, i.e. the sludge blanket level is continuously defined as being at 0.16m.

2. Underflow concentration

Figure 8.22 compares the measured and predicted underflow concentrations with difbot (calculated) and difbot (real) over the 6h test.

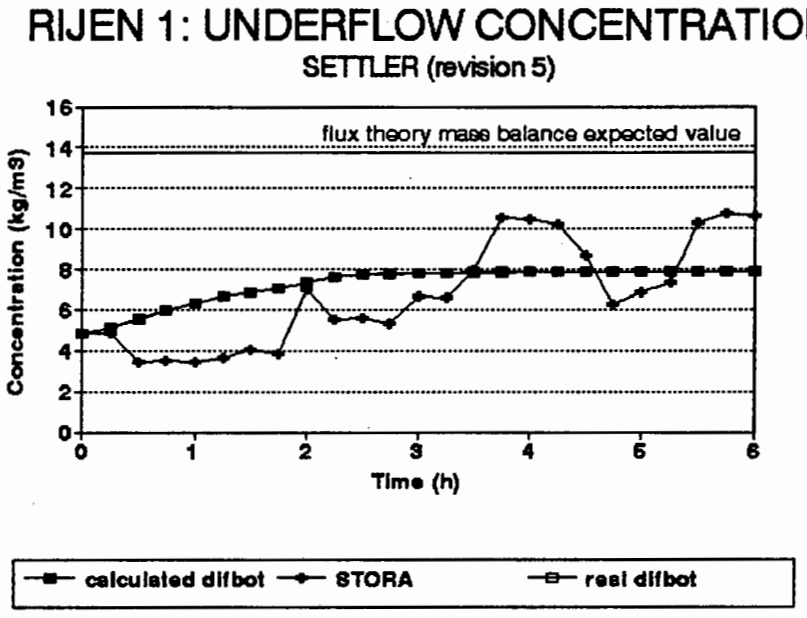

Figure 8.22 Predicted and measured underflow concentrations for Rijen 1 with SETTLER (revision 5)

The damping effect caused by the inclusion of a CSTR in the model, although limiting the rate at which the underflow concentration rises, does not affect the maximum value which the underflow concentration attains. This was tested by running the Rijen 1 simulation for a period of 80 hours without diffusivity, but with the CSTR. It was found that, under these conditions, the flux theory predicted underflow concentration of 13.3kgm^{-3} was attained after 67h. When diffusivity was included in the 80h simulation, however, the flux theory predicted underflow concentration was not attained during the 80h. This confirms the fact that the presence of diffusivity in the bottom layers of the tank effectively prevents the (possibly unrealistic) degree of thickening from taking place and means that the flux theory - mass balance predicted mass abstracted from the bottom of the tank via the underflow is not achieved. Because SETTLER preserves the mass balance, the difference between the flux theory - mass balance predicted mass abstracted via the underflow (at a maximum concentration of

13.3kgm^{-3}) and the SETTLER predicted mass abstracted via the underflow lost with the underflow (at a maximum concentration of $\pm$7.8kgm^{-3}) is sludge that does not flow downwards in the settling tank and therefore is lost with the effluent. This is a third mode of settling tank failure not considered by the flux theory itself, and is the reason that the tank continues to manifest overloaded conditions even though the flux theory indicates that the settling tank is overloaded only for the first 2.5h of the test (see Section 8.2). This limitation of the underflow concentration by the diffusivity is a very important aspect in simulating full scale settling tank behaviour, and is discussed in detail in Section 8.19 below. It was realised from the ATV and STORA design experience that some feature would be necessary to model this behaviour, as its presence in SETTLER on the basis of the flux theory alone was not expected. Finding that it was already accounted for with the presence of diffusivity was a fortuitous result.

The predicted results with the calculated value of difbot and the real value of difbot are almost indistinguishable. Both predicted results show a gradual rise in the underflow concentration from a starting value of 4.84kgm^{-3} to a value of 7.79kgm^{-3} (calculated difbot) and 7.81kgm^{-3} (real difbot) at approximately 3h. Thereafter, the underflow concentration rises very slowly to its maximum of 7.86kgm^{-3} (calculated difbot) and 7.89kgm^{-3} (real difbot) which is attained at 6h. The slight difference between the underflow concentrations with difbot (real) and difbot (calculated) is to be expected given that difbot (calculated) is slightly higher than difbot (real) and thus would have a more pronounced effect in mixing the bottom layers of the tank and in preventing thickening from taking place.

The measured underflow concentration shows an erratic rise from a starting concentration of 4.84kgm^{-3} to a maximum value of 10.56kgm^{-3} at 3.75h. After this, it decreases rapidly to 6.25kgm^{-3} at 4.75h and then immediately rises again to a value of 10.59kgm^{-3} at 6h. The erratic values of the underflow concentration up to approximately 4h into the test are probably a function of construction details of the tank, such as the scraper, sludge hopper and other bottom effects which are not

modelled by the CSTR. The decrease at about 5h probably also arises from these effects but is exacerbated by the switching on and off of the influent flow. It was considered to be sufficient if the program reflected the general trend of the measured results i.e. a gradual rise in concentration, rather than the individual fluctuations, and it was deemed that this has been adequately achieved.

3. Effluent concentration

Figure 8.23 compares the measured and predicted (using the real value of difbot) effluent concentrations for Rijen 1. The effect of using the calculated value of difbot is discussed later.

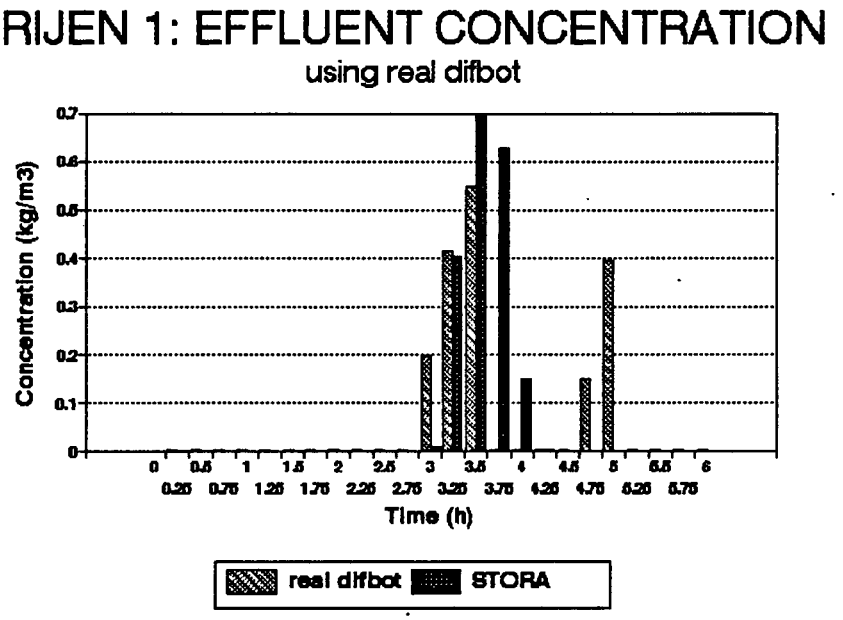

Figure 8.23 **Predicted (with real difbot) and measured effluent concentrations for Rijen 1 with SETTLER (revision 5)**

The predicted effluent concentration with the real value of difbot is negligible until 3h into the test, when a series of concentration peaks is predicted (198mgl^{-1} at 3h, 413mgl^{-1} at 3.25h and 594mgl^{-1} at 3.5h). The time that these peaks occur (although not their magnitude) closely matches that measured by STORA, which shows three concentration peaks of 405mgl^{-1} at 3.25h, 698mgl^{-1} at 3.5h and 628mgl^{-1} at 3.75h. The predicted results (using real difbot) show a second series of peaks at 4.75h (150mgl^{-1})

and 5h ($394gl^{-1}$), which are not reflected in the measured results. The total predicted mass lost over the 6 hour period is 779kg (2.20% of the total influent solids mass), whilst the measured mass lost is 773kg (2.18% of the total influent solids mass), an error of approximately 0.7%. With the real value of difbot, the measured and predicted results match very closely in terms of both the total solids mass lost in the effluent and the manner in which the mass is lost. This is to be expected, as the real value of difbot was selected on the basis of its ability to predict the correct solids mass lost in the effluent. The manner of the mass loss i.e. effluent concentration - time profile is not governed by the choice of difbot but by diftop and α_2.

Figure 8.24 compares the measured and predicted effluent solids concentrations using the calculated value of difbot during the 6h test at Rijen 1.

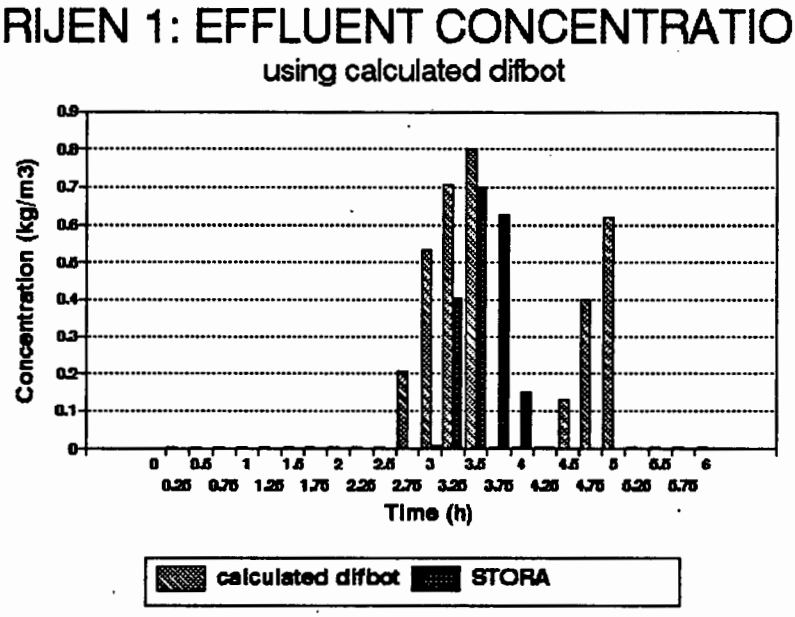

Figure 8.24 **Predicted (with calculated difbot) and measured effluent concentrations for Rijen 1 with SETTLER (revision 5)**

With the calculated value of difbot, the predicted effluent concentration over the 6 hour simulation shows negligible concentration values in the effluent until 2.75h, after which a series of concentration peaks is predicted ($207mgl^{-1}$ at 2.75h, $535mgl^{-1}$ at 3h, $708mgl^{-1}$ at 3.25h and $800mgl^{-1}$ at 3.5h). The predicted results also show a second

series of peaks at 4.5h (131mgl^{-1}), 4.75h (400mgl^{-1}) and 5h (620gl^{-1}), which are not reflected in the measured results. The total predicted mass lost over the 6 hour period is 1521kg (4.39% of the total influent solids mass) compared to 773kg (2.18% of the total influent solids mass) for the measured results.

For the calculated value of difbot, the time of the onset of solids loss is about 0.5h earlier than that measured and the magnitudes of the predicted peaks in the effluent concentration are considerably larger than the magnitude of the measured effluent concentration peaks. It therefore follows that the predicted effluent solids mass lost does not correspond with the measured effluent solids mass lost. This confirms the earlier finding that the effluent solids mass lost is very sensitive to small changes in the value of difbot. In this case a $\pm$7% increase in difbot almost doubles the predicted effluent solids mass lost. However, this increase in predicted effluent solids mass lost should be seen in the context of the fact that the total effluent solids mass lost is still only 4.39% of the total influent solids mass, indicating that the settling tank has processed the remaining 95.61% of the influent solids mass (34336kg). The time at which the first peak occurs matches the measured results fairly closely, giving a good indication of when failure in the tank will occur, although the existence of a second series of peaks in the predicted results is a cause for concern, as no comparable mass loss occurs in the measured results. The second series of peaks was also predicted with the real difbot value.

8.5.1 PROPAGATION OF THE SLUDGE BLANKET ABOVE THE FEED POINT

In comparing Figure 8.21 and Figure 8.23, it can be noted that the time at which the predicted sludge blanket level first reaches the top of the tank is not concurrent with the time at which failure is predicted. The onset of failure is defined as the time at which the first gross solids loss in the effluent occurs. For the real value of difbot, failure occurs 3h into the test although the sludge blanket reached the top of the tank at 1.75h. Between 1.75h and 3h, a total of 3509kg is accumulated in the settling tank (the

mass in the tank increases from 29140kg to 32649kg) before its storage capacity is exceeded. The concentration of sludge in the second layer (and all the other layers above the feed point) first exceeds 3kgm^{-3} (the sludge blanket level definition) at 1.75h. Therefore, at this time, the sludge blanket level is defined as being at the top of the tank. However, the concentration in all these layers is still permitted by the flux theory to increase to 4.80kgm^{-3} before solids loss in the effluent is predicted. The concentration to which these layers is permitted to increase is X_{af}, the maximum limiting solids concentration for the layers above the feed point for these operating conditions. Figure 8.25 illustrates the changing sludge concentration depth profile every 0.5h for 1.75h after the start of the test (sludge blanket reaches the top of the tank) to 3.5h after the start of the test (gross solids loss is predicted in the effluent). The figure clearly shows that the first instance of gross solids loss occurs only after the sludge blanket in the layers above the feed point has exceeded X_{af} (4.80kgm^{-3}).

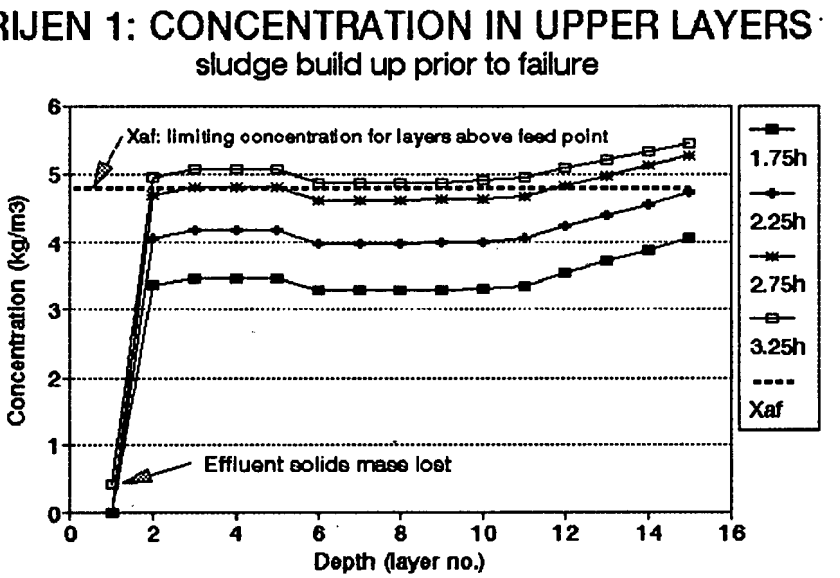

Figure 8.25 **Sludge blanket concentration increase in the layers above the feed point for 1.75h to 3.5h into the Rijen 1 test**

8.5.2 CONCLUSIONS FOR THE RIJEN 1 TEST SIMULATION

Predicted and measured sludge concentration - depth profiles could not be compared because in the Rijen 1 test these were not measured. For the remaining parameters, the real value of difbot was found to predict more accurate results than the calculated value, especially the effluent solids mass lost. The calculated value of difbot, although predicting fairly accurate results for the other two parameters (sludge blanket rise rate and underflow concentration), gave relatively poor results for the effluent solids mass lost. This can be ascribed to the fact that the effluent solids mass lost is very sensitive to the value of difbot and the calculated value of difbot is 6% higher than the real value (see Table 8.9). However, when seen in the context of the total mass of solids processed by the settling tank, the increase in effluent solids mass lost is not really significant. Examination of the graph showing the real vs calculated difbot values indicates that for the Rijen 1 and Rijen 4 tests, the real difbot values lie below the regression line. This means that for these two cases, the calculated value of difbot will be higher than the real value, thereby making the settling tank more sensitive to an overloaded situation with the calculated difbot than with the real difbot which gives the best simulation results. Because the effluent solids mass lost is very sensitive to the value of difbot, it can be seen that this parameter will be over predicted for the Rijen 1 test, and even more so for the Rijen 4 test because the real value of difbot for the Rijen 4 test lies furthest below the regression line. On the other hand, for Rijen 7 and Rijen 8, the calculated values of difbot lie above the regression line, indicating that the calculated value of difbot will be less than the real value and consequently simulations carried out with the calculated value of difbot will make the settling tank less sensitive to the overloaded situation. This means that the predicted effluent solids mass lost using the calculated difbot is expected to be lower than the measured values for these two tests. For Rijen 5, the real and calculated values of difbot are the same, and thus the predicted effluent solids mass lost for both the real and calculated values of difbot is expected to match the measured results.

8.6 SIMULATING THE RIJEN 4 TEST WITH SETTLER (revision 5)

As mentioned above, the calculated and real values of difbot for the Rijen 4 test are $0.776m^{-2}h^{-1}$ and $0.579m^{-2}h^{-1}$ respectively and simulations based on both of these are compared with the measured data below. Details of the operating parameters for the Rijen 4 test are give in Section 8.3.

1. Sludge blanket level

Figure 8.26 compares the measured and predicted sludge blanket levels with both the calculated and real values of difbot for the 7h Rijen 4 test during which the influent was shut off at 5.5h and not turned on again.

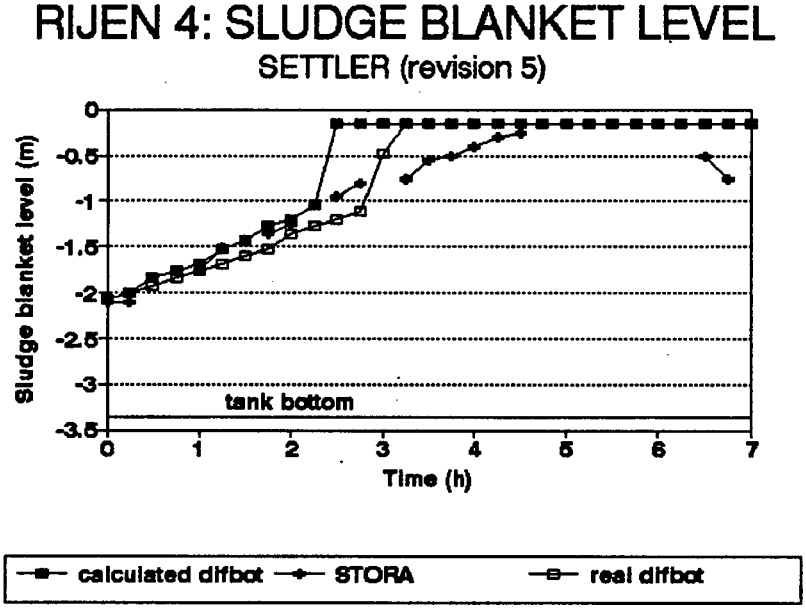

Figure 8.26 Predicted and measured sludge blanket levels for Rijen 4 with SETTLER (revision 5)

The predicted results using the calculated value of difbot show a rapid rise in sludge blanket level from 2.08m below the surface at the start of the test to 0.16m (effectively the top of the tank) at 2.5h after the start of the test. The predicted results with the real value of difbot show a similar, although less rapid, sludge blanket rise rate from 2.08m at the start of the test to 0.16m at 3.25h into the test. Thereafter, the sludge

blanket level remains constant for both sets of predicted results until the end of the test.

The measured results show a similar sludge blanket rise rate from 2.11m below the surface at the start of the test to 0.16m (top of the tank) 5h into the test. Thereafter, the sludge blanket level remains constant until 6.5h after the start of the test, when the sludge blanket level falls to 0.76m below the surface due to the shutting off of the influent flow.

The predicted and measured sludge blanket rise rates show a close correspondence for the first 2.25h of the test, although the predicted sludge blanket rise rate using the real value of difbot is slightly faster than the measured rise rate. The predicted sludge blanket rise rate using the calculated value of difbot is even more rapid after this point. Both sets of predicted sludge blanket levels reach the top of the tank sooner than the measured sludge blanket level with the difference in times between the predicted and measured sludge blanket levels reaching the top of the tank, being 2h and 1.75h respectively for the calculated and real difbot values.

As far as rise rate of the sludge blanket is concerned, both sets of predicted results correspond well with the measured results for the first part of the test, although after that there is poor correspondence between the measured results and both sets of predicted results for the same reasons as identified in the Rijen 1 test. The time at which the sludge blanket reaches the top of the tank is poorly identified by both sets of predicted results. It appears that for this test, as for the Rijen 1 test, the sludge blanket level is too sensitive to the overloaded situation, underestimating the storage capacity of the settling tank and thus prematurely allowing the sludge blanket to reach the top of the tank. The over sensitivity is worse for the calculated value of difbot, as expected, because the calculated value of difbot is 25% higher than the real value.

2. Underflow concentration

Figure 8.27 compares the measured and predicted underflow concentrations using both the calculated and real values of difbot for the Rijen 4 test.

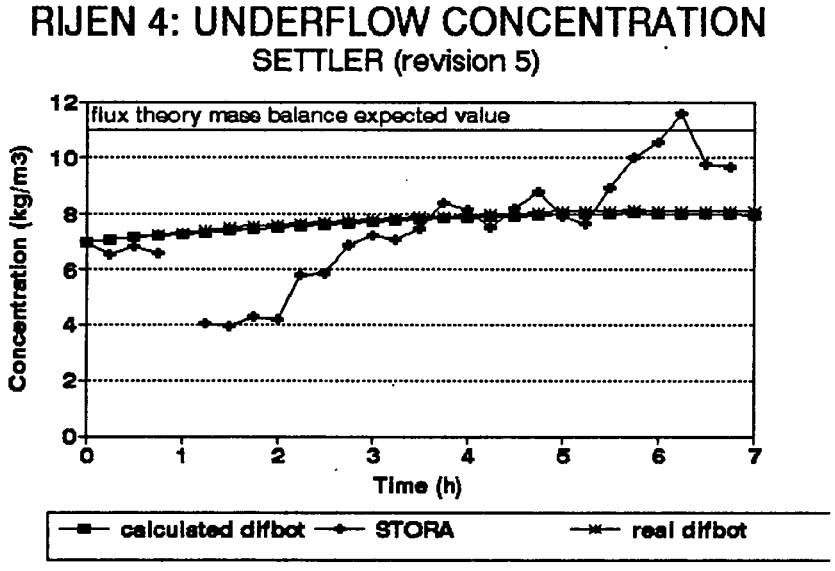

Figure 8.27 Predicted and measured underflow concentrations for Rijen 4 with SETTLER (revision 5)

The predicted underflow concentration using the real value of difbot and that using the calculated value of difbot are almost indistinguishable. The predicted underflow concentration rises slowly and constantly from 7.01kgm^{-3} at the start of the test to 8.11kgm^{-3} (real difbot) and to 8.03kgm^{-3} (calculated difbot) at the end of the test.

The measured results are rather erratic throughout the test. From an initial underflow concentration of 7.01kgm^{-3}, the underflow concentration remains approximately constant for 1h, when it drops suddenly from 6.6kgm^{-3} to 3.92kgm^{-3} at 1.5h. At approximately 2h, the underflow concentration begins to rise fairly quickly but erratically, reaching 8.4kgm^{-3} at 3.75h. This concentration is maintained (with some fluctuations) until 5.25h, when it increases sharply to attain its maximum value of 11.57kgm^{-3} at 6.25h into the test. At the end of the test, the underflow concentration drops slightly to its final value of 9.67kgm^{-3}.

Both sets of predicted results show a change in underflow concentration that is very smooth, with none of the erratic behaviour that characterises the measured results. As for Rijen 1, this erratic behaviour in the measured results is ascribed to settling tank construction details. The only period in which the predicted results correspond closely with the measured results is in the period from 3.5h to 5.25h, which is the only time when the measured results show some degree of constancy. The difference between the final underflow concentration predicted with the real value of difbot ($8.11 kgm^{-3}$) and that predicted with the calculated value ($8.03 kgm^{-3}$) can be attributed to the increased degree of mixing in the bottom layers of the settling tank brought about by the higher calculated value of difbot.

The fact that the program reflected reasonably accurately the general trend of the measured results (i.e. a rise in underflow concentration with a period of constant concentration at approximately $8 kgm^{-3}$) was regarded as sufficient for the purposes of the simulation.

3. Effluent concentration

Figure 8.28 compares the measured and predicted (using the real value of difbot) effluent concentrations for the Rijen 4 test. The effect of using the calculated value of difbot is discussed later.

The measured effluent solids concentration shows a negligible concentration of solids in the effluent until 5h, when three peaks of $110 mgl^{-1}$, $558 mgl^{-1}$ and $700 mgl^{-1}$ occur. Thereafter, the effluent concentration is very low until the end of the test. The total measured effluent solids mass lost is 740kg.

The predicted effluent concentration using the real value of difbot also shows negligible values during most of the test until 4.75h, when a concentration of $219 mgl^{-1}$ is predicted in the effluent. Thereafter, three further peaks in the effluent concentration occur ($432 mgl^{-1}$, $617 mgl^{-1}$ and $786 mgl^{-1}$) until 5.5h, when the concentration again

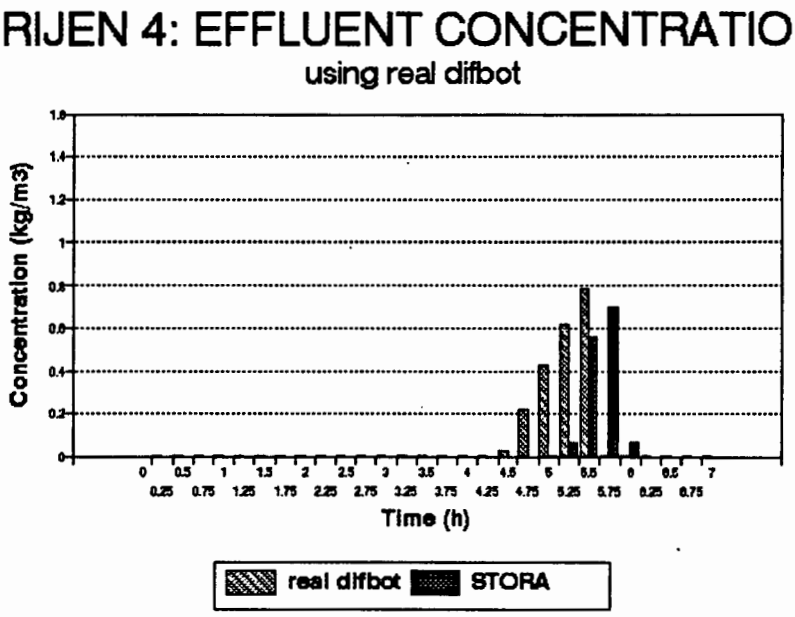

Figure 8.28 **Predicted (with real difbot) and measured effluent concentrations for Rijen 4 with SETTLER (revision 5)**

declines to negligible values. The predicted effluent solids mass lost with the real value of difbot is 752kg.

The predicted peaks in the effluent solids concentration occur sooner than the measured peaks, although the manner in which the mass is lost is the same for both the measured and predicted results. The total effluent solids mass lost for the predicted results using the real value of difbot is 1.77% of the total solids processed and 1.75% for the measured values. This close correlation between measured and predicted effluent solids mass lost is to be expected, as the real value of difbot was chosen such that the predicted effluent solids mass lost would be the same as the measured value.

Figure 8.29 compares the measured and predicted (using the calculated value of difbot) effluent concentrations for the Rijen 4 test.

The predicted effluent solids concentration with the calculated value of difbot shows negligible values until 3.5h, when the concentration increases progressively from 154mgl^{-1} at 3.5h to 1583mgl^{-1} at 5.5h. Thereafter, the effluent solids concentration is

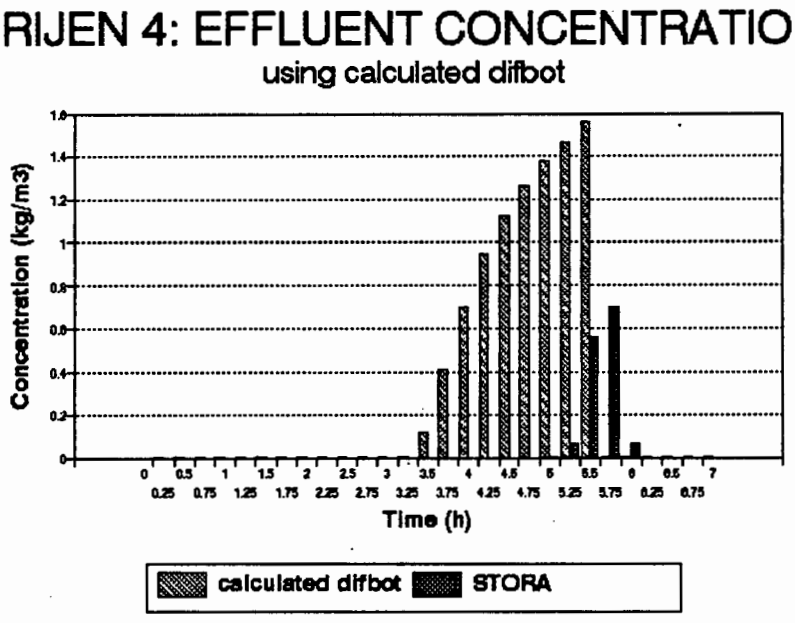

Figure 8.29 **Predicted (with calculated difbot) and measured effluent concentrations for Rijen 4 with SETTLER (revision 5)**

negligible. The total predicted effluent solids mass lost is 3192kg, which is 7.5% of the total solids mass processed by the settling tank.

The correspondence between the measured and predicted results using the calculated value of difbot is poor. Not only is the predicted total effluent solids mass lost more than four times that of the measured results, but the time at which the first concentration peak occurs is 2h earlier than the first measured peak. Since it has been found that the effluent solids mass lost is highly sensitive to the value of difbot, this poor correspondence between predicted (using the calculated value of difbot) and measured results is expected, the excessive predicted effluent solids mass lost being attributed to the fact that the calculated value of difbot is significantly higher (35%) than the real value.

4. Concentration profile

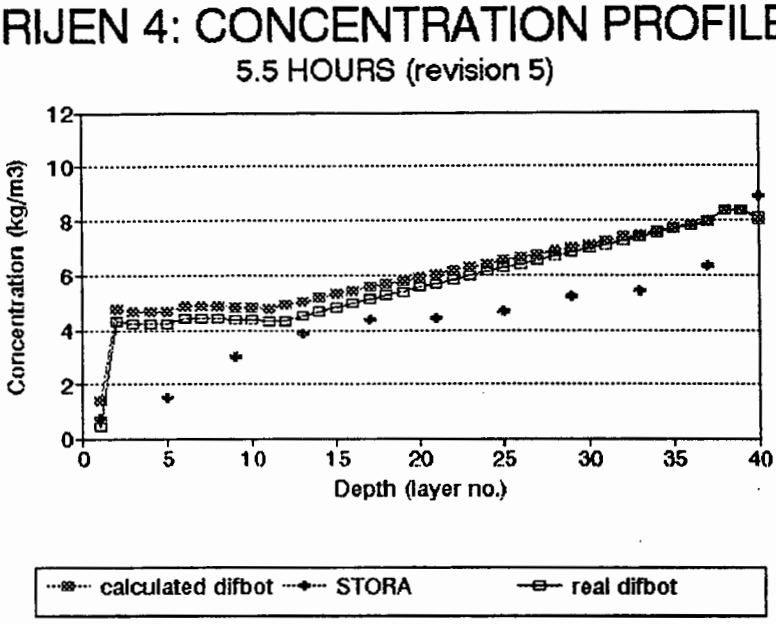

Figure 8.30 Predicted and measured concentration profiles at 5.5h for Rijen 4 with SETTLER (revision 5)

Figure 8.30 compares the measured and predicted sludge concentration depth profiles (with both the real and calculated values of difbot) for the Rijen 4 test at 5.5h. This is a critical point in the test because the influent flow to the tank is shut off at 5.5h, causing the tank to be underloaded from this time until the end of the test.
The predicted concentration profiles at 5.5h have an underflow concentration of $8.09kgm^{-3}$ (real difbot) and $8.04kgm^{-3}$ (calculated difbot) and a sludge blanket that extends through the entire tank (layers 39 to 2) at a concentration of between $4.32kgm^{-3}$ and $8.36kgm^{-3}$ (real difbot) and between $4.78kgm^{-3}$ and $8.36kgm^{-3}$ (calculated difbot). The effluent solids concentration for the real value of difbot is $0.432kgm^{-3}$, and that for the calculated value of difbot is $1.399kgm^{-3}$. The predicted total mass of sludge in the tank is 31222kg (real difbot) and 32933 (calculated difbot).

The measured concentration profile has an underflow concentration of $8.89kgm^{-3}$, and a sludge blanket extending from layer 39 to layer 13 at a concentration of approximately $5kgm^{-3}$. Above layer 13, the concentration decreases from $3.88kgm^{-3}$

(layer 13) to 1.49kgm^{-3} (layer 5). The measured effluent solids concentration is 0.77kgm^{-3} and the measured total mass of sludge in the tank is 219311kg.

The total predicted sludge mass in the settling tank is 42% higher and 50% higher than the measured mass for the real and calculated difbot values respectively. This is due to the generally higher concentration of the predicted sludge blanket, as well as a higher predicted concentration in the layers above the sludge blanket. Although the predicted concentration profiles contain substantially more mass than the measured profile, the general trends of the profiles (such as the existence of a well developed sludge blanket) and salient features (such as the underflow concentration) correspond quite satisfactorily.

Figure 8.31 compares the measured and predicted results (using both the real and calculated values of difbot) for the Rijen 4 test at 7h, which is at the end of the test, 1.5h after the influent flow has been shut off.

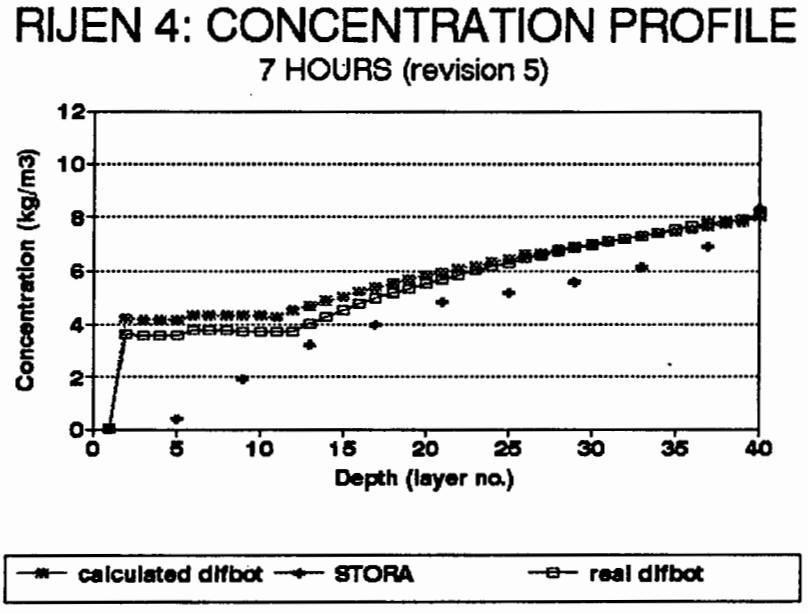

Figure 8.31 Predicted and measured concentration profiles at 7 hours for Rijen 4 with SETTLER (revision 5)

The predicted concentration profile has an underflow concentration of 8.11kgm^{-3} (real difbot) and 8.03kgm^{-3} (calculated difbot) and a sludge blanket that extends through

most of the tank, from 39 to layer 11. The average concentration of the sludge blanket is approximately 6kgm^{-3} for both the real and the calculated values of difbot. From layer 11 to layer 2, there is a region of constant concentration which is approximately 3.7kgm^{-3} for the real value of difbot and 4.3kgm^{-3} for the calculated value of difbot. The effluent concentration is 0.0027kgm^{-3} (2.7mgl^{-1}) for the real value of difbot and 0.0032kgm^{-3} (3.2mgl^{-1}) for the calculated value of difbot. The total sludge mass in the tank is 29764kg (real difbot) and 31272kg (calculated difbot).

The measured concentration profile at 7h has an underflow of 8.33kgm^{-3}, and a well developed sludge blanket that extends from layer 39 to layer 13 at an average concentration of approximately 5kgm^{-3}. Above layer 13, the measured concentration decreases from 3.22kgm^{-3} to 0.39kgm^{-3} in layer 5. The measured effluent concentration is 0.04kgm^{-3}. The total measured mass in the settling tank at 7h is 20989kg. The predicted sludge mass in the settling tank is higher than the measured value by 41% (real difbot) and 49% (calculated difbot).

Both the predicted and measured results indicate that the sludge blanket level has declined since 5.5h, and that the total mass in the settling tank has decreased. This is to be expected, as the influent flow was shut off at 5.5h, causing the settling tank to be underloaded from then until the end of the test. There is good correspondence between the measured and predicted underflow concentrations, although the average predicted sludge blanket concentration is slightly higher than the measured value. The predicted results do not reflect the region of low concentration above the feed point that is found in the measured results.

8.6.1 CONCLUSIONS FOR THE RIJEN 4 TEST SIMULATION

In general, the results for this test are good, with the major trends and salient factors of the measured results being well reflected in the predicted results. However, there are some discrepancies between them. Most of the discrepancies in predicted and measured results are related to the oversensitivity of the program to the overloaded

situation for the test resulting from the too high calculated and, to a much lesser extent, real difbot values. The rapid rise rate of the sludge blanket after 2.25h, the premature effluent solids mass lost and the over- estimation of the sludge mass in the settling tank at both 5.5h and 7h are all reflections of this same phenomenon. For this test, the settling tank is over sensitive to the overloaded situation (due to the high calculated difbot value compared with the real one (see Table 8.9) and hence the storage capacity of the settling tank and its ability to process the influent solids mass is underestimated. This results in the sludge blanket level building up in the tank too soon and at too low a concentration, causing failure to be prematurely predicted.

The calculated value of difbot for this test gives poorer predictions than the real difbot value because higher difbot values render the settling tank more sensitive to the overloaded situation. Consequently, the simulation with the calculated value of difbot is expected to show a somewhat poorer correspondence with the measured results than the simulation with using the real value of difbot.

8.7 SIMULATING THE RIJEN 5 TEST WITH SETTLER (revision 5)

The fifth settling tank test carried out at Rijen (hereafter referred to as Rijen 5) was run for a total of 7 hours, with the influent flow being shut off for 0.75h from 4h to 4.75h after the start of the test. At 4.75h, the influent flow to the settling tank was restarted for 1.417h until 6.17h into the test. At 6.17h the influent flow was shut off again until the end of the test. The flux theory constants, V_o and n, were calculated from the measured $SSVI_{3.5}$ using the relationship for extended aeration plants derived in Chapter 4. From the measured $SSVI_{3.5}$ of $110 ml g^{-1}$, the equations give $V_o = 5.762 m h^{-1}$ and $n = 0.407 m^3 kg^{-1}$. With these values of V_o and n, the steady state (idealised hyperbolic equations) flux theory indicated that the settling tank was overloaded from 1.5h until 2h into the test. At all other times the settling tank was, according to the flux theory, underloaded. The data measured by STORA for the Rijen 5 test is given in Table 8.10 and a summary of the operating parameters for Rijen 5 is presented in Table 8.11.

Table 8.10 Data measured by STORA for the Rijen 5 test

Test Rijen 5 Begin test: 9:00h
Date: 21 November 1978 End test: 13:00h

Q_i = 1425m^3h^{-1} Q_r = 1006.5m^3h^{-1}

Time (h)	Feed conc (kg/m3)	Underflow conc (kg/m3)	Effluent conc (mg/l)	Sludge blanket height (m)	Remarks
09:00					influent started
09:20		5.59		2.40	
09:30				2.20	
09:40	3.69	3.79			
10:00			7.00		
10:07		4.06			
10:10				1.80	
10:30				1.65	
10:35	4.72	4.14			
11:00	3.87	4.86	< 0.1		
11:30		4.95		1.20	
12:10	3.62	4.76	< 0.1		
12:20				0.90	
12:30			2.00		
12:35	3.65	5.58	34.00		flocs coming
12:40				0.85	over the weir
12:45			34.00		
12:50				0.65	
12:55			393.00		
13:00	3.32	6.39			influent stopped
13:05			858.00		
13:15			494.00		
13:20		7.14			
13:30			39.00		
13:40	3.20	9.26		0.90	
13:45					influent restarted
14:00		7.62	10.00		
14:20	4.03	5.48			
14:30			0.80	0.90	
14:40		5.90			
14:50				0.70	
14:55			22.00		flocs coming
15:00	3.07	6.31	334.00		over the weir
15:05			537.00		
15:10					influent stopped
15:15			349.00		
15:20		7.36			
15:25				0.70	
15:40	3.24	9.04		0.75	
15:45			178.00		
16:00	3.38	8.95		1.00	

The initial conditions for Rijen 5 are illustrated in Figure 8.32. They were generated in the same way as for the two previous Rijen tests.

The calculated and real values of difbot were found to be the same for the Rijen 5 test i.e. difbot = 1.693m^2h^{-1}. Because they are the same, the results will also be the same and so only the results for the real value of difbot will be presented and compared to the measured results.

Table 8.11 Summary of operating parameters for the Rijen 5 test

PARAMETER	VALUE
Q_i	$1425m^3h^{-1}$
Q_r	$1006.5m^3h^{-1}$
X_o (max)	$4.72kgm^{-3}$
X_o (min)	$3.07kgm^{-3}$
Area	$1625m^2$
Depth (from overflow weir to bottom of tank)	3.35m
Feed point layer	5
Duration of test	7 hours
$SSVI_{3.5}$	$110mlg^{-1}$
DSVI	$130mlg^{-1}$
V_o	$5.762mh^{-1}$
n	$0.407m^3kg^{-1}$

1. Sludge blanket level

Figure 8.33 compares the measured and predicted sludge blanket levels for the 7h Rijen 5 test.

The predicted results show an almost constant sludge blanket level for the first hour of the test whilst the sludge in the tank is being redistributed to overcome the sharp discontinuity at layer 18 (1.5m depth) in the initial concentration profile (see Figure 8.32). The sudden rise in sludge blanket level at 1.25h is an artefact of the definition of the sludge blanket level, and does not indicate a discontinuity in the settling tank behaviour. This has been discussed earlier for the Rijen 1 test (see Figure 8.25) and is confirmed by observing the slow but gradual increase in sludge mass in

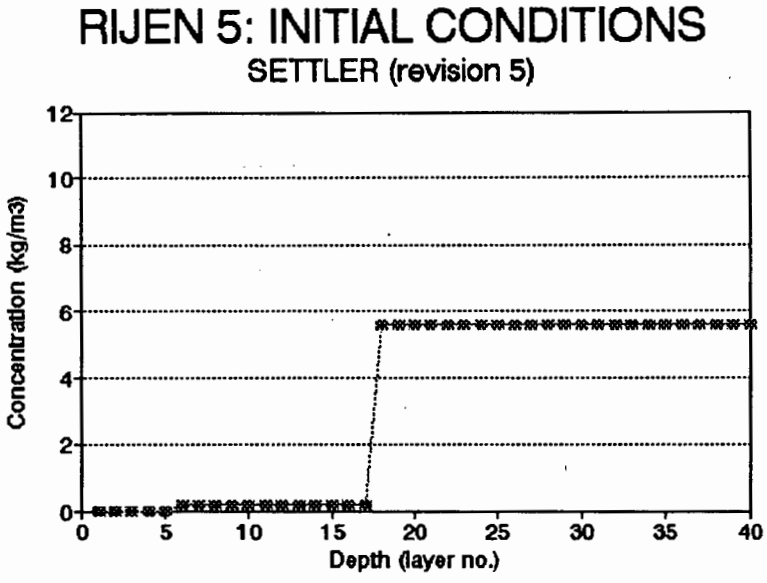

Figure 8.32 Initial concentration profile for Rijen 5

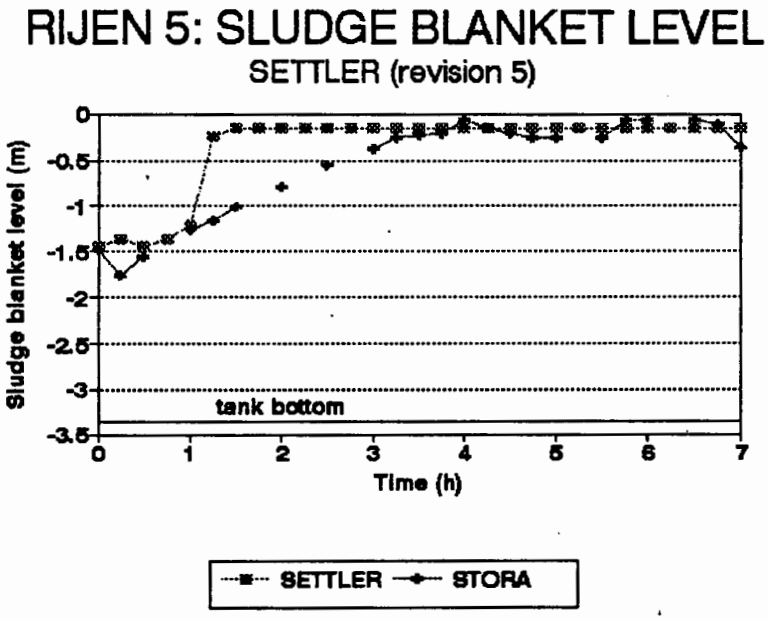

Figure 8.33 Predicted and measured sludge blanket levels for Rijen 5 with SETTLER (revision 5)

the tank during the first 1.5h of the test, as illustrated in Figure 8.34, where the rate of mass accumulation in the tank is gradual throughout the 1.6h but accelerates as the test progresses.

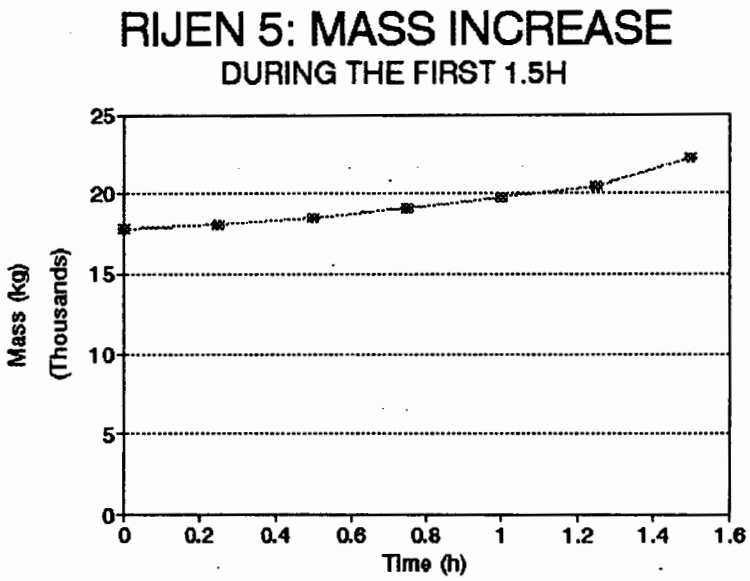

Figure 8.34 **Predicted sludge mass increase in the tank during the first 1.5h of the Rijen 5 test**

At 1.5h, the predicted sludge blanket level reaches 0.16m (the top of the tank) and the sludge blanket level remains at this level throughout the remainder of the test.

The measured results initially show a slight drop in sludge blanket level, but thereafter the sludge blanket level rises progressively from 1.76m at 0.25h into the test to 0.16m (effectively the top of the tank) at 3.75h. Thereafter, the sludge blanket level remains constant (aside from slight fluctuations) at the top of the tank. During the last 0.25h of the test, the measured sludge blanket level drops from 0.11m to 0.36m below the surface of the tank as a result of the shutting off of the influent flow for the second time at 6.17h.

The measured and predicted results correspond well only for the first hour of the test, after which the predicted sludge blanket level rises more quickly than that measured. The predicted sludge blanket level reaches the top of the tank prematurely at 1.5h as opposed to at 3.75h for the measured results.

2. Underflow concentration

Figure 8.35 compares the measured and predicted underflow concentrations for the Rijen 5 test.

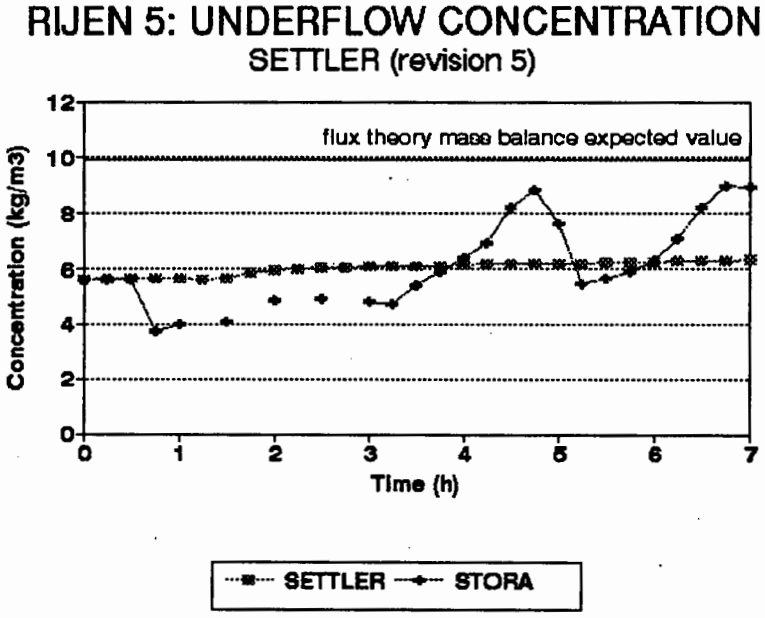

Figure 8.35 Predicted and measured underflow concentrations for Rijen 5 with SETTLER (revision 5)

The predicted underflow concentration rises very slightly during the test, beginning at 5.59kgm^{-3} at the start of the test and attaining its maximum of 6.33kgm^{-3} at the end of the test.

The measured underflow concentration is erratic throughout the test, dropping from 5.59kgm^{-3} at the start of the test to 3.79kgm^{-3} at 0.75h into the test. Thereafter, the underflow concentration rises gradually but erratically to reach a maximum concentration of 8.85kgm^{-3} at 4.75h. From 4.75h, the underflow concentration suddenly drops to 5.69kgm^{-3} at 5.5h and then rises suddenly to reach 9.02kgm^{-3} at 6.75h. As for the other Rijen tests, this erratic behaviour is not an indication of erratic flux effects in the tank, but can be attributed both to the switching on and off of the influent flow and to sludge collection effects such as the action of the sludge scraper in the bottom of the tank.

The fact that the predicted underflow concentration increases marginally during this test can be ascribed to the fact that the difbot value for Rijen 5 is relatively high ($1.693 m^2h^{-1}$), which is near the top of the acceptable range for difbot. This causes a significant degree of mixing in the bottom layers of the tank, and has the effect of severely damping the underflow concentration rise. However, as before, the predicted underflow concentration is considered to be sufficiently accurate if it reflects the general trend of the measured underflow concentration and this was considered to have been adequately achieved for this test. However, it does seem that the Rijen tank underflow concentration is very sensitive to changes in the influent flow, a sensitivity not well reflected by SETTLER.

3. Effluent concentration

Figure 8.36 compares the measured and predicted effluent concentrations for the Rijen 5 test.

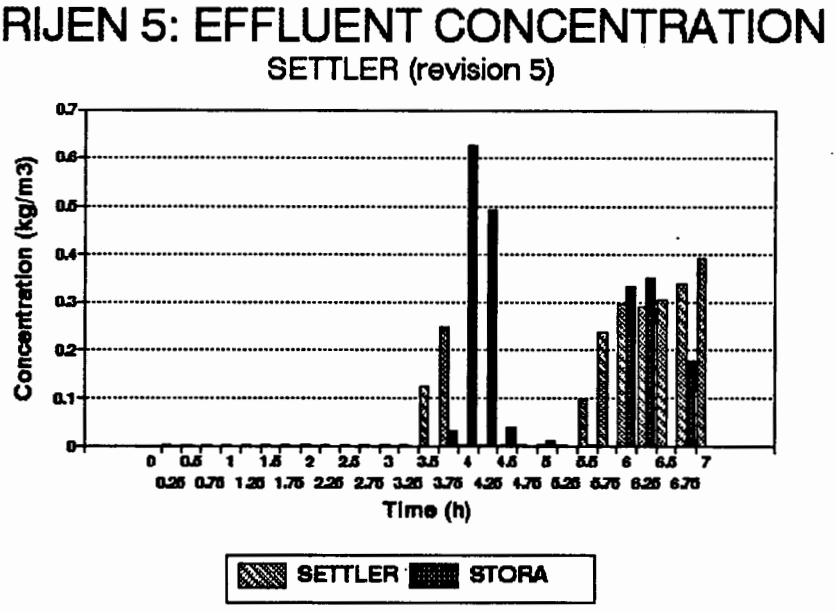

Figure 8.36 Predicted and measured effluent concentrations for Rijen 5 with SETTLER (revision 5)

The predicted results show a negligible concentration in the effluent until 3.5h, at which two concentration peaks are predicted ($127 mgl^{-1}$ at 3.5h and $248 mgl^{-1}$ at 3.75h).

The predicted effluent solids concentration then declines to negligible values again until 5.5h, when a second series of peaks is recorded ($97mgl^{-1}$, $238mgl^{-1}$, $298mgl^{-1}$, $292mgl^{-1}$, $303mgl^{-1}$, $337mgl^{-1}$ and $392mgl^{-1}$) until the end of the test at 7h. The total predicted effluent solids mass lost is 845kg, which is 1.45% of the total solids mass processed by the settling tank during this period.

The measured results also show a negligible effluent solids concentration for the first 3.75h of the test. At 4h the measured results show two large concentration peaks ($625mgl^{-1}$ at 4h and $494mgl^{-1}$ at 4.25h). Thereafter, the effluent solids concentration declines again until 6h, when the measured results show a further surge of effluent solids mass lost ($334mgl^{-1}$ at 6h, $349mgl^{-1}$ at 6.25h and $178mgl^{-1}$ at 6.75h). The total measured effluent solids mass lost is 843kg, 1.44% of the total solids mass processed.

The two peaks in the predicted and measured effluent solids concentration are responses to the switching of the influent flow off and on at 4h and 4.75h respectively and then off again at 6.25h. Although the first peak in the predicted effluent solids concentration occurs 15min earlier than the measured peaks, the total predicted effluent solids mass lost is less than the measured effluent solids mass lost during this first peak of solids mass loss in the effluent. The second peak of mass loss is more accurately predicted. Although the predicted effluent solids mass lost for the second peak still occurs sooner than the measured effluent solids mass lost (5.5h as opposed to 6h), the magnitude of the effluent solids concentrations correspond very well. The predicted and measured results match relatively well for the overall pattern of mass lost i.e. two distinct periods of high effluent solids concentration, although the predicted effluent solids mass lost occurs consistently earlier than the measured effluent solids mass lost. The predicted and measured effluent solids mass lost over the 7h test period correspond almost exactly (845 and 843kg respectively) because the difbot value of $1.693m^2h^{-1}$ was chosen for its ability to accurately predict this parameter.

4. Concentration profile

Figure 8.37 compares the measured and predicted concentration profiles at 4.5h for the Rijen 5 test.

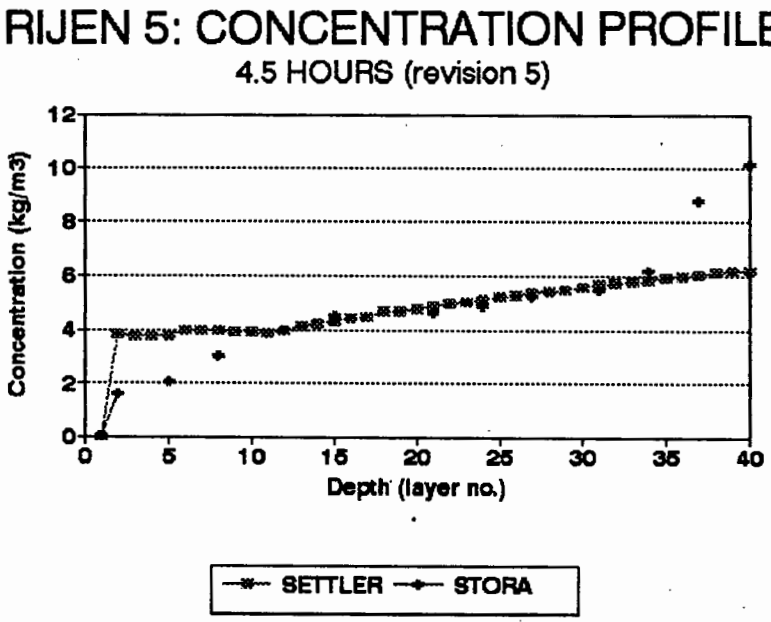

Figure 8.37 Predicted and measured concentration profiles at 4.5h for Rijen 5 with SETTLER (revision 5)

The predicted sludge concentration depth profile at 4.5h (0.5h after the influent flow has first been shut off and between the two effluent solids loss peaks) shows little variation throughout the tank. The underflow concentration of 6.2kgm^{-3} is very similar to the concentration of the entire sludge blanket which extends from layer 39 (6.18kgm^{-3}) to layer 2 (3.81kgm^{-3}). The decrease in predicted concentration from the bottom to the top of the tank is very small, and the effluent solids concentration is negligible at 0.027kgm^{-3} (2.7mgl^{-1}). The total predicted mass of sludge in the settling tank for the 4.5h profile is 25918kg.

The measured results show an underflow concentration of 10.15kgm^{-3}. Above this, a small region of high concentration exists (8.77kgm^{-3} in layer 37 and 6.21kgm^{-3} in layer 34). From layer 34 upwards, the concentration of the sludge blanket is relatively

constant at approximately 5kgm^{-3} until layer 8, when the concentration decreases to 3.03kgm^{-3}. Above the feed point layer, the concentration is constant at approximately 2kgm^{-3}. The measured effluent solids concentration is 0.039kgm^{-3}. The measured sludge mass in the settling tank at 4.5h is 25109kg.

The correspondence between the measured and predicted sludge concentration depth profiles is not too good in the bottom three layers of the tank, with the predicted concentrations being significantly lower than those measured in these layers. The concentration of the sludge blanket for the predicted and measured results corresponds very well up to the feed point, but above the feed point the predicted concentrations are higher than the measured values. Both predicted and measured effluent concentrations are very low. The measured and predicted masses of sludge in the settling tank correspond well at 25109kg and 25918kg respectively.

8.7.1 CONCLUSIONS FOR THE RIJEN 5 TEST SIMULATION

The predicted results for the Rijen 5 test are somewhat oversensitive to the overloaded condition. This is apparent from the too rapid rise rate of the sludge blanket as well as the premature prediction of effluent solids mass lost. This oversensitivity can be attributed to the relatively high value of difbot for this test (1.693m^{2}h^{-1}) which reduces the sludge storage capacity of the settling tank and causes the settling tank to fail too soon. The high value of difbot also has the effect of limiting the increase in the underflow concentration and of damping the influence of the influent flow on the underflow concentration. However, since this is the only test for which the calculated and measured values of difbot are the same, the predicted effluent solids mass lost matches almost exactly with the measured effluent solids mass lost. In addition, it should be noted that the time at which the predicted sludge blanket level reaches the top of the tank (1.5h) does not correspond to the time of failure (i.e. onset of solids loss with the effluent), which occurs at the first gross loss of solids mass in the effluent (3.5h). Thus, although the predicted sludge blanket rise rate is too rapid, the first predicted effluent solids mass loss occurs only 0.5h before the first measured

gross effluent solids mass loss. Indeed, the sensitivity of the effluent solids concentration and mass to the switching on and off of the influent flow is predicted very well. In addition, the general trend of the measured underflow concentration is well reflected by the predicted results. In summary, most of the salient features of the measured results have been accurately predicted by SETTLER for this test.

8.8 SIMULATING THE RIJEN 8 TEST WITH SETTLER (revision 5)

The eighth settling tank test carried out at Rijen (hereafter referred to as Rijen 8) was run for a total of 7 hours, with the influent flow being shut off for 0.83h from 6.17h until the end of the test. The flux theory constants, V_o and n, were calculated from the measured $SSVI_{3.5}$ using the relationship for extended aeration plants derived in Chapter 4. From the measured $SSVI_{3.5}$ of $120 ml g^{-1}$, the equations give $V_o = 5.407 m h^{-1}$ and $n = 0.429 m^3 kg^{-1}$. From these values of V_o and n, the flux theory indicates that the settling tank is overloaded for only the first 1.25h of the test, thereafter being underloaded. The data measured by STORA for Rijen 8 is given in Table 8.12 and a summary of the operating parameters for Rijen 8 is presented in Table 8.13.

The initial conditions for Rijen 8 are illustrated in Figure 8.38. They were generated in the same way as those for the earlier Rijen tests. The calculated value of difbot for Rijen 8 was found to be difbot = $1.259 m^2 h^{-1}$ compared to the real value of difbot = $1.476 m^2 h^{-1}$. The Rijen 8 test was simulated with both the calculated and real values of difbot, the predicted results being discussed and compared with the measured results below.

1. Sludge blanket level

Figure 8.39 compares the measured and predicted sludge blanket levels with the real and calculated difbot values for the 7h Rijen 8 test.

Table 8.12 Data measured by STORA for the Rijen 8 test

Test Rijen 8 Begin test: 9:30h
Date: 28 November 1978 End test: 14:00h

Q_i = 1200m^3h^{-1} Q_r = 1006.5m^3h^{-1}

Time (h)	Feed conc (kg/m3)	Underflow conc (kg/m3)	Effluent conc (mg/l)	Sludge blanket height (m)	Remarks
09:30	5.19	6.03			influent started
09:45				2.10	
09:50		4.32			
10:10	4.49	4.34			
10:30				1.70	
10:40		5.38	4.2		
10:50	4.09				
11:05		5.12			
11:20		4.30			
11:25				1.35	
11:30	3.91		4.4		
11:40		4.45			
11:50				1.20	
12:00		4.91			
12:05				1.15	
12:15				1.15	
12:20	3.68	7.30			
12:30			4.8	1.05	
12:35		5.59			
13:00	3.47	6.55			
13:20		6.24			
13:25			2.6	0.75	flocs coming over the weir
13:40	3.44	6.61			
13:50			4.2	0.65	solids loss
14:00		6.46	213		
14:08				0.60	
14:15			556	0.60	
14:20	3.36	6.12		0.60	
14:35			580	0.55	
14:40		6.97			
14:45			1076		
15:00	3.45	6.47			
15:05			1180		
15:10				0.60	influent stopped
15:15		4.11 (?)	800		
15:25		7.89			
15:30			477	0.70	
15:45	3.45	9.64			
15:50				0.90	
16:00	3.27	11.17	17		
16:15				1.10	

The predicted results with the calculated and real values of difbot show a gradual rise in sludge blanket level for the first 0.5h of the test from 1.44m below the surface at the start of the test to 1.12m at 0.5h. At 0.75h both predicted sludge blanket levels suddenly rise to the top of the tank (0.16m). The sudden drop and subsequent rise in sludge blanket level at 1h for the calculated difbot case is a consequence of the redistribution of sludge mass above the feed point to cope with the step change in influent feed at the start of the test. This redistribution also takes place for the real

Table 8.13 Summary of operating parameters for the Rijen 8 test

PARAMETER	VALUE
Q_i	$1200m^3h^{-1}$
Q_r	$1006.5m^3h^{-1}$
X_o (max)	$5.19kgm^{-3}$
X_o (min)	$3.27kgm^{-3}$
Area	$1625m^2$
Depth (from overflow weir to bottom of tank)	3.35m
Feed point layer	5
Duration of test	7 hours
$SSVI_{3.5}$	$120mlg^{-1}$
DSVI	$130mlg^{-1}$
V_o	$5.407mh^{-1}$
n	$0.429m^3kg^{-1}$

difbot case but is not manifested in the sludge blanket level profile because it occurs at concentrations less than $3kgm^{-3}$, which is the concentration that defines the sludge blanket level. For the calculated difbot case, the redistribution occurs around $3kgm^{-3}$ and therefore exhibits the dip in the profile as this redistribution takes place. A detailed sludge concentration profile at 15 minute intervals from 0.5h to 1.25h after the start of the test for the calculated difbot value is given in Figure 8.40 which also shows the sludge blanket definition concentration of $3kgm^{-3}$. It can be seen that the sludge concentration oscillates from less than $3kgm^{-3}$ to greater than $3kgm^{-3}$ over the time interval which causes the dip in the sludge blanket level (see Figure 8.39).

After 1.25h, the predicted sludge blanket level with the calculated value of difbot remains constant at the top of the tank (0.16m) until the end of the test at 7h even

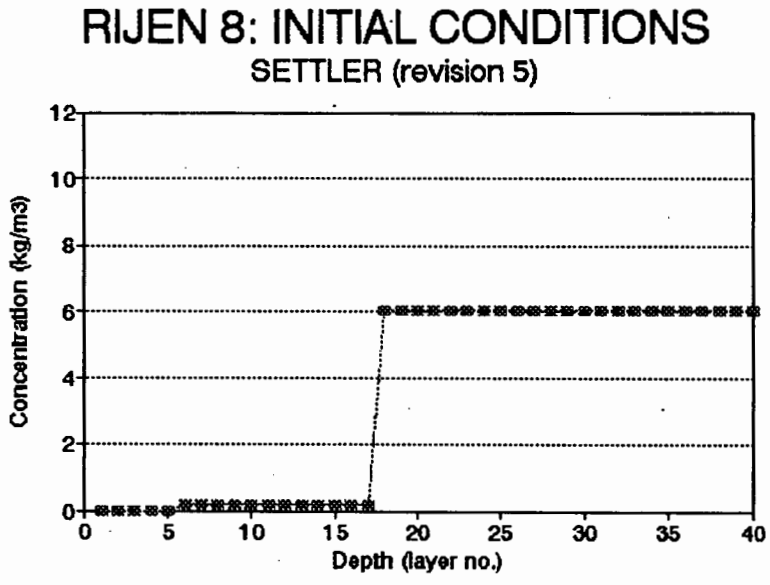

Figure 8.38 Initial concentration profile for Rijen 8

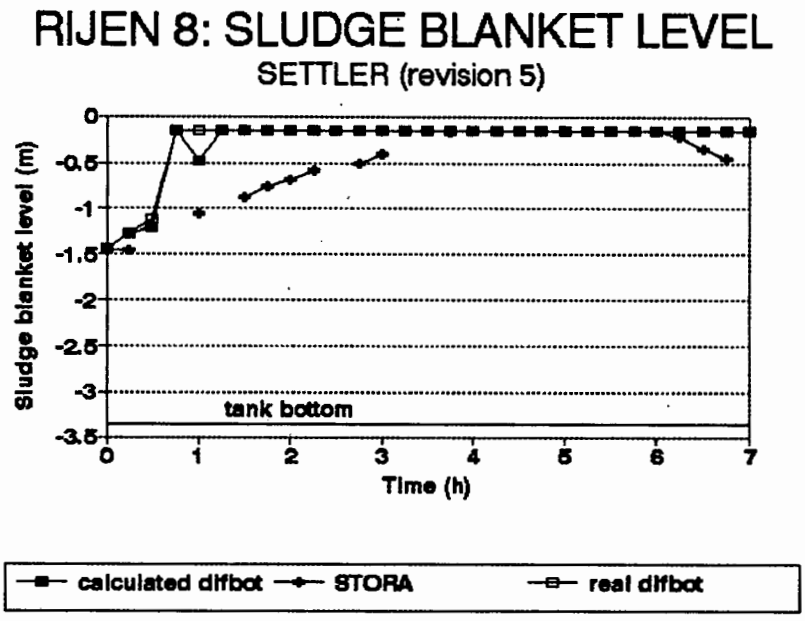

Figure 8.39 Predicted and measured sludge blanket levels for Rijen 8 with SETTLER (revision 5)

though the influent flow was shut off at 5.5h.

The predicted results with the real difbot value are similar to those for the calculated difbot value and show a gradual rise in sludge blanket level for the first 0.5h of the

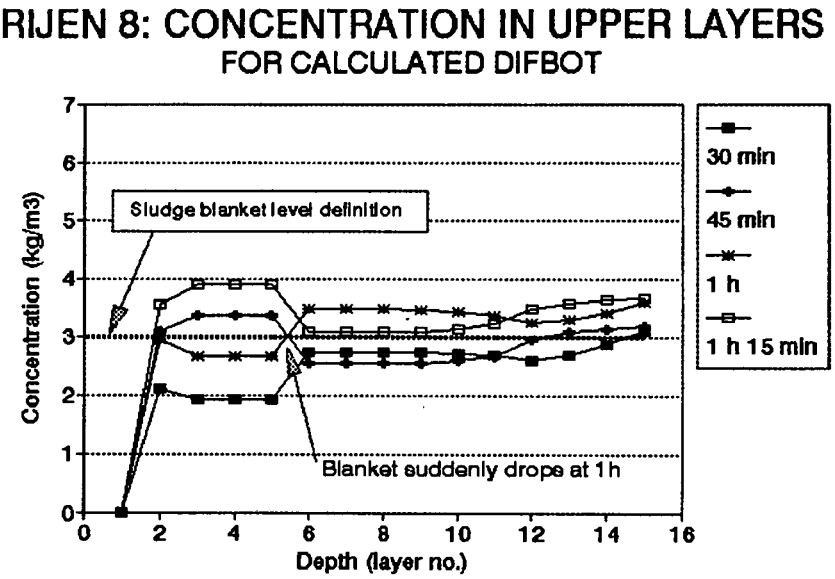

Figure 8.40 **Mass redistribution in the upper layers of the settling tank for the Rijen 8 test with calculated difbot**

test from 1.44m at the start of the test to 1.2m below the surface at 0.5h into the test. At 0.75h, a sharp rise in sludge blanket level is predicted, and the sludge blanket reaches the top of the tank (0.16m) at this time. Thereafter, the sludge blanket level remains at 0.16m (without exhibiting the dip observed in the results for the calculated difbot value) until the end of the test at 7h even though the influent flow was shut off at 5.5h.

The measured results show a gradual rise in sludge blanket level from 1.46m at the start of the test to 0.16m at 4.25h into the test. The sludge blanket level remains constant at 0.16m for 1.75h until 6h, whereupon it falls gradually, reaching 0.46m below the surface by the end of the test due to the shut off of the influent flow at 5.5h.

For this parameter, the correspondence between measured and predicted results (for both values of difbot) is poor. The predicted sludge blanket rise rate is much faster than the measured one, and thus the predicted sludge blanket level reaches the top of the tank 3.5h earlier than the measured sludge blanket. The jump in the predicted sludge blanket is also noticeable in the earlier simulations, but it did not occur so early

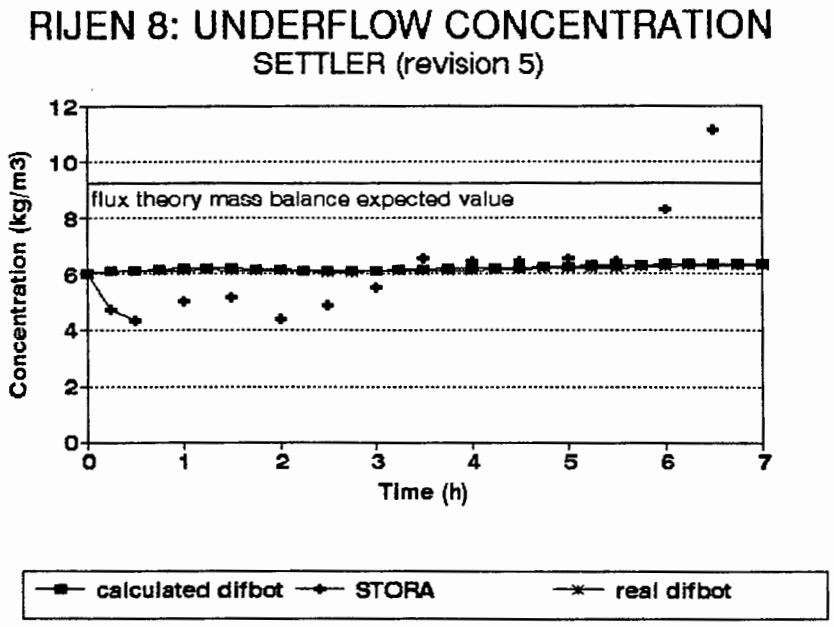

Figure 8.41 Predicted and measured underflow concentrations for Rijen 8 with SETTLER (revision 5)

The almost constant predicted underflow concentration for this test is caused by the high values of difbot (both real ($1.476 m^2h^{-1}$) and calculated($1.259 m^2h^{-1}$)) which introduce a marked degree of mixing in the bottom layers of the tank and thus prevent thickening from taking place. It is to the model's credit that the predicted underflow concentration matches the measured value for most of the first 5h of the test; only for the final 2h is there a marked difference with the predicted values remaining around $6 kgm^{-3}$ while the measured value increases to $11 kgm^{-3}$. Large and rather erratic changes in measured underflow concentration have been observed in earlier tests, these being ascribed to the switching of the influent flow on and off and to sludge collection bottom effects. This increase in the measured results at the end of the test could be due to the same effects but it seems strange that in this test the underflow concentration increases after the influent flow has been switched off. In earlier tests, the underflow concentration decreased when the influent flow was switched off. Nevertheless, in general, the high difbot value seems to be the best possible choice for the simulation of the underflow concentrations for the Rijen 8 test.

3. Effluent concentration

Figure 8.42 compares the measured and predicted effluent concentrations with the real difbot value for the Rijen 8 test. The effect of using the calculated value of difbot is discussed later.

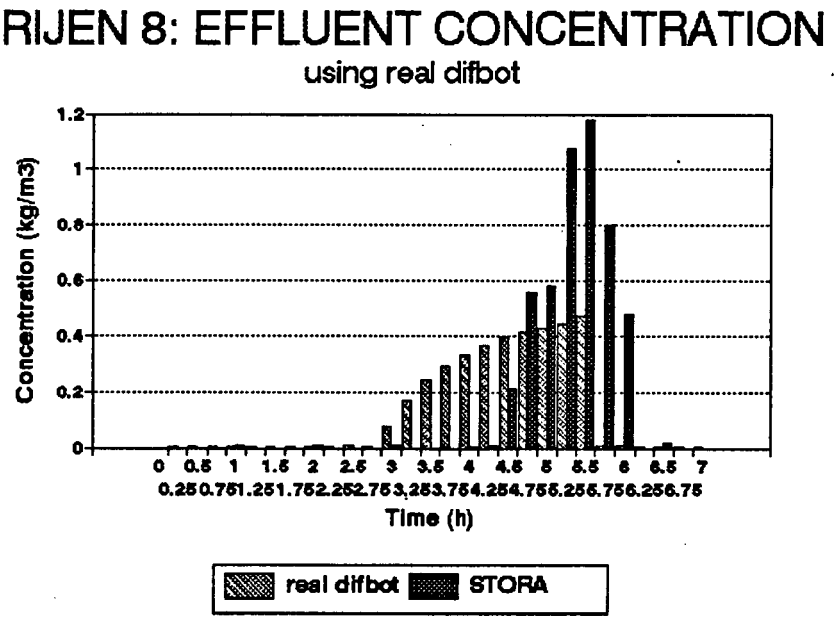

Figure 8.42 Predicted (with real difbot) and measured effluent concentrations for Rijen 8 with SETTLER (revision 5)

The predicted effluent solids concentration with the real value of difbot shows negligible effluent solids concentration until 3h, when the effluent solids concentration begins to increase gradually from 77mgl^{-1} at 3h to a maximum of 470mgl^{-1} at 5.5h at which time the influent flow was switched off. The total predicted effluent solids mass lost is 1094kg, which is 2.1% of the total solids mass processed by the settling tank over the 7h test.

The measured results also show a negligible effluent solids concentration until 4.5h, when a series of peaks of effluent solids concentration is recorded. These peaks continue until 6h, 0.5h after the influent flow was switched off, when the effluent solids concentration again declines to negligible values. The total measured effluent

solids mass lost is 1068kg, 3.04% of the total solids mass processed by the settling tank.

Although the total effluent solids mass lost for the measured and predicted results is approximately the same (the real value of difbot was chosen on the basis of this parameter), the manner in which the mass is lost is not so well predicted. The predicted results show an effluent solids mass loss that occurs over a period of 2.5h, with the magnitude of the effluent solids concentration peaks gradually increasing over this period, but never exceeding 470mgl^{-1}. In contrast, the measured effluent solids mass loss occurs over a period of only 1.5h, with much greater effluent solids concentration being recorded, the maximum being 1180mgl^{-1} at 5.5h.. The manner of the measured effluent solids loss can be described as more focused or intensified than the predicted effluent solids mass loss. Because the manner of effluent solids mass loss is governed by α_2 and diftop, this would seem to indicate that the diffusivity in the upper layers of the tank for SETTLER is too high for this test.

Figure 8.43 compares the measured and predicted effluent solids concentrations for the Rijen 8 test where the predicted results are based on the calculated difbot value. The predicted effluent solids concentration using the calculated value of difbot shows an almost negligible concentration in the effluent until 4.25h, when effluent solids mass loss begins to occur. This solids loss occurs for 1.25h until 5h, when the influent flow was switched off, after which the predicted effluent solids concentration declines again to negligible values. The total predicted effluent solids mass lost over the 7h test is 286kg, which is 0.54% of the total solids mass processed by the settling tank.

As in earlier tests, this test also shows the sensitivity of the predicted effluent solids concentration to small changes in the value of difbot. In this case, a 14% decrease in the value of difbot (the difference between the real and the calculated values of difbot) resulted in a 73% decrease in the total predicted effluent solids mass lost. Although the correspondence between measured and predicted (with calculated difbot) effluent solids mass lost is not as good as that with the real difbot value predictions, the calculated

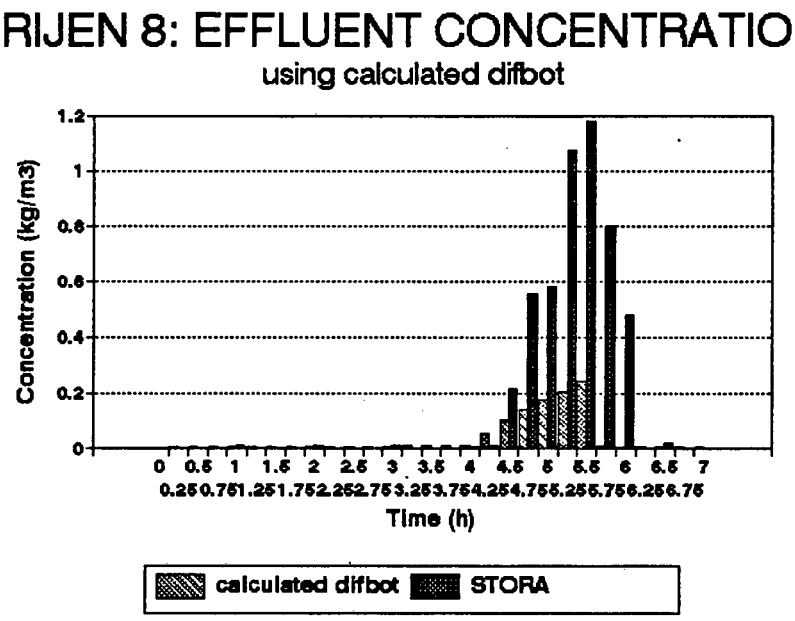

Figure 8.43 **Predicted (with calculated difbot) and measured effluent concentrations for Rijen 8 with SETTLER (revision 5)**

difbot value predictions give a much closer correspondence with the measured time of onset of failure than the real difbot predictions.

4. Concentration profile

Figure 8.44 compares the measured and predicted concentration profiles for both the real and calculated values of difbot at 7h for the Rijen 8 test and shows that the two predicted profiles are virtually the same.

The predicted sludge concentration depth profiles (with the calculated and real values of difbot) have an underflow concentration of 6.36kgm^{-3} and a sludge blanket that extends throughout the tank, decreasing gradually from a concentration of 6.28kgm^{-3} at layer 39 to 3.57kgm^{-3} (calculated difbot) and 3.76kgm^{-3} (real difbot) in layer 11. From layer 11 to layer 6, the concentration is approximately constant and slightly higher at 3.9kgm^{-3} (calculated difbot) and 4kgm^{-3} (real difbot). Between layers 5 and 3, there is a region of constant concentration at $\pm$3.09kgm^{-3} (calculated difbot) and 3.2kgm^{-3} (real

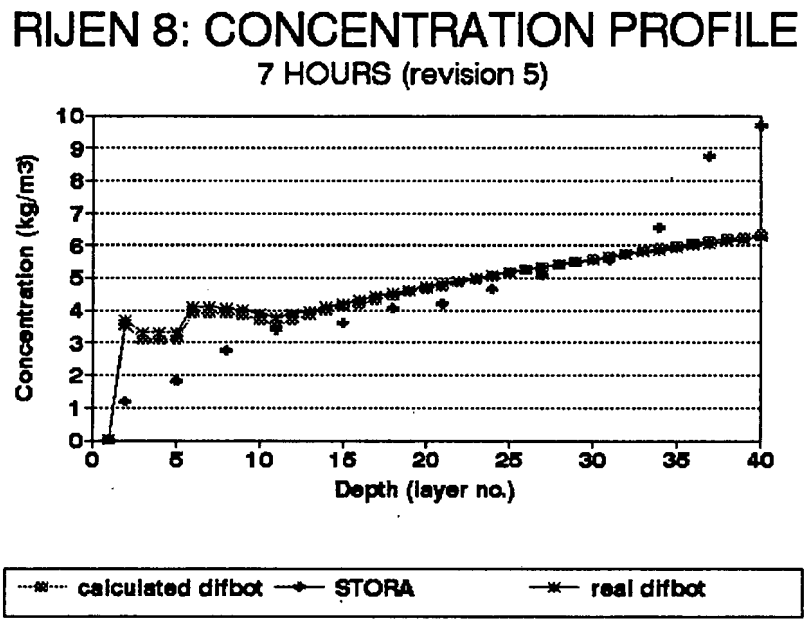

Figure 8.44 **Predicted and measured concentration profiles at 7h for Rijen 8 with SETTLER (revision 5)**

difbot). In layer 2, the concentration is slightly higher, and the predicted effluent solids concentration is 0.0026kgm^{-3} (calculated difbot) and 0.0028kgm^{-3} (real difbot). The total predicted sludge mass in the tank is 25264kg (calculated difbot) and 25544kg (real difbot).

The measured solids concentration depth profile at 7h has an underflow concentration of 9.7kgm^{-3} and a region of high measured concentration in the bottom five layers of the tank: 8.74kgm^{-3} at layer 37 and 6.56kgm^{-3} at layer 34. From layer 31 to layer 2, the concentration in the tank decreases gradually from 5.53kgm^{-3} to 1.22kgm^{-1}. The measured effluent solids concentration at 7h is negligible, and the total measured sludge mass in the tank is 26100kg.

The predicted results do not reflect the region of high and low concentration recorded in the measured results for the bottom and top layers of the tank, but in the middle two thirds of the tank the concentration corresponds well. At the start of the test, the predicted sludge concentration depth profile for the upper 11 layers is somewhat unstable, showing some concentration variation, but this dies down after approximately

1.5h. The total mass of sludge in the tank is less for both sets of predicted results than for the measured results, because the predicted results lack the substantial contribution made by the region of high concentration in the lower layers of the tank. However, the difference between measured and predicted results is only 2.13% and 3.20% lower for the real and calculated values of difbot respectively. The fact that the total sludge mass in the tank is less for the calculated value of difbot than for the real value is expected, because the higher real value of difbot makes the settling tank more sensitive to overloaded conditions and thus reduces its sludge storage capacity.

8.8.1 CONCLUSIONS FOR THE RIJEN 8 TEST SIMULATION

For this test, the correspondence between measured and predicted results is generally fairly good. As with the earlier tests, the predicted sludge blanket rise rate is too rapid, with the sludge blanket reaching the top of the tank 2h earlier than the measured results. In earlier simulations this problem was not as marked as in this simulation and consequently this aspect was only investigated in detail at this stage. The jump in the sludge blanket level was found to arise at 0.5h in this test because the initial sludge blanket level was high, and therefore close to the layers of high diffusivity at the feed point. The higher diffusivity in the layers near the feed point layer causes considerable mixing in these layers and results in an almost uniform concentration in these layers. When the concentration in these layers exceeds $3kgm^{-3}$, which is the sludge blanket definition concentration, the sludge blanket level jumps to the uppermost layer which is at this concentration. The measured sludge blanket level shows a more gradual rate of increase through the layers around the feed point, indicating, for the real tank, the diffusivity in these layers is not as high as that in SETTLER. However, it was found that, without this high diffusivity, it was not possible to accurately simulate the effluent solids concentration time profile for the other Rijen test simulations. This phenomenon, therefore, is a consequence of both the high diffusivity required in the upper layers of the tank and the definition of the sludge blanket level.

The predicted effluent solids mass lost for the calculated value of difbot does not correspond as well with the measured results as the predictions for the real difbot value. However, the onset of failure is predicted accurately for the calculated value of difbot but not for the real value of difbot. The predicted underflow concentration corresponds fairly well with the measured results. The predicted sludge concentration depth profile, although reflecting the general trend of the measured results, such as the existence of a sludge blanket through most of the tank, exhibits some concentration differences compared with the measured results in the top and bottom of the tank. With regard to the bottom, the difference in all likelihood arises from sludge collection effects in the bottom of the real tank. With regard to the top, the difference is caused by the relatively high diffusivity in the layers around the feed point and by the definition of the sludge blanket level concentration.

8.9 SIMULATING THE RIJEN 7 TEST WITH SETTLER (revision 5)

The seventh settling tank test carried out at Rijen (hereafter referred to as Rijen 7) was run for a total of 7 hours, with the influent running into the settling tank throughout the test. The flux theory constants, V_o and n, were calculated from the measured $SSVI_{3.5}$ using the relationship for extended aeration plants derived in Chapter 4. From the measured $SSVI_{3.5}$ of $120mlg^{-1}$, the equations give $V_o = 5.407mh^{-1}$ and $n = 0.429m^3kg^{-1}$. From these values of V_o and n, the flux theory indicated that the settling tank was overloaded from 0.25h into the test until the end of the test. For the first 0.25h, the settling tank was underloaded. The data measured by STORA for the Rijen 7 test is given in Table 8.14 and a summary of the operating parameters for the test is presented in Table 8.15.

Table 8.14 Data measured by STORA for the Rijen 7 test

Test Rijen 7 Begin test: 9:45h
Date: 21 November 1978 End test: 16:20h

Q_i = 1200m^3h^{-1} Q_r = 531m^3h^{-1}

Time (h)	Feed conc (kg/m3)	Underflow conc (kg/m3)	Effluent conc (mg/l)	Sludge blanket height (m)	Remarks
09:30	4.99	5.11		2.9	influent started
09:40				2.9	
09:45	5.09	5.26			
09:50				2.9	
10:00	4.87	5.32			
10:20		4.39		2.65	
10:40	5.32	5.08		2.45	
11:00			1.20		
11:20	5.09	4.79		2.00	
11:35				1.95	
11:40		5.73			
12:00	4.94	6.12	< 0.1		
12:15				1.70	
12:20		7.26			
12:35				1.55	
12:40	4.75	7.41			
13:00		7.30	3.00		
13:20	4.37	8.10			
13:30				1.30	
13:40		8.02		1.20	
14:00	4.31	8.88	0.40	1.15	
14:20		9.03		1.10	
14:35				1.05	
14:40	4.02	8.66			
14:45				1.05	
15:00		8.64	4.00	1.00	
15:20	3.97	9.33		0.95	
15:40		9.03			
15:50				0.85	
16:00	3.82	9.01	0.40	0.75	flocs coming over the weir
16:15			0.65		
16:20		9.31	21.00		solids loss
16:25			285.00		
16:40	3.78	8.30	354.00		
16:45			320.00		influent stopped
16:50		9.20	79.00	0.60	
17:00		10.92	0.65		
17:10		10.30			
17:20	3.92	9.75			

The initial conditions for Rijen 7 are illustrated in Figure 8.45. They were generated in the same way as for the four previous Rijen tests.

The calculated value of difbot for Rijen 7 was found to be difbot = 0.342m^2h^{-1} compared to the real value of difbot = 0.423m^2h^{-1}. The Rijen 7 test was carried out using both the calculated and real values of difbot, the results being discussed and compared with the measured results below.

Table 8.15 Summary of operating parameters for the Rijen 7 test

PARAMETER	VALUE
Q_i	$1200m^3h^{-1}$
Q_r	$531m^3h^{-1}$
X_o (max)	$5.32kgm^{-3}$
X_o (min)	$3.78kgm^{-3}$
Area	$1625m^2$
Depth (from overflow weir to bottom of tank)	3.35m
Feed point layer	5
Duration of test	7 hours
SSVI	$120mlg^{-1}$
DSVI	$120mlg^{-1}$
V_o	$5.407mh^{-1}$
n	$0.429m^3kg^{-1}$

1. Sludge blanket level

Figure 8.46 compares the measured and predicted sludge blanket levels with difbot (real) and difbot (calculated) for the 7h Rijen 7 test.

The predicted results with the calculated value of difbot show an initial drop in the sludge blanket level from 2.08m below the surface at the start of the test to 2.24m at 0.75h into the test. This drop in sludge blanket level is caused by the redistribution of sludge mass in the tank to overcome the sharp discontinuity at layer 26 in the initial conditions. During this time, the concentration in the lower layers of the tank is increasing which necessitates a decrease in the concentration of the layers higher up in the tank. This causes the drop in the predicted sludge blanket level. Thereafter, the

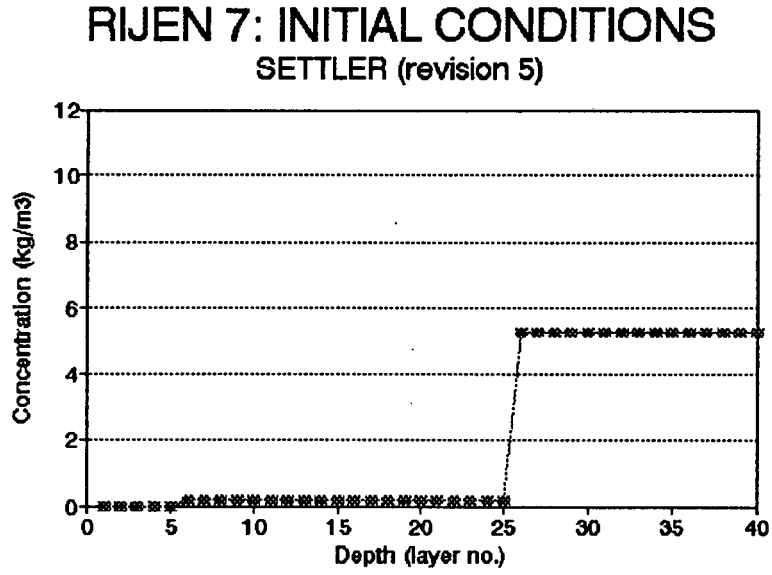

Figure 8.45 Initial concentration profile for Rijen 7

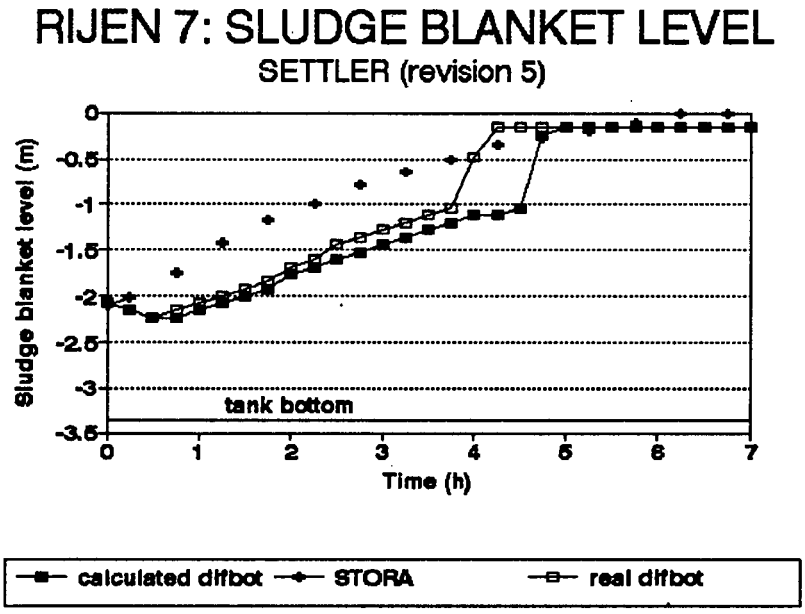

Figure 8.46 Predicted and measured sludge blanket levels for Rijen 7 with SETTLER (revision 5)

sludge blanket rises gradually and constantly to a level of 1.04m below the surface at 4.5h. At 4.75h, a sudden rise in sludge blanket level to 0.24m is predicted and at 5h the predicted sludge blanket level is at 0.16m (effectively the top of the tank). From 5h

until the end of the test, the predicted sludge blanket level with the calculated value of difbot is constant at 0.16m.

The predicted results with the real value of difbot are similar to those with the calculated difbot except, because the real difbot value is higher than the calculated difbot, the sludge blanket rises slightly faster and the sludge blanket level reaches the top of the tank 0.75h earlier at 4.25h. From 4.25h until the end of the test, the sludge blanket level remains constant at 0.16m.

The measured results show a constant rise in sludge blanket level from 2.11m below the surface at the start of the test to 0.2m below the surface at 5.25h into the test. Thereafter, the sludge blanket level continues to rise until it reaches the top of the tank at 5.75h.

There is a good correspondence between the measured and predicted sludge blanket rise rates, although the initial drop in predicted sludge blanket level causes a phase difference in the results for approximately the first 4h of the test. The predicted results with the real value of difbot show a sludge blanket level that prematurely reaches the top of the tank whereas with the calculated value of difbot the time that the sludge blanket level reaches the top of the tank corresponds better with the measured results. It should be noted that in this test, as in all the previous predicted results, the same phenomenon of a sudden rapid rise in sludge blanket from 1m upwards takes place and this also, as discussed for the Rijen 8 test, is a result of the sludge blanket entering the layers of high diffusivity around the feed point as well as an artefact of the definition of the sludge blanket concentration. As in all the earlier tests, even though the sludge blanket is at the top of the tank, gross solids loss with the effluent is not yet taking place. This occurs only at 6h into the test, which is 1h after the sludge blanket has reached the top of the tank (for the real difbot value)(see Figure 8.48). As in earlier tests, during this hour, sludge is accumulating in the sludge blanket above the feed point as the concentration in these layers increases. Only when the concentration in the

layers above the feed point has increased to X_{af} (the limiting concentration for the layers above the feed point), does gross solids loss occur.

2. Underflow concentration

Figure 8.47 compares the measured and predicted underflow concentrations with difbot (real) and difbot (calculated) for the Rijen 7 test.

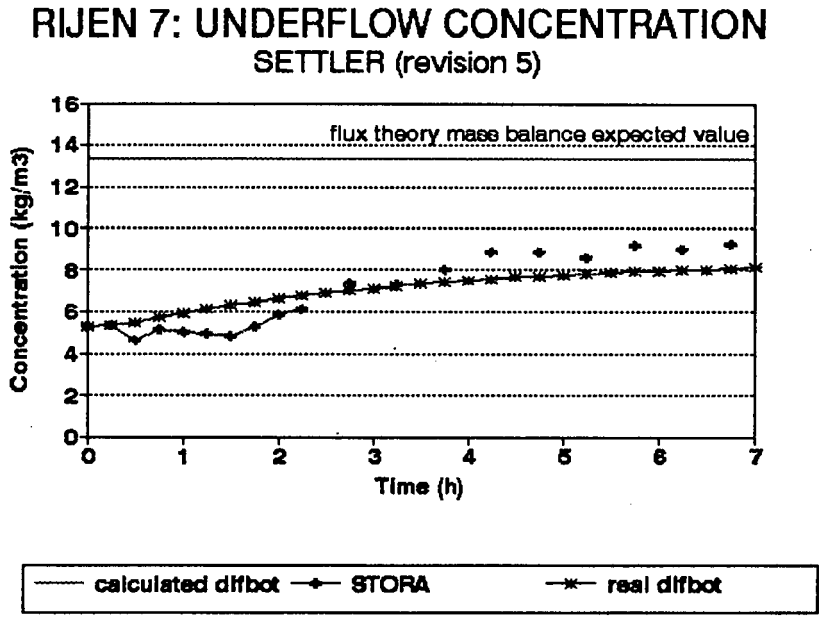

Figure 8.47 Predicted and measured underflow concentrations for Rijen 7 with SETTLER (revision 5)

The predicted results with the real and calculated difbot values are almost indistinguishable. The predicted results show an underflow concentration that rises gradually from an initial concentration of 5.26kgm^{-3} to a final underflow concentration of 8.11kgm^{-3} (real difbot) and 8.13kgm^{-3} (calculated difbot) at the end of the test.

The measured underflow concentration is erratic throughout the test, but generally remains constant at $\pm$5kgm^{-3} until 1.5h into the test. At 1.5h, the measured underflow concentration shows a gradual rise from 4.826kgm^{-3} at 1.5h to 8.88kgm^{-3} at 4.25h. Thereafter, the measured underflow concentration remains fairly constant, although it fluctuates between 9.273kgm^{-3} (maximum) and 8.64kgm^{-3} (minimum) during this time.

The gradual increase in predicted underflow concentration (as opposed to an almost constant value) can be attributed to the fact that the difbot values (both real and calculated) for this test are relatively low and thus only the minimum amount of mixing takes place in the bottom layers of the tank. Thus the degree of thickening that is permitted to take place is not inhibited by the diffusivity in the bottom of the tank, but rather by the time lag introduced by the CSTR. The magnitude of the increase in the underflow concentration during the 7h test reflects this accordingly.

Aside from the erratic behaviour of the measured results, the correspondence between measured and predicted underflow concentrations is excellent for this test. The predicted underflow concentration accurately reflects the general trend of the measured underflow concentration, and the final maximum predicted underflow concentration attained ($\pm 8.12 kgm^{-3}$) is close to the measured value ($9.27 kgm^{-3}$).

3. Effluent concentration

Figure 8.48 compares the measured and predicted effluent concentrations with difbot (real) and difbot (calculated) for the Rijen 7 test.

The predicted effluent solids concentration using the calculated difbot value (being smaller than the real difbot value) is negligible throughout the test. On the bar graph in Figure 8.48, the bars representing the effluent solids concentration for the calculated value of difbot are almost indiscernible. The total predicted effluent solids mass lost is 13.98kg, 0.03% of the total solids mass processed by the settling tank. However, if the simulation is run for 1h longer, then at 7.75h, gross solids loss with the effluent is predicted i.e. 1.5h after the onset of solids loss with the real difbot value.

The predicted effluent solids concentration with the real value of difbot shows a negligible concentration of solids in the effluent until 6.5h, when solids mass loss in the effluent begins to occur. The manner in which this solids mass loss occurs is in the form of three major peaks of concentration over the final 0.75h of the test ($145 mgl^{-1}$ at

6.5h, 339mgl^{-1} at 6.75h and 515mgl^{-1} at 7h). The total predicted effluent solids mass

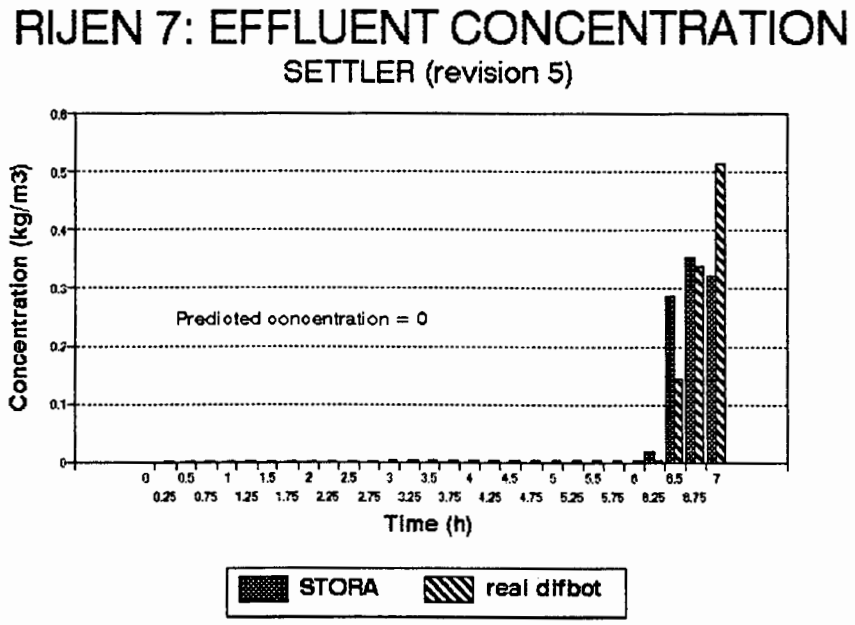

Figure 8.48 Predicted and measured effluent concentrations for the Rijen 7 test with SETTLER (revision 5)

loss with the real value of difbot is 313kg, 0.58% of the total solids mass processed during the test.

The measured effluent solids concentration is also negligible until 6h into the test, when a small peak of effluent solids concentration is measured. The major effluent solids mass loss occurs between 6.25h and 7h, with effluent solids concentration peaks of 285mgl^{-1} at 6.25h, 354mgl^{-1} at 6.5h and 320mgl^{-1} at 6.75h. The total measured effluent solids mass lost is 294kg, 0.54% of the total solids mass processed by the settling tank during the test.

The correspondence between measured and predicted results for the calculated value of difbot is not as good as the correspondence between the measured and predicted results for the real value of difbot. The correspondence between measured and predicted results using the real value of difbot is excellent, with the both the manner and the magnitude of the effluent solids mass loss matching well. This is to be expected, given that the real value of difbot was chosen on the basis of this parameter. Examination of

the difference between the predicted results using the calculated and real values of difbot confirms that the effluent solids mass lost is sensitive to the value of this parameter and that the 20% lower difbot value causes the 1.25h delay in the onset of solids loss with the effluent.

4. Concentration profile

Figure 8.49 compares the measured and predicted concentration profiles with both the real and calculated values of difbot at 7h (end of test) for the Rijen 7 test.

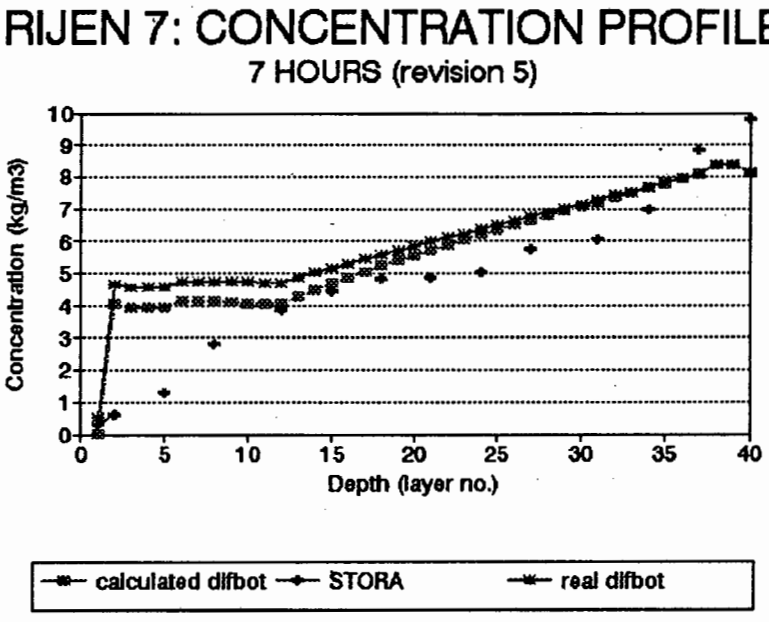

Figure 8.49 Measured and predicted concentration profiles at 7h for Rijen 7 with SETTLER (revision 5)

The predicted sludge concentration depth profile with the calculated value of difbot has an underflow concentration of 8.13kgm^{-3} and a sludge blanket that extends through most of the tank below the feed point from layer 39 at 8.36kgm^{-3} to layer 13 at 4.30kg^{-3}. From layer 11 upwards, the concentration is almost constant at $\pm$4kgm^{-3}. The predicted effluent solids concentration using the calculated value of difbot is 0.03kgm^{-3} and the total mass of sludge in the tank is 30850kg.

The predicted sludge concentration depth profile with the real value of difbot has an underflow concentration of 8.11kgm^{-3} and, similar to the calculated difbot result, has a sludge blanket that extends from layer 39 at 8.36kgm^{-3} to layer 12 at 4.8kgm^{-3}. From layer 11 upwards, the concentration is constant at $\pm$4.6kgm^{-3}. The predicted effluent solids concentration is 0.515kgm^{-3} and the total mass of sludge in the tank is 32851kg. In this profile it can be seen that for the calculated difbot case, even though the sludge blanket is at the top of the settling tank and has been there for already 2h (see Figure 8.46), no gross solids loss with the effluent has yet taken place. The sludge concentration above the feed point is still lower than that for the real difbot case (for which solids loss is taking place) and needs to still increase by about 0.7kgm^{-3} before solids loss with the effluent will take place.

The measured solids concentration depth profile has an underflow concentration of 9.80kgm^{-3} and a region of high concentration in the bottom of the tank: 8.84kgm^{-3} at layer 37 and 6.98kgm^{-3} at layer 34. From layer 31 to layer 15, the concentration in the tank is more or less constant at $\pm$5kgm^{-3}. Above the feed point, the concentration drops sharply from 2.79kgm^{-3} in layer 8 to 0.63kgm^{-3} in layer 2. The measured effluent solids concentration is 0.320kgm^{-3} and the total measured sludge mass in the tank is 25091kg.

The measured and predicted results do not correspond very well in the bottom layers of the tank, although the sludge blanket concentration matches reasonably well. The region of low concentration above the feed point for the measured results is not reflected in the predicted results. There is a good correspondence between the measured effluent concentration and the predicted effluent concentration using the real value of difbot. The total mass of sludge in the tank is greater for the predicted results ($\pm$30000kg) than for the measured results ($\pm$25000kg), and greater for the real value of difbot than for the calculated value. The difference between the real and calculated values of difbot is to be expected, as the higher real value of difbot renders the tank more sensitive to overloaded conditions and tends to reduce the ability of the tank to process the influent solids mass.

8.9.1 CONCLUSIONS FOR THE RIJEN 7 TEST SIMULATION

This test highlights the sensitivity of the predicted results to the value of difbot. The difference between the real and calculated values of difbot is 20% and this causes some differences in the four parameters examined, one of which is the 1.25h delay in the onset of effluent solids mass loss. The relatively low value of difbot (both real and calculated) causes the sludge blanket rise rate to be fairly slow, and ensures that the blanket reaches the top of the tank fairly late in the test. With the higher (real) value of difbot the sludge blanket reaches the top of the tank 1h earlier than with the lower (calculated) value. For the low values of difbot with this test, an excellent correspondence between measured and predicted underflow concentrations is obtained, as low values allow the underflow concentration to rise substantially during the test which does not happen for higher difbot values due to their limiting effect. On the whole, the predicted sludge concentration depth profiles match the measured profile very well although the predicted mass in the tank is higher than the measured mass. The predicted results deviate from the measured results for the sludge concentration in the bottom of the tank and in the layers above the feed point, which can be attributed to the sludge collection mechanism in the real tank, the high diffusivity in the layers near the feed point and the definition of the sludge blanket concentration. In summary, it appears that the value of difbot needs to be carefully chosen to establish the correct sensitivity of the increase in the underflow concentration, the rise rate of the sludge blanket and the delay in the onset of effluent solids mass loss. It appears that, with the difbot values linked to the feed flow rate (Q_i+Q_r), this sensitivity is satisfactorily simulated.

8.10 ASSESSING THE QUALITY OF THE RIJEN SIMULATIONS

The most notable phenomenon emerging from the Rijen simulations is the sensitivity of the four settling tank parameters (sludge blanket level and rise rate, underflow concentration, effluent solids mass lost and sludge concentration depth profile) to the value of difbot.

The quality of the simulations was significantly altered even for small changes in difbot. For example, the effluent solids mass lost for Rijen 7, 4 and 8 is not as well predicted with the calculated value of difbot as with the real value of difbot. A summary of the change in the predicted effluent solids mass lost with the real and calculated values of difbot is presented in Table 8.16 for the Rijen tests.

Table 8.16 Effects of real and calculated difbot on effluent solids mass lost for the Rijen tests

TEST	REAL DIFBOT (m^2h^{-1})	CALCULATED DIFBOT (m^2h^{-1})	% CHANGE	EFFLUENT SOLIDS MASS LOST (kg)		
				WITH REAL DIFBOT	WITH CALCULATED DIFBOT	% CHANGE
Rijen 7	0.423	0.342	19.1% less	313	14	95.5% less
Rijen 4	0.579	0.776	35.5% more	752	3192	324.5% more
Rijen 1	1.367	1.461	6.7% more	779	1521	95.3% more
Rijen 8	1.476	1.259	14.6% less	1094	286	73.9% less
Rijen 5	1.689	1.693	0% (same)	845	845	0% (same)

It was found that the simulations with the higher values of difbot (Rijen 8 and 5) are not as good as those with the lower values of difbot. The high value of difbot has two effects:

1. It renders the tank more sensitive to the overloaded situation, causing the sludge blanket to rise too rapidly and effluent solids mass loss to be prematurely predicted.

2. It blurs the definition of the various concentration regions in the tank and creates a sludge concentration depth profile that changes relatively little with depth and lacks distinct concentration regions. This damping effect also causes the predicted underflow concentration to vary relatively little during the test.

The lower values of difbot (Rijen 7, 4, and 1) tend to give more accurate simulation results. Good correspondence of the sludge blanket rise rate and an accurate reflection of both the time and the manner of effluent solids mass lost (at least for the real values of difbot) is found for these tests. The lower values of difbot also tend to generate well defined concentration regions in the sludge concentration depth profile. They permit a considerable degree of thickening to take place and result in the underflow concentration increasing substantially during the test, thereby better reflecting the measured results.

Despite the finding that lower difbot values perform better than the higher ones, it was not possible to reduce the real difbot values for Rijen 8 and Rijen 5. This is because the basis for the selection of the value of difbot was that the predicted effluent solids mass lost matched that measured. This means that, for fixed values of α_1, α_2 and diftop, difbot has a unique value which will ensure that the predicted effluent solids mass loss matches the measured mass.

The sensitivity of the program to the value of difbot means that the precise determination of this parameter is critical for accurate predictions. The function that is used to calculate the value of difbot was developed on the basis of only five data points and selected because it is simple and directly related to the phenomenon that causes turbulent diffusion i.e. the feed flow rate. Considering the five Rijen simulations as a whole, and taking into account that all the important results of the simulations were examined: underflow concentration, manner of effluent solids loss, time of first gross effluent solids loss, sludge blanket level and rise rate and concentration depth profile, surprisingly good simulations were obtained with the model. Indeed, remembering that the programme is a single dimension model seeking to simulate full scale tanks with large diameter to depth ratios where solids and liquid flows are not only in the vertical direction, it would be unrealistic to expect it to give much better simulations. The inclusion of diffusivity, which is used as a lumped parameter for all the different effects in the settling tank that cause disturbance and mixing such as density currents, hydraulic flows, weir effects, temperature differences, viscosity changes, turbulence,

etc. appears to go a long way to introducing the necessary degree of deviation from the idealized hyperbolic (non-diffusivity) case. The simple linear difbot/feed flow relationship produced a satisfactory multiple correlation coefficient ($r^2 = 0.921$), t statistic and simulations. Further investigation into the form and influencing factors of the diffusivity function fail to reveal any other parameters that significantly affect difbot on their own. There were also no factors that improved the linear relationship by being included with the feed flow term. Thus, although the equation for determining difbot is simple, it nonetheless was found to be the best possible relationship that could be derived from the available information.

A further factor in favour of the established diffusivity function is that the Rijen tests are severe tests of the simulation program. The duration of all the tests is relatively short (not more than 7 hours), and the simulations were initiated with idealized discontinuous initial conditions (step changes in the initial concentration profile). The initial conditions significantly affect the progress of the simulation results because the redistribution of sludge mass in the settling tank to overcome the effect of discontinuities in the initial sludge concentration depth profile is barely accomplished before the test is ended. In addition, the tests themselves consisted of step changes in the influent flow to the settling tank. This allows no opportunity for discontinuities to be propagated out of the system, as the system is continuously acted upon by step changes in the forcing function, which prevents it from reaching any equilibrium.

In real time simulations, the duration of the tests will almost certainly be longer (up to 10 days). This will reduce the influence of the initial conditions on the final predictions and the final results will be far more significantly influenced by the operating parameters themselves. In addition, it is unlikely that the forcing functions for real time simulations will be step changes. They are more likely to consist of gradually changing influent flows and feed concentrations, with an occasional peak representing storm flow. Under these conditions, there will be ample opportunity for dynamic steady state to be established in the settling tank.

The simulations have so far been only at the Rijen full scale (45.5m diameter) settling tank. Because the same settling tank was used for all the tests, and α_2 and diftop are fixed for a particular tank, it was not possible to establish the manner in which α_2 and diftop change for different tanks. To establish this, other settling tank tests needed to be simulated. Unfortunately, the STORA data presents only two other overloaded cases, i.e. at the settling tanks at

1. Wijk bij Duurstede and
2. Uden - Veghel

It was decided to use the test at Wijk bij Duurstede (hereafter referred to as Wijk) to establish how α_2 and diftop change for a different tank. Following this, the generality of the equation for determining difbot would also be examined. Finally the test at Uden - Veghel would be used to evaluate the validity of the general equations developed for determining α_2, diftop and difbot.

8.11 CALIBRATION OF α_1, α_2 AND DIFTOP IN TERMS OF GEOMETRY WITH THE TEST AT WIJK BIJ DUURSTEDE

It was established in the previous tests that, for the Rijen tank, α_2 and diftop could be fixed at constant values. This finding, which appeared reasonable in terms of the nature of diffusivity in the settling tank, led to the hypothesis that α_2 and diftop are related to the geometry of the settling tank. The simulation of the settling tank test at Wijk served to determine how α_2 and diftop change with changing tank dimensions.

The settling tank test at Wijk was carried out for a total of 5 hours, with the influent flow running into the settling tank throughout the test. The flux theory constants, V_o and n, were calculated from the measured $SSVI_{3.5}$ using the relationship for extended aeration plants derived in Chapter 4. From the measured $SSVI_{3.5}$ of $80 ml g^{-1}$, the equations give $V_o = 6.974 m h^{-1}$ and $n = 0.342 m^3 kg^{-1}$. With these values of V_o and n, the flux theory indicated that the settling tank was overloaded for the first 2.25h of the test. Thereafter it was underloaded due to the decrease in feed concentration as the test progressed. The data measured by STORA for the Wijk test is given in Table 8.17 and a summary of the operating parameters is presented in Table 8.18.

Table 8.17 Data measured by STORA for the Wijk bij Duurstede test

Test: Wijk bij Duurstede Begin test: 11:15h
Date: 20 November 1979 End test: 16:05h

Q_i = 900m^{3}h^{-1} Q_r = 350m^{3}h^{-1}

Time (h)	Feed conc (kg/m^3)	Underflow conc (kg/m^3)	Effluent conc (mg/l)	Sludge blanket height (m)	Remarks
11:15					influent started
11:20		5.4			
11:40	5.5	6.4			
12:00		7.5			
12:10				1.25	
12:20	5.0	8.9			
12:30				1.25	
12:40		10.0			
12:50				1.15	
13:00	4.4	10.3			
13:10				1.00	
13:20		10.0			
13:30			12.2	1.00	
13:40	3.8	10.3			
13:50				0.90	
14:00		10.0			
14:10			7.30	0.85	
14:20	3.6	10.3	4.8		
14:30			10.5	0.75	
14:40		10.6			
14:50				0.75	
15:00	3.3	10.3	156		
15:10				0.75	
15:20		12.0?			
15:30			286	0.75	
15:40	3.3	12.0?			
15:50				0.80	
16:05	3.1	214			influent stopped

The initial conditions for the simulation of the Wijk test are illustrated in Figure 8.50 and were generated in the same way as those for the Rijen tests.

The next step was to determine how the values of α_2 and diftop change with the changing dimensions of the tank. The dimensions of the settling tank at Wijk compared to those of the Rijen tank are set out in Table 8.19.

From Table 8.19 it can be seen that the Wijk settling tank is smaller in all dimensions than the Rijen settling tank, with the Rijen tank having more than 2.3 times the volume and 1.6 times the area of the Wijk tank.

Table 8.18 Summary of operating parameters for Wijk bij Duurstede

PARAMETER	VALUE
Q_i	$900m^3h^{-1}$
Q_r	$350m^3h^{-1}$
X_o (max) (start)	$5.5kgm^{-3}$
X_o (min) (end)	$3.1kgm^{-3}$
Area	$1000m^2$
Depth (from overflow weir to bottom of tank)	2.183m
Feed point layer	5
Duration of test	5 hours
$SSVI_{3.5}$	$80mlg^{-1}$
DSVI	$75mlg^{-1}$
V_o	$6.974mh^{-1}$
n	$0.342m^3kg^{-1}$

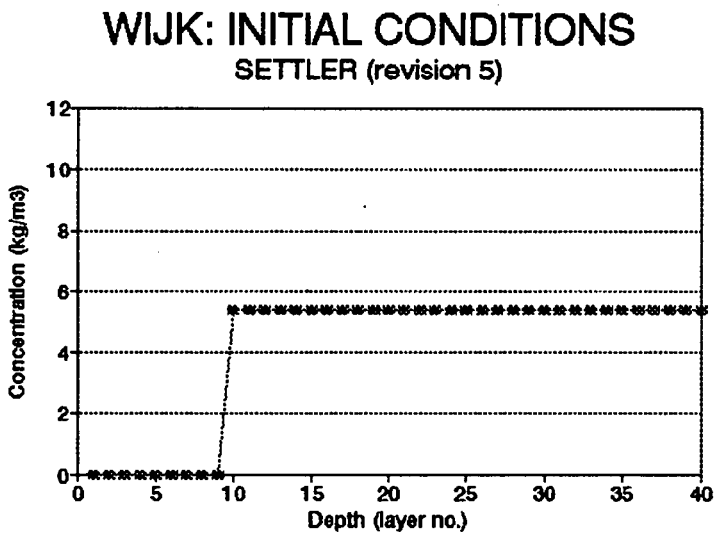

Figure 8.50 Initial concentration profile for Wijk

Table 8.19 Dimensions of the Wijk settling tank relative to the Rijen tank

PARAMETER	WIJK	RIJEN	RATIO (RIJEN/WIJK)
Volume (m^3)	1990	4690	2.357
Area (m^2)	1000	1625.97	1.626
Depth (m)	2.183	3.35	1.535

Because there is little quantitative literature on the changes in turbulence and diffusivity with changes in geometry of settling tanks, the dependence of α_2 and diftop were evaluated empirically from the results of trial and error experimentation with the simulation program and an assessment of the reasonableness (or not) of the results obtained.

For the earlier simulations on the Rijen tank, it was found that the simulation results were quite insensitive to changes in the α_1 value i.e. the die off rate of the diffusivity above the feed point. This insensitivity was kept in mind with the Wijk simulations and tested from time to time as empirical functions in terms of settling tank geometry for diftop and α_2 (the die off rate of the diffusivity below) were developed. It also should be noted that the α_1 and α_2 values determined for the Rijen tank were specified in terms of $layer^{-1}$ and equivalent m^{-1} units. It was realised that, because tanks with different depths (and areas) were now being simulated, the 40 layers into which the tank is divided would be shallower for a smaller tank and deeper for a larger tank. This means that, if α_1 and α_2 are specified as $layer^{-1}$, the die off rate for shallower tanks will effectively be faster due to the shallower tank depth. This was kept in mind as the empirical functions for relating α_2 and diftop to the settling tank dimensions were developed. Although from the Rijen simulations it was found that the influence of α_1 on the simulation results was small, it nevertheless does influence the total diffusivity in the tank in the following way: a large value of α_1 means that the die off rate of diffusivity above the feed point is fast, causing the total diffusivity in the upper

layers of the tank to be small; a small value of α_1 means that the die off rate of diffusivity above the feed point is slow, causing the total diffusivity in the upper layers of the tank to be large. Generally, the greater the amount of diffusivity above the feed point, the greater the degree of mixing in these layers. A small value of α_1 reduces the time between the sludge blanket reaching the top of the tank and the onset of solids loss with the effluent. As discussed earlier for the Rijen tests, a delay in onset of solids loss arises because sludge accumulation in the upper layers continues until the sludge has reached the critical concentration. Once the critical concentration has been reached, then solids loss occurs with the effluent. It was found that the higher the total diffusivity in the upper layers of the tank, the lower the critical concentration at which onset of solids loss commences.

In the trial and error simulations, it was found that it was generally necessary to delay the onset of failure rather than to accelerate it, thus necessitating a high α_1 value. As discussed earlier in the Rijen tests, the value of difbot also influences the time of failure since difbot influences the total diffusivity in the tank. Consequently there is a considerable degree of interaction between the three diffusivity constants which determine the total diffusivity in the settling tank. Considering that (i) α_1 affects the diffusivity in the layers above the feed point only which is small part of the settling tank (5 out of 40 layers) and (ii) a fast die off rate is required to allow the correct critical concentration above the feed point to develop and (iii) inaccuracies in the α_1 value will be counteracted by fine tuning of the difbot value, it was concluded that the best results would be obtained when (i) α_1 remained at the $10 layer^{-1}$ value found for the Rijen tests and (ii) would remain specified per layer even though this means a greater diffusivity die off rate in terms of m^{-1} due to the shallower tank depth for the Wijk tank. It would have been preferable to find that an "absolute" diffusivity die off rate in m^{-1} units gave the best simulation results, but the trial and error simulations indicated that this was not the case. Consequently, for the Wijk and other settling tanks, an α_1 value of $10 layer^{-1}$ was accepted as a general value. This means that, for the layers between the top of the settling tank and the feed point, the diffusivity dies off by the same degree irrespective of the depth of the feed point. For all the settling

tanks simulated in this investigation, the feed point depth was retained at layer 5. The effect on the simulation results of changing the feed point layer is discussed in Section 8.17. Maintaining a constant value for α_1 for all the tests was not considered to be a serious deficiency in the program, as it was considered that the change in diffusivity with both tank dimensions and operating parameters was adequately modelled with the diftop, α_2 and difbot values.

With regard to the α_2 and diftop values, it was hypothesised that the value of diftop increases as the size of the tank decreases. This hypothesis is based on the supposition that the effect of the diffusivity at the feed point would be relatively more powerful for the same feed flow should it enter a tank with smaller dimensions, both surface area and volume. It was also hypothesised that α_2 increases as the size of the settling tank decreases. This means that, for smaller tank dimensions, the effect of the diffusivity below the feed point will die away more quickly with distance from the feed point so that the function for diffusivity in the bottom layers of the tank (difbot) will start to be effective higher up in the tank. This hypothesis stems from the fact that α_2 and diftop govern only the diffusivity at and around the feed point and not the bottom layers of the tank. Thus, for a smaller tank, α_2 will need to die away more quickly to ensure that the phenomenon of diffusivity at the feed point does not extend too far down the tank and interfere with the diffusivity in the bottom layers. In addition, it was found that low values of α_2 cause the diffusivity function to die away too slowly, resulting in an inaccurate pattern of effluent solids loss and poor sludge concentration depth profiles. Thus, in scaling the variables to account for the smaller tank size, care needed to be taken to ensure that the new α_2 value was not so low that it caused this phenomenon when scaled for a smaller settling tank. Although these proposals give some guidelines as to how α_2 and diftop should change with changing tank size, they give no indication as to which dimensions of the settling tank are important in scaling the values of α_2 and diftop.

The effect of basing the values for α_2 and diftop on the three major dimensions of the Wijk tank and two combinations of the area and volume dimensions was investigated.

The scaled versions of α_2 and diftop for each of the dimensions (depth, area and volume) and two combinations of the area and volume dimensions are presented in Table 8.20. The units of α_2 were maintained as layer^{-1} for similar reasons to those motivated earlier for retaining the units of α_1 as layer^{-1}.

Table 8.20 Scaled up values of α_2 and diftop for the Wijk test

PARAMETER:	SCALED ON THE BASIS OF:	DIMENSIONS		RATIO: RIJEN/ WIJK	VALUE
		RIJEN	WIJK		
diftop	depth	3.35m	2.183m	1.5345	184150 m^2h^{-1}
α_2	depth	3.35m	2.183m	1.5345	2.302$layer^{-1}$
diftop	area	1625m^2	1000m^2	1.6259	195116 m^2h^{-1}
α_2	area	1625m^2	1000m^2	1.6259	2.439$layer^{-1}$
diftop	volume	4690m^3	1990m^3	2.3568	282814 m^2h^{-1}
α_2	volume	4690m^3	1990m^3	2.3568	3.535$layer^{-1}$
diftop	area	1625m^2	1000m^2	1.6259	195116 m^2h^{-1}
α_2	volume	4690m^3	1990m^3	2.3568	3.535$layer^{-1}$
diftop	volume	4690m^3	1990m^3	2.3568	282814 m^2h^{-1}
α_2	area	1625m^2	1000m^2	1.6259	2.439$layer^{-1}$

For example, in order to scale diftop on the basis of depth, the value of diftop for the Rijen test (120000m^2h^{-1}) was multiplied by the ratio of the depth of the Rijen tank to the depth of the Wijk tank. See Equation (8.14).

$$\begin{aligned} diftop_{WIJK} &= diftop_{RIJEN} * \frac{depth_{RIJEN}}{depth_{WIJK}} \\ &= 120000 * \frac{3.35}{2.183} \\ &= 184150 m^2h^{-1} \end{aligned} \qquad (8.14)$$

The Wijk test was simulated with each of the five α_2 and diftop pairs in Table 8.20 and the predicted results examined. For each of the simulations, the value of difbot was uniquely determined by trial and error to ensure that the predicted effluent solids mass lost corresponded with the measured results. It was not possible to use the equation for calculating difbot developed in Section 8.4 because this equation is

specific to the values of α_2 and diftop determined for the Rijen tests and thus specific to the geometry of the Rijen tank. The equation for difbot will be extended later to apply to other tank geometries and thus to other values of α_2 and diftop. The size of the CSTR for the thickening zone was scaled down on the basis of the smaller size of the Wijk tank. The cross sectional area of the CSTR is determined by the cross sectional area of the Wijk tank ($1000m^2$). The depth of the CSTR was scaled downwards directly proportionally to account for the smaller depth of the Wijk tank (2.183m) compared to that of the Rijen tank (3.35m). As the CSTR depth for the Rijen tank was set at 1m, the CSTR depth for the Wijk tank was reduced proportionally to 0.651m. The five diffusivity constant sets for each of the tests, with α_2 in terms of $layer^{-1}$ being the scaled parameter, are set out in Table 8.21.

Table 8.21 The five different sets of diffusivity constants to be used for the test carried out at Wijk

TEST NAME	DIFTOP (m^2h^{-1})	α_2 ($layer^{-1}$)	DIFBOT (m^2h^{-1})
Wijk D (depth)	184150	2.302	0.446
Wijk A (area)	195116	2.439	0.446
Wijk V (volume)	282814	3.535	0.477
Wijk AV	195116	3.535	0.450
Wijk VA	282814	2.439	0.420

where depth of layer for the Wijk tank = 0.0545m

$\alpha_2(m^{-1})$ = $\alpha_2(layer^{-1})$/layer depth

Wijk D = both diftop and α_2 scaled on the basis of depth

Wijk A = both diftop and α_2 scaled on the basis of area

Wijk V = both diftop and α_2 scaled on the basis of volume

Wijk AV = diftop scaled on the basis of area and α_2 scaled on the basis of volume

Wijk VA = diftop scaled on the basis of volume and α_2 scaled on the basis of area

Because of the relative insensitivity of the simulation results to the α_2 and diftop values, all the scaleup methods give essentially the same results. This is reflected in the similarity of the difbot values.

Scaling both diftop and α_2 on the basis of depth (Wijk D) was immediately rejected as a scale up method because the diffusivity in the settling tank cannot be completely characterised by this dimension on its own. It is apparent, at least intuitively, that the cross sectional area of the settling tank plays a major role in influencing the total diffusivity in the tank, and it would be incorrect to exclude it from the scale up method. Scaling diftop and α_2 on the basis of volume only (Wijk V) and area and volume (Wijk AV) were also rejected as scale up methods because they lead to what is considered to be an unrealistically high value for α_2 (3.535layer^{-1}). The remaining scaling methods are Wijk A (area only) and Wijk VA (volume and area). The final sludge concentration depth profile generated with these two scale up methods is illustrated in Figure 8.51.

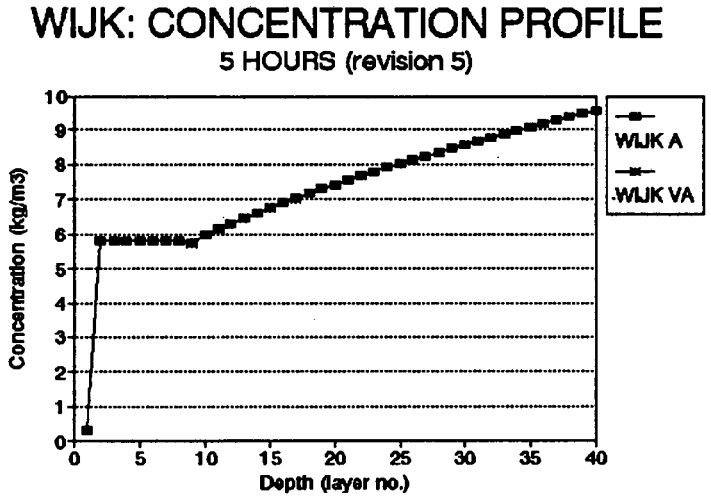

Figure 8.51 Sludge concentration depth profile for Wijk with two different sets of diffusivity constants

The STORA data does not present any sludge concentration depth profiles for the Wijk test, so it is not possible to compare the predicted results with measured values. However, it is possible to assess the performance of SETTLER on the basis of the expected shape of the concentration profile for these operating conditions. Almost identical results were obtained for both sets of diffusivity constants, both showing a well developed sludge blanket extending through most of the tank as well as reasonable underflow and effluent concentrations.

The sludge blanket rise rate for both sets of diffusivity constants was also examined. The predicted results are compared with the measured results in Figure 8.52. Both sets of diffusivity constants give identical results.

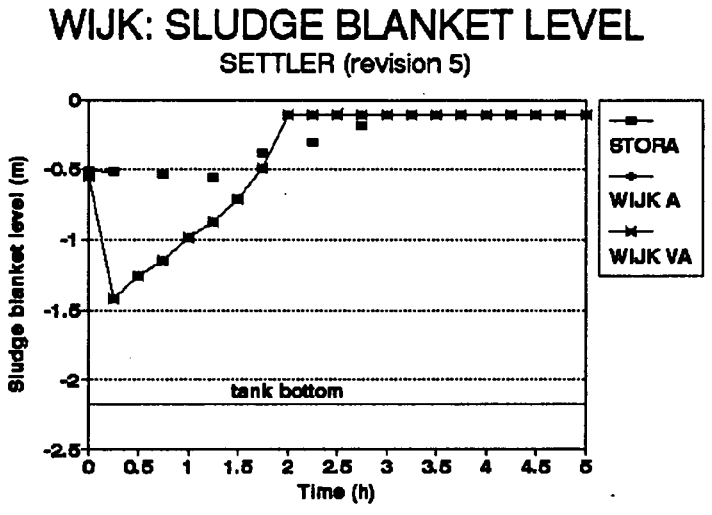

Figure 8.52 Sludge blanket level for Wijk with two different sets of diffusivity constants

On the basis of these findings it seems that there is very little to choose between the two sets of diffusivity constants. Intuitively, it appears necessary to include the depth of the settling tank in the scale up for at least one of the diffusivity constants, as it is apparent that if the feed flow is high and the cross sectional area and depth are both small, there will be a high degree of diffusivity in the tank at the feed point. Conversely, if the cross sectional area and depth of the tank are large, the turbulent effect of a high feed flow to the tank will be less, as it has a relatively greater tank

volume in which to disperse. Consequently, Wijk VA was chosen as the scale up method, implying that α_2 is cross sectional area dependent and diftop is both cross sectional area and depth dependent.

The results of the simulation at Wijk with area as the scale up basis for α_2 and volume as the scale up basis for diftop were then isolated and evaluated. The values of α_2, diftop and difbot are given in Table 8.21 (Wijk VA). The parameters examined for the Wijk test are the same as those for the Rijen 1 test i.e. sludge blanket level, underflow concentration and effluent solids concentration. No sludge concentration depth profiles were measured, so only these three parameters could be examined.

1. Sludge blanket level

Figure 8.53 compares the measured and predicted sludge blanket levels for the Wijk test.

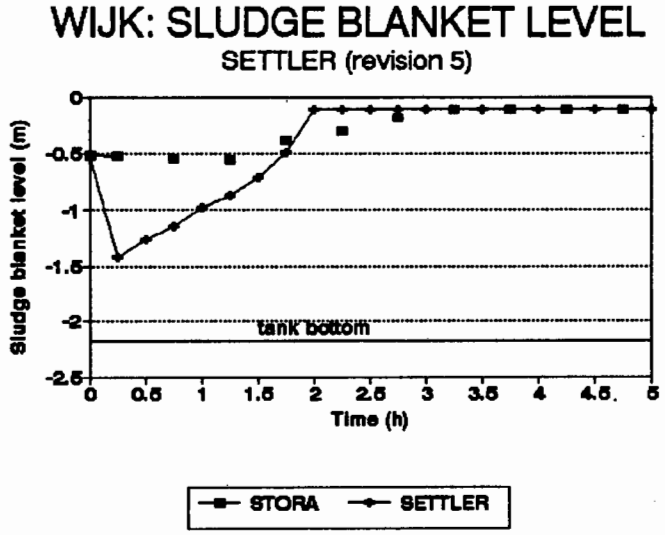

Figure 8.53 Predicted and measured sludge blanket levels for Wijk with SETTLER (revision 5)

The predicted sludge blanket level initially drops from 0.546m below the surface at the start of the test to 1.419m at 0.25h into the test. Thereafter the sludge blanket level rises steadily to reach its maximum height of 0.109m (layer 2) below the surface at 2h

into the test. After 2h, the sludge blanket level remains constant at this value, which is effectively the top of the tank, until the end of the test.

The measured sludge blanket level remains fairly constant at approximately 0.5m for the first 1.5h of the test. Thereafter the sludge blanket level rises slowly to reach its maximum level of 0.109m (effectively the top of the tank) at 3.25h into the test. From 3.25h until the end of the test, the sludge blanket remains at this level.

As for the Rijen tests, the correspondence between measured and predicted sludge blanket rise rate is fairly good, although the predicted sludge blanket level reaches the top of the tank earlier than measured, in this case 1.25h earlier. However, although the predicted sludge blanket reaches the top of the settling tank sooner, failure does not occur until considerably later on in the test (see discussion of effluent concentration results). For the measured results (the Rijen tank also), generally there is no delay between the sludge blanket reaching the top of the tank and the onset of solids loss with the effluent.

2. Underflow concentration

Figure 8.54 compares the measured and predicted underflow concentrations for the Wijk test.

The predicted underflow concentration increases relatively rapidly from 5.4kgm^{-3} at the start of the test to 9.33kgm^{-3} at 2h into the test. Thereafter, the predicted rate of increase of the underflow concentration is very gradual. The maximum predicted underflow concentration of 9.56kgm^{-3} is reached at the end of the test.

The measured underflow concentration rises rapidly from 5.4kgm^{-3} at the start of the test to 10.3kgm^{-3} at 2h into the test. Thereafter, the measured underflow concentration fluctuates around 10.3kgm^{-3} until 4.25h into the test. At 4.25h, the measured underflow concentration rises to 12kgm^{-3}, where it remains until the end of the test.

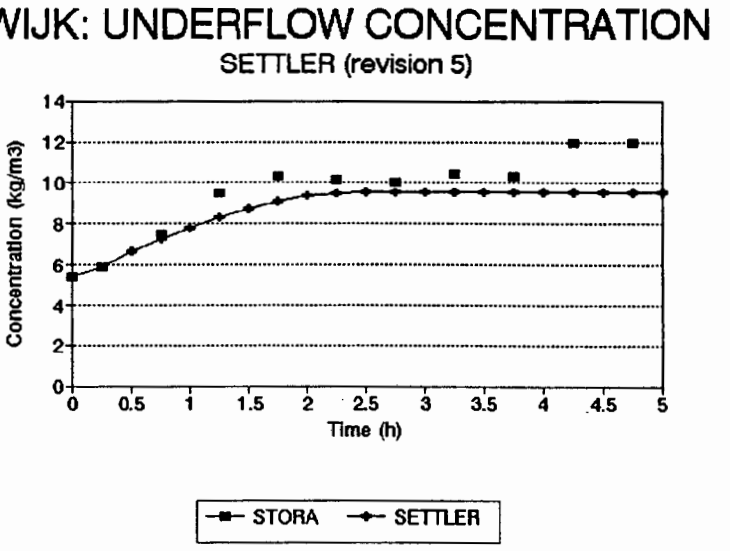

Figure 8.54 Predicted and measured underflow concentrations for Wijk with SETTLER (revision 5)

The correspondence between measured and predicted results for this parameter is very good. The general trend of the measured results is accurately reflected by the predicted results, although the fluctuations in the measured results are not reflected in the predicted results. The predicted results appear to be slightly overdamped, as the predicted underflow concentration is consistently less than the measured underflow concentration. This could possibly be corrected by reducing the depth of the thickening zone.

3. Effluent concentration

Figure 8.55 compares the measured and predicted effluent solids concentration profiles for the Wijk test.

The predicted results show a negligible effluent solids concentration until 3.75h into the test, when a sudden increase in effluent solids loss is predicted. The effluent solids concentration increases steadily from 44.8mgl^{-1} at 3.75h to 302mgl^{-1} at 5h. The total predicted effluent solids mass lost is 306kg, 1.17% of the total solids mass processed by the settling tank during the test.

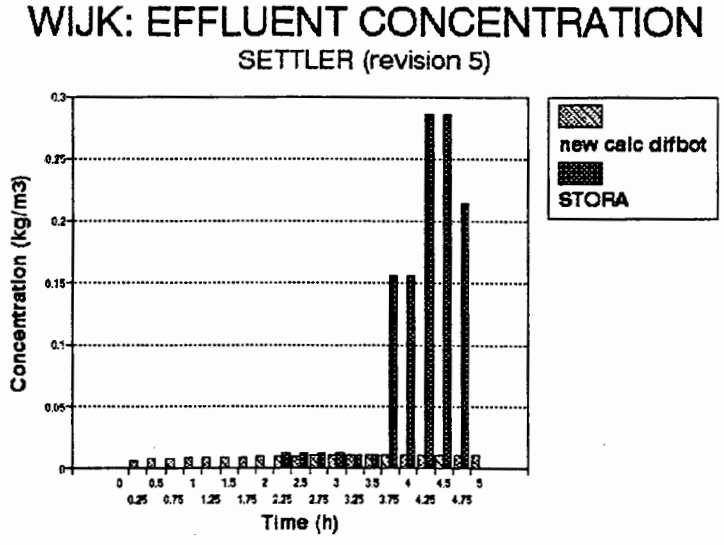

Figure 8.55 Predicted and measured effluent concentrations for Wijk with SETTLER (revision 5)

The measured effluent solids concentration is negligible until 3.75h into the test, when an effluent solids concentration of 156mgl^{-1} is measured. Thereafter, the peaks in effluent solids concentration continue until 4.75h, when the final peak of 214mgl^{-1} is measured. The total measured effluent solids mass lost is 295kg, 1.14% of the solids processed by the settling tank during the test.

The correspondence between measured and predicted results for this parameter is good. Both the time and manner of failure are accurately predicted by SETTLER. The fact that the predicted effluent solids mass lost matches the measured value so closely is due to the fact that, as in the Rijen simulations, the difbot value was selected to achieve this.

8.11.1 CONCLUSIONS FOR THE WIJK TEST SIMULATION

The correspondence between measured and predicted parameters for the Wijk test is generally good. Although the predicted sludge blanket level reaches the top of the tank earlier than the measured sludge blanket level, this is not a major cause for concern, as predicted failure only occurs much later on in the test and corresponds with the

measured time of failure. As discussed earlier, once the predicted sludge blanket level has reached the top of the tank, it is still possible for the mass of sludge in the tank to increase before failure occurs.

The correspondence between measured and predicted underflow concentrations is good, with the general trend of the measured underflow concentration being accurately reflected in the predicted results.

The effluent solids mass lost is accurately predicted, although it should be born in mind that the value of difbot for this test was chosen on the basis of its ability to accurately predict this parameter. However, the manner in which the effluent solids mass is lost is not governed by difbot, but by α_2 and diftop. The fact that the manner of effluent solids mass loss is correctly predicted by the program indicates that appropriate values of α_2 and diftop were selected for SETTLER. Thus, the scaling procedure used to determine the magnitude of α_2 and diftop appears to be quantitatively acceptable.

From this simulation it was concluded that the hypothesis regarding the tank geometry dependence of α_2 and diftop is valid. It remains therefore to integrate the relationship between tank geometry and the α_2 and diftop diffusivity parameters with the relationship between feed flow and difbot in order to develop a function allowing the diffusivity parameters to be calculated for different circular settling tanks. This development is presented in the next section and checked with the Uden - Veghel settling tank test.

8.12 DEVELOPING EQUATIONS FOR α_2 AND DIFTOP FOR ANY SETTLING TANK

At the outset it should be stated that the data available for developing equations relating α_2 and diftop to the dimensions of a settling tank is somewhat limited. Any functions proposed are therefore only tentative, and should not be considered to be more than general guidelines. Because only two different settling tanks (Rijen and Wijk) have been simulated, only two different values of α_2 and diftop are available. The two values are set out in Table 8.22.

Table 8.22 Values of α_2 and diftop for the Rijen and Wijk tests

TEST	α_2 (layer^{-1})	DIFTOP (m^2h^{-1})
RIJEN	1.5 (17.94m^{-1})	120000
WIJK	2.439 (44.67m^{-1})	282814

There are an infinite number of possible mathematical relationships that can link these points and, because there are only two, it is impossible to identify which is the most appropriate. Because of the limited data, initially the simplest possible relationship was adopted and the two points were joined by a straight line. If this is found to be inadequate, then more settling tank calibration tests and more complex mathematical relationships would be required to develop empirical functions relating the diffusivity constants to settling tank dimensions and operating parameters.

The two linear relationships proposed for α_2 and diftop respectively are illustrated in Figure 8.56 and Figure 8.57 respectively. These relationships are intended only to reflect the general trend of the change in α_2 and diftop with changing cross sectional area and volume. The general trend is that α_2 and diftop are inversely proportional to cross sectional area and volume respectively.

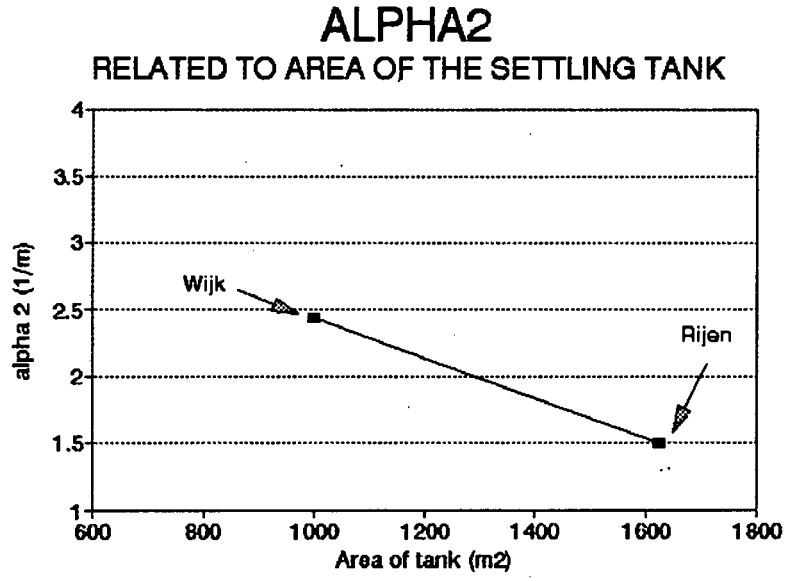

Figure 8.56 **Relationship of α_2 to cross sectional area of the settling tank where the diameters of the Wijk and Rijen tanks are 35.7 and 45.5m respectively**

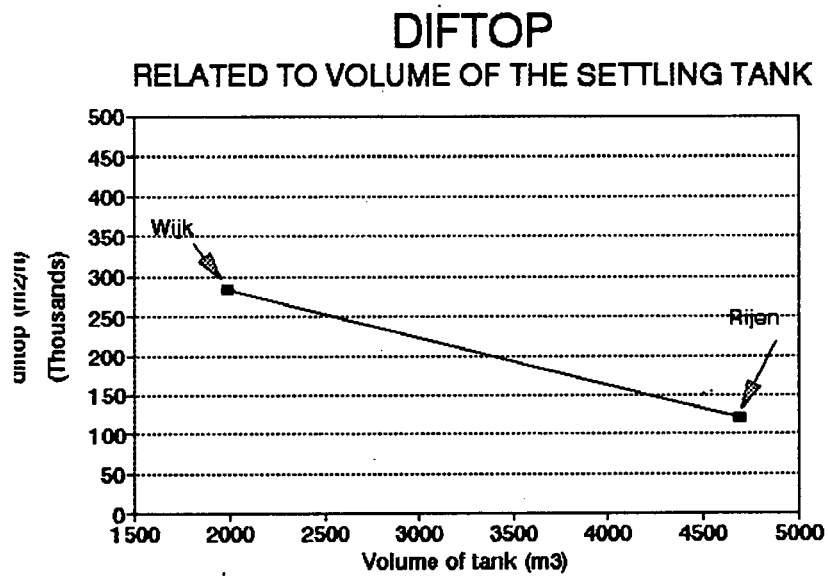

Figure 8.57 **Relationship of diftop to volume of the settling tank**

The equation of the line for α_2 is:

$$\alpha_2 = 3.939 - 0.0015 * A \text{ (in } m^2) \qquad (8.15)$$

The equation of the line for diftop is:

$$\text{diftop} = 402814 - 60.30 * V \text{ (in } m^3) \quad (8.16)$$

Obviously, these relationships cannot be applied indiscriminately, as their frame of reference is extremely small. However, because the slopes of both the lines are relatively flat, this indicates that α_2 and diftop are not very sensitive to changing settling tank dimensions and remain fairly constant over the expected range of areas and volumes for full scale settling tanks. This relative insensitivity to α_2 and diftop has been corroborated in the simulation results presented so far and therefore it seems that the danger of obtaining incorrect values by interpolation is not very great.

8.13 DEVELOPING AN EQUATION FOR DIFBOT FOR ANY SETTLING TANK

Previously (see Section 8.4) a linear relationship was developed for the Rijen tank whereby the value of difbot could be calculated as a function of the feed flow rate (Q_i+Q_r). The relationship developed is

$$\text{difbot} = -2.995 + 0.0019 * (Q_i+Q_r) \quad (8.17)$$

As stated earlier, Equation (8.17) applies exclusively for the α_2 and diftop values determined for the geometry of the Rijen tank i.e. $\alpha_2 = 1.5 \text{layer}^{-1}$ and diftop $= 120000 m^2h^{-1}$ respectively. For the Rijen 1 test it was found that the necessary value of difbot changed if the values of α_2 and diftop changed. This confirmed that difbot for the Rijen tank is dependent on the values of α_2 and diftop and therefore also on the tank dimensions. In order to transform Equation (8.17) so that it can be applied to other settling tanks, the terms α_2 and diftop must be made explicit in the equation.

It has been found from the Rijen tests that the necessary value of difbot decreases with increasing diftop and decreasing α_2 i.e. the higher the total diffusivity in the top of the tank the lower the required diffusivity in the bottom of the tank. This makes difbot inversely proportional to diftop and directly proportional to α_2. Therefore, if diftop and

α_2 are to be included explicitly in the difbot equation, diftop should appear in the denominator and α_2 should appear in the numerator.

In addition, the relative influence of the feed flow term on the value of difbot in Equation (8.17) depends on the cross sectional area of the tank. If both the feed flow and the cross sectional area of the tank are small, then the relative influence of the feed flow on difbot is great i.e. difbot is large. Conversely, if the feed flow is small and the cross sectional area is large, then difbot is small. This suggests that the feed flow term should be scaled on the basis of the cross sectional area, which should appear in the denominator of the proposed function. This approach also ensures that the equation may be used to calculate a value of difbot that is dimensionally consistent.

The form of the proposed equation is one which expresses difbot as a function of settling tank area, feed flow rate, α_2 and diftop as follows:

$$\text{difbot} = L + M * \left[\frac{Q_i+Q_r}{A}\right]\left[\frac{\alpha_2}{\text{diftop}}\right] \qquad (8.18)$$

where L, M = constants determined by linear regression (m^2h^{-1}) and ($m^3layerh^{-1}$)

(Q_i+Q_r) = feed flow rate to the settling tank (m^3h^{-1})

A = cross sectional area of the settling tank (m^2)

α_2 = diffusivity constant ($layer^{-1}$)

diftop = diffusivity constant (m^2h^{-1})

In order to determine the values of the constants L and M in Equation (8.18), the relevant parameters from the five Rijen simulations and the simulation at Wijk were grouped together as illustrated in Table 8.23, where the difbot value was that determined from simulations to give the best simulation results compared with the measured results.

Table 8.23 Relevant parameters for the STORA simulations

TEST	Q_i+Q_r (m^3h^{-1})	AREA (m^2)	α_2 ($layer^{-1}$)	DIFTOP (m^2h^{-1})	SLOPE FACTOR (m^{-2})	DIFBOT (m^2h^{-1})
RIJEN 7	1731	1625.97	1.5	120000	1.331E-5	0.423
RIJEN 4	1956	1625.97	1.5	120000	1.504E-5	0.579
RIJEN 8	2206.5	1625.97	1.5	120000	1.777E-5	1.476
RIJEN 1	2311	1625.97	1.5	120000	1.696E-5	1.367
RIJEN 5	2431.5	1625.97	1.5	120000	1.869E-5	1.693
WIJK	1250	1000	2.439	282814	1.078E-5	0.420

where

$$\text{slope factor (in Table 8.23)} = \frac{Q_i+Q_r}{A} * \frac{\alpha_2}{\text{diftop}} \qquad (8.19)$$

A linear regression was carried out with difbot on the slope factor. The multiple correlation coefficient for the regression was found to be $r^2 = 0.834$, which means that the regression equation explains 83.4% of the total variance in the slope factor data. The t value for the estimate of the slope of the regression line was found to be 4.480, compared to a critical t value of $t(4,0.975) = 2.776$, indicating that the null hypothesis (that there is no relationship between the slope factor and difbot) can be rejected. This t value gives a probability level of 0.00830, indicating that there is a 99.2% probability of being correct in accepting that there is a linear relationship between the slope factor and difbot. Figure 8.58 shows the regression of difbot on the slope factor with the 95% confidence limits indicated. Also shown are the real difbot values and the previously calculated difbot values for the Rijen tanks (see Table 8.24). Therefore, the functional relationship accepted for difbot is:

$$\text{difbot} = -1.73781 + 176981.6 * \frac{(Q_i+Q_r)}{A} * \frac{\alpha_2}{\text{diftop}} \qquad (8.20)$$

This functional relationship can be applied to any settling tank. Provided the cross sectional area of the tank is known, α_2 and diftop can be calculated from Equations (8.15) and (8.16). Then, with a knowledge of the feed flow rate, Equation (8.20) can

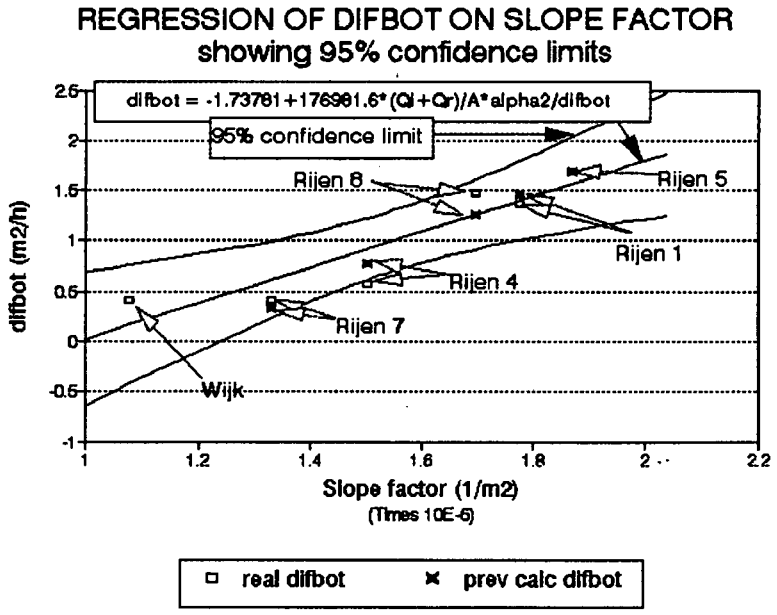

Figure 8.58 Regression of difbot on the slope factor

be used to calculate the value of difbot for any settling tank. Table 8.24 shows the calculated values of difbot for all the Rijen tests and the Wijk test using Equation (8.20).

It can be seen from Figure 8.58 and Table 8.24 that for Rijen 7, Rijen 4 and Wijk the calculated difbot values obtained from the extended empirical function deviate quite considerably (>30%) from the real difbot value. For the remaining three tests, the deviation is less than 15%. From the Rijen tests, it was found that, although the simulation results are very sensitive to difbot, deviations less than 15% did not cause significant inaccuracies in the predicted results. Consequently, except for Wijk, Rijen 7 and Rijen 4, the simulations will remain good.

In order to establish the effect of the deviation of the new calculated values of difbot for Rijen 7, Rijen 4 and Wijk on the simulations, the Rijen 4, 7 and Wijk tests were repeated with the new calculated value of difbot. As expected, it was found that, for the Rijen 4 and 7 tests, the high calculated difbot value caused the sludge blanket rise rate to be too rapid and the onset of predicted failure to be premature. In addition, the total predicted effluent solids mass loss was overpredicted. However, the effect on the

Table 8.24 Table showing real and calculated values of difbot for Rijen and Wijk simulations

TEST	SLOPE FACTOR (m^{-2})	"REAL" DIFBOT (m^2h^{-1})	CALCULATED DIFBOT (m^2h^{-1})	PREVIOUSLY CALCULATED DIFBOT (m^2h^{-1})
RIJEN 7	1.331E-5	0.423	0.617 (+31.44%)	0.342 (-19.10%)
RIJEN 4	1.504E-5	0.579	0.923 (+37.26%)	0.776 (+25.4%)
RIJEN 1	1.777E-5	1.367	1.406 (+2.85%)	1.461 (+6.87%)
RIJEN 8	1.696E-5	1.476	1.264 (-14.37%)	1.259 (-14.70%)
RIJEN 5	1.869E-5	1.693	1.570 (+7.05%)	1.693 (+0%)
WIJK	1.078E-5	0.420	0.170 (-59.5%)	

(where figures in brackets are % deviations from the real difbot values)

underflow concentration and sludge concentration depth profile was not pronounced. To avoid repetitious discussion, a detailed analysis of the results for these tests is not included. However, the general trend of the results is well reflected in the previous analysis of the Rijen 4 test in Section 8.6.

For the Wijk test, the low calculated value of difbot caused the opposite trend, with the sludge blanket rise rate being too slow and the onset of predicted failure being too late. In addition, the total effluent solids mass loss was underpredicted. As for the previous tests, the effect on the underflow concentration and sludge concentration depth profile was not pronounced, and the results were very similar to those with the real value of difbot.

In summary, although the value of difbot exerts a marked influence on the predicted results, its effect is mainly to change the magnitude of the trends observed, but not the trends themselves.

The next step was to simulate the test at Uden - Veghel with calculated values of α_2, diftop and difbot.

8.14 SIMULATING THE TEST AT UDEN - VEGHEL WITH CALCULATED VALUES OF α_2, DIFTOP AND DIFBOT

Unfortunately, there is only one remaining overloaded test documented in the STORA data i.e. the test at Uden - Veghel (hereafter referred to as Veghel). This test was used to check the validity of the equations for the diffusivity constants developed in the above section.

The settling tank test at Veghel was carried out for a total of 3 hours, with the influent flow running into the settling tank throughout the test. The flux theory constants, V_o and n, were calculated from the measured $SSVI_{3.5}$ with the aid of the relationship for extended aeration plants derived in Chapter 3. From the measured $SSVI_{3.5}$ of $90mlg^{-1}$, the equations give $V_o = 6.544mh^{-1}$ and $n = 0.363m^3kg^{-1}$. With these values of V_o and n, the flux theory indicated that the settling tank was overloaded for the first 2.25h of the test. Thereafter, the settling tank was underloaded due to the reduction in feed concentration. The data measured by STORA for the Veghel test is given in Table 8.25 and a summary of the operating parameters is presented in Table 8.26. The initial conditions for Veghel are illustrated in Figure 8.59. These were generated in the same way as for the Rijen tests.

The size of the CSTR for the thickening zone was scaled down on the basis of the smaller size of the Veghel tank. The cross sectional area of the CSTR is fixed by the cross sectional area of the Veghel tank ($1320m^2$). The depth of the CSTR was scaled linearly downwards to account for the smaller overall depth of the Veghel tank which was 2.908m compared with 3.35m for the Rijen tank. Because the CSTR for the Rijen tank was set at 1m, the CSTR depth for the Veghel tank proportionally reduced was calculated to be 0.869m.

Table 8.25 Data measured by STORA for the Uden - Veghel test

Test: Uden - Veghel Begin test: 10:20h
Date: 23 November 1979 End test: 13:10h

Q_i = 1550m^3h^{-1} Q_r = 720m^3h^{-1}

Time (h)	Feed conc (kg/m^3)	Underflow conc (kg/m^3)	Effluent conc (mg/l)	Sludge blanket height (m)	Remarks
10:20					influent started
10:30					
10:40		3.5			
10:50			1.75		
11:00	4.9	3.2			
11:10				1.70	
11:20		3.5			
11:30				1.30	
11:40	4.4	3.7			
11:50			12.5	1.20	
12:00		4.0			
12:10				0.95	
12:20	4.0	3.9			
12:30			390	0.85	
12:40		3.7	390		
13:00	3.4	3.7	390		
13:10			770	0.55	
14:15			770	1.10	

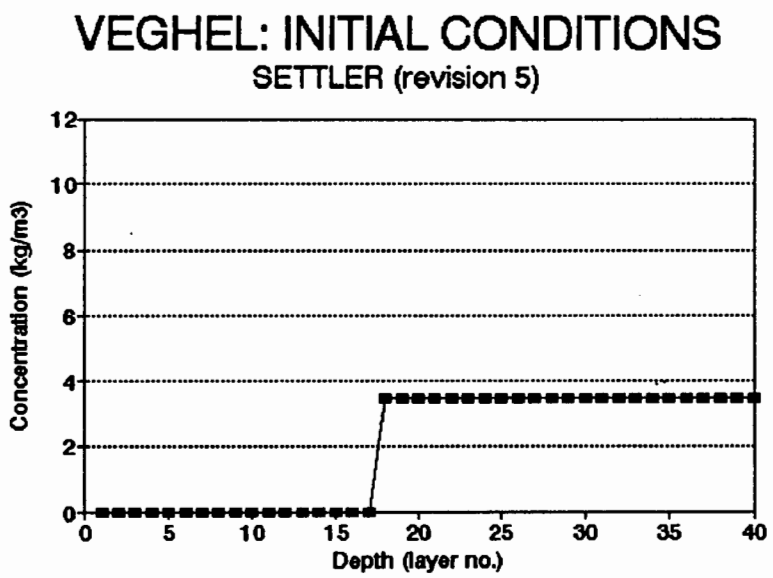

Figure 8.59 Initial concentration profile for Veghel

The value of α_1 was set at 10$layer^{-1}$ as for all the earlier simulations. The values of α_2 and diftop were calculated from Equations 8.15 and 8.16 to be α_2 = 1.959$layer^{-1}$ and 198391m^2h^{-1} respectively. The value of difbot was calculated from Equation 8.18 to be

Table 8.26 Summary of operating parameters for Uden - Veghel

PARAMETER	VALUE
Q_i	$1550m^3h^{-1}$
Q_r	$720m^3h^{-1}$
X_o (max)	$4.9kgm^{-3}$
X_o (min)	$3.4kgm^{-3}$
Area	$1320m^2$
Depth (from overflow weir to bottom of tank)	2.908m
Feed point layer	5
Duration of test	3 hours
$SSVI_{3.5}$	$90mlg^{-1}$
DSVI	$90mlg^{-1}$
V_o	$6.544mh^{-1}$
n	$0.363m^3kg^{-1}$

difbot = $1.267m^2h^{-1}$. The test at Veghel was then simulated with SETTLER (revision 5) and the following parameters extracted and analysed:

1. Sludge blanket level and rise rate
2. Underflow concentration
3. Effluent solids concentration
4. Sludge concentration depth profile at 3h

1. Sludge blanket level

Figure 8.60 compares the measured and predicted sludge blanket levels for the Veghel test.

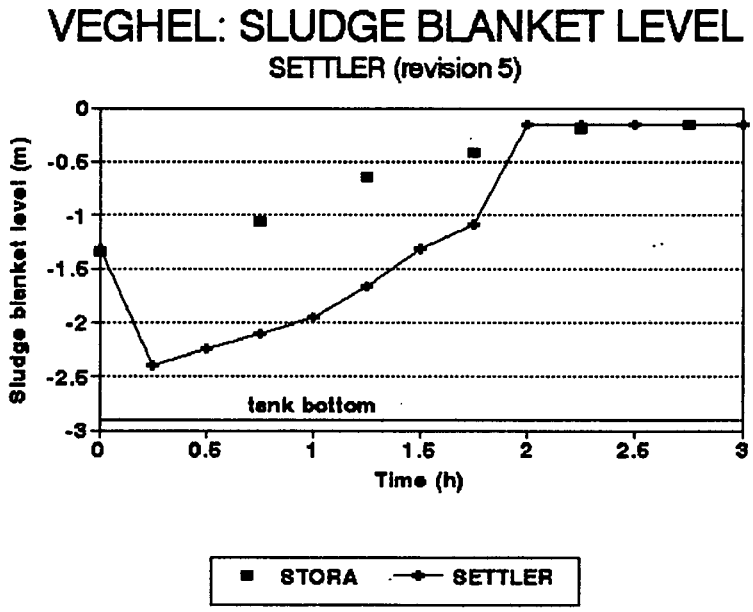

Figure 8.60 **Predicted and measured sludge blanket levels for Veghel with SETTLER (revision 5)**

The predicted sludge blanket level falls from 1.3m to 2.4m below the surface of the tank during the first 0.25h as the sludge redistributes itself in the tank to overcome the discontinuities in the initial concentration profile. It then rises rapidly to reach 0.145m (effectively the top of the tank) at 2h after the start of the test. From 2h until the end of the test at 3h, the sludge blanket level remains constant at 0.145m.

The measured sludge blanket rises progressively from 1.35m below the surface at the start of the test to 0.65m below the surface at 1.25h after the start of the test. Thereafter, the sludge blanket rises slowly to attain its maximum height of 0.145m (effectively the top of the tank) at 2.75h into the test.

Apart from the initial drop in the sludge blanket level, there is a reasonable correspondence between the measured and predicted sludge blanket rise rates from 0.25h until 2h into the test. However, because of the initial drop in predicted sludge blanket level, there is a phase difference between the predicted and measured sludge blanket levels for the remainder of the test. The predicted sludge blanket level reaches the top of the tank at 2h, whereas the measured sludge blanket level only reaches the

top of the tank at 2.75h. As noted in the earlier simulations, there is a difference between the predicted and measured results with respect to the onset of solids loss with the effluent. For the measured results, there is no delay between the time that the sludge blanket reaches the top of the tank and the onset of solids loss with the effluent, whereas there is with the predicted results. Therefore, the fact that the predicted and measured sludge blankets reach the top of the tank at different times does not mean that the onset of solids loss with the effluent commences at different times. Indeed, in this test, the predicted time of failure is later than the measured time even though the predicted sludge blanket level reaches the top of the tank before the measured sludge blanket level (see below).

2. Underflow concentration

Figure 8.61 compares the measured and predicted underflow concentrations for the Veghel test.

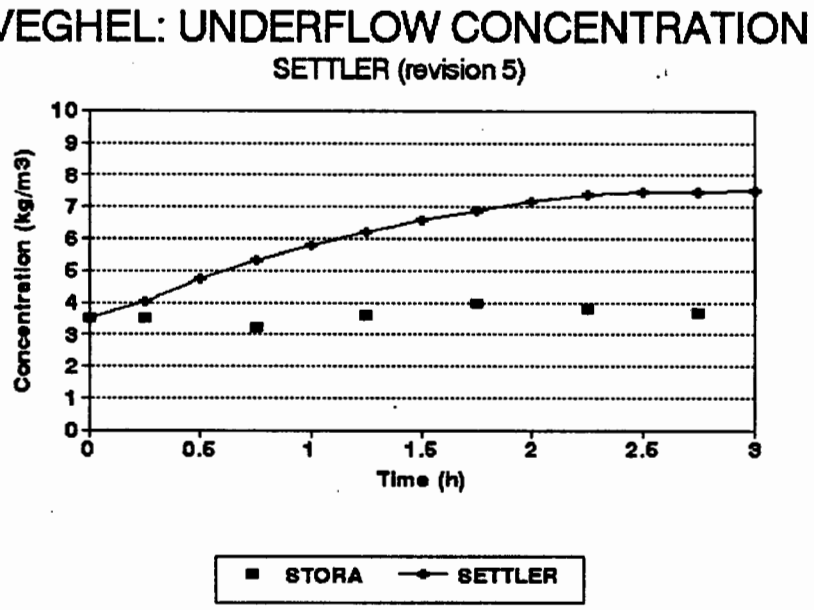

Figure 8.61 Predicted and measured underflow concentrations for Veghel with SETTLER (revision 5)

The predicted underflow concentration increases gradually from 3.5kgm^{-3} at the beginning of the test to 7.38kgm^{-3} at 2.25h into the test. Thereafter, the increase in

predicted underflow concentration becomes slightly less rapid, and the maximum predicted underflow concentration of 7.51kgm^{-3} is reached at the end of the test.

The measured underflow concentration decreases slightly from 3.5kgm^{-3} at the start of the test to 3.2kgm^{-3} at 0.75h into the test. Thereafter, the measured underflow concentration rises slightly to reach its maximum concentration of 4kgm^{-3} at 1.75h into the test. From 1.75h until the end of the test, the measured underflow concentration decreases again to 3.7kgm^{-3}.

The predicted underflow concentration is higher than the measured underflow concentration throughout the test and there is not a good correspondence between measured and predicted results. However, for an overloaded test like this one, it is difficult to understand why the measured underflow concentration remained virtually constant throughout the test. Intuitively, the underflow concentration should increase and the fact that it did not is probably a consequence of tank bottom effects such as sludge scraper and collection effects. This is confirmed in the concentration profile results, which show a concentration of over 5kgm^{-3} over a considerable depth of the tank. Consequently, a satisfactory basis for comparison between measured and predicted results for this parameter was not possible.

3. Effluent concentration

Figure 8.62 compares the measured and predicted effluent solids concentrations for the Veghel test.

The predicted effluent solids concentration shows negligible values in the effluent until 2.5h, when the predicted effluent solids concentration is 383mgl^{-1}. From 2.5h until the end of the test, two further peaks of high effluent solids concentration are predicted (682mgl^{-1} and 842mgl^{-1}. The total effluent solids mass lost during the test is 753kg, 2.34% of the total solids processed by the settling tank during the test.

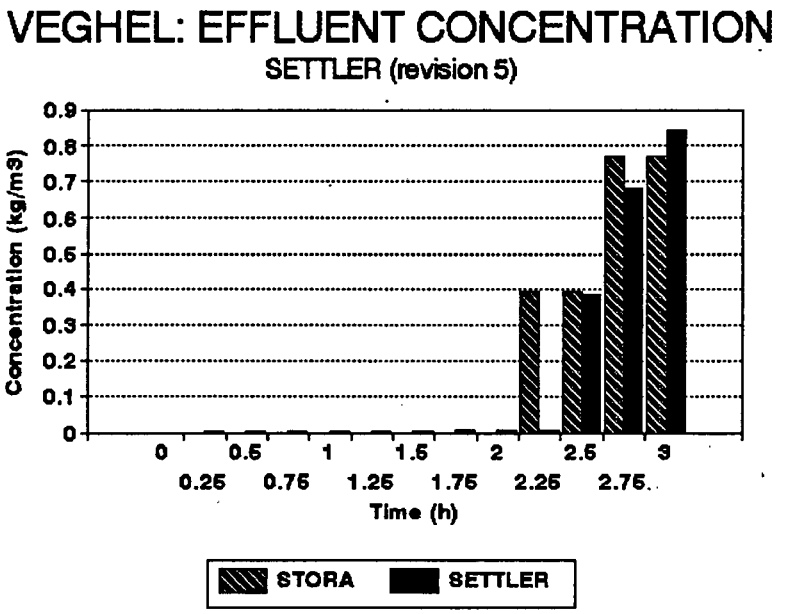

Figure 8.62 **Predicted and measured effluent concentrations for Veghel with SETTLER (revision 5)**

The measured effluent solids concentration shows negligible values until 2.25h, when two peaks of concentration 390mgl^{-1} are measured. Two further peaks of 770mgl^{-1} are measured at 2.75h and at 3h. The total measured effluent solids mass lost is 736kg, 2.3% of the total solids processed.

The measured and predicted effluent solid concentration time profiles match very closely considering that the diffusivity constants were not obtained by calibration but by calculation from the empirical relationships. The predicted effluent solids mass lost also closely matches the measured values, both in terns of time of the first effluent solids mass lost and the manner of the total effluent solids mass lost.

4. Concentration profile at 3h

Figure 8.63 compares the measured and predicted sludge concentration depth profiles for the Veghel test at 3h.

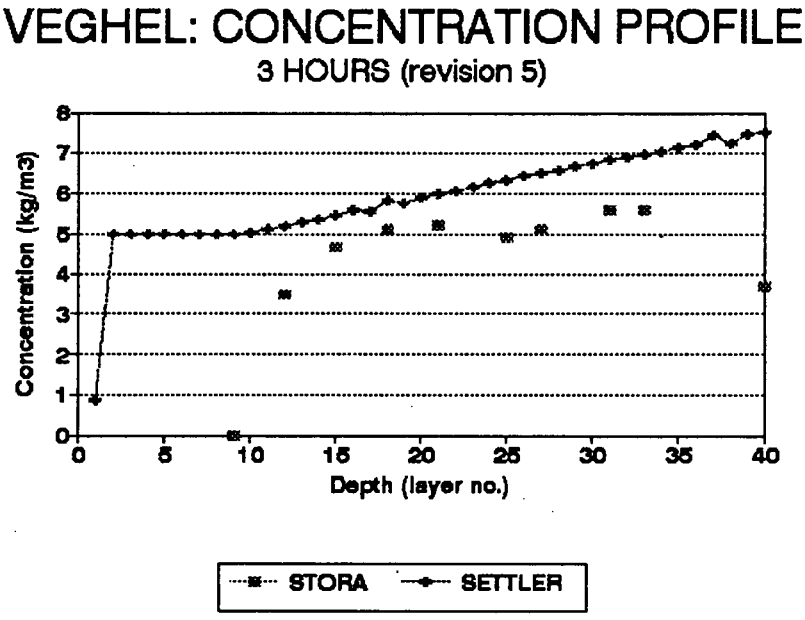

Figure 8.63 **Predicted and measured concentration profiles at 3h for Veghel with SETTLER (revision 5)**

The predicted results at 3h show a sludge concentration depth profile with a sludge blanket that extends throughout the tank, gradually decreasing in concentration from 7.51kgm^{-3} at layer 39 to 4.99kgm^{-3} at layer 7 (the feed point layer). From the feed point layer upwards, the concentration in the tank remains constant at 4.99kgm^{-3}. The predicted effluent solids concentration at 3h is 0.842kgm^{-3}. There are two concentration anomalies apparent in the predicted sludge concentration depth profile; one at layer 38 and 37, and one at layer 27 and 26. These are layers in which the concentration in the layer above is greater than the concentration in the layer below. No explanation could be found for these anomalies although they are small enough not to be a major cause for concern.

The measured sludge concentration depth profile at 3h (0.75h after failure) contains two aspects contrary to expectation (i) an unusually low measured underflow concentration of 3.7kgm^{-3} and (ii) an absence of a sludge blanket in the top of the tank.

The correspondence between measured and predicted results for this parameter is poor, mostly because of the unexpected concentrations in the measured sludge concentration

depth profile. In comparing the two sludge blanket regions (between layers 34 and 15), it is apparent that the predicted concentration profile has somewhat higher concentrations than the measured profile. Further comparisons between measured and predicted results for this parameter are not possible.

8.14.1 CONCLUSIONS FOR THE VEGHEL TEST SIMULATION

For this simulation, the predicted and measured sludge blanket rise rates correspond well, apart from the initial drop in predicted sludge blanket level, which causes the predicted and measured sludge blanket levels to be out of phase for the remainder of the test. The predicted sludge blanket level reaches the top of the tank only 0.25h earlier than the measured sludge blanket. However, the time at which the predicted sludge blanket level reaches the top of the tank is not concurrent with the time at which failure is predicted, as this occurs 2.5h into the test. Between 2h, when the sludge blanket reaches the top of the tank and 2.5h, when the first solids are lost in the effluent, a further 1090kg of sludge is accumulated in the settling tank before its storage capacity is exceeded. The fact that there is a difference between the time that the predicted sludge blanket level reaches the top of the tank and the time that the first gross effluent solids mass loss occurs indicates that the sludge blanket level is not a critical parameter in assessing the predicted performance of the settling tank under overloaded conditions. This is confirmed by the previous simulations at Rijen and Wijk.

The pattern of the predicted underflow concentrations is unexpected for this test. For other tests, when the value of difbot is high, the predicted underflow concentration is overdamped, whereas for this test the reverse is true. In addition, it appears that the measured underflow concentrations exhibit aberrant values for this test due to factors not taken into account by the model. Consequently, for this parameter, a comparison between measured and predicted values is not valid.

The predicted effluent solids mass lost matches the measured value very closely, and the time and manner in which the solids are lost are accurately predicted. This suggests that the defined value of α_1 and the calculated values of α_2, diftop and difbot for this test are appropriate.

Generally, the correspondence between measured and predicted results for this test is good for the critical parameters (time of failure, manner of failure and total effluent solids mass lost). The correspondence between measured and predicted sludge blanket levels is not so good, but this is not a very critical parameter with regard to failure. A comparison between measured and predicted results for the underflow concentration and sludge concentration depth profiles cannot be made because of the questionable validity of the measured data.

Because of the sparsity of the data available for overloaded situations in full scale settling tanks, it is difficult to draw any more general conclusions as to the accuracy of the equations developed for the determination of α_2, diftop and difbot for full scale settling tanks under overloaded conditions. However, the STORA data does present four underloaded cases that fall close to the dividing line between failed and safe cases. In order to ascertain whether or not SETTLER can correctly identify a situation that is found in practice to be safe, these four test cases were also simulated. These tests are as important as the overloaded cases, as the ability of SETTLER to discriminate between failed and safe cases is an important criterion for measuring its usefulness as a simulation program.

8.15 SIMULATING UNDERLOADED CASES WITH SETTLER (revision 5)

In order to further test the applicability and generality of the diffusivity values and functions developed in the above simulations with overloaded cases, these were applied to simulating four underloaded test cases, two at Oss, one at Rijen and one at Gieten. Underloaded tests are as valuable as overloaded tests for checking the simulation results of SETTLER when the applied solids loading is close to the maximum permissable solids loading because these cases effectively test the discriminating ability of the program. For these cases, it is possible that, even though, according to the flux theory they will be found to be underloaded, in practice they might fail. Ekama and Marais (1986) showed that the flux theory tends to overpredict the limiting flux (G_L) so that the maximum permissible applied flux (G_{per}) is only 80% of the calculated limiting flux (G_L) i.e. $G_{per} = 0.80*G_L$. Therefore, there will be some situations which are defined by the flux theory as underloaded ($G_{ap} < G_L$), but in practice are found to fail ($G_{per} < G_{ap} < G_L$). (This aspect was first discussed in Chapter 2 and is again discussed in greater detail in Section 8.16 below.) Figure 8.64 illustrates the applied vs limiting flux for the four selected safe STORA tests and for comparative purposes also shows the failed test cases already simulated. From the figure, it can be seen that the overloaded tests at Rijen 1, 5 and 8, Wijk and Veghel are examples of conditions where $0.8*G_L < G_{ap} < G_L$ (i.e. $G_{ap} > G_{per}$). SETTLER, although based on the flux theory, nevertheless correctly predicted settling tank failure in these cases, even though they were found to be underloaded by the flux theory for large portions of the test periods. The reason for this is the inclusion of diffusivity in the model which, as previously discussed, makes the settling tank more sensitive to the solids flux loading. The presence of diffusivity in the model (and specifically difbot in the lower layers of the tank) effectively reduces the permissable limiting solids flux (G_L), shifting the under/overloaded dividing line closer to $G_{per} = 0.8*G_L$.

In order to ascertain whether or not SETTLER can correctly identify a situation that is found in practice to be safe, the first test case chosen for simulation was one which falls close to the dividing line between cases that are failed and safe **in practice** i.e.

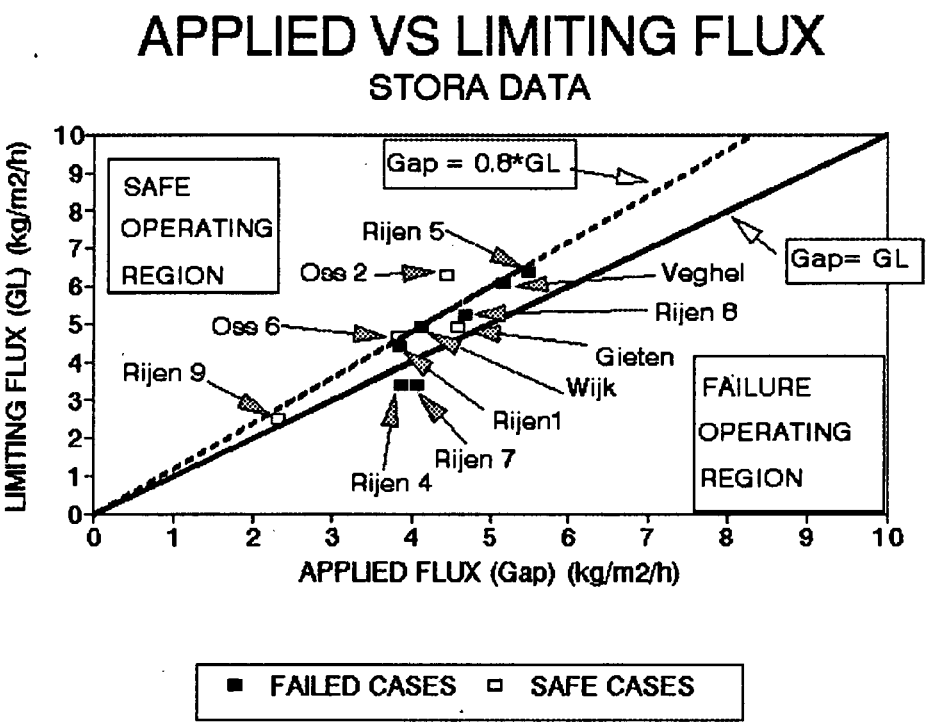

Figure 8.64 Applied vs limiting flux for the STORA test cases

the line that defines $G_{ap} = G_{per} = 0.8*G_L$. The Oss 6 test was found to be the closest safe case to the $G_{ap} = 0.8*G_L$ line and this test therefore was selected first for simulation. A detailed description of the test simulation follows.

8.15.1 SETTLER (revision 5) APPLIED TO THE OSS 6 UNDERLOADED CASE

The sixth settling tank test at Oss (hereafter referred to as Oss 6) was carried out for a total of 6 hours, with the influent flow running into the settling tank throughout the test. The flux theory constants, V_o and n, and the initial conditions for the test were found in the same manner as for previous tests. With the calculated values of V_o and n, the flux theory indicated that the system was in an underloaded state throughout the test with G_{ap} at about 80% of G_L i.e. approximately equal to G_{per}. The data measured by STORA for the Oss 6 test is given in Table 8.27 and a summary of the operating parameters is presented in Table 8.28.

Table 8.27 Data measured by STORA for the Oss 6 test

Test: Oss 6 Begin test: 11:20h
Date: 12 July 1979 End test: 17:15h

Q_i = 933m^{3}h^{-1} Q_r = 849m^{3}h^{-1}

Time (h)	Feed conc (kg/m^3)	Underflow conc (kg/m^3)	Sludge blanket height (m)	Remarks
11:20			2.20	influent started
11:40	3.44	4.23	2.10	
12:00		4.24		
12:10			1.60	
12:40		4.47		
12:50	3.0		1.90	
13:10		4.51		
13:35		4.87		
13:50	3.09		1.85	
14:10		4.82		
14:20			1.75	
14:35		5.05		
14:50	2.81			
15:10		5.19	1.70	
15:30			1.67	
15:40	2.91	5.4		
16:00			1.70	
16:40	2.91	5.73	1.65	
17:00			1.65	
17:10		5.94	1.65	
17:15	2.95	5.94	1.70	

The Oss tank is slightly smaller than the Rijen tank i.e. 1370m^2 (a diameter of 41.76m) compared to 1625m^2 (a diameter of 45.5m) for the Rijen tank. The depth is also less, being 2.94m compared to 3.35m for the Rijen tank. These dimensions means that the size of the Oss tank falls between the sizes of the Wijk and Rijen tanks. The sludge settleability is also poorer than for previous simulations (130mlg^{-1} $SSVI_{3.5}$). The initial conditions for Oss 6 are illustrated in Figure 8.65. These were generated in the same way as for the previous tests.

With regard to the diffusivity value, α_1 was fixed at 10layer^{-1} as in all the earlier simulations. The values of α_2 and diftop were calculated from the empirically derived relationships linking diftop, α_2 and difbot to the tank dimensions and operating parameters. From Equations (8.15) and (8.16) α_2 and diftop were calculated to be 1.884layer^{-1} and 189346m^{2}h^{-1} respectively. The value of difbot was calculated from Equation (8.20) to be 0.553m^{2}h^{-1}. The size of the CSTR for the thickening zone was scaled down on the basis of the shallower depth of the Oss tank compared to the Rijen

Table 8.28 Summary of operating parameters for Oss 6

PARAMETER	VALUE
Q_i	$933m^3h^{-1}$
Q_r	$849m^3h^{-1}$
X_o (max)	$3.44gm^{-3}$
X_o (min)	$2.81gm^{-3}$
Area	$1370m^2$
Depth (from overflow weir to bottom of tank)	2.942m
Feed point layer	7
Duration of test	6 hours
$SSVI_{3.5}$	$130mlg^{-1}$
DSVI	$200mlg^{-1}$
V_o	$5.074mh^{-1}$
n	$0.451m^3kg^{-1}$

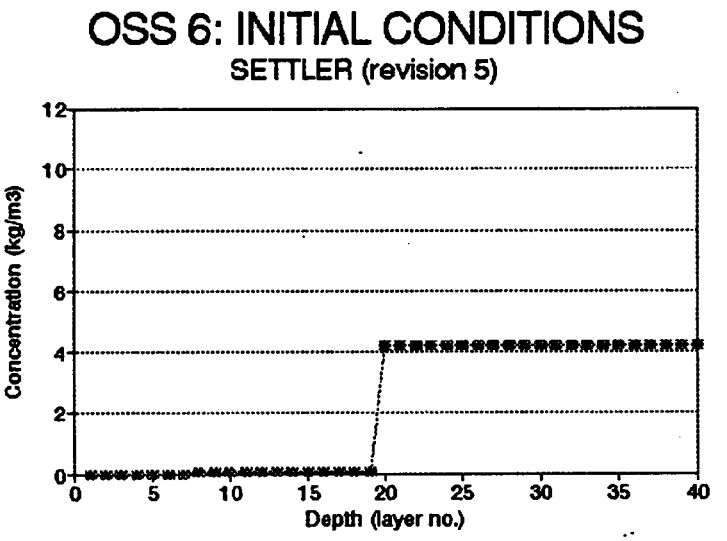

Figure 8.65 Initial concentration profile for the Oss 6 test

tank and was calculated to be 0.879m. The test at Oss 6 was then simulated with

SETTLER (revision 5) and the following predicted and measured parameters were compared:

1. Sludge blanket level and rise rate
2. Underflow concentration
3. Effluent solids concentration

Sludge concentration depth profiles were not measured for this test, so this parameter could not be evaluated.

1. Sludge blanket level

Figure 8.66 compares the measured and predicted sludge blanket levels for the Oss 6 test.

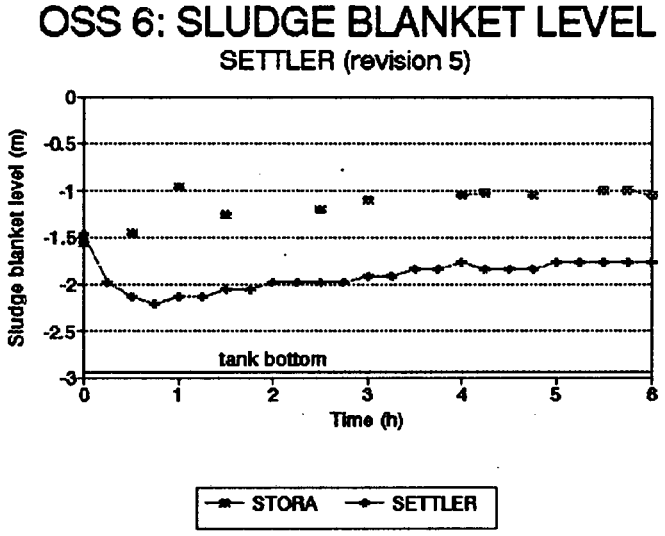

Figure 8.66 Predicted and measured sludge blanket levels for Oss 6 with SETTLER (revision 5)

The predicted sludge blanket level drops from 1.47m below the surface at the start of the test to 2.13m at 0.5h. It then rises 0.5m very slowly over 4.5h until 5h into the test, after which the sludge blanket level remains constant for 1h until the end of the test.

The measured sludge blanket rises from 1.5m below the surface at the start of the test to 1.09m below the surface at 3h after the start of the test. Thereafter, the sludge blanket remains constant at this level until the end of the test.

There is a good correspondence between the measured and predicted sludge blanket rise rates for the whole test. However, because of the drop in the predicted sludge blanket level during the first 0.5h of the test (due to sludge redistribution in the tank to overcome the discontinuity in the initial concentration profile), it consistently remains at a lower level in the tank than the measured sludge blanket. More importantly, however, neither the measured nor the predicted sludge blankets reach the top of the tank during the test. It should be noted that the discontinuity in the initial concentration profile adversely affects the simulation results and that more favourable results could have been achieved if the initial concentration profile had been "tailored" for each test. However, this was regarded as an unacceptable method of ensuring good simulation results and thus the original method of determining the initial concentration profile was maintained for all the simulations.

2. Underflow concentration

Figure 8.67 compares the measured and predicted underflow concentrations for the Oss 6 test.

The predicted underflow concentration remains fairly constant throughout the test, rising from its minimum concentration of 4.23kgm^{-3} at the start of the test to 5.23kgm^{-3} at the end of the test. The measured underflow concentration also remains fairly constant throughout the test, rising from its minimum concentration of 4.23kgm^{-3} at the start of the test to 5.94kgm^{-3} at the end of the test. The correspondence between measured and predicted results for this parameter is excellent.

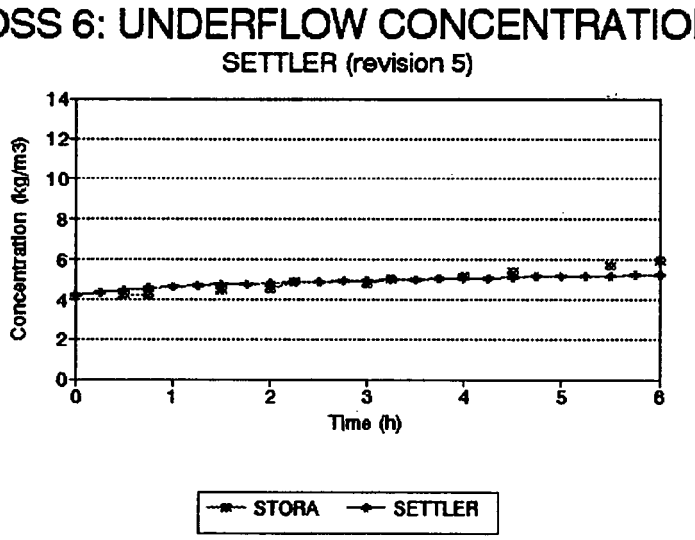

Figure 8.67 **Predicted and measured underflow concentrations for Oss 6 with SETTLER (revision 5)**

3. Effluent concentration

Neither the predicted nor the measured results show any effluent solids loss during this test.

Conclusions for the Oss 6 test simulation

The correspondence between measured and predicted results for this test is remarkably good considering that (i) no calibration runs were undertaken and that the values of the diffusivity function constants (diftop, α_1, α_2 and difbot) were calculated from the earlier developed relationships based on tank size and operating parameters and used without modification and (ii) that the loading conditions are close to overload i.e. G_{ap} is close to $0.8*G_L$ (see Figure 8.64). Both the measured and predicted sludge blanket levels remain fairly constant throughout the test (besides the initial drop in the predicted sludge blanket level). Although the sludge blanket level rises during the test, SETTLER correctly predicts that it will not reach the top of the tank. Both measured and predicted underflow concentrations remain almost constant during the test and

SETTLER correctly predicts that no solids will be lost with the effluent during the test.

The program SETTLER correctly identified the Oss 6 test as an underloaded case, and generated accurate predictions. The fact that the Oss 6 test is very close to the $G_{ap} = 0.8*G_L$ line in Figure 8.64 and was correctly identified as a safe case whereas earlier simulated cases also close to the $G_{ap} = 0.8*G_L$ line (Rijen 5, 8 and 1, Veghel and Wijk) were correctly identified as failure cases, confirms the ability of SETTLER to distinguish quite precisely between failure and safe cases.

8.15.2 SETTLER (revision 5) APPLIED TO THE REMAINING THREE UNDERLOADED CASES

Three other underloaded (or safe) settling tank tests were also simulated: one with $G_{ap} < 0.8*G_L$ (Oss 2) and two with $0.8*G_L < G_{ap} < G_L$ (Rijen 9 and Gieten). The detailed results of these simulations are not given because their primary objective was only to determine whether or not SETTLER correctly distinguishes between failed and safe situations. A secondary objective was to generally examine the behaviour of SETTLER for underloaded cases and to establish whether or not any modifications need to be made to the program for accurate simulation of these cases.

The simulation of the Oss 2 test yields very similar results to those for the Oss 6 test. From Figure 8.64, it can be seen that Oss 2 is defined by the flux theory as being underloaded throughout the test period. The calculated values of α_2, diftop and difbot for this test were found to be $1.884 layer^{-1}$, $189346 m^2h^{-1}$ and $0.803 m^2h^{-1}$ respectively.

The Oss 2 sludge blanket level, similarly to the Oss 6 sludge blanket level, falls during the first part of the test and then rises slowly during the remainder of the test. SETTLER correctly predicts that the sludge blanket will not reach the top of the tank during the test and that no solids will be lost with the effluent during the test. Both

measured and predicted underflow concentrations remain almost constant during the test. SETTLER correctly identified the Oss 2 test as an underloaded case and generated accurate predictions.

The other two safe cases simulated (those with $G_{ap} > 0.8G_L$), Rijen 9 and Gieten, present a different problem. For these tests, the slope factor in the difbot - diffusivity function (See Equations 8.19 and 8.20) leads to very small or negative values of difbot. This is illustrated in Figure 8.68. For comparative purposes, the slope factors and difbot values for the other safe tests are also plotted on the graph.

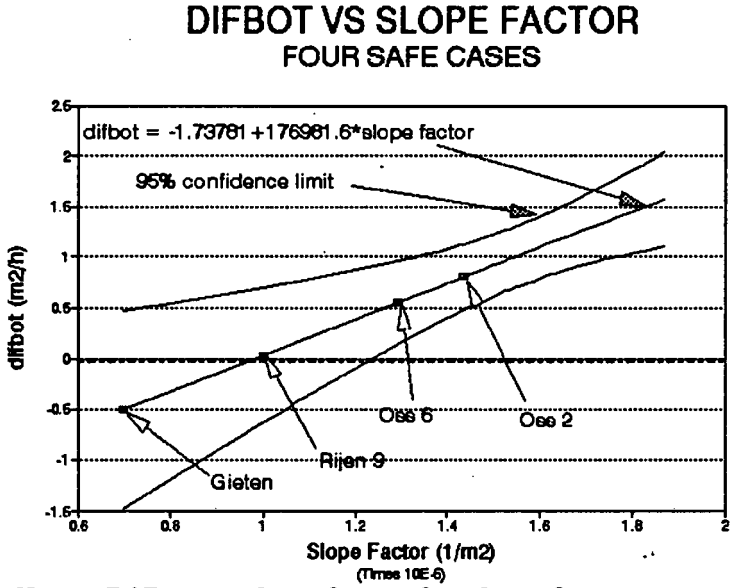

Figure 8.68 Difbot vs slope factor for the safe cases

It is obvious that negative values of difbot are not physically possible and, indeed, even difbot very close to zero is not physically realistic. Earlier, (see Section 8.4) it was noted that difbot cannot be set $>2.5m^2h^{-1}$ for reasons of entropy restrictions, but up until now, no minimum value of difbot has been discussed. This is because all the tests so far (both underloaded and overloaded) have had slope factors that led to values of difbot somewhat greater than zero. From experimental observation, it is clear that, even for underloaded cases, diffusivity is present at all depths in the tank. For cases with low slope factors i.e. $((Q_i + Q_r)/A)$ small, the diffusivity in the lower layers of the tank is not so much caused by the influence of turbulence resulting from the

influent and recycle flows, but rather by bottom effects such as scraper action and the bulk velocity caused by the underflow recycle. These bottom effects will be present at all times, even when the influent flow rate is zero. It is thus necessary to specify a minimum value of difbot for the cases where a low slope factor would otherwise generate negative or very small values for difbot.

The test at Gieten was used as an example to examine the effect of different minimum values of difbot. Figure 8.69 illustrates the effect on the sludge blanket level for difbot = 0, 0.04 and 0.121m^2h^{-1} respectively.

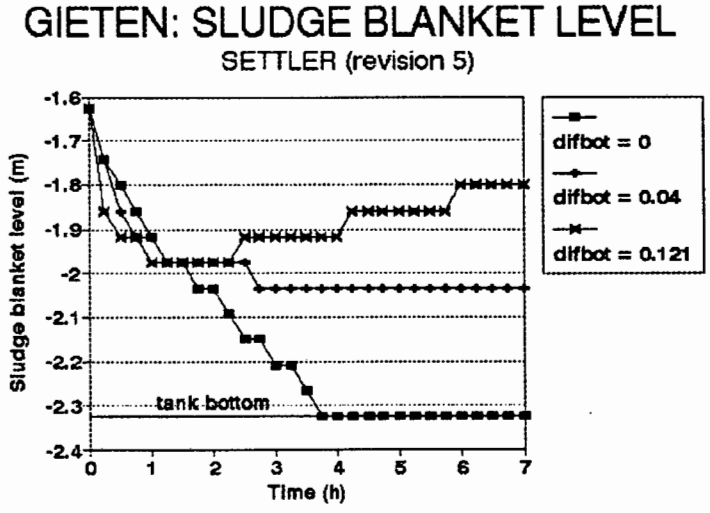

Figure 8.69 Effect of difbot on the sludge blanket level for Gieten with SETTLER (revision 5)

It is obvious that difbot =0m^2h^{-1} is not a realistic value, for reasons stated above. Difbot = 0.04m^2h^{-1} is also not realistic, as it is known from experience that in practice the sludge blanket will not fall to the bottom of the tank, even if the settling tank is underloaded. Difbot = 0.121m^2h^{-1} seems to be a realistic value, as it permits the sludge blanket to develop in the tank during the test, but does not cause it to rise to the surface of the tank. For the Rijen 9 test with difbot = 0.121m^2h^{-1}, similar satisfactory results to those for the Gieten test were obtained, and thus difbot = 0.121m^2h^{-1} was selected as the minimum value. An additional reason for selecting 0.121m^2h^{-1} as a realistic minimum value for difbot is the relatively good correspondence that results

between predicted and measured underflow concentrations at the end of the tests for the Gieten and Rijen 9 cases. The predicted vs measured final underflow concentrations for all four safe cases are illustrated in Figure 8.70.

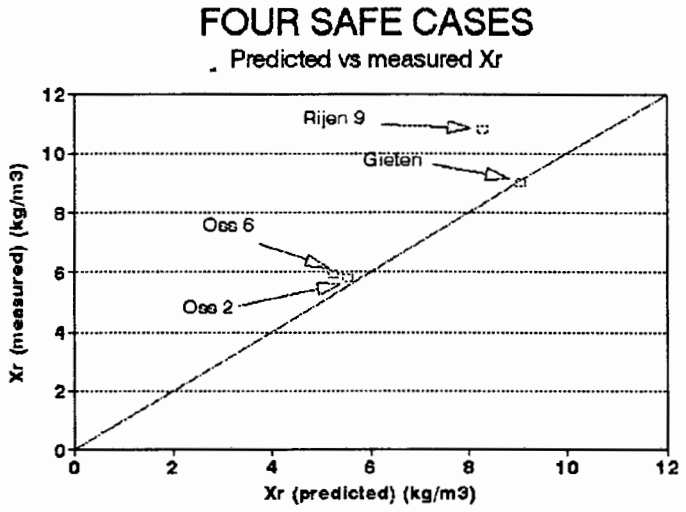

Figure 8.70 Predicted vs measured underflow concentrations for the four safe cases.

In conclusion, SETTLER has been found to correctly distinguish between test cases that were found to be safe and those that fail in practice and generates satisfactorily accurate predictions for the safe cases when these are simulated. It therefore seems that, by including diffusivity in the flux model, it implicitly incorporates the conclusion of Ekama and Marais that for full scale tanks the flux theory overestimates the maximum solids loading with the result that the permissable solids loading should be only about 80% of the calculated maximum solids loading. In order to further explore SETTLER's implicit incorporation of this conclusion, further theoretical simulations were carried out with the program. These are described in detail in the next section.

8.16 DETERMINING THE PREDICTED VS MEASURED LIMITING FLUX: SETTLER (revision 5) APPLIED TO FIVE THEORETICAL FULL SCALE CASES

Because none of the available full scale cases was appropriate for the purposes of accurately determining the limiting flux predicted by the now appropriately calibrated and tested SETTLER program incorporating diffusivity, it was necessary to create five theoretical test situations. The theoretical cases were based on the Rijen 1 data, with the dimensions of the tank and the sludge settleability parameters being the same as for the Rijen 1 test (see Section 8.2). With this data as a basis, five theoretical test cases were created and simulations carried out for each of the following conditions:

1. $G_{ap} = G_L$ (critically loaded)
2. $G_{ap} = 0.90*G_L$
3. $G_{ap} = 0.85*G_L$
4. $G_{ap} = 0.80*G_L$
5. $G_{ap} = 0.75*G_L$

where G_{ap} = applied flux ($kgm^{-2}h^{-1}$)
G_L = flux theory limiting flux ($kgm^{-2}h^{-1}$)

The operating parameters that remain constant for all five test cases are presented in Table 8.29. The physical dimensions of the Rijen tank are given in Table 8.2 in Section 8.2 and the operating parameters that are specific to each test case are listed in Table 8.30.

Each of the test cases was simulated for a 36h period with an identical initial concentration profile (the same as that for the Rijen 1 test). During the course of each simulation the sludge blanket level and effluent solids concentration were noted every 0.25h. Figure 8.71 shows the effluent solids concentration for each of the five test cases over the 36h simulation.

Table 8.29 Operating parameters that apply to all five full scale test cases

PARAMETER	VALUE
V_o	$6.544mh^{-1}$
n	$0.363m^3kg^{-1}$
X_o	$3.16kgm^{-3}$
Q_r	$531m^3h^{-1}$
diftop	$120000m^2h^{-1}$
α_2	$1.5m^{-2}$

Table 8.30 Specific operating parameters for each of the five full scale test cases

TEST CASE	% OF LIMITING FLUX	Q_i+Q_r (m^3h^{-1})	difbot (m^2h^{-1})
1.	100%	2311	1.406
2.	90%	2080	1.092
3.	85%	1964	0.934
4.	80%	1849	0.778
5.	75%	1733	0.620

For the critically loaded test, the first gross solids loss in the effluent occurs at 11h, whereafter the effluent solids concentration increases continuously until the end of the test. For the test with the applied flux equal to 90% and 85% of the limiting flux, the first gross solids loss in the effluent occurs at 18.75h and 26.5h respectively. For both these tests, once the first gross solids loss has occurred in the effluent, the effluent solids concentration continues to increase until the end of the test. For the two remaining test cases where the applied flux is 80% and 75% of the limiting flux respectively, no gross solids loss occurs in the effluent at any stage during the test.

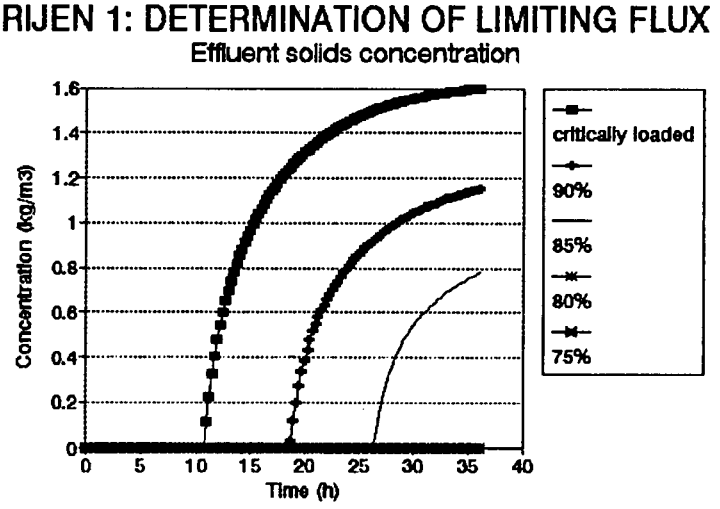

Figure 8.71 **Effluent concentration for the five full scale test cases with SETTLER (revision 5)**

Figure 8.72 shows the sludge blanket level for each of the five test cases over the 36h test period.

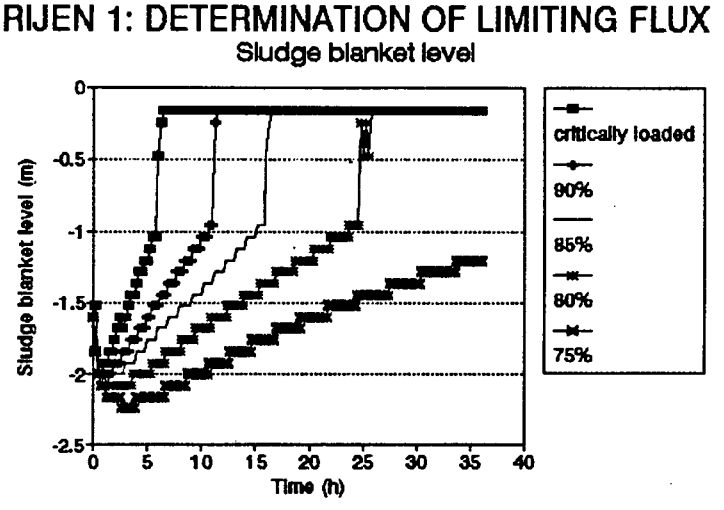

Figure 8.72 **Sludge blanket level for the five full scale test cases with SETTLER (revision 5)**

For the critically loaded test, the sludge blanket level rises from an initial level of 1.6m below the surface and reaches the top of the tank 6.5h after the start of the test. For the other tests, where the applied flux is 90%, 85% and 80% of the limiting flux respectively, the sludge blanket level reaches the top of the tank at 11.5h, 16.5h and

25.75h after the start of the test respectively. For the test case with the applied flux equal to 75% of the limiting flux, the sludge blanket level rises and levels out at approximately 1.2m below the surface of the tank and does not reach the top of the tank during the 36h test.

8.16.1 CONCLUSIONS FOR THE FIVE THEORETICAL FULL SCALE SIMULATIONS

The cases that ended in gross effluent solids loss are clearly failed cases i.e. those with $G_{ap} = G_L$ (critically loaded), $G_{ap} = 0.90*G_L$ and $G_{ap} = 0.85*G_L$. For all these cases, the sludge blanket level rises rapidly from the start of the test and reaches the top of the tank relatively early on in the test. The test with $G_{ap} = 0.75*G_L$ is clearly an underloaded case, as indicated both by the fact that no effluent solids were lost during the test and by the fact that the sludge blanket does not rise to the top of the tank.

For the remaining case with $G_{ap} = 0.80*G_L$, the fact that no effluent solids were lost during the test indicates that this case is predicted by the model to be a safe situation, at least for the 36h duration of the simulation. Although for this test the sludge blanket level did rise to the top of the tank after 25.75h, this, as discussed previously, is not an indication of settling tank failure. These results suggest that this test lies on the dividing line between those cases that are found to be safe and those that fail. The results of these simulations therefore appear to confirm the conclusions of Ekama and Marais, that for large diameter (30 to 50m diameter) full scale settling tanks, the maximum permissable solids loading should only be 80% of the calculated maximum solids loading according to the flux theory (see Chapter 2).

8.17 EXAMINING THE EFFECT OF CHANGING THE FEED POINT LAYER

Up until now, all the full scale simulations have been carried out with the feed point at layer 5, where layer 1 is the topmost layer in the settling tank, and layer 40 is the bottommost layer. In order to check that the form of the diffusivity function is valid if

the feed point layer is located at other depths in the tank, four hypothetical full scale tests were created and simulated.

The theoretical simulations were based on the Rijen data, with the dimensions of the tank and the sludge settleability parameters being the same as for the Rijen 1 test. The same initial concentration profile as for the Rijen 1 test was used for each of the four simulations. The operating conditions that remain constant for all four theoretical simulations are presented in Table 8.31, and are the same as those for the $G_{ap} = 0.8*G_L$ case in Section 8.16 above.

Table 8.31 Parameters that are constant for all four test cases

PARAMETER	VALUE
V_o	$6.544 mh^{-1}$
n	$0.363 m^3kg^{-1}$
X_o	$3.16 kgm^{-3}$
Q_i+Q_r	$1849 m^3h^{-1}$
Q_r	$531 m^3h^{-1}$
diftop	$120000 m^2h^{-1}$
α_2	$1.5 m^{-2}$
difbot	$0.778 m^2h^{-1}$

The simulations were each carried out for 30h and the concentration depth profile for each test at the end of the 30h period was recorded. The concentration profiles for all four tests are presented in Figure 8.73.

From Figure 8.73, it can be seen that the higher the feed point layer in the tank, the closer the settling tank approaches failure during the test. At the end of the 30h period, the test case with the feed point at layer 5 has a sludge blanket that extends throughout the settling tank from layer 39 to layer 2, although no gross effluent solids loss has been predicted. For the test with the feed point at layer 7, the sludge blanket extends

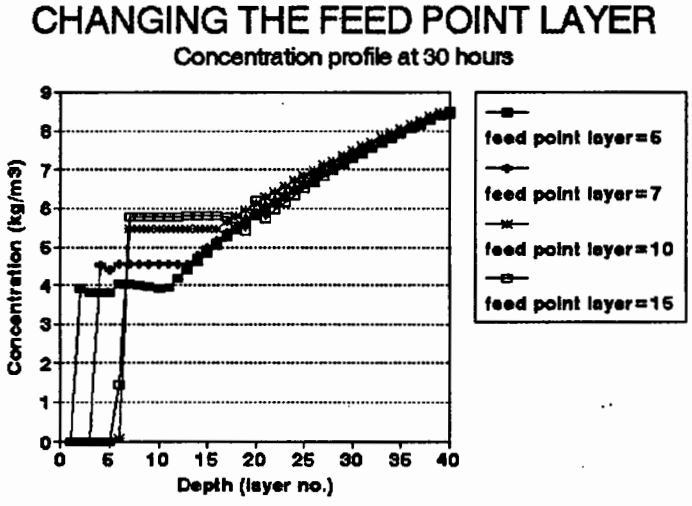

Figure 8.73 Concentration depth profiles for each of the four test cases carried out with different feed point layers

from layer 39 to layer 4. The remaining two tests with feed points at layers 10 and 15 respectively both have a sludge blanket that extends from layer 29 to layer 7 at the end of the 30h test.

For all the tests, the concentration profiles from layer 39 to layer 17 are almost identical because each simulation has the same difbot value and therefore the same diffusivity in this region. Above these layers, the sludge blanket concentrations decrease with decreasing feed point layer depth i.e. the "extra" portion of the sludge blanket is at a concentration of 5.8kgm^{-3} when the feed point is at layer 15, 5.4kgm^{-3} when the feed point is at layer 10, 4.5kgm^{-3} when the feed point is at layer 7 and 3.8kgm^{-3} when the feed point is at layer 5. This phenomenon is related to the shape of the diffusivity function, which is illustrated for each of the four test cases in Figure 8.74. Although the diffusivity in each of the feed point regions is the same, The depth at which diftop occurs is different, causing the concentration of the sludge blankets to diverge at the layer at which the diffusivity begins to increase.

From Figure 8.74 it can be seen that, although the shape of the diffusivity function for each of the four test cases is identical, the position of the diffusivity function is shifted

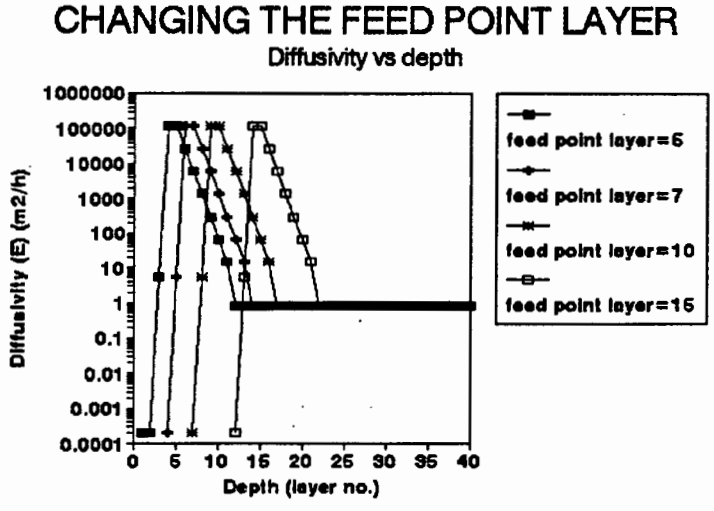

Figure 8.74 **Diffusivity vs depth profile for each of the four test cases with different feed point layers**

upwards or downwards in the tank such that the layer at which the maximum diffusivity occurs corresponds to the feed point layer. Hence, the deeper the feed point layer, the greater the diffusivity in the **lower** layers of the tank. The **total** diffusivity in the tank (area between the diffusivity curve and the y axis) therefore increases as the depth of the feed point layer moves upwards. Previously (see Section 8.4) it was observed that as the total diffusivity in the tank increased, the tank became more sensitive to the applied solids loading and thus more susceptible to failure. This observation is confirmed by these simulations because the test with the feed point at layer 5 has the greatest amount of total diffusivity in the tank and is also closest to failure. Conversely, the test with the feed point at layer 15 has the least amount of total diffusivity in the tank and is furthest from failure (see Figure 8.73). It was also previously observed that the presence of diffusivity encourages the propagation of the sludge blanket by virtue of its mixing effect between layers. This is also confirmed in these tests because it can be seen that the layers in which the "extra" constant concentration portion of the sludge blanket occurs (e.g. layers 17 to 7 for the feed point at layer 10) correspond to the layers in which the diffusivity function is high. This is illustrated in Figure 8.75, in which the diffusivity function has been superimposed on the concentration profile for the case of the feed point at layer 10.

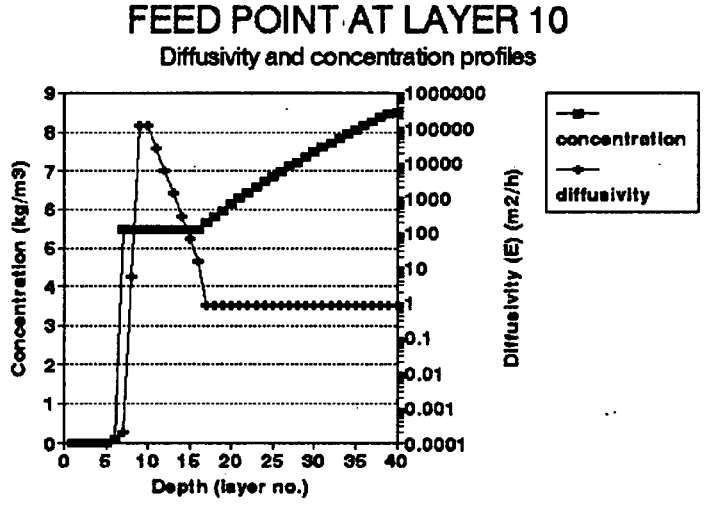

Figure 8.75 Diffusivity and concentration profile for the test case with feed point at layer 10

From Figure 8.75, it can be seen that the region of the concentration profile which exhibits the "extra" portion of the sludge blanket is the same as the layers in which the diffusivity is high. For layers 18 to 40, where the diffusivity is reduced to difbot = $0.778 m^2h^{-1}$ and is the same for all four tests, the concentration profiles for all four tests correspond almost exactly. These four theoretical full scale test cases demonstrate that the program SETTLER performs satisfactorily for a range of different feed point layers but that the onset of failure will be delayed for the same diffusivity constants as the feed point is placed deeper in the tank. Calibration simulations to estimate the values of the diffusivity constants for feed point depths lower than layer 5 were not conducted.

8.18 COMPACTION RELATED SETTLING TANK FAILURE

Up until now, all the underloaded cases that have been simulated have either had recycle ratios ($s = Q_r/Q_i$) greater than 0.25 or relatively good sludge settleability ($SSVI_{3.5} \leq 120 ml g^{-1}$), or both. Table 8.32 summarises the recycle ratios and $SSVI_{3.5}$ values for the four underloaded cases simulated so far. From Table 8.32 it can be seen

that all except one of the underloaded cases have $SSVI_{3.5}$ values $\leq$ 120mlg^{-1}, and the one case that has $SSVI_{3.5}$ > 120mlg^{-1} (Oss 2) has a high recycle ratio.

Table 8.32 Summary of recycle ratios and $SSVI_{3.5}$ values for the four underloaded cases

TEST CASE	RECYCLE RATIO (Q_r/Q_i)	$SSVI_{3.5}$ (mlg^{-1})
Oss 2	0.753	130
Oss 6	0.910	100
Gieten	0.667	80
Rijen 9	0.278	100

For cases which have both a low recycle ratio (s < 0.25) and a poor sludge settleability ($SSVI_{3.5} \geq$ 120mlg^{-1}), it is possible for the settling tank to fail even though the operating point on the design and operating chart is in the safe operating region. An example of such a case is illustrated in Figure 8.76.

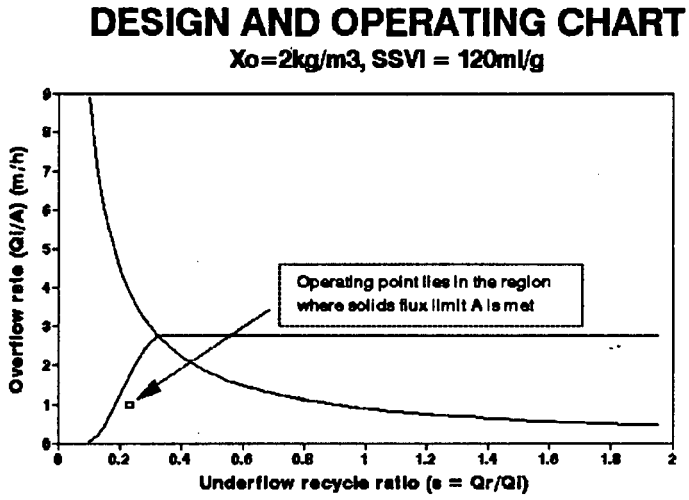

Figure 8.76 Design and operating chart for a test case with a low recycle ratio

In the example illustrated, the recycle ratio (Q_r/Q_i = s) = 0.23, $SSVI_{3.5}$ = 120mlg^{-1} and the feed concentration (X_o) = 2kgm^{-3}. In order to preserve the material balance over the tank under these underloaded operating conditions, a high underflow concentration (X_r) is required i.e. $X_r = X_o (1+s)/s$ = 10.69kgm^{-3}. If the sludge settleability is good, this presents no problems, as the time required for the concentrating process is not long, and this can be accommodated during the retention time of the sludge in the tank. If, on the other hand, the sludge settleability is poor, then the time required for the sludge concentrating process is too long to be accommodated during the retention time of the sludge in the tank. Consequently, the mass abstracted via the underflow is less than that entering the tank and solids will build up in the tank. If this situation persists it can lead to solids overflow with the effluent. This compaction related solids loss is different to that caused by the limiting flux because the solids can reach the bottom of the tank but do not densify fast enough to the concentration required by the recycle ratio to preserve the mass balance. This is an aspect not hitherto considered by the flux theory (see Chapter 2).

Compaction related settling tank failure is taken into account in the ATV and STORA design procedures. These procedures define a maximum attainable underflow concentration which is related to the sludge settleability, in their case the DSVI, as follows:

$$X_{rmax} = \frac{1200}{DSVI} \text{ for DWF (kgm}^{-3}) \qquad (8.21)$$

where DWF = dry weather flow

and

$$X_{rmax} = \frac{1200}{DSVI} + 2 \text{ for WWF (kgm}^{-3}) \qquad (8.22)$$

where WWF = wet weather flow

With the X_{rmax} at DWF and WWF known, the minimum underflow rates or recycle ratios can be calculated from the mass balance to ensure that higher underflow

concentrations than the maximum are not required. A graphical representation of the maximum attainable underflow concentration at DWF and WWF for a range of DSVI values is given in Figure 8.77.

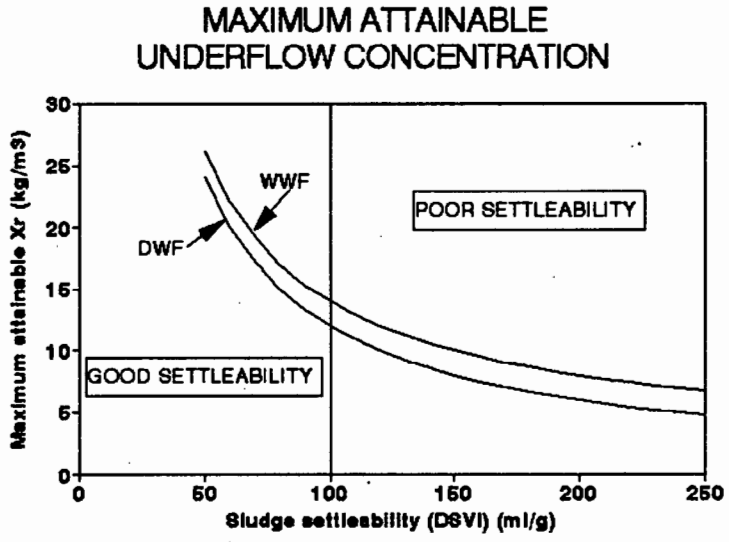

Figure 8.77 Maximum attainable underflow concentration vs DSVI

The figure shows that as the sludge settleability deteriorates (DSVI increases), so the maximum attainable underflow concentration decreases. This implies that in design, low underflow recycle ratios that require high underflow concentrations in order for the mass balance to be preserved can only be allowed for good settling sludges but must be avoided for poorly settling sludges. Hence, in terms of the ATV and STORA design procedures, a minimum underflow recycle ratio according to sludge settleability must be set to avoid solids loss due to poor compaction of the sludge in the bottom of the settling tank. It is the intention in this final section to demonstrate that SETTLER implicitly incorporates this third mode of settling tank failure (i.e. additional to solids flux limits A and B failure) by virtue of the inclusion of diffusivity in the flux model.

Accepting the validity of the strategy for restricting the maximum attainable underflow concentration, and recognising that settling tank failure usually takes place under WWF conditions, Equation (8.22) was incorporated into the program SETTLER. A tag line was also incorporated into the program with this equation. The function of the tag line

was to report whether or not the restriction on the maximum attainable underflow concentration was used. If the restriction was not used, then no report was made. In order to test the ability of SETTLER to reflect sludge compaction failure, the test case illustrated on the design and operating chart in Figure 8.76 was simulated. The simulation is based on the Rijen 4 test, the tank dimensions, sludge settleability and initial concentration profile being the same as for that test (see Section 8.3). The influent flow rate, underflow rate and feed concentration were changed from those of the Rijen 4 test to ensure that the operating point for this test fell into the region of interest on the design and operating chart. The values of α_1, α_2, diftop and difbot were calculated from the diffusivity functions derived earlier from the Rijen tank dimensions and operating conditions given in Table 8.33 (see Equations 8.15, 8.16 and 8.20). The V_o and n values were calculated from the Rijen 4 test $SSVI_{3.5}$ value of $120mlg^{-1}$ from the empirical relationships linking V_o and n and $SSVI_{3.5}$ derived in Chapter 4 and yielded $V_o = 5.188mh^{-1}$ and $n = 0.429m^3kg^{-1}$. The gravity flux curve for these operating conditions is illustrated in Figure 8.78, which shows clearly that the tank is underloaded.

Table 8.33 Summary of operating parameters for the compaction related solids loss test

PARAMETER	VALUE
Q_i	$1625.97m^3h^{-1}$
Q_r	$373.97m^3h^{-1}$
Q_r/Q_i (=s)	0.23
X_o	$2.0kgm^{-3}$
Area	$1625m^2$
DSVI*	$180mlg^{-1}$
V_o	$5.188mh^{-1}$
n	$0.429m^3kg^{-1}$
$SSVI_{3.5}$	$120mlg^{-1}$

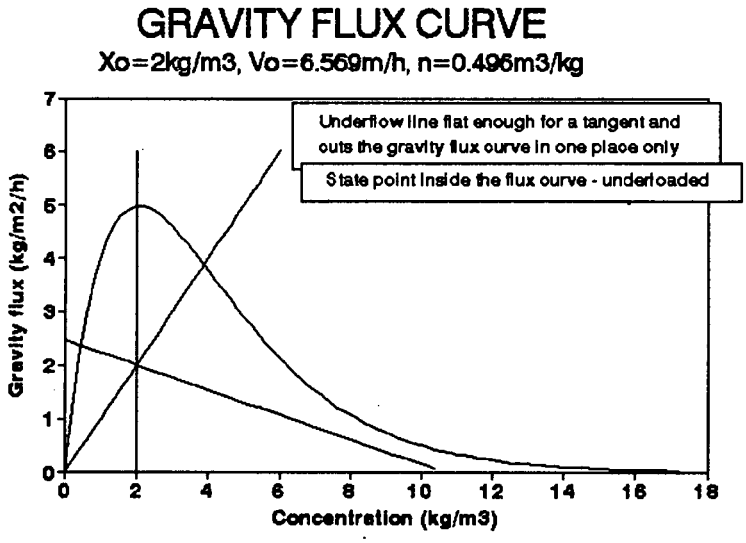

Figure 8.78 Flux curve for the compaction related solids loss test

The measured DSVI for the Rijen 4 test was 130mlg^{-1}. This value does not conform well to the general trend of the STORA data that the DSVI = 1.54*$SSVI_{3.5}$ (see Ekama and Marais (1986)). From measurements at 13 Western Cape plants, Ekama and Marais established that DSVI = 1.50*$SSVI_{3.5}$, confirming that of the STORA data. In terms of these relationships, the DSVI is more realistically around 180mlg^{-1} and this value was adopted to compare the maximum underflow concentration predicted by SETTLER with that of Equations (8.21) and (8.22) (see Figure 8.77). The simulation was carried out for a total of 30h, the effluent solids concentration being recorded every 15min during the simulation and the sludge concentration depth profile being recorded at the end of the 30h simulation. The effluent solids concentration is illustrated in Figure 8.79.

From the figure, it can be seen that SETTLER predicts the onset of gross solids loss at 8.75h into the test. From 8.75h until the end of the test, the predicted effluent solids concentration continually increases although the rate of increase levels off towards the end of the test.

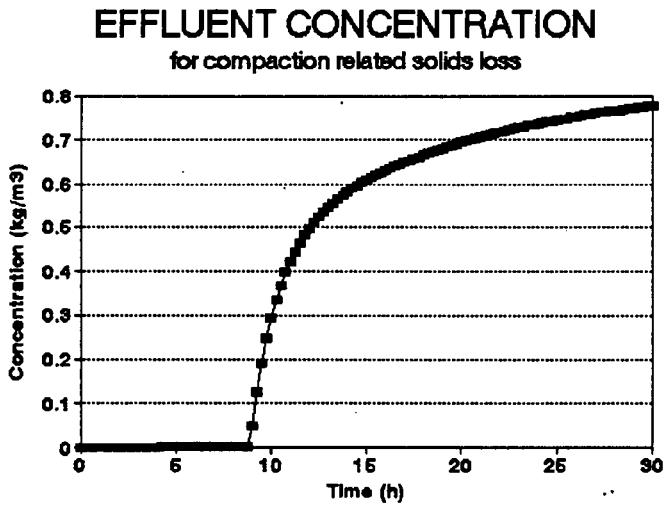

Figure 8.79 **Effluent solids concentration for the compaction related solids loss test with SETTLER (revision 5)**

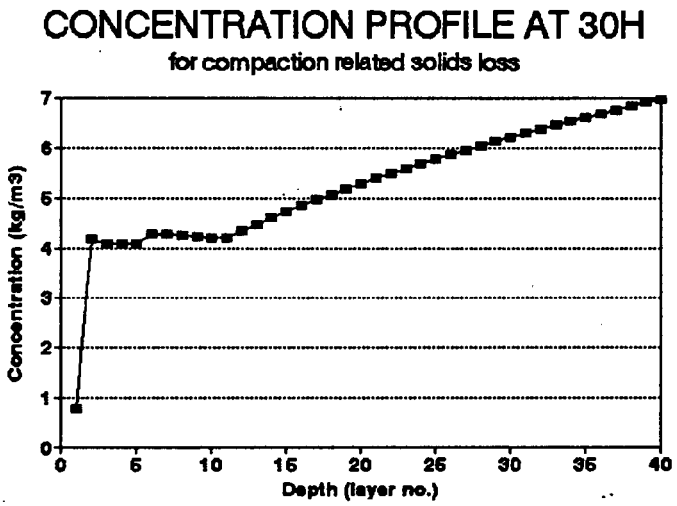

Figure 8.80 **Concentration profile at 30h for the compaction related solids loss test with SETTLER (revision 5)**

Figure 8.80 illustrates the predicted sludge concentration depth profile at the end of the test. From the figure, it can be seen that solids have built up in the tank during the 30h simulation, and that the sludge blanket extends throughout the tank. The concentration in the first layer of the concentration profile indicates that effluent solids loss at a concentration of 778mgl^{-1} is predicted.

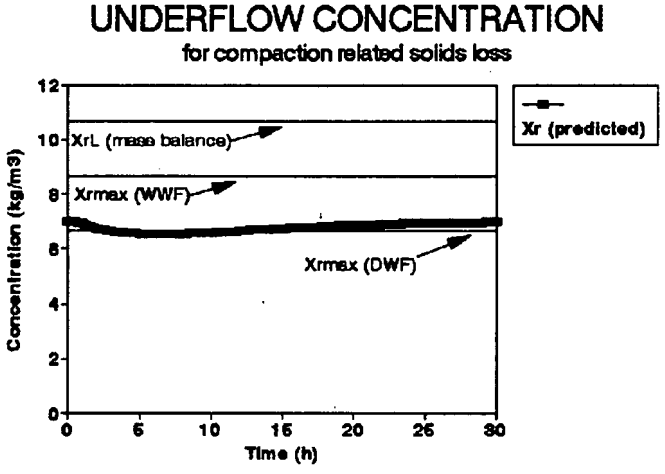

Figure 8.81 **Predicted underflow concentration compared to maximum values as specified by the mass balance and the ATV procedure**

Figure 8.81 illustrates the predicted underflow concentration over the 30h simulation. Also on the figure are the predicted maximum underflow concentration as calculated from the flux theory mass balance (X_{rL}) and the maximum attainable underflow concentration as specified by ATV for DWF ($X_{rmax(DWF)}$) and WWF ($X_{rmax(WWF)}$) for the estimated DSVI of 180mlg^{-1}. The predicted underflow concentration initially decreases about from 7.0kgm^{-3} to $\pm$6.6kgm-3 over the first 5h, but thereafter gradually increases to $\pm$7.0kgm^{-3} again towards the end of the test at 30h. At no stage did the predicted underflow concentration rise above 7.0kgm^{-3} even though, to preserve the mass balance for underloaded conditions, an underflow concentration of 10.69kgm^{-3} was required. During the course of the simulation, the tag line at no stage reported that the maximum attainable WWF underflow concentration (8.67kgm^{-3}) restriction was used and it appears therefore that the limit on the increase in the underflow concentration does not originate from the flux theory itself but is already restricted by the presence of diffusivity in the lower layers of the tank.

All the earlier overloaded and underloaded cases were rerun with the program SETTLER containing the tag line and, for all of these simulations, the tag line at no stage reported that the restriction on the maximum attainable WWF underflow

concentration was required. While these cases do not have low recycle ratios (<0.25) or poor sludge settleability ($SSVI_{3.5}$ > 120mlg^{-1}), they nevertheless confirm the observation that the presence of diffusivity in the flux model SETTLER takes into account the ATV and STORA experience that the underflow concentration is limited at some maximum attainable value depending on the sludge settleability. This aspect needs considerably more investigation than that outlined above in that the accuracy of the predicted maximum underflow concentration of 7.0kgm^{-3} compared to the ATV empirical value of 6.67kgm^{-3} could be purely fortuitous. Many different sludge settleabilities, recycle ratios and magnitudes of diffusivity need to be tested before a general conclusion of this mode of failure in the SETTLER flux model can be made. It nevertheless is interesting that the flux theory with diffusivity implicitly incorporates this feature, which is already recognised in the ATV and STORA design procedures.

8.19 CONCLUSIONS

After carrying out the 11 simulations based on the data collected by STORA and 10 further theoretical full scale simulations, it was concluded that SETTLER (revision 5) with diffusivity at all layers in the tank and a CSTR to simulate the thickening region was able to predict satisfactory results for all the cases.

1. For the seven overloaded cases, SETTLER (revision 5) generated acceptably accurate predictions for sludge blanket level and rise rate, underflow concentration, the time of onset of failure and the effluent solids concentration. Where applicable, the sludge concentration depth profiles generated by SETTLER approximately matched the measured data. The underflow concentration, time of onset of failure and the effluent solids concentration were considered to be more critical parameters than the sludge blanket level and rise rate and the sludge concentration depth profiles. Accordingly, they were given more weight in assessing the performance of SETTLER, the latter parameters being merely qualitatively evaluated.

2. For the four underloaded cases, SETTLER (revision 5) accurately predicted that these would be safe cases, and generated appropriate results.

3. The inclusion of diffusivity in the program enables SETTLER to implicitly incorporate the findings of Ekama and Marais (1986), that the flux theory tends to overpredict the maximum permissable solids loading for full scale tanks. For a series of five theoretical tests cases, SETTLER predicted that failure will occur when the solids loading is greater than 80% of the maximum permissable solids loading predicted by the idealised (hyperbolic) flux theory.

4. SETTLER is valid for all reasonable feed point depths.

5. SETTLER is also able to simulate compaction related failure, implicitly incorporating restrictions on the maximum attainable underflow concentration by virtue of the diffusivity in the lower layers of the tank.

With the incorporation of the diffusivity function and the inclusion of a CSTR to model the thickening region, SETTLER is an improvement on previous layer based sedimentation models based purely on the steady state flux theory. Deficiencies in the flux theory are overcome with the inclusion of these features into the model, with the result that the maximum permissable solids loading and underflow concentration restrictions may now be accurately predicted. These findings hopefully will promote greater confidence in the predictive power of the flux theory and its ability to accurately simulate dynamic secondary settling tank behaviour. As a consequence, there are good prospects for transferring the flux theory out of its essentially research realm into the realm of design, practice and operation.

REFERENCES

Alkema K.L., "The effect of settler dynamics on the activated sludge process", MSc Thesis, Univ of Colorado, (1971)

Collins M.A. and R.M. Crosby, "Impact of flow variation of secondary clarifier performance", Paper presented at 53rd Annual Conference of the Water Pollution Control Federation, Las Vegas, Nevada, (1980)

Ekama G.A. and G.V.R. Marais, "Sludge settleability and secondary settling tank design procedures", Wat Pollut Control, Vol 5, No. 1, (1986)

Takacs I., Patry G.G. and D. Nolasco, "A dynamic Model of the clarification-thickening process", Wat Res, Vol 25, No. 10, pp 1263-1271, (1991)

Vitasovic Z.Z., "An integrated control strategy for the activated sludge process", PhD dissertation, Rice University, Houston, Texas, (1986)

CHAPTER 9
CONCLUSIONS

9.1 INTRODUCTION

Theoretical understanding and modelling of secondary settling tanks has developed relatively separately from design and practice. Even though the flux theory is acknowledged as the best model for describing settling tank behaviour, it has not been accepted into full scale settling tank design and operation practice. The problems with the flux theory appear to be threefold: (i) it requires sludge settleability to be defined in terms of the multiple batch zone settling velocity - concentration (ZSV-X) test which is tedious and time consuming and therefore not carried out in practice (ii) it has not been definitively verified which has led to a lack of confidence in it as a design tool and (iii) it has deficiencies as regards settling tank design in that it does not give guidelines for sludge storage capacity, settling tank depth and maximum underflow concentration.

The main objective of this investigation was to bring the theoretical modelling and practical design aspects of secondary settling tanks closer together. This was sought to be achieved in following two ways:

1. by evaluating and developing empirical relationships from which the flux theory constants, V_o and n, (usually obtained from the ZSV-X test) may be derived from the simpler sludge settleability measures: sludge volume index (SVI), stirred specific volume index ($SSVI_{3.5}$) and diluted sludge volume index (DSVI),

2. by developing a computer model for the simulation of dynamic behaviour of full scale secondary settling tanks and evaluating its performance with regard to important design requirements such as maximum underflow concentration and sludge storage capacity.

The first objective was required in order to meet the second. This was because the full scale data against which the dynamic model was to be verified did not include reliable flux theory constants V_o and n linking the zone settling velocity and concentration. These values therefore needed to be calculated from the measured $SSVI_{3.5}$ or DSVI.

The first objective was achieved by collecting all the available data sets comprising ZSV-X and SVI, $SSVI_{3.5}$ and DSVI data. By applying various statistical significance tests to the data, the data sets that could be legitimately pooled were identified. From the pooled data sets, best fit constants for the relationship linking the ZSV (V_s) to the sludge concentration and particular sludge settleability parameter (SSP) were evaluated by a single step least squares regression on the function:

$$\ln V_o = \ln\alpha - \beta * SSP - \gamma * X - \delta * SSP * X \qquad (9.1)$$

This function results from accepting that the flux theory constants V_o and n (in the semilog relationship $V_s = V_o e^{-nX}$) are exponential and linear respectively i.e.

$$V_o = \alpha e^{-\beta * SSP} \qquad (9.2)$$

$$n = \gamma + \delta * SSP \qquad (9.3)$$

The linear least squares regression to determine the α, β, γ and δ constants was also conducted by the more usual double step method i.e. first obtaining V_o and n from the ZSV-X data and then obtaining α, β, γ and δ by correlating the determined V_o and n values on the SSP.

It was found that, the higher the multiple correlation coefficient (r^2) for the data set (or poled data set), the more closely the single and double step methods matched. The single step method was always found to have the better fit and, for multiple correlation coefficients (r^2) better than 0.9, the two methods gave almost identical results. From the largest data set that could be pooled, which for the SVI, $SSVI_{3.5}$ and DSVI were

1. They render the flux theory more accessible for use in practise, as the simpler sludge settleability tests may still be performed and subsequently transformed into V_o and n values for use with the flux theory design and operating chart.

2. They provide a link between empirical design procedures and the flux theory so that different design procedures may be compared. This offers the potential for the two paths of theoretical and practical developments to be brought closer together and areas of integration to be created.

3. They allow the $SSVI_{3.5}$ measurements of the STORA data to be transformed into V_o and n values so the simulation program based on the flux theory may be calibrated and verified for full scale tanks using this data.

It is realised that the idea of developing empirical relationships between V_s (or V_o and n) and the SSP is not new and has been done by a number of researchers since White developed the Water Research Centre settling tank design procedure in 1975 (see also Daigger and Roper (1985), Pitman (1984), Koopman and Cadee (1983) and Riddel *et al* (1983). However, for this investigation, the main objective of conducting the statistical evaluation was to facilitate the development of the dynamic simulation model for secondary settling tank behaviour. The evaluation was done quite comprehensively because of the vital importance of the V_o and n values in describing the settling behaviour of the sludge and therefore also of the settling tank. It therefore needed to be shown that the V_o and n values could be reliably obtained from $SSVI_{3.5}$ or DSVI values, if not for general use in design, then at least for use in this particular investigation. With regard to the former, this was considered to have been satisfactorily achieved. However, with regard to the latter, these relationships do not appear to be general because certain data sets could not be pooled and needed to considered individually.

The second objective of this investigation was achieved by adopting, modifying, refining and testing the secondary settling tank model developed by Anderson (1981).

Apart from a number of deficiencies in the algorithm, a major deficiency in Anderson's program was that the diffusivity function appeared to have been calibrated specifically for Anderson's application and thus was not applicable to the general case. The relevant section of Anderson's program was reconstructed into a self contained, dedicated, FORTRAN settling tank program called SETTLER (revision 1) and tested against

1. Anderson's own data collected at one of the Detroit Wastewater Treatment Plant settling tanks,

2. idealised flux theory predictions (hyperbolic case, no diffusivity),

3. laboratory scale measurements (hyperbolic case, no diffusivity),

4. full scale data collected by STORA (parabolic case, with diffusivity).

In testing the program against Anderson's data, it was concluded that SETTLER (revision 1) was an accurate reconstruction of the secondary settling tank component of Anderson's program. The results obtained for the simulation with SETTLER were the same as those obtained by Anderson. It was also noted in these tests that neither the measured data nor the results generated by SETTLER (revision 1) preserved the mass balance over the settling tank.

For the purposes of testing SETTLER against idealised flux theory predictions, it was assumed that the effects of diffusivity were negligible, and hence it was possible to avoid having to define a general diffusivity function at this stage. Without diffusivity, the basic partial differential equation (PDE) is hyperbolic, a feature of such PDE's being that their solutions are not uniquely defined by their initial conditions, resulting in the generation of physically meaningless solutions. To guide SETTLER to the physically meaningful solution for the hyperbolic case, seeding was introduced into the program. A number of other modifications and refinements in the algorithm were also

required. Once complete, it was found that SETTLER (revision 3) generated accurate solutions matching the idealised flux theory predictions for each of the idealised test cases with a variety of initial conditions. For the settling tank, four different steady state modes of operation can be identified and SETTLER was found to predict the correct sludge depth concentration profile, underflow concentration and effluent concentration for each of these modes, irrespective of the initial conditions. The program also preserved the mass balance.

From these results, it was concluded that SETTLER represented an accurate embodiment of the idealised flux theory and that conceptual and algorithm errors had been, as best as could be established, eliminated. SETTLER was ready to be tested against measured results: laboratory scale settling column data representative of hyperbolic (no diffusivity) conditions and full scale settling tank performance data measured by STORA (1981) on 22 different tanks.

Because all the laboratory data was representative of only two of the four possible modes of steady state operation, SETTLER was tested against only two of the cases. For the two cases, SETTLER correctly predicted that they were underloaded and overloaded respectively, and generated predictions that matched the measured data reasonably well.

SETTLER was then tested against the full scale data collected by STORA (1981). This data represented 44 cases of solids loading at 22 different sewage treatment plants in Holland. The settling tanks at these plants were all circular, conically bottomed tanks with diameters of between 30 and 50m. The STORA data reported the final outcome of each test as safe (underloaded), failed (overloaded) or inconclusive, and reported measurements of important parameters such as sludge blanket level and rise rate, underflow concentration, effluent solids concentration and sludge concentration depth profiles. All of the overloaded cases and four of the underloaded cases were used for the purposes of calibrating and verifying the simulation program.

In order to test SETTLER against this data, it was necessary to take into account that flows in the full scale tanks could not be assumed to be in the vertical direction only. To this end, a diffusivity function was formulated and incorporated into the program. A CSTR was also included at the bottom of the settling tank to simulate the thickening zone. The final form of the diffusivity function is as follows:

$$E_i = \text{diftop}.(Q_i+Q_r).e^{+\alpha_1(i-i_{feed})} \text{ for } i<i_{feed} \quad (9.7)$$

$$E_i = \text{diftop}.(Q_i+Q_r).e^{-\alpha_2(i-i_{feed})} \text{ for } i \geq i_{feed} \quad (9.8)$$

$$\text{IF}(E_i<\text{difbot}) \text{ THEN } E_i = \text{difbot} \quad \text{for } i>i_{feed} \text{ only} \quad (9.9)$$

where E_i = diffusivity at layer i (m^2h^{-1})

i = layer number

Q_i+Q_r = feed flow rate to the settling tank (m^3h^{-1})

diftop = diffusivity at the feed point (m^2h^{-1})

α_1 = die off rate of diffusivity above the feed point ($layer^{-1}$)

α_2 = die off rate of diffusivity below the feed point ($layer^{-1}$)

difbot = diffusivity in the lower layers of the tank (m^2h^{-1})

Six overloaded settling tank tests were used to calibrate SETTLER (revision 5) and to determine the values of the constants in the diffusivity function. It was proposed that the value of α_1 should remain constant at a value of $10 layer^{-1}$ for all the full scale settling tank tests. It was proposed that the values of α_2, diftop and difbot should be determined as follows:

$$\alpha_2 = 3.939 - 0.0015 * A \text{ (in } m^2) \quad (9.10)$$

$$\text{diftop} = 402814 - 60.30 * V \text{ (in } m^3) \quad (9.11)$$

where Q_i+Q_r = feed flow rate to the settling tank (m^3h^{-1})

$$\text{difbot} = -1.73781 + 176981.6 * \frac{(Q_i+Q_r)}{A} * \frac{\alpha_2}{\text{diftop}} \qquad (9.12)$$

A	=	surface area of the settling tank (m^2)
V	=	volume of the settling tank (m^3)
diftop	=	diffusivity at the feed point (m^2h^{-1})
α_2	=	die off rate of diffusivity below the feed point ($layer^{-1}$)
difbot	=	diffusivity in the lower layers of the tank (m^2h^{-1})

For the thickening zone simulation, it was proposed that the depth of the CSTR should be proportional to the depth of the settling tank. The last remaining available overloaded case was used to verify SETTLER (revision 5) by simulating the test case with calculated values of the diffusivity constants.

For the overloaded cases, it was found that:

1. The inclusion of diffusivity in the program has the effect of rendering the settling tank more sensitive to solids overload, reducing the effective storage capacity of the tank and thus making it more susceptible to failure.

2. For the predicted results, the time at which the sludge blanket reaches the top of the tank does not correspond to the time at which failure occurs, as the settling tank is still able to accumulate sludge above the feed point until the critical concentration has been exceeded. The onset of failure is thus determined solely by the first solids loss in the effluent. In contrast, for the measured results, the time at which the sludge blanket reaches the top of the settling tank coincides with the onset of failure. In addition, the predicted results manifested a rapid rise in sludge blanket level once the sludge blanket entered the region of high diffusivity around the feed point. This was not reflected in the measured results. Because of the discrepancy between measured and predicted results for the sludge blanket level, it was concluded that the sludge blanket level should not be

regarded as a very reliably predicted parameter. However, it was also concluded that it is not a critical parameter.

3. High values of difbot had a greater effect on limiting the maximum attainable underflow concentration than low values of difbot.

In general, the simulations for the overloaded cases produced reasonably good correspondence with the measured results.

In order to test the ability of SETTLER to discriminate between under and overloaded cases, four underloaded cases that were found to be close to the dividing line between under- and overloaded cases were simulated. It was found that a minimum value of difbot needed to be specified in order for SETTLER to generate realistic results. This minimum value of difbot was set at $0.121 m^2 h^{-1}$. It was concluded that, with this specified minimum value of difbot, SETTLER accurately identified these cases as safe situations and generated appropriate results. Sludge blanket behaviour and underflow concentration were correctly predicted and no solids loss was predicted in the effluent for any of the underloaded cases.

In the simulations for the overloaded cases, it was found that both the maximum solids loading and underflow concentration were affected by the diffusivity. To further examine these effects, five further theoretical test cases were simulated. This was specifically to see if SETTLER confirmed the findings of Ekama and Marais (1986), which were that the flux theory tends to overpredict the maximum permissable solids loading, thus overestimating the storage capacity of full scale settling tanks. Five theoretical full scale cases were simulated, each at a different percentage of the flux theory maximum solids loading. SETTLER predicted failure for the cases where the applied solids loading was greater than 80% of the predicted maximum solids loading, thus verifying earlier findings.

Further simulations were carried out with SETTLER to examine the effect of changing the depth of the feed point. The program was found to be valid for all reasonable feed point depths.

A last simulation was carried out to determine if SETTLER is able to predict compaction related settling tank failure. This form of failure arises at low recycle ratios and poor sludge settleabilities and is caused by the inability of the compression zone to sufficiently thicken the sludge during the available retention time. This form of failure is not accounted for in the flux theory. A hypothetical test case was created and simulated, and it was found that the presence of diffusivity in the lower layers of the tank enabled SETTLER to predict this form of failure.

It was concluded that SETTLER, with the incorporation of diffusivity at all layers in the tank and a CSTR to model the thickening region, is an improvement on previous simulation programs based purely on the steady state flux theory. The inclusion of diffusivity in the program enables it to correctly predict the limitations on the maximum attainable underflow concentration and to overcome the tendency in the flux theory to overpredict the maximum solids loading. These aspects are not considered by the flux theory, although they have been recognised by and incorporated into the ATV and STORA design procedures.

It should be further noted that, although SETTLER was considered to have successfully achieved the major objective of bringing practical and theoretical developments in settling tanks closer together, it is not appropriate in its present form for design and operation. Its value as a model lies primarily in its usefulness in assessing the applicability of the idealised flux theory to full scale tanks.

9.2 RECOMMENDATIONS

The work in this investigation has been largely preliminary, and has touched only briefly on the many area of interest for workers in this field. It is recommended that:

1. the relationships formulated in this thesis that link V_o and n to the sludge settleability measures SVI, $SSVI_{3.5}$ and DSVI be used with caution, as they are known to be applicable only under certain conditions. The relationship for $SSVI_{3.5}$ particularly, appears to be plant type specific, and should only be applied to plants of the extended aeration type from which the pooled data was collected.

2. if further work is carried out in collecting sludge settleability data, then other relevant parameters besides the concentration and SSP measurements must also be collected. These parameters include plant type, temperature and organism type, as well as other parameters that could possibly influence the sludge settleability measure,

3. the progress made in this investigation in verifying the flux theory should be used as a starting point for developing design strategies based on the flux theory that incorporate important settling tank features such as maximum underflow concentration and sludge storage capacity,

4. greater cognisance be taken of the ATV and STORA design procedures, which already contain some of the ideas outlined in this investigation.

Ultimately, it is hoped that this investigation will further the unification of the many different approaches to sludge settleability and secondary settling tank design and at least provide the potential for greater integration of the divergent paths.

REFERENCES

Abwasser Technik Verband, "Erlaterungen und erganzungenzum arbeitsbericht des ATV-fachausschiusses 2.5 absetzverfarhen. Die demessung der nachlarbecken von belebungsanlangen", Korrespondenz Abwasser, 8, 23, 231, (1976)

Abwasser Technik Verband, "Arbeitsbericht des ATV-fachausschiusses 2.5 absetzverfarhen. Die bemussung der nachlarbecken von belebungsanlangen", Korrespondenz Abwasser, 8, 20, 193 (1973)

Anderson H.M., "A dynamic simulation model for wastewater renovation systems", PhD thesis, Wayne State University, Detroit, Michigan, (1981)

Daigger G.T. and R.E. Roper, "The relationship between SVI and activated sludge settling characteristics", JWPCF, Vol 57, No 8, pp 859-866, (1985)

Ekama G.A. and G.v.R. Marais, "Sludge settleability and secondary settling tank design procedures", Wat Pollut Control, Vol 5, No. 1, (1986)

Koopman B. and K. Cadee, "Prediction of thickening capacity using diluted sludge volume index", Water Research, 17, 10, pp 1427-1431, (1983)

Pitman A.R., "Settling of nutrient removal activated sludges", Procs of 12th IAWPRC Conference, Amsterdam, Wat Sci Tech, 17, 493, (1984)

Pitman A.R., "Settling properties of extended aeration sludge", JWPCF, 52, (3), 524 (1980)

Riddel M.D.R., Lee J.S. and T.E. Wilson, "Method for estimating the capacity of an activated sludge plant", JWPCF, Vol 55, No. 4, (1983)

STORA (Stichting Toegepast Onderzoek Reiniging Afvalwater), "Hydraulische en technologische aspecten van het nabezink-process", Rapport 1-Literatuur, Rapport 2-Ronde nabezinktanks (Praktijkonderzoek), Rapport 3-Rondenabezinktanks (Ontwerpgegevens en bedrijfservaring), (1981)

White M.J.D., "Settling of activated sludge", Technical Report TR11, Water Research Centre, England, (1975)

APPENDIX A
THE FLUX THEORY

Much of what follows has been taken directly from Chapter 8 of "Theory, Design and Operation of Nutrient Removal Activated Sludge Processes", published by the Water Research Commission of South Africa, (1984), although some of the terminology regarding design and operating charts has been changed.

In continuous settling tank operation, the sludge entering the settler is transferred to the bottom by two flux components: (a) the gravity flux and (b) the flux caused by the downdraught flow generated by the sludge abstraction flow from the bottom of the settler, called the bulk flux. The gravity flux is given by the product of the settling velocity V_s, and the concentration of the sludge, X:

$$G_s = V_s * X \qquad (A.1)$$

where G_s = solids flux ($kgm^{-2}d^{-1}$)
V_s = settling velocity (md^{-1})
X = sludge concentration ($kgMLSSm^{-3}$)

The bulk flux (G_b) is given by the product of the underflow velocity and the sludge concentration where the underflow velocity is the downdraught velocity caused by the underflow sludge removal:

$$G_b = u_u * X \qquad (A.2)$$

$$u_u = \frac{Q_r}{A} \qquad (A.3)$$

where G_b = bulk flux ($kgm^{-2}d^{-1}$)
u_u = underflow velocity (md^{-1})
Q_r = underflow rate (m^3d^{-1})

A = surface area of settling tank (m^2)

For a fixed underflow rate, the bulk flux is proportional to the sludge concentration. This is depicted graphically in Figure A.1.

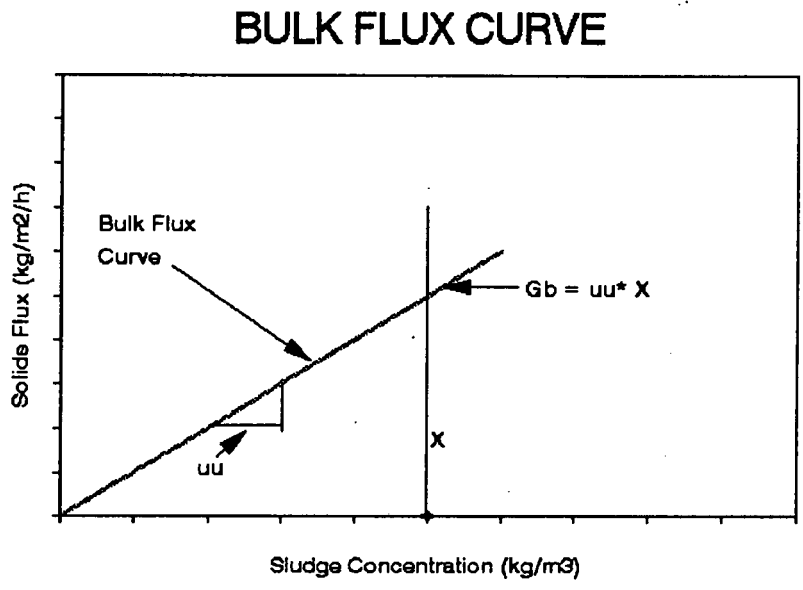

Figure A.1: Bulk flux vs sludge concentration

The total flux (G_t) to the bottom of the settler is the sum of the two flux components:

$$G_t = G_s + G_b = X(V_s + u_u) \quad (A.4)$$

For a selected value of the underflow velocity u_u, the sum of the two flux components can be represented graphically, as shown in Figure A.2.

For the particular choice of u_u, the total flux G_t attains a minimum value G_L at a concentration X_L. This minimum limits the rate at which sludge can reach the bottom of the settling tank. Hence, to ensure that all the sludge reaches the bottom, the sludge mass applied to the tank per unit surface area i.e. the applied flux (G_{ap}) must be equal to or less than the limiting flux (G_L).

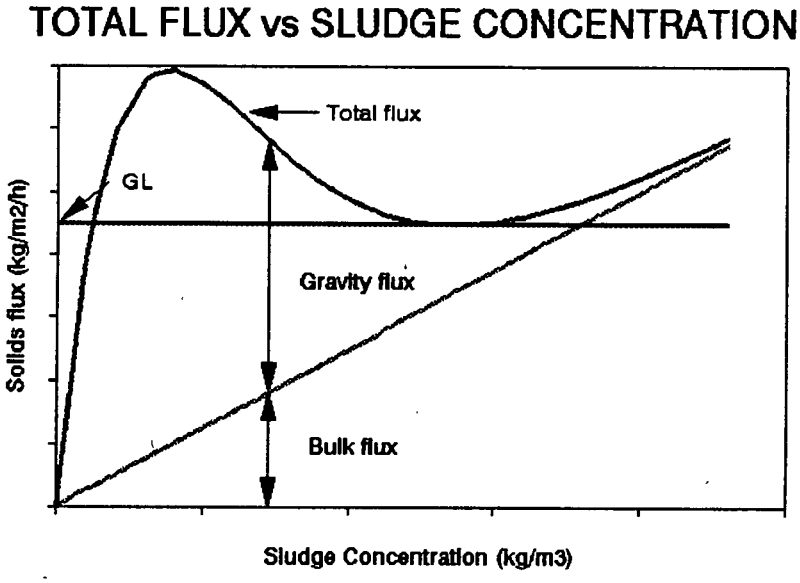

Figure A.2: Total flux vs sludge concentration

The applied flux on the settling tank is given by the product of the sludge concentration in the reactor (X_o) and the combined recycle and influent flow ($Q_i + Q_r$) per unit area:

$$G_{ap} = X_o \frac{(Q_i + Q_r)}{A} = X_o(u_o + u_u) \quad \text{(A.5)}$$

where G_{ap} = applied flux ($kgm^{-2}d^{-1}$)

X_o = operating MLSS sludge concentration in the biological reactor (kgm^{-3})

u_o = overflow rate (md^{-1})

$$u_0 = \frac{Q_i}{A} \quad \text{(A.6)}$$

where Q_i = influent wastewater to process (m^3d^{-1})

Hence, for safe operation of the settling tank:

$$G_{ap} \leq G_L \qquad (A.7)$$

where G_L = limiting flux ($kgm^{-2}d^{-1}$)

From a mass balance around the settling tank, if no sludge is lost over the effluent weirs, the mass of sludge applied is equal to the mass of sludge removed in the sludge underflow i.e.

$$Q_r X_r = X_o(Q_i + Q_r) \qquad (A.8)$$

where X_r = MLSS concentration in underflow recycle (kgm^{-3})

For design purposes, for a specified MLSS concentration (X_o), influent flow (Q_i), and selected underflow recycle (Q_r), the area (A) is found by trial and error. Firstly, Equations (A.3) to (A.5) are used to determine the applied flux (G_{ap}) for the selected operating parameters. Then the limiting flux (G_L) is found as illustrated on the total flux curve in Figure A.2.

The correct area of the settling tank is the value which makes Equation (A.7) an equality. Values of A which result in $G_{ap} > G_L$ are too small and settling tank failure will occur. Values of A which result in $G_{ap} < G_L$ are too large, and although the tank will operate successfully, it will be oversized and thus not economically optimum. The value of A found by this method is only valid for the specified X_o and Q_i and selected Q_r. By repeating the procedure for different values of Q_r, different values of A will be obtained. The maximum expected value of Q_r should be selected in determining A for the proposed plant.

Under safe conditions, no solids will be lost with the effluent if the overflow velocity u_o is less than or equal to the settling velocity of the sludge at the concentration at which it is discharged to the tank (X_o) i.e.:

$$u_o \leq V_s \text{ at } X_o \qquad (A.9)$$

Clearly, the above procedure is extremely tedious because for every choice of Q_r, different total flux curves need to be constructed.

Yoshioka et al (1957) (see also Dick and Young (1972), Pitman (1980) and White (1975)) have streamlined the procedure by introducing the concept of the state point. Their graphical design procedure is carried out using the gravity flux curve, which is specific only to the settling characteristics of the sludge and does not depend on the settling tank parameters.

On the gravity flux plot (Figure A.3), the operating sludge concentration (X_o), is represented by a vertical line at the specified X_o value. The overflow rate ($u_o = Q_i/A$) is represented by a line (called the overflow line) from the origin with the slope equal to the overflow rate. The intersection of the overflow line and the operating concentration line is called the state point. The underflow rate ($u_u = Q_r/A$) is represented by a line (called the underflow line) with the slope equal to the underflow rate passing through the state point, as illustrated in Figure A.3.

Figure A.3 illustrates an underloaded situation, where $G_{sp} < G_L$. In this case, the intersection of the underflow line with the horizontal axis gives the underflow concentration (X_r) as given by Equation (A.8) and that with the vertical axis gives the applied flux G_{sp} as given by Equation (A.5).

The state point is defined as the point of intersection of the three operating lines (the feed concentration line, the underflow line and the overflow line) and may fall either within or outside the envelope of the gravity flux curve.

1. When the state point is within the envelope of the flux curve, the following four situations are possible:

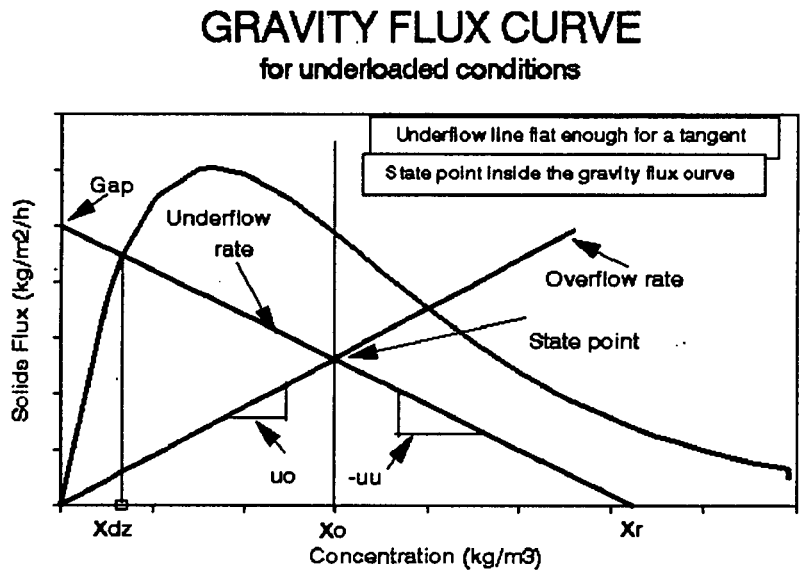

Figure A.3: The gravity flux curve onto which is superimposed the settling tank behaviour - underloaded conditions.

a. When the underflow line is sufficiently flat to enable a tangent to be drawn to the gravity flux curve and cuts the flux curve at only one point, then the tank is underloaded, and safe operating conditions prevail. See Figure A.3.

b. When the underflow line is sufficiently flat to enable a tangent to be drawn to the gravity flux curve and cuts the flux curve at one point only and is tangential at another, critically loaded conditions prevail. See Figure A.4.

c. When the underflow line is sufficiently flat to enable a tangent to be drawn to the gravity flux curve and cuts the flux curve at 3 points, overloaded conditions prevail. This type of failure is termed solids flux limit A failure. See Figure A.5.

d. When the underflow line is too steep to enable a tangent to be drawn to the gravity flux curve and cuts the gravity flux curve in one place only, underloaded conditions prevail. See Figure A.6.

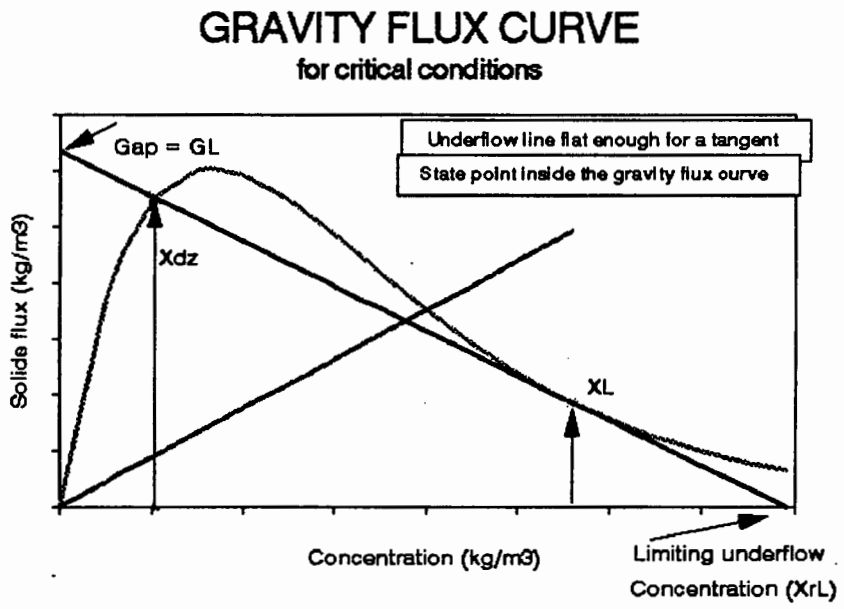

Figure A.4: Gravity flux curve showing critically loaded conditions in the settling tank.

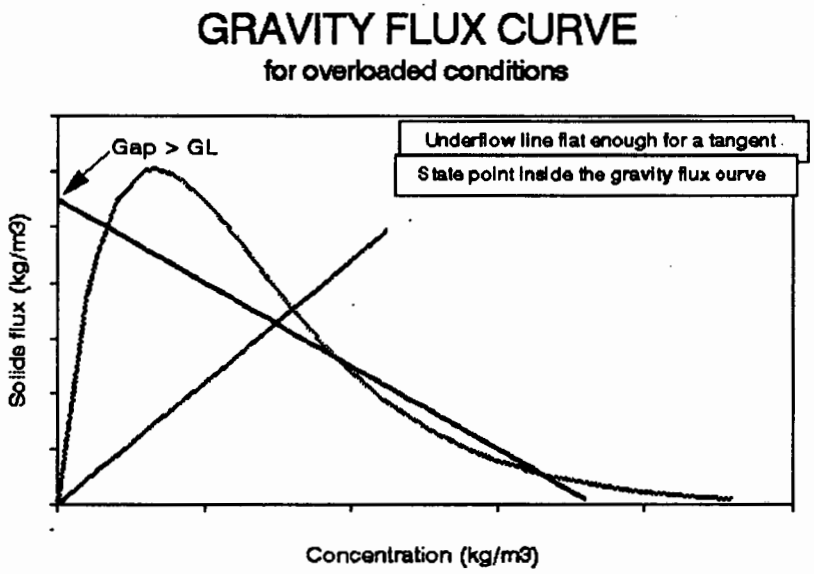

Figure A.5: Gravity flux curve showing overloaded conditions in the settling tank - state point inside flux curve.

2. When the state point is outside the envelope of the flux curve, overloaded conditions will always prevail, but the following two conditions are possible:

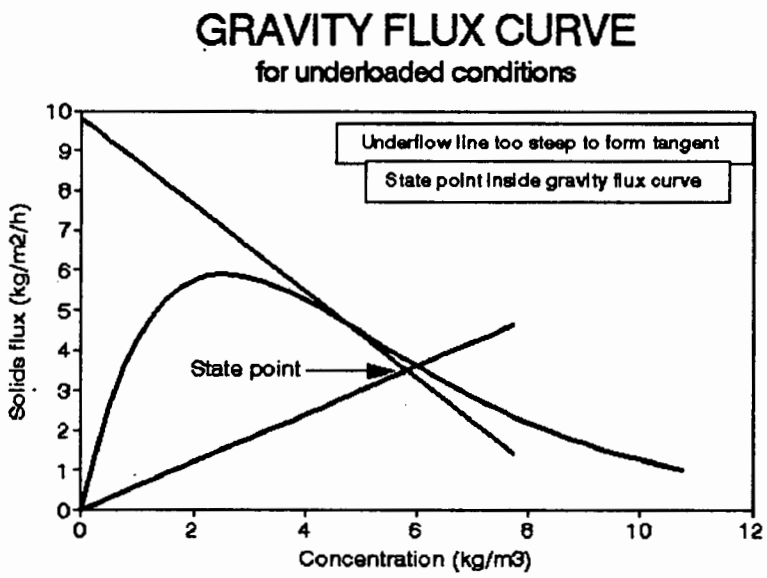

Figure A.6: Gravity flux curve showing underloaded conditions in the settling tank - underflow line too steep to form a tangent

a. when the underflow line is sufficiently flat to enable a tangent to be drawn to the gravity flux curve (see Figure A.7) the type of failure is termed solids flux limit A failure.

b. when the slope of the underflow line is too steep to make a tangent to the flux curve of the flux curve (see Figure A.8) the type of failure is termed solids flux limit B failure.

The above conditions can be readily applied to design. For a given Q_i and X_o, select A, which gives u_o (Equation (A.6)) and, with X_o, fixes the state point. The area A should be selected so that the state point falls on or within the flux curve. Through the state point, draw the underflow line such that it makes a tangent to the flux curve. From the slope of the underflow line and the selected A, determine Q_r (Equation (A.3). Observe that this procedure actually solves Equations (A.5) to (A.9) graphically. The intercept of the underflow line with the vertical is the applied flux (G_{ap}), and, when the underflow line makes a tangent to the flux curve, the applied flux

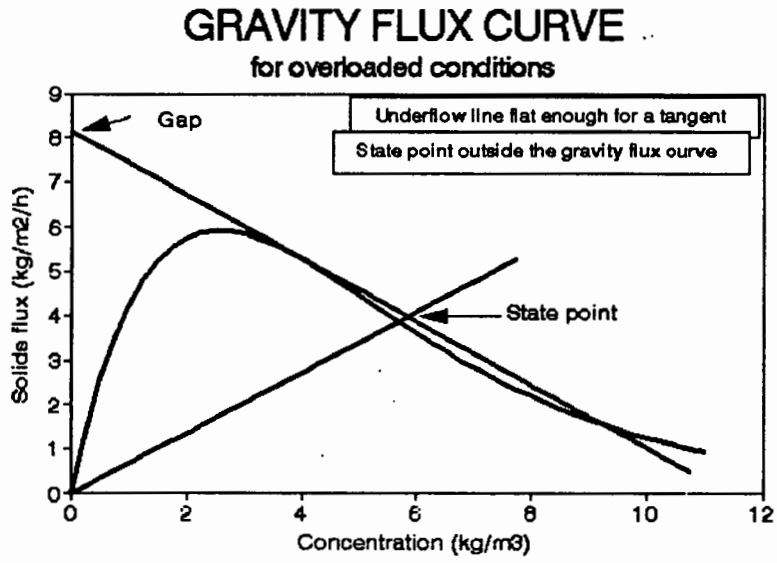

Figure A.7: **Gravity flux curve showing overloaded conditions in the settling tank - underflow line flat enough to form a tangent.**

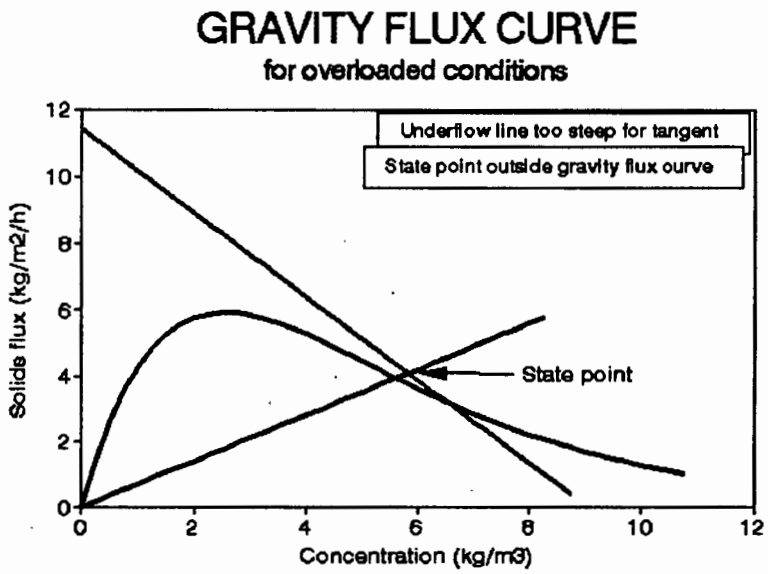

Figure A.8: **Gravity flux curve showing overloaded conditions in the settling tank - underflow line too steep to form a tangent.**

equals the limiting flux. See Equation (A.7) and Figure A.4.

Although the above procedure is still a trial and error one in that a repeated selection of A is made and the corresponding Q_r for safe operation is calculated, it is far simpler than the total flux curve method because each selected A can be analysed on the same flux curve. Thus, the need for constructing different total flux curves (Figure A.2) is obviated. Note that the two methods give identical results; the condition described by the horizontal line from G_L in Figure A.2 is identical to that described by the underflow line tangential to the flux curve in Figure A.4.

In order to avoid the difficulties associated with having to carry out a graphical procedure every time, a relationship between sludge settling velocity and concentration is required. Such a relationship would allow direct analytical solutions to the design equations.

Accepting the Vesilind (1968) semi-log expression:

$$V_s = V_o.e^{-n.X} \qquad (A.10)$$

where V_s = settling velocity (md^{-1})

X = sludge concentration ($kgMLSSm^{-3}$)

V_o, n = constants describing settling characteristics of the sludge (md^{-1} m^3kg^{-1})

and substituting Equation (A.10) into Equation (A.1) yields the gravity flux in terms of the concentration and settling characteristics. i.e.:

$$G_s = X.V_o\, e^{-nX} \qquad (A.11)$$

Equation (A.11) describes the gravity flux curve shown in Figure A.3.

The slope of the flux curve is given by the derivative of Equation (A.11) i.e:

$$\frac{dG_s}{dX} = V_o e^{-nX} (1-nX) \qquad (A.12)$$

which, when set to zero, gives a turning point at X = 1/n and a maximum flux of V_o/ne. Differentiating Equation (A.12) with respect to X and substituting 1/n for X shows that the turning point with co-ordinates (1/n, V_o/ne) is a maximum. Setting the second derivative to zero shows that there is an inflexion point in the flux curve at co-ordinates ($2/n$, $2V_o/ne^2$).

From an inspection of the flux curve, no tangential underflow line can be constructed on the flux curve with a slope greater than that of the flux curve at the inflexion point. The intercepts of the tangent at the inflexion point with the vertical and horizontal axes therefore give respectively the maximum limiting flux (G_{lmax}) and the minimum underflow concentration (X_{rmin}) for the underflow line tangent limit. The slope of this tangent is $-V_o/e^2$ (from Equation (A.12)) and hence:

$$G_{lmax} = \frac{4V_0}{ne^2} = 2G_{IP} = 4.\frac{G_{max}}{e} \qquad (A.13)$$

$$X_{rmin} = \frac{4}{n} = 2X_{IP} = 4X_{TP} \qquad (A.14)$$

where subscripts IP and TP refer to the inflexion and turning points respectively. The above features of the flux curve are illustrated in Figure A.9.

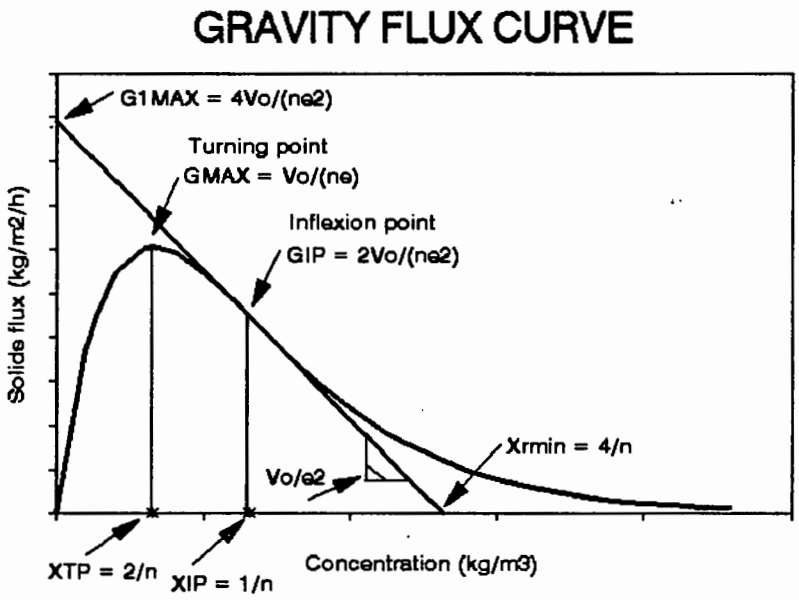

Figure A.9: Mathematical properties of the flux curve

CONCENTRATION REGIONS IN THE SETTLING TANK

The gravity flux curve is a useful tool in identifying the expected concentration regions in the settling tank.

1. for safe (underloaded) conditions, only two concentration regions are expected. See Figure A.10:

   a. the dilute zone settling region of concentration X_{dz}. This point is found on the flux curve at the intersection of the underflow line with the flux curve to the left of the turning point (see Figure A.3),

$$X_{dz} V_o e^{-nX_{dz}} = -u_u X_{dz} + G_{sp}$$

$$X_{dz} = \frac{G_{sp}}{(V_o e^{-nX_{dz}} + u_u)} \qquad (A.15)$$

   b. the underflow concentration zone of concentration X_r, where X_r is given by the intercept of the underflow line with the horizontal axis. See Figure A.3.

$$-u_u X_r + G_{ap} = 0$$

$$X_r = \frac{G_{ap}}{u_u} \qquad \text{(A.16)}$$

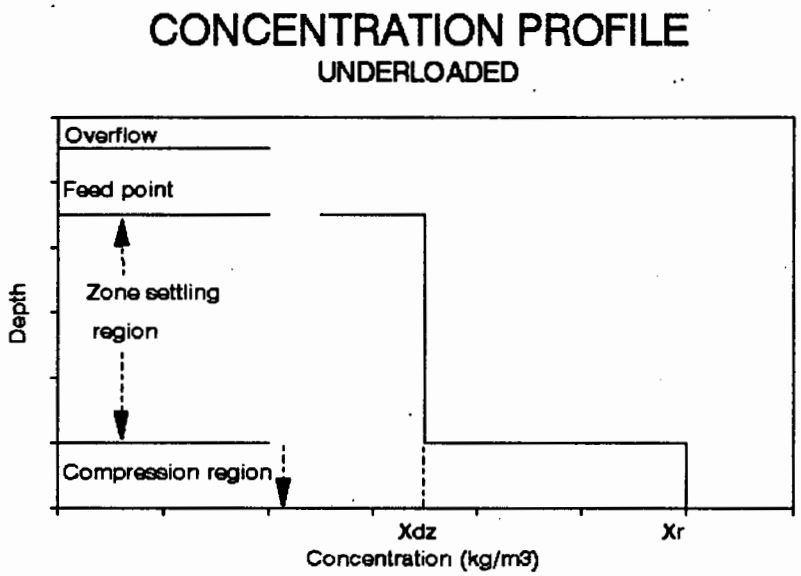

Figure A.10: Concentration profile for underloaded conditions

2. For critically loaded conditions, three concentration zones occur in the settling tank (see Figure A.11):

   a. X_{dz}, the dilute zone concentration,

   b. X_{rL}, the limiting underflow concentration and

   c. an additional region of concentration X_L. This is the zone settling region where the concentration is that which causes the limiting flux, G_L. For critical conditions with respect to solids flux limit A, X_L is found where the slope of the gravity flux curve is equal to the slope of the underflow line (see Figure A.4). The equation of the gravity flux curve is:

$$G = X(V_o e^{-nX}) \tag{A.17}$$

The slope of the gravity flux curve is:

$$\frac{\delta G}{\delta X} = V_o e^{-nX}(1-nX) \tag{A.18}$$

The slope of the underflow line is:

$$\frac{\delta G}{\delta X} = -u_u \tag{A.19}$$

Equating the two slopes at X_L gives:

$$-u_u = V_o e^{-nX_L}(1-nX_L) \tag{A.20}$$

Thus

$$X_L = -\frac{1}{n} LN\left[\frac{u_u}{V_o(1-nX_L)}\right] \tag{A.21}$$

which is solved iteratively.

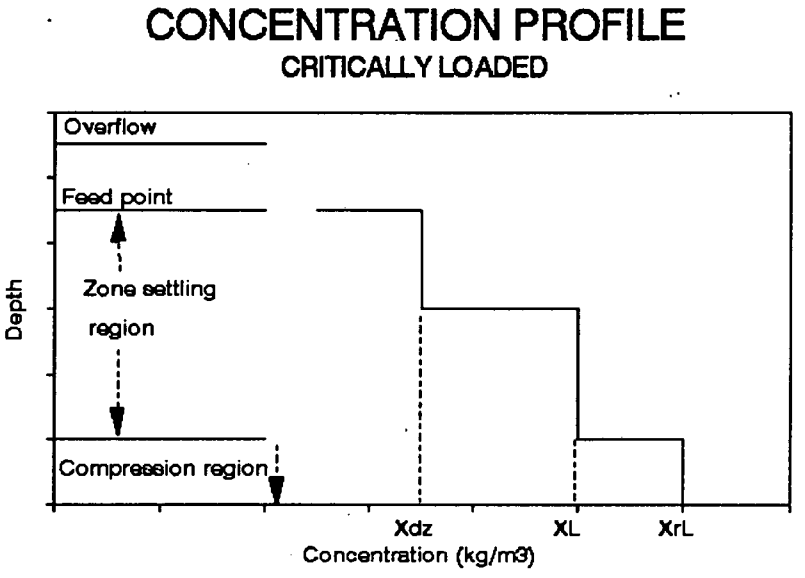

Figure A.11: Concentration profile for critically loaded conditions

For critical conditions with respect to solids flux limit B (see Figure A.8), X_L is found where the state point is on the gravity flux curve and is equal to the feed concentration:

$$X_L = X_o \tag{A.22}$$

For both forms of critical conditions, X_{rL} is found where the limiting underflow line intersects the X axis. Firstly, finding G^*, the point on the gravity flux curve which corresponds to X_L:

$$G^* = X_L V_o e^{-nX_L} \tag{A.23}$$

which gives G_L, the limiting flux:

$$G_L = G^* + u_u X_L \quad (A.24)$$

The intersection of the limiting underflow line with the X axis is thus:

$$-u_u X_{rL} + G_L = 0 \quad (A.25)$$

Thus:

$$X_{rL} = \frac{G_L}{u_u} \quad (A.26)$$

3. For overloaded conditions, the limiting concentration zone settling region will expand upwards (consuming the dilute zone settling concentration layer) until it reaches the height of the feed point. A sludge layer above the feed point then develops. This layer will be of concentration X_{af}, caused by the difference between the applied and the limiting flux i.e. the flux which has been forced to move in an upward direction.

For solids flux limit A and solids flux limit B failure, calculating the flux above the feed point:

$$G_{up} = G_{ap} - G_L \quad (A.27)$$

This flux is composed of a bulk flux term (moving upwards) and a gravity flux term (moving downwards) as follows:

$$G_{up} = X_{af} u_u - X_{af} V_o e^{-nX_{af}} \quad (A.28)$$

Thus

$$X_{af} = \frac{-1}{n} LN\left[\frac{u_i}{V_o} - \frac{G_{up}}{V_o X_{af}}\right] \quad (A.29)$$

which is solved iteratively. For solids flux limit B failure, X_{af} is always equal to X_o.

When this layer reaches the effluent overflow, sludge loss with the effluent will begin. The concentration that is lost with the effluent, X_{ef}, is given by:

$$X_{ef} = \frac{(G_{ap} - G_L)}{u_o} \qquad (A.30)$$

See Figure A.12.

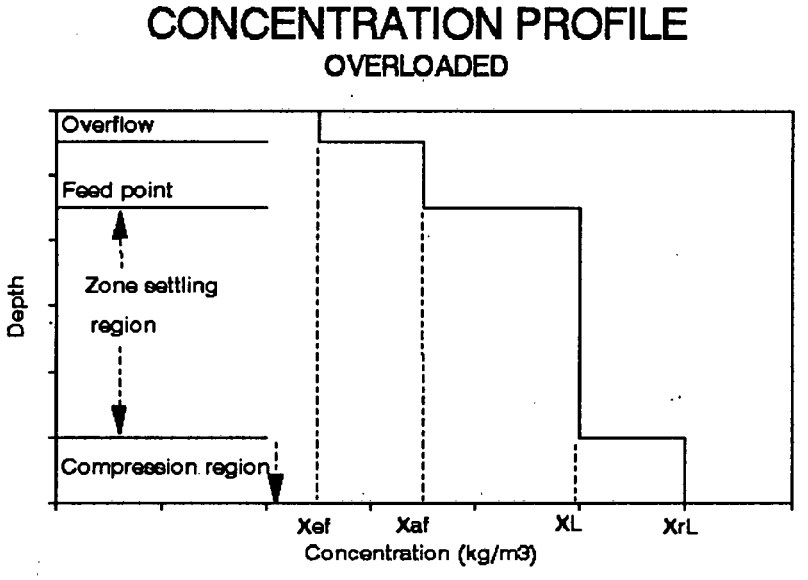

Figure A.12: Concentration profile for overloaded conditions

$$X_1 = \left(\frac{X_r}{2}\right)\left[1 + \sqrt{1 - \frac{4}{(nX_r)}}\right] \qquad (A.36)$$

Substituting Equation (A.36) into Equation (A.11) gives the limiting flux. i.e:

$$G_1 = V_o \alpha X_r \frac{(1 + \alpha)}{(1 - \alpha)} e^{\left(-nX_r \frac{(1 + \alpha)}{2}\right)} \qquad (A.37)$$

where

$$\alpha = \sqrt{1 - \frac{4}{nX_r}} \qquad (A.38)$$

If $\alpha < 0$, there is no solution for G_1. Setting $\alpha = 0$ yields $X_r = 4/n$ and hence $G_1 = 4V_o/ne^2$ which corresponds to X_{rmin} and G_{1max} respectively as found above (see Figure A.9). No solution for G_1 is possible for $X_r < 4/n$ because the curvature of the flux curve is such that no valid underflow line can be constructed within the envelope of the flux curve. This result can be interpreted as the solids flux limit A criterion having no relevance in a design when $X_r < 4/n$, this region being governed by the solids flux limit B criterion.

Substituting Equation (A.33) for X_r into Equation (A.37) and (A.38) and substituting Equation (A.37) into Equation (A.32) yields:

$$\frac{Q_i}{A} = \frac{V_o}{s} \frac{(1+\alpha)}{(1-\alpha)} e^{-n(1+s)X_o \frac{(1+\alpha)}{2s}} \qquad (A.39)$$

where

$$\alpha = \sqrt{1 - \frac{4s}{n(1+s)X_o}} \qquad (A.40)$$

Equation (A.39) relates the overflow rate to the recycle ratio for a selected value of the sludge concentration in the reactor and settling characteristics of the sludge to meet the

solids flux limit A criterion. If $\alpha = 0$, $X_o = 4s/(n(1+s))$. Hence, from Equation (A.39), if $\alpha = 0$

$$\frac{Q_i}{A} = \frac{V_o}{e^2 s} \qquad (A.41)$$

Consequently, if Q_i/A is less than $V_o/(e^2 s)$, then the solids flux limit A criterion governs the design. If Q_i/A is greater than $V_o/(e^2 s)$, then the solids flux limit B criterion governs the design. The solids flux limit B criterion is met if the overflow rate is less than the settling velocity of the sludge at the feed concentration i.e. from Equation (A.9)

$$\frac{Q_i}{A} < V_o e^{-nX_o} \qquad (A.42)$$

THE SETTLING TANK DESIGN AND OPERATING CHART

By plotting Q_i/A versus s from Equations (A.39) to (A.42) for different values of X_o, a steady state design and operating chart for the settling tank is obtained (see Figure A.13).

Figure A.14 shows the same design and operating chart drawn for a feed concentration of 5 kgm^{-3} only.

The hyperbola in Figure A.14 described by Equation (A.41) distinguishes between the domain in which, on the gravity flux curve, the underflow line is sufficiently flat to enable a tangent to be drawn to the gravity flux curve (area between axes and hyperbola) and in which the underflow line is too steep to enable a tangent to be drawn (area above hyperbola). The solids flux limit A criterion is given by Equation (A.39) which, for different X_o values, is a family of curves from the hyperbola to the origin. These curves show that, as the underflow recycle ratio decreases, the allowable overflow rate decreases. The solids flux limit B criterion is given by Equation (A.42) and, being independent of s, is a family of horizontal lines. In the region below the hyperbola, both solids flux limit A and solids flux limit B are met. In some instances

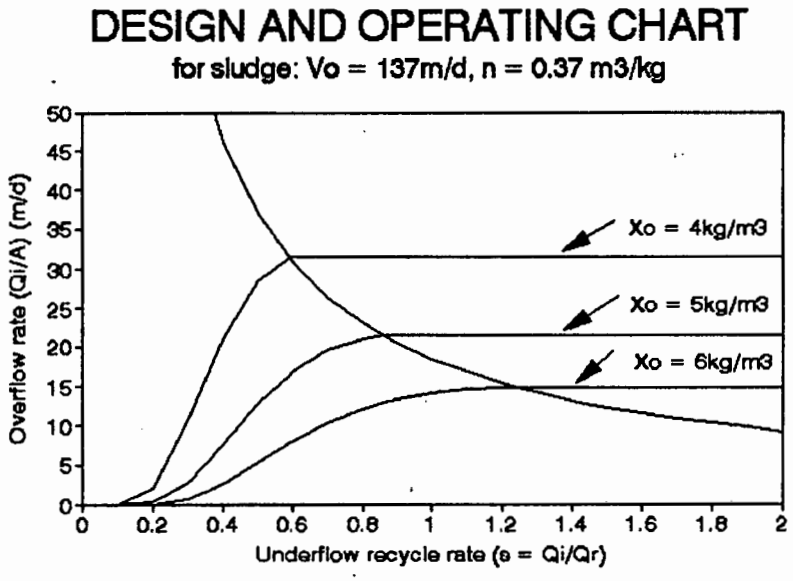

Figure A.13: Design and operating chart showing the effects of different feed concentrations

in this region, the allowable overflow rate is higher for solids flux limit A than for solids flux limit B, in which case solids flux limit B is the governing criterion for the settling tank. Consequently, for a specified rector concentration, X_o, failure of the settling tank is represented by overflow rate-underflow recycle ratio data pairs falling above the solids flux limit A and solids flux limit B lines.

It should be noted that the design and operating chart is also valid for daily cyclic conditions. For successful operation of the settling tank, the conditions prescribed by the design and operating chart need to be met at any instant of the day. For example, for a fixed settling tank area (A), and underflow rate (Q_r), as the influent flow (Q_i) to the plant increases, so the overflow rate (Q_i/A) increases and the recycle ratio (s) decreases, which moves the intersection point of the overflow rate and the recycle ratio upwards and to the left in Figure A.14. At each instant of the day, the overflow rate and the recycle ratio intersection point must subscribe to the solids flux limit A and the solids flux limit B criteria in the diagram i.e. must at all times be below the solids flux limit A and the solids flux limit B lines.

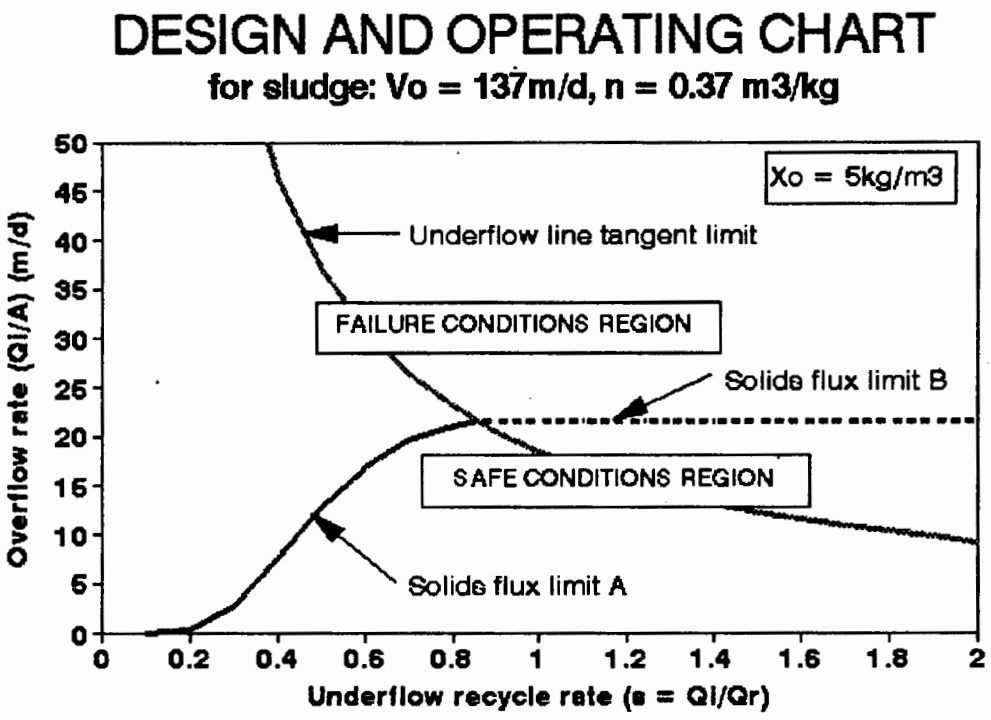

Figure A.14: Design and operating chart showing failed and safe regions of settling tank operation

REFERENCES

Dick R. I., and K. W. Young, "Analysis of thickening performance of final settling tanks", Procs 27th Purdue International Waste Conf, Lafayette, Indiana, (1972)

Pitman A.R., "Settling properties of extended aeration sludge", JWPCF, 52, (3), 524 (1980)

Smollen M., "Behaviour of secondary settling tanks in activated sludge processes", MSc Thesis, Dept of Civil Engineering, University of Cape Town, (1981)

Vesilind P.A., "Design of prototype thickeners from batch settling tests", Water and Sewage Works, 115, 302, (1968)

White M.J.D., "Settling of Activated Sludge", Technical Report TR11, Water Research Centre, England, (1975)

Yoshioka N., Hotta Y., Naito S., Tanaka S. and S. Tsugami, "Continuous thickening of homogenous flocculated suspension", Chem Eng Tokyo, 21, 66, (1957)

APPENDIX B

STATISTICAL CALCULATIONS FOR POOLING THE DATA

The statistical questions that need to be answered to determine whether or not all the data belongs to a single population are as follows. Suppose we have k groups and n_i observations (on both X and Y) in the ith group,

1. Can one regression line be used for all the data?

2. If b_i represents the estimate of β_i, where b_i is the estimated slope for the ith group and β_i is the true slope of the regression function in the population from which the ith group is a sample, does $\beta_1 = \beta_2 = \ldots = \beta_k$? In other words, are all the sample slopes estimates of the same true slope?

3. Assuming $\beta_1 = \beta_2 = \ldots = \beta_k$, would a regression fitted to the group means be linear?

4. Assuming $\beta_1 = \beta_2 = \ldots = \beta_k$ and that the regression of the group means is linear, is $\beta_w = \beta_m$, where β_m is the true regression coefficient for the means and β_w is the true pooled within groups regression coefficient?

The necessary calculations are as follows:

$$A_i = \sum_{j=1}^{n_i} (X_{ij} - \bar{X}_i)^2 = \sum_{j=1}^{n_i} X^2_{ij} - \frac{\left[\sum_{j=1}^{n_i} X_{ij}\right]^2}{n_i} \tag{B.1}$$

$$B_i = \sum_{j=1}^{n_i} (X_{ij} - \bar{X}_i)(Y_{ij} - \bar{Y}_i) = \sum_{j=1}^{n_i} X_{ij}Y_{ij} - \frac{\left[\sum_{j=1}^{n_i} X_{ij}\right]\left[\sum_{j=1}^{n_i} Y_{ij}\right]}{n_i} \tag{B.2}$$

$$C_i = \sum_{j=1}^{n_i} (Y_{ij} - \bar{Y}_i)^2 = \sum_{j=1}^{n_i} Y^2_{ij} - \frac{\left[\sum_{j=1}^{n_i} Y_{ij}\right]^2}{n_i} \tag{B.3}$$

$$A_T = \sum_{i=1}^{k}\sum_{j=1}^{n_i} (X_{ij} - \bar{X})^2 = \sum_{i=1}^{k}\sum_{j=1}^{n_i} X^2_{ij} - \frac{\left[\sum_{i=1}^{k}\sum_{j=1}^{n_i} X_{ij}\right]^2}{\sum_{i=1}^{k} n_i} \tag{B.4}$$

$$\begin{aligned} B_T &= \sum_{i=1}^{k}\sum_{j=1}^{n_i} (X_{ij} - \bar{X})(Y_{ij} - \bar{Y}) \\ &= \sum_{i=1}^{k}\sum_{j=1}^{n_i} X_{ij}Y_{ij} - \frac{\left[\sum_{i=1}^{k}\sum_{j=1}^{n_i} X_{ij}\right]\left[\sum_{i=1}^{k}\sum_{j=1}^{n_i} Y_{ij}\right]}{\sum_{i=1}^{k} n_i} \end{aligned} \tag{B.5}$$

$$C_T = \sum_{i=1}^{k}\sum_{j=1}^{n_i} (Y_{ij} - \bar{Y})^2 = \sum_{i=1}^{k}\sum_{j=1}^{n_i} Y^2_{ij} - \frac{\left[\sum_{i=1}^{k}\sum_{j=1}^{n_i} Y_{ij}\right]^2}{\sum_{i=1}^{k} n_i} \tag{B.6}$$

$$A_w = \sum_{i=1}^{k} A_i \tag{B.7}$$

$$B_w = \sum_{i=1}^{k} B_i \tag{B.8}$$

$$C_w = \sum_{i=1}^{k} C_i \tag{B.9}$$

Designate S_1 as the pooled sum of squares of deviations from the regression.

$$S_1 = \sum_{i=1}^{k} C_i - \sum_{i=1}^{k} \left[\frac{B_i^2}{A_i} \right] \tag{B.10}$$

Designate S_2 as the sum of squares of deviations among the k group regression coefficients, that is, if S_2 is a sum of squares expressing the amount of variation among $b_1, b_2 \ldots, b_k$, where b_j is the regression coefficient in the jth group, it may be shown that:

$$\begin{aligned} S_2 &= C_w - \frac{B^2{}_w}{A_w} - S_1 \\ &= \sum_{i=1}^{k} \frac{B^2{}_i}{A_i} - \frac{B^2{}_w}{A_w} \end{aligned} \tag{B.11}$$

Similarly, we may designate the sum of squares of the deviations of the Y-means from the regression of Y-means on X-means by S_3, where S_3 is calculated as follows:

$$S_3 = C_m - \frac{B^2{}_m}{A_m} \tag{B.12}$$

The square of the difference between the regression coefficient computed from the "pooled within" values (b_w) and the regression coefficient for the regression of the means (b_m) is given by $(b_w - b_m)^2$. If we multiply this by a suitable factor, it becomes another estimate of the standard deviation (σ_E), assuming a constant variance of Y for all X. This may be expressed as:

$$S_4 = (b_w - b_m)^2 \frac{A_w A_m}{A_T} \tag{B.13}$$

Since S_1 is the pooled sums of squares of deviations from regression, we can show that:

$$S_T = S_1 + S_2 + S_3 + S_4 \tag{B.14}$$

Furthermore, the degrees of freedom associated with S_T may be subdivided in the following fashion:

$$\sum_{i=1}^{k} n_i - 2 = \left[\sum_{i=1}^{k} n_i - 2k\right] + (k - 1) + (k - 2) + 1 \tag{B.15}$$

and these are associated with S_1, S_2, S_3, and S_4 respectively.

We are now in a position to answer the questions posed earlier. The correct test procedures for each question are as follows:

1. Can one regression line be used for all the regressions?

$$F_1 = \frac{(S_T - S_1)/2(k - 1)}{S_1 / \left[\sum_{i=1}^{k} n_i - 2k\right]} \tag{B.16}$$

If $F_1 < F_{0.95}(\upsilon_1, \upsilon_2)$ where $\upsilon_1 = 2k\text{-}1$, $\upsilon_2 = \Sigma n_i\text{-}2k$, then one regression line can be used for all the equations.

2. To test the hypothesis that $\beta_1 = \beta_2 = \ldots = \beta_k$. This test and the succeeding ones are only considered If F_1 turns out to be significant.

$$F_2 = \frac{S_2/(k-1)}{S_1/\left[\sum_{i=1}^{k} n_i - 2k\right]} \qquad \text{(B.17)}$$

If $F_2 < F_{0.95}(\upsilon_1,\upsilon_2)$ where $\upsilon_1 = k\text{-}1$, $\upsilon_2 = \Sigma n_i\text{-}2k$, then $\beta_1 = \beta_2 = \ldots = \beta_k$.

3. To test whether the regression of the means is linear (assuming $\beta_1 = \beta_2 = \ldots = \beta_k$).

$$F_3 = \frac{S_3/(k-2)}{(S_1 + S_2)/\left[\sum_{i=1}^{k} n_i - k - 1\right]} \qquad \text{(B.18)}$$

If $F_3 < F_{0.95}(\upsilon_1,\upsilon_2)$ where $\upsilon_1 = k\text{-}2$, $\upsilon_2 = \Sigma n_i\text{-}k\text{-}1$, then the regression of the means is linear.

4. To test whether $\beta_w = \beta_m$ (assuming the regression of the means is linear and $\beta_1 = \beta_2 = \ldots = \beta_k$).

$$F_4 = \frac{S_4/1}{(S_1 + S_2)/\left[\sum_{i=1}^{k} n_i - k - 1\right]} \qquad \text{(B.19)}$$

If $F_4 < F_{0.95}(\upsilon_1,\upsilon_2)$ where $\upsilon_1 = 1$, $\upsilon_2 = \Sigma n_i\text{-}k\text{-}1$, then $\beta_w = \beta_m$.

REFERENCES

Ostle B., "Statistics in Research", 2nd Edition, Iowa State University Press, (1963)

APPENDIX C
SWITCHING FUNCTION ALLOCATION IN THE CALCULATION ALGORITHM

In the settling tank, a shock is a step change or concentration discontinuity in the sludge depth concentration profile which may move upwards or downwards in the tank. The switching functions are a means by which the direction of shocks and their associated shock fronts are appropriately dealt with in the algorithm by ensuring that the shocks in the system are propagated in the correct directions and that mass is conserved in the system.

Because the fixed grid numerical method assumes that the concentration in each layer is the same throughout the layer, it assumes that the potential location of an allowable (one that does not violate entropy restrictions) shock can only be at the boundary of each layer. The velocity (speed and direction) of the allowable shock at any cell boundary can be calculated by the derivative $\delta G/\delta X$ (rate of change of flux with concentration) between two adjacent layers. The magnitude of this derivative represents the allowed shock speed at each layer in the network whilst its sign indicates the direction in which the shock is travelling.

A discrete approximation to the derivative $\delta G/\delta X$ across the boundary of each layer is calculated in the following way:

At each time interval, the difference between the concentration in layer (i-1) and layer (i) in the tank is calculated. This quantity is called cdif and can be represented as follows:

$$cdif(i) = conc(i-1) - conc(i) \qquad (C.1)$$

where conc(i) = concentration in the ith layer

conc(i-1) = concentration in the (i-1)th layer

cdif(i) = the difference between the two.

The same procedure is carried out for the flux difference at each layer as follows:

$$fdif(i) = flux(i-1) - flux(i) \qquad (C.2)$$

where flux(i) = flux in the ith layer

flux(i-1) = flux in the (i-1)th layer

fdif(i) = the difference between the two.

If the signs of cdif and fdif in layer (i) are the same or zero (i.e. $\delta G/\delta X$ is zero or positive), then a shock direction (jsw) of +1 is assigned to layer (i). If cdif and fdif have different signs (and are not zero) (i.e. $\delta G/\delta X$ is negative), then a shock direction (jsw) of -1 is assigned to layer (i). These values of jsw indicate the direction in which the shocks are travelling in the layer. A value of jsw = +1 indicates a shock moving downwards and a value of jsw = -1 indicates a shock moving upwards. Once the shock direction in each layer has been established, the next step is to ascertain how the shock direction in each layer relates to the shock direction in the adjacent layers. See Figure C.1.

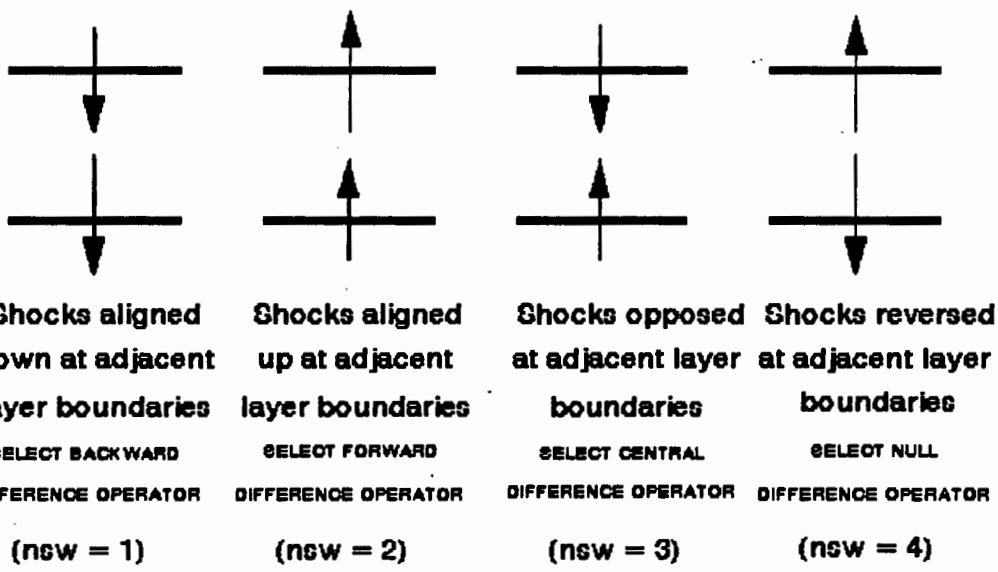

Figure C.1 The spatial differencing criteria

If the shock directions in layer (i-1) and layer (i) are both downwards (i.e. jsw(i-1) = +1 and jsw(i) = +1), then the shocks are said to be aligned downwards at adjacent layer boundaries, and a backwards difference operator (nsw = 1) is selected for layer (i). This difference operator aligns itself with the direction that the shock is travelling, and indicates that the shock is moving downwards through layer (i-1) into layer (i).

If the shock directions in layer (i-1) and layer (i) are both upwards (i.e. jsw(i-1) = -1 and jsw(i) = -1), then a forwards difference operator (nsw = 2) is selected for layer (i), also aligning itself with the direction in which the shock is travelling. In this case, the selection of a forwards difference operator indicates that the shock is moving upwards through layer (i) into the next one above (i-1).

If the shock direction in layer (i-1) is downwards and that in layer (i) is upwards (i.e. jsw(i-1) = +1 and jsw(i) = -1), in other words, the shock velocities are opposed at adjacent layer boundaries, then a central difference operator is selected (nsw = 3) for layer (i). This indicates that layer (i) contains the shock front and that solids will accumulate in this layer. This accumulation will continue until the continuously calculated quantities cdif and fdif indicate that the slope of the derivative between layers (i-1) and (i), and hence the relative shock directions, have changed. Subsequently, no further solids will be permitted to accumulate in this layer and the shock front location will move to an adjacent layer.

If the shock direction in layer (i-1) is upwards and that in layer (i) is downwards (i.e jsw(i-1) = -1 and jsw(i) = +1), in other words, the shock velocities are reversed at adjacent layer boundaries, then the null difference operator (nsw = 4) is selected.

The selection of the null difference operator is a peculiarity of the switching function scheme, and is necessary in order for mass to be correctly conserved in the system. Whenever adjacent layer boundaries have shocks in reversed directions, no shocks can exist in the layer, since it is behind the shock front and loses material to the layers

both above and below it. In the case of sedimentation processes, the concentration of material in this layer must equal the limiting flux concentration. Since regions exist above and below this layer which also contain the limiting flux concentration, it is clear that this layer can accumulate no further material by convective transport. The algorithm, therefore, selects a null difference operator for this layer to follow the central difference operator used at the layer containing the shock.

A graphical summary of the criteria for spatial differencing is presented in Figure C.1.

In order to clarify the manner in which the difference operators (1,2,3 and 4) are selected, two examples are given below:

EXAMPLE 1: THE CASE OF A FALLING SLUDGE BLANKET

In the case of a falling sludge blanket, one would expect to observe the following progression of difference operators (nsw values), where nsw = 3 represents the position of the shock front, which is observed to be falling in the tank. See Table C.1.

Table C.1 Selection of nsw values for a falling sludge blanket

TIME	5 min	10 min	15 min
LAYER NUMBER	nsw	nsw	nsw
9	1	1	1
10	1	1	1
11	1	1	1
12	1	1	1
13	1	1	1
14	**3**	1	1
15		1	1
16		**3**	1
17			**3**

EXAMPLE 2: THE CASE OF A RISING SLUDGE BLANKET

In the case of a rising sludge blanket, one would expect to observe the following progression of difference operators (nsw values) in the lower section of the settling tank, where nsw = 3 represents the position of the shock front, which is rising upwards in the tank. See Table C.2.

In order for the sludge blanket to move above the feed point, the following pattern of concentration differences (cdif), flux differences (fdif), shock velocities (jsw values) and difference operators (nsw values) is necessary in the feed point region of the tank. See Table C.3.

In this case, the sludge blanket (location of the shock front) has risen up to the feed point layer (7), as indicated by the selection of the central difference operator (nsw (nsw = 3) in that layer. In layer 6, above the feed point layer, the null difference

Table C.2 Selection of nsw values for a rising sludge blanket

TIME	5 min	10 min	15 min
LAYER NUMBER	nsw	nsw	nsw
30			3
31			2
32		3	2
33		2	2
34	3	2	2
35	2	2	2
36	2	2	2
37	2	2	2
38	2	2	2

Table C.3 Spatial differencing at the feed point

LAYER NUMBER	cdif	fdif	jsw	nsw
4	<0	<0	1	3
5	<0	>0	-1	2
6	>0	<0	-1	4
7	<0	<0	1	3
8	<0	>0	-1	2
9	<0	>0	-1	2

operator is selected (nsw = 4), indicating that this layer is at the limiting flux concentration, X_{af}, and that material is being lost both upwards (to layer 5) and downwards (to layer 7).

For the reasons of mass conservation discussed above, the difference operator used in series with the central difference operator identifying the location of the shock must be the null difference operator (nsw = 4) in layer 6.

In layer 5, the forward difference operator (nsw = 2) has been selected, indicating that the shock is travelling upwards through this layer. At the point in time represented by this table, the shock front associated with the upwards moving shock above the feed point is located at layer 4, as indicated by the selection of the central difference operator (nsw = 3) for that layer. In other words, the shocks representing the two limiting flux concentrations are both propagating upwards in the tank

1. from the bottom of the tank towards the feed point at X_L (shock front located at the feed point layer) and

2. above the feed point at a concentration of X_{af}. (In this example, the shock front is located at layer 4, but is moving upwards).

For the case of a rising sludge blanket, if the overwriting condition is not activated i.e. the concentration at the feed point layer (7) and the one above it (6) are **not** set equal to one another, the sludge blanket will rise upwards from the bottom of the tank at a concentration X_L until the following pattern of difference operators occurs near the feed point. See Table C.4.

Note that in the table jsw = -1 for layer 8, where it should be jsw = +1 according to the values of cdif and fdif. The incorrect allocation of jsw for this layer is a consequence of the statement in Anderson's program that sets the shock direction in layer 8 equal to that in layer 9 (when the feed point is at layer 7), regardless of the actual shock direction that has been calculated for layer 8. This statement in the program was later eliminated.

Table C.4 Spatial differencing at the feed point in the absence of the overwriting condition

LAYER NUMBER	cdif	fdif	jsw	nsw
5	<0	<0	1	1
6	<0	<0	1	1
7	<0	<0	1	3
8	>0	>0	-1	2
9	<0	>0	-1	2

Although the central difference operator has been selected for layer 7, as expected, in the absence of Anderson's feed point layer condition, the null difference operator (which is necessary for the sludge blanket to move upwards) will never be selected for layer 6 and instead, material will continue to accumulate in layer 7, whilst the concentration in layer 6 will remain very small or zero. The reason for this is that layer 6 is the first layer above the feed point layer, and therefore is the first layer where one process occurs upwards (bulk flux) and one process occurs downwards (gravity flux), as opposed to one where both processes occur downwards (bulk and gravity flux) as in the feed point layer and the ones below it.

This discontinuity in the flux curve means that the algorithm is unable to permit the necessary concentration increase to occur in layer 6.

If, however, Anderson's overwriting condition at the feed point is activated, the calculated concentrations in layer 6 and layer 7 are averaged and this average value is inserted in both layers (see Equations (6.1) and (6.2)). These equations have the effect of ensuring that material is passed to layer 6, thus initiating the propagation of the sludge blanket above the feed point. A consequence of this averaging procedure, however, is that the calculated concentration in layer 5 will be higher than that in layer 6, which is an entropy rule violation, since there is no change in gravity or bulk flux

between these two layers. Hence, once the sludge blanket has risen to the top of the tank, the final predicted concentration profile will always exhibit 2 layers (6 and 7) where the concentration is lower than that of layer 5 and those above it.

Once Anderson's condition has been eliminated in the program, and diffusivity has been added at the feed point, the contents of layers 6 and 7 are "mixed" within the algorithm, and thus the discontinuity in the total flux curves at the feed point is overcome.

This initiates the sludge blanket propagation upwards above the feed point and allows it to continue until solids loss is experienced in the effluent.

REFERENCES

Von Neumann J. and R.D. Richtmyer, "A method for the numerical calculation of hydrodynamic shocks", Journal of Applied Physics, Vol 21, Page 231, (1950)

APPENDIX D

PROGRAM LISTING

```
c.....
c     program SETTLER (revision 5)
c     purpose      Mathematical simulation of dynamic secondary
c                  settling tank behaviour

c     this revision:    *  with seeding for the overloaded case
c                       *  diffusivity function determined by alpha1, alpha2, diftop
c                          and difbot
c                       *  using a CSTR to simulate the time lag for thickening

c     programmer   Alison Emslie Ozinsky
c     date         27 June 1993
c     language     WATFOR-FORTRAN 77
c     input files: simdat1.dat  -  contains initial concentration profile,
c                                  tank dimensions, sludge settleability
c                  newdat1.dat  -  contains Xo, Qi and Qr every 15min
c     output files: conc.dat    -  contains concentration profile and
c                                  total mass in tank
c                  uflow.dat    -  contains sbl, Xef, Xr
c.....
c
      write(*,*)'Enter total length of simulation in hours'
      write(*,*)'  - data will be read every fifteen minutes'
      read(*,*)nruns
      call SETUP(nruns)
      stop
      end
```

```
      subroutine SETUP(nruns)
c.....
c           variable names
c
c           nfq = height of feed point
c           npc = number of layers in the tank
c.....
            real *8         conc,v2,cdif,fdif,fit1,fit2,dx,dt,
     &                      coef,rhs,z,flux,aug,vf,v3,v1,vel,vec,E
            common          q0,qt,uflow,a,dCSTR,diftop,difbot,alpha2
     &                      conc(40),v2,cdif(40),fdif(40),coef(40,3),rhs(40),z(40),
     &                      flux(40),aug(40,4),vf,v3(40),nfq,qup,qdown,qfeed,xfeed,
     &                      E(41),v1,vel(40),vec(40),dx,dt,fit1,fit2,npc,
     &                      nf(40,3),nsw(40),jsw(40),sconc(40),nsp(4,3),iload,xl
c .....
            t0 = 0
            npc = 40

            open(1,file='c:\stora\simdat1.dat')
            read(1,2214)a,dx
 2214       format(3f10.5)
            read (1,2215)SSVI,DSVI
 2215       format (F6.4,1X,F8.6)
            read(1,2202)nfq
 2202       format(I5,1X,F10.8)
            read(1,2201)(conc(k),k=1,npc)
 2201       format(5f10.2/5f10.2/5f10.2/5f10.2/5f10.2/5f10.2/5f10.2/
     &      5f10.2)
            close(1)


c       converting SSVI3.5 to Vo and n
c       and normalising them with respect to velocity and concentration
c       assuming the relationship for extended aeration

            fit1v = exp(2.45095-0.00636*SSVI)
            fit2n = (0.16756+0.00218*SSVI)
            fit1 = fit1v/1.646
            fit2 = fit2n*4.0


c       printing out initial concentrations

            do 5433 j = 1,npc
 5433       sconc(j) = sngl(conc(j))*4.0
            write(*,*)'INITIAL CLARIFIER CONCENTRATIONS'
            write(*,1109)t0,(sconc(i),i=1,npc)
 1109       format(f5.2/5(7f10.2/)5f10.2)

c       initialising the underflow concentration and mass in settler
            uconc = sconc(npc)
            totmass = 0.0

            do 630 iti = 1,nruns
```

```
c     q to be read every fifteen minutes

      lkl = 0
8888  lkl = lkl + 1

      open(2,file = 'c:\stora\newdat1.dat')
      read(2,2217)cas0,cast,q0,qt,uflow
2217  format(2f10.4,3f10.7)

      alpha1 = 10.00
      diftop = 315115.0-120.0*a
      alpha2 = 3.931-0.0015*a
      difbot = -1.71854+175964.3*qt/a*alpha2/diftop
          if (difbot.lt.0.121)difbot = 0.121
      dCSTR = dx/0.0836

c     normalising the feed concentrations

      scin0 = cas0/4.0
      scint = cast/4.0

      call FLUXCALC(cas0,cast,xrl,xdz)
      call DIFFUS(t0)
      call CLAR2(DSVI,nruns,totmass,scin0,scint,t0,lkl,xrl,uconc)

      t0 = t0 + 0.25
      if (lkl.ne.4) go to 8888
630   continue

      return
      end
```

```
      subroutine FLUXCALC(cas0,cast,xrl,xdz)
c .....................................................................
c       variable names
c
c       uu  = underflow velocity
c       ui  = overflow velocity
c       qup = Qi
c       gap = applied flux
c       fit1v =  Vo
c       fit2n  = n
c       xl    = limiting concentration
c       gtemp = g*
c       gl    = limiting flux
c       xrl   = limiting underflow conc
c .....................................................................
      real *8       conc,v2,cdif,fdif,fit1,fit2,dx,dt,
     &              coef,rhs,z,flux,aug,vf,v3,v1,vel,vec,E
      common        q0,qt,uflow,a,dCSTR,diftop,difbot,alpha2
     &              conc(40),v2,cdif(40),fdif(40),coef(40,3),rhs(40),z(40),
     &              flux(40),aug(40,4),vf,v3(40),nfq,qup,qdown,qfeed,xfeed,
     &              E(41),v1,vel(40),vec(40),dx,dt,fit1,fit2,npc,
     &              nf(40,3),nsw(40),jsw(40),sconc(40),nsp(4,3),iload,xl
c .....................................................................

      iload = 0

c     calculate applied flux
      qup = (q0+qt)/2.0 - uflow
      uu = uflow/a
      ui = qup/a
      if(ui.gt.0)s = uu/ui
      xf = (cas0 + cast)/2.0
      gap = xf * (uu + ui)

c     calculate xl for case of solids flux limit A

      fit1v = fit1*1.646
      fit2n  = fit2/4.
      xl = (1+uu/fit1v)/fit2n + 2.0

      if ((ui.lt.fit1v/EXP(2.0)/s).and.(ui.gt.0)) then

643       xlold = xl
          xl = -1/fit2n * ALOG(-uu/fit1v/(1-fit2n*xlold))
          if (abs(xl - xlold).gt.0.00001) go to 643

c     calculate gtemp
          gtemp = fit1v * xl * exp(-fit2n * xl)

c     calculate gl
          gl = gtemp + uu * xl

c       calculate xrl
          xrl = gl/uu
```

```
c      compare limiting and applied fluxes
                if (gap.gt.gl) then
                    iload = 1
                    write(*,*)' ... System overloaded ...'
                    xaf = xl
 645                xafold = xaf
                    xaf = -1/fit2n*ALOG(ui/fit1v-(gap-gl)/fit1v/xafold)
                    if (abs(xafold-xaf).gt.0.00001) goto 645
                    xef=(gap-gl)/ui
                else
                    iload = 0
                    write(*,*)' ... System underloaded ...'
                    xr = gap/uu
                    xdz = xf/2.
 644                xdzold = xdz
                    xdz = gap/(fit1v*exp(-fit2n*xdzold)+uu)
                    if (abs(xdz - xdzold).gt.0.00001) go to 644
                endif

            else
                 write(*,*)' ... Solids flux limit B ...'
                xl = xf
                gxf = xl*fit1v*exp(-fit2n*xl)
                gl = gxf + uu* xl
                xrl = gl/uu
                if (ui .lt. fit1v * EXP(-fit2n * xf)) then
                    write(*,*)' ... Safe ...'
                else
                    iload = 1
                endif
            endif

            return
            end


subroutine DIFFUS(st0)
c.....
c
c    Purpose:
c    Calculate the diffusivity for the settling tank
c.....
      real *8       conc,v2,cdif,fdif,fit1,fit2,dx,dt,
     &              coef,rhs,z,flux,aug,vf,v3,v1,vel,vec,E
      common        q0,qt,uflow,a,dCSTR,diftop,difbot,alpha2
     &              conc(40),v2,cdif(40),fdif(40),coef(40,3),rhs(40),z(40),
     &              flux(40),aug(40,4),vf,v3(40),nfq,qup,qdown,qfeed,xfeed,
     &              E(41),v1,vel(40),vec(40),dx,dt,fit1,fit2,npc,
     &              nf(40,3),nsw(40),jsw(40),sconc(40),nsp(4,3),iload,xl
c .....
            qav = (q0+qt)/2.
            qf = qav
            qup = qav-uflow
            qdown = uflow
```

```
      vf = qf/(a*1.646)
      v1 = qdown/(a*1.646)
      v2 = -qup/(a*1.646)
      dt = 5./60.0
      nfu = nfq-1
      nfd = nfq+4
      nf0 = nfd+1

      do 895 j = 2,nfu
      if((alpha1*(j-nfu)).lt.-85) then
          E(j) = 0.0
      else
          E(j) = diftop*exp(alpha1*(j-nfu))*dt/dx**2
      end if
895   continue

      icount = 0
      j = nfq
394   E(j) = diftop*exp(alpha2*(j-nfq))*dt/dx**2
      if (E(j).lt.difbot) icount = j-1
      if (j.lt.npc.and.icount.eq.0) then
          j = j+1
          go to 394
      end if

      if (icount.ne.0) then
          do 393 j = icount,npc
          E(j) = difbot*dt/dx**2
393       continue
      end if

      E(1) = E(2)
      E(41) = E(npc)

      nfd = nfq+1
      do 3 i=1,nfu
 3    v3(i) = v2
      v3(nfq) = v1
      do 4 i=nfd,npc
 4    v3(i) = v1

      open(9,file = 'c:\stora\uflow.dat')
      if (st0.eq.0.0) then
          write(9,'(7Hdiftop = f20.5)')diftop
          write(9,'(9Halpha1 = f10.4)')alpha1
          write(9,'(9Halpha2 = f10.4)')alpha2
          write(9,'(9Hdifbot = f10.4)')difbot
          write(9,'( )')
      end if
996   format(f10.2)

      return
      end
```

```
      subroutine CLAR2 (DSVI,nruns,totmass,scin0,scint,st0,lkl,xrl,uconc)
      c.....................................................................
      c
      c     Purpose:
      c     Computes the unsteady state concentration profile
      c     in one dimension using a modified crank-nicholson method
      c     suitable for handling non-linearities in the gravity flux.
      c     The profiles define concentration in the secondary clarifiers.
      c     Anderson/Edwards difference version
      c.....................................................................
            real *8       conc,v2,cdif,fdif,fit1,fit2,dx,dt,
           &              coef,rhs,z,flux,aug,vf,v3,v1,vel,vec,E
            common        q0,qt,uflow,a,dCSTR,diftop,difbot,alpha2
           &              conc(40),v2,cdif(40),fdif(40),coef(40,3),rhs(40),z(40),
           &              flux(40),aug(40,4),vf,v3(40),nfq,qup,qdown,qfeed,xfeed,
           &              E(41),v1,vel(40),vec(40),dx,dt,fit1,fit2,npc,
           &              nf(40,3),nsw(40),jsw(40),sconc(40),nsp(4,3),iload,xl
      c .....................................................................
                  lt = 0
                  nfu = nfq -1
                  jpc = npc +1
                  np1 = npc -1
                  if (st0.ne.0) go to 1002
                  nsp(1,1) = 1
                  nsp(1,2) = 2
                  nsp(1,3) = -1
                  nsp(2,1) = -1
                  nsp(2,2) = -2
                  nsp(2,3) = 1
                  nsp(3,1) = 1
                  nsp(3,2) = 0
                  nsp(3,3) = 1
                  nsp(4,1) = -1
                  nsp(4,2) = 0
                  nsp(4,3) = -1

      c     write initial conditions

       1002       continue
                  cin0 = dble(scin0)
                  cint = dble(scint)
                  cdiff = cint-cin0

      c     establish coefficient matrix

       1001       continue

                  if(lt.eq.0) c0 = cin0
                  if(lt.eq.0) ct = 1./3.*cdiff+cin0
                  if(lt.eq.1) c0 = 1./3.*cdiff+cin0
                  if(lt.eq.1) ct = 2./3.*cdiff+cin0
                  if(lt.eq.2) c0 = 2./3.*cdiff+cin0
                  if (lt.eq.2) ct = cint
```

```
      cav = (c0+ct)/2.

c     establish flux relationships

      do 20 i=1,npc
      z(i) = fit1*dexp(-fit2*conc(i))
      flux(i) = conc(i)*(v3(i)+z(i))
      vel(i) = v3(i)+z(i)-fit2*conc(i)*z(i)
 20   vec(i) = v3(i)+z(i)
      do 19 i=2,npc
      fdif(i)=flux(i-1)-flux(i)
 19   cdif(i) = conc(i-1)-conc(i)

c     set switching pattern

      jsw(1) = 1
      do 21 i=2,npc
      jsw(i) = -1
      if (fdif(i).ge.0..and.cdif(i).ge.0.) jsw(i) = 1
      if (fdif(i).le.0..and.cdif(i).le.0.) jsw(i) = 1
      if(jsw(2).eq.-1) jsw(1) = -1
 21   continue
      n=0
      j=1
 111  j = j+1
      if (jsw(j-1).ge.0.and.jsw(j).ge.0) nsw(j-1) = 1
      if (jsw(j-1).lt.0.and.jsw(j).lt.0) nsw(j-1) = 2
      if (jsw(j-1).ge.0.and.jsw(j).lt.0) nsw(j-1) = 3
      if (jsw(j-1).lt.0.and.jsw(j).ge.0) nsw(j-1) = 4
      if (jsw(j-1).ge.0.and.jsw(j).lt.0) n = n+1
      do 112 i=1,3
 112  nf(j-1,i) = nsp(nsw(j-1),i)
      if (j.ne.np1) go to 111
      if (jsw(np1).gt.0) nsw(np1) = 1
      if (jsw(np1).lt.0) nsw(np1) = 4
      do 113 i=1,3
 113  nf(np1,i) = nsp(nsw(np1),i)
      if(nf(1,2).eq.-2) nf(1,2) = 0
      nf(npc,1) = 1
      nsw(npc) = 1

c     establish lhs matrix

      coef(1,2) = 2.0+E(1) + nf(1,2)*.5*vel(1)
      coef(1,3) = -E(2) +(1+nf(1,3))*.5*vel(2)
      do 30 i=2,np1
      coef(i,1) = -E(i) - (nf(i,1)+1)*.5*vel(i-1)
      coef(i,2) = 2.+E(i)+E(i+1)+nf(i,2)*.5*vel(i)
      coef(i,3) = -E(i+1) + (1+nf(i,3))*.5*vel(i+1)
 30   continue
      coef(npc,1) = -E(npc) - (nf(npc,1) + 1) *.5*vel(np1)
      coef(npc,2) = 2.0+E(jpc)
```

```
c     establish the rhs vector

            rhs(1) =  (2.-E(1)+nf(1,2) * .5*(vel(1)-2.*vec(1)))*
     &      conc(1)  +(E(2)+(1+nf(1,3))*.5*(vel(2)-2.*vec(2)))
     &      *conc(2)
            do 40 i=2,np1
            rhs(i) =   (+E(i)-(nf(i,1)+1)*.5*(vel(i-1)-2.*vec(i-1)))* conc(i-1)
     &      +(2.-E(i)-E(i+1)+nf(i,2)*.5*(vel(i)-2.*vec(i))) * conc(i)
     &      +(E(i+1)+(1+nf(i,3))*.5*(vel(i+1)-2.*vec(i+1))) * conc(i+1)
    40      continue
            rhs(npc) =      (E(npc)-(nf(npc,1)+1)*.5*(vel(np1)-2.*vec(np1)))*
            &               conc(np1)+(2.-E(jpc))*conc(npc)


c     add sources and sinks

            coef(1,2) = coef(1,2) -v3(1)
            rhs(1) = rhs(1) + v3(1) * conc(1)
            coef(npc,2) = coef(npc,2) + v3(npc)
            rhs(npc) = rhs(npc) - v3(npc) * conc(npc)
            rhs(nfu) = rhs(nfu) + vf*cav
            rhs(nfq) = rhs(nfq) + vf*cav

c     solve for the current time step
c     using tridiagonal gauss elimination

            coef(1,1) = 0.0
            coef(npc,3) = 0.0
            do 59 i=1,npc
            do 59 j=1,3
            aug(i,j) = coef(i,j)
            aug(i,4) = rhs(i)
    59      continue
            do 60 i=2,npc
            aug(i,2) = aug(i,2) -aug(i,1)/aug(i-1,2)*aug(i-1,3)
            aug(i,4) = aug(i,4) -aug(i,1)/aug(i-1,2)*aug(i-1,4)
    60      continue
            aug(npc,4) = aug(npc,4)/aug(npc,2)
            do 70 i=1,np1
            m=npc-i
            aug(m,4) = (aug(m,4) - aug(m,3) *aug(m+1,4))/aug(m,2)
    70      continue
            do 75 i=1,npc
            conc(i) = aug(i,4)
            if(conc(i).lt.0) conc(i) = 0.0010
    75      continue

c     seeding a value for zone settling
c     (seeded at every time interval)

            if (iload.eq.1) then
                if (conc(38).lt.xl/4.) conc(38) = xl/4.
                if (conc(39).lt.xl/4.) conc(39) = xl/4.
            end if
```

```
          sconc(38) = conc(38)*4.
          sconc(39) = conc(39)*4.
          sconc(40) = conc(40)*4.

c     single CSTR time lag for compression zone
          uconc = sconc(40)-(sconc(40)-uconc)/exp(uflow/a/dCSTR*dt)
          conc(npc) = uconc/4.

c     compaction limitation on the underflow

          if (uconc.gt.1200./DSVI) then
              uconc = 1200./DSVI
              write(*,*)'Underflow compaction limited'
          end if

c     advance to the next time step

          lt = lt + 1
          tp = st0+lt*0.25/3.

          do 90 i=1,npc
          if (conc(i).lt.1E-37) conc(i) = 0.0
          sconc(i) = sngl(conc(i))*4.
 90       continue

          if (lt.ne.3) go to 1001

          write(*,*)'Time = ',st0,' Step = ',lt
          if (lkl.ne.4) go to 776
          if (st0+1.lt.nruns) go to 776
          open(8,file = 'c:\stora\run2.dat')
          write(8,998)st0,lt
 998      format(f6.2,i4)
          do 901 i=1,npc
          write(8,999)-i,sconc(i),E(i)/dt*dx**2.
 901      continue
 999      format(i4,4f15.4)
 776      continue
          concmass = 0.0
          do 908 i = 1,npc
 908      concmass = concmass + sconc(i)*a*dx
          write(8,925)concmass
 925      format(33X,'Conc mass 'f10.2)

          qup = -v2*a*1.646
          qdown =v1*a*1.646
          qfeed = vf*a*1.646
          xfeed = (scin0+scint)*4./2.
          if (st0.eq.0.0)
     &    write(9,*)'  time blan uflow  Xrmass  eff '
     &,'  Xeffmass Feedmass Concmass'
          i = 0
 553      i=i+1
          if(i.lt.40.and.conc(i)*4..lt.xfeed)then
```

```
            go to 553
        else
            write(9,994)st0+0.25,i,sconc(40),uconc*qdown*15/60.,
     &      sconc(1),sconc(1)*qup*15/60.,
     &      xfeed*qfeed*15/60.,concmass
        endif
994     format(f9.2,i4,f8.2,2f10.4,3f10.2)
        totmass = totmass + sconc(1)*qup*15/60.
        if ((st0+0.25).eq.nruns) write(9,995)totmass
        if ((st0+0.25).eq.nruns) write(*,995)totmass
        if ((st0+0.25).eq.nruns) write(*,996)sconc(npc)
995     format(30X,'Total mass in settling tank 'f10.2)
996     format(27X,'Underflow conc 'f10.2)

        return
        end
```

EXAMPLE OF SIMDAT1.DAT (FROM RIJEN 4 TEST)

```
1625.97  0.0836
120.00 130.00
5
0.0       0.0       0.0       0.0       0.0
0.0475    0.0475    0.0475    0.0475    0.0475
0.0475    0.0475    0.0475    0.0475    0.0475
0.0475    0.0475    0.0475    0.0475    0.0475
0.0475    0.0475    0.0475    0.0475    0.0475
1.7525    1.7525    1.7525    1.7525    1.7525
1.7525    1.7525    1.7525    1.7525    1.7525
1.7525    1.7525    1.7525    1.7525    1.7525
```

EXAMPLE OF NEWDAT1.DAT (FROM RIJEN 4 TEST)

```
3.81      3.81      1956.0    1956.0    531.0
3.81      3.81      1956.0    1956.0    531.0
3.81      3.81      1956.0    1956.0    531.0
3.81      3.81      1956.0    1956.0    531.0
3.81      3.81      1956.0    1956.0    531.0
3.81      3.81      1956.0    1956.0    531.0
3.81      4.10      1956.0    1956.0    531.0
4.10      4.39      1956.0    1956.0    531.0
4.39      4.215     1956.0    1956.0    531.0
4.215     4.04      1956.0    1956.0    531.0
4.04      3.945     1956.0    1956.0    531.0
3.945     3.85      1956.0    1956.0    531.0
3.85      3.63      1956.0    1956.0    531.0
3.63      3.41      1956.0    1956.0    531.0
3.41      3.44      1956.0    1956.0    531.0
3.44      3.47      1956.0    1956.0    531.0
3.47      3.36      1956.0    1956.0    531.0
3.36      3.25      1956.0    1956.0    531.0
3.25      3.225     1956.0    1956.0    531.0
3.225     3.20      1956.0    1956.0    531.0
3.20      3.26      1956.0    1956.0    531.0
3.26      3.32      1956.0    1956.0    531.0
3.32      3.095     531.0     531.0     531.0
3.095     2.87      531.0     531.0     531.0
2.87      3.08      531.0     531.0     531.0
3.08      3.29      531.0     531.0     531.0
3.29      3.06      531.0     531.0     531.0
3.06      3.06      531.0     531.0     531.0
```